Sensitization of prostate cancer cells to cytotoxic drugs induced by the small adenoviral E1A12S protein through multiple cell death/signalling pathways.

Héctor Rubén Maya-Pineda

Centre for Molecular Oncology
Barts Cancer Institute
Barts and the London School of Medicine and Dentistry
Queen Mary University of London
Charterhouse Square
London
United Kingdom

A thesis submitted for the degree of Doctor of Philosophy

September 2013

Declaration

I hereby declared that the work presented in this thesis is an original work done by the author, Héctor Rubén Maya-Pineda, at the Centre for Molecular Oncology, Barts Cancer Institute, Barts and The London School of Medicine and Dentistry, Queen Mary, University of London. All external sources have been properly acknowledged.

Acknowledgements

I would like to thank CONACYT for the financial support awarded. I would also like to thank all the people, friends and family that helped me to get here and made this possible, in particular Dr Ingeborg Becker, Dr Magdalena Aguirre and Dr Alejandro Zentella for the support and a special thanks to Dr Gloria Vizcaino for her friendship.

I would like to thank my supervisor Dr Gunnel Halldén for giving me the opportunity to accomplish one of my most important goals in life, I am really grateful for all your support, guidance and patience throughout this exciting journey, and also for giving me the tools to further develop my career in research. I would also like to thank Professor Nick Lemoine for the support during my thesis.

I would like to thank the past and present group members Constantia, Maria, Ana, Virginie, Stella, Carmen, Camilla and Gioia for all their time, advice, support and friendship, and for all the good time in the lab and the memories. Will like to thank especially Katrina Sweeney for the friendship and for always being there when I need it; I'm very grateful to you Katrina. Additionally, to all the members of the VGT group that helped during my research and all past and present people of Molecular Oncology and Tumour Biology, it was a great pleasure to meet you all; with special thanks and mention to Barbara Delage for your friendship and all the people in the G28 office, it was great to share the office with friends for almost four years.

I would also like to thank you, Michaela M, for your support, patience, your friendship and for being a very important part of my life; TAM.

Finally, I would like to thank my parents and my brother, who have always supported me, encouraged me, and made me forget the long distance; I'm always going to be extremely grateful to you; LQM.

Abstract

Replication-selective oncolytic adenoviruses represent a promising anticancer approach with proven efficacy in cancer cell lines and tumour xenografts *in vivo*. Anti-tumour efficacy, both in preclinical studies and clinical trials, was significantly improved in combination with chemotherapeutics in numerous cancers, including prostate cancer. It has been established that expression of the viral E1A gene is essential for the enhancement of cell killing in combination with cytotoxic drugs.

The overall goal of this project is to identify specific E1A gene regions involved in the sensitization to the cytotoxic drugs mitoxantrone and docetaxel, the current standard of care for late stage prostate cancers, to enable the development of improved anti-cancer therapies. Specific regions in the E1A proteins bind to numerous cellular factors to regulate the host cell function and the viral life cycle, including the p300, p400 and pRb family proteins. This work was aimed at determining the mechanisms involved in the synergistic cell killing in prostate cancer cells in response to the combination of the replication-selective (oncolytic) mutant AdΔΔ with cytotoxic drugs. Previous findings suggested an enhancement of drug-induced apoptosis. I found that the small E1A12S protein, unable to induce viral replication, is sufficient to sensitize the prostate cancer cells, 22Rv-1 (AR+), and PC-3 and DU145 (AR-), to drugs. The non-replicating AdE1A12S-mutant AdE1A1104 (defective in p300-binding) could not sensitize the cells while mutants with intact E1A-p300 binding (AdE1A12S, AdE1A1102, AdE1A1108) and defective in p400- (AdE1A1102) or pRb-binding (AdE1A1108) potently sensitized all tested cell lines. In fact, all mutants except AdE1A1104 potently synergised with mitoxantrone and docetaxel to kill the prostate cancer cells. When comparing the non-replicating E1A12S mutants with the corresponding replicating E1A-deletion mutants (expressing E1A12S and 13S) synergy was demonstrated with all replicating mutants except *dl*1104, which caused an additive effect with mitoxantrone. We hypothesised that the synergistic cell killing is the result of pathway convergence through E1A-p300 and mitoxantrone-activated DNA-damage/apoptosis events. To address this I employed an extensive miRNA array screen to identify potential pathways. Several miRNAs were found to be differentially regulated in response to the combination of AdE1A12S with mitoxantrone compared to each single agent treatment. The majority of these miRNAs are reported to be part of cell death and survival pathways (*e.g.* apoptosis and autophagy) and to be differentially regulated in prostate cancer. To further investigate the role of these pathways, I determined changes in expression levels of key proteins that had previously been suggested to be targeted by the identified miRNAs, thereby preventing translation of the respective mRNAs. The greatest changes in protein levels in response to AdE1A12S and mitoxantrone were observed for Bcl-2, p-Akt, LC3BII and p62. Finally, I verified similar mechanisms of action when the oncolytic AdΔΔ was combined with mitoxantrone under synergistic conditions. These findings will direct future investigations aimed at dissecting the mechanisms of action for virus-induced sensitization to cytotoxic drugs and may aid in the development of improved therapies for prostate cancer by design of novel oncolytic mutants and combination strategies and/or identification of targets for small molecules inhibitors.

List of Abbreviations

Ab: antibody

Abs: absorbance

Ad: adenovirus

ADP: adenovirus death protein

AR: androgen receptor

ATCC: American Type Tissue Culture Collection

Bik: BCL2-interacting killer

BMF: Bcl-2-modifiying factor

BNIP3: BCL2/Adenovirus E1B 19 KDa Protein-Interacting Protein 3

BSA: bovine serum albumin

CAR: Coxsackie and adenovirus receptor

CBP: CREB binding protein

CD: cytosine deaminase

Cdk: cyclin-dependent kinase

CI: combination index

CMV: cytomegalovirus

COX2: cyclooxygenase 2

CREB: cAMP response element binding

CR: conserved region

CtBP: carboxy-terminal binding protein

Cyt C: cytochrome C

CRUK: Cancer Research UK

DHT: dihydrotestosterone

DMEM: Dubelcco's modified Eagle medium

EC_{50}: effective concentration at inducing 50% cell death

EGFR: epithelial growth factor receptor

EMT: epithelial-mesenchymal transition

FCS: foetal calf serum

GFP: green fluorescence protein

h: hours

HAT: histone acetyltransferase

HDAC: histone deacetylase

HRK: Harakiri, BCL2 Interacting Protein

Ig: immunoglobulin

ITR: inverted terminal repeat

LHRH: Luteinising hormone releasing hormone

min: minutes

mRNA: messenger RNA

NMR: nuclear magnetic resonance

Noxa: Latin for damage

OD: optical density

Orf: open reading frame

P/CAF: p300/CBP associated factor

PCR: polymerase chain reaction

Pfu: plaque forming unit

PIN: prostatic intraepithelial neoplasia

PP2A: protein phosphatase 2A

ppc: particles per cell

pRb: retinoblastoma protein

PSA: prostate-specific antigen

PSMA: prostate specific membrane antigen

qPCR: quantitative PCR

rpm: revolutions per minute

SDS: sodium dodecyl sulphate

TBP: TATA-binding protein

$TCID_{50}$: tissue culture inhibitory dose 50%

TMRE: tetramethylrhodamine

TNF: Tumour Necrosis Factor

TRRAP: transactivation/transformation domain protein

Contents

1. Introduction

1.1 Prostate cancer

Prostate cancer (PCa) is a major public health problem in Western industrialized countries and is the third most common cause (after lung cancer) of cancer-related deaths in men.[1] The initial treatment of advanced metastatic PCa is to deprive tumours of androgens by chemical castration, achieved by the use of Gonadotropin-releasing hormone (GnRH) agonists or antagonists; inhibition of steroidogenic enzymes; and the use of anti-androgens that block the binding of androgens to the androgen receptor (AR).[2] For most patients, the cancer becomes insensitive to androgen ablation therapy, spreads further, and ultimately patients will die from hormone-refractory metastatic PCa (HRPC).[3] The development of PCa to a hormone-independent stage invariably results in advanced disease, with limited therapeutic options, poor prognosis and death.[4,5] HRPC frequently displays alterations in AR signalling, cell cycle and apoptosis pathways or neuroendocrine differentiation.[6] No effective treatment is yet available for HRPC with radiation and chemotherapy (e.g. mitoxantrone and docetaxel) mainly being palliative.[7] Therefore, novel therapeutic strategies that target treatment-resistant PCa are needed.[8] The key goal when developing new, targeted cancer treatments is to disable signalling mechanisms that are essential for tumour maintenance without affecting normal tissue.[9,10] Development of novel drugs is urgently needed because the current standard of care such as cytotoxic drugs [11] and radiation therapy [12] are not curative in the majority of cases, and efficacy is invariably reduced by side effects and treatment resistance.[13]

1.1.1 Epidemiology and Risk Factors

With the advent of prostate-specific antigen (PSA) testing, one in six men in the United States will be diagnosed with prostate cancer at some point in their life.[14] In 2008, PCa was the second most frequently diagnosed cancer and the sixth highest cause of all cancer-related death in men worldwide.[1] In the United Kingdom, the

incidence rate of PCa is the highest of all cancers in men and is the second leading cause of cancer-related deaths in men.[15]

Age is considered to be the most important risk factor, with increasing incidence in men of advanced age, being 15-30% by the age of 50, and up to 60-80% by the age of 80.[16] Cultural origin and environmental factors can also increase the risk of developing the disease. North America has the highest incidence of PCa (92 cases per 100,000 men),[16] however men of African descent in the Caribbean have the highest mortality rate in the world.[1] In contrast, in East Asia, the rates remain below those of western countries. For example, Chinese men have the lowest incidence (1 case per 100,000 men).[16] However, both incidence and mortality has increased in the last 20 years in Asian countries.[17] Asian immigrants in the United States have a higher incidence of PCa compared to the incidence in their own countries, suggesting that environmental and dietary factors play a role.[18] Studies have suggested that first degree male relatives of men with PCa have a 2- to 3-fold higher risk of developing PCa, and up to 10-fold if three or more relatives are affected, implying a hereditary and genetic link.[16]

Diet has been strongly implicated as a risk factor for PCa. A Health Professionals Follow up study of 51,000 men suggested a positive correlation between PCa incidence and the intake of red meat and a diet high in fat.[16] In contrast, the consumption of a diet rich in fatty fish, isoflavones, lycopenes and high systemic levels of vitamin D, showed an inverse correlation with the incidence of PCa.[16] Also, reduction of cholesterol levels in the blood decreases the incidence of PCa by 50%.[17]

Inflammation is another possible risk factor for PCa. Although the reasons for the inflammatory responses are unclear, there are many potential sources, including direct infection, urine-reflux-induced chemical and physical trauma, dietary factors, oestrogens, or a combination of two or more of these factors (Fig. 1).[18]

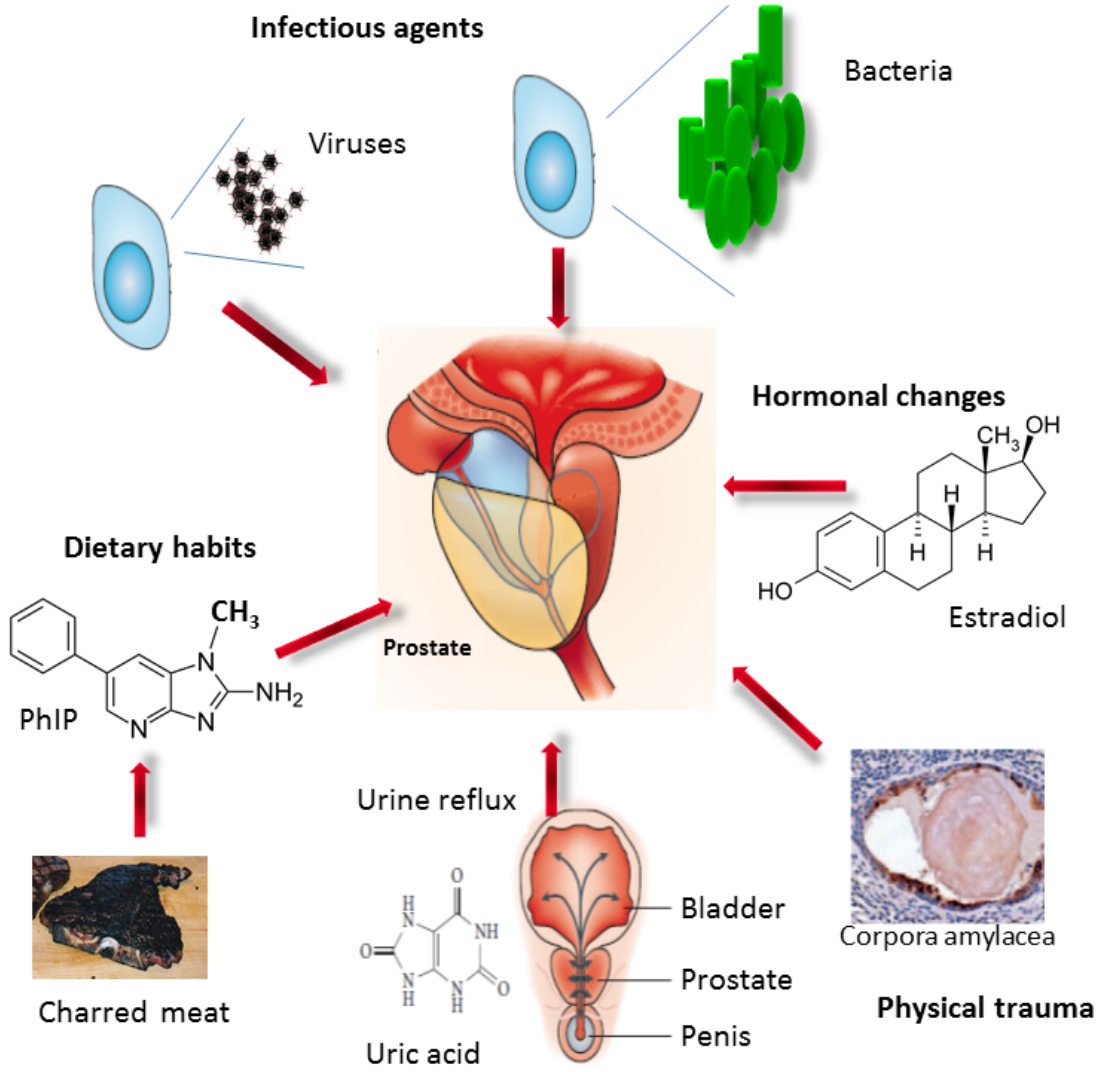

Figure 1. Potential sources of prostate inflammation. Factors that could trigger an inflammatory response within the prostate and induce PCa, adapted from [18].

Another potential source of inflammation is pathogens such as virus and bacteria. The induction of PCa by bacteria has not been proven definitively, but there is strong evidence connecting bacterial infection with chronic inflammation of the prostate tissue.[19] Moreover, bacteria responsible for the inflammation of the prostate can be divided into sexually transmitted and non-sexually transmitted pathogens, and among the sexually transmitted *Neisseria gonorrhoea, Chlamydia trachomatis, Trichomonas vaginalis* and *Treponema pallidum* have been associated with PCa.[18] The non-sexually transmitted bacteria include *Propionibacterium acnes* that is also found in the skin and is associated with acne. These bacteria have a high prevalence in prostate cancer tissue (35%) and show a strong correlation with inflammation in

PCa tissue.[20] *Propionibacterium acnes* in a mouse model was found to induce acute chronic inflammation of prostate tissue and favour cell proliferation, although the induction of PCa by these bacteria remains to be elucidated.[21] Other pathogens such as human papillomavirus (HPV), human herpes simplex virus type 2 (HSV2), cytomegalovirus (CMV) and human herpes virus type 8 (HHV8) are known to infect the prostate tissue, although a correlation between virus-induced inflammation of the prostate and the induction of PCa has not been proved definitively.[18] In 2006, Urisman and colleagues[22] reported that the xenotropic murine leukaemia virus-related virus (XMRV) was associated with prostate cancer. However, this finding was not verified and has been dismissed since the identification of the virus in prostate tissue has been shown to be related to a contamination of the samples rather than the result of an infection.[19] In contrast, both HPV and Epstein Barr virus (EBV) sequences have been identified simultaneously in 55% of human prostate cancer samples, indicating a strong correlation of HPV and EBV with prostate cancer.[23] Although the results indicated a correlation between HPV and EBV and prostate cancer, the number of samples were low (n=40) and a direct link between viral infection and prostate cancer was not shown. Thus, the implications of viral infections as inducers of prostate cancer remain unclear. However, despite the facts mentioned above the only risk factors that have been established are old age, ethnicity (African descent), familial history and dietary habits.[1,19]

1.1.2 Biology of prostate cancer

The prostate is a gland that reaches maturity in an androgen-dependent manner after puberty. The mature prostate is the size and shape of a walnut (20g and 4cm × 2.5cm) in an adult man.[24] It is localized in the pelvis, anterior to the rectum surrounding the urethra at the base of the bladder.[16] The human prostate has a zonal architecture, corresponding to central, periurethral, transitional, and peripheral zones, together with an anterior fibromuscular stroma (Fig. 2).[25,26] The gland produces part of the seminal fluid and may facilitate sperm motility. The prostate is composed of branching glands with ducts that are lined by luminal secretory and

basal epithelial cells.[16] Most tumours initially develop gradually from the luminal secretory epithelial cells (Fig. 3).[27,28] The prostate tissue is mainly composed of glandular tissue and growth is androgen-dependent. Luminal secretory epithelial cells represent the major cell type in the gland and produce PSA and prostatic acid phosphatase.[29] PCa is a multifocal disease that develops from multiple histological foci of cancer cells that are often genetically heterogeneous.[30] Over 95% of PCas are adenocarcinomas with a luminal phenotype; of these, the vast majority are acinar adenocarcinomas (Fig. 3).[28] Androgen deprivation results in apoptosis of the luminal epithelium.[31]

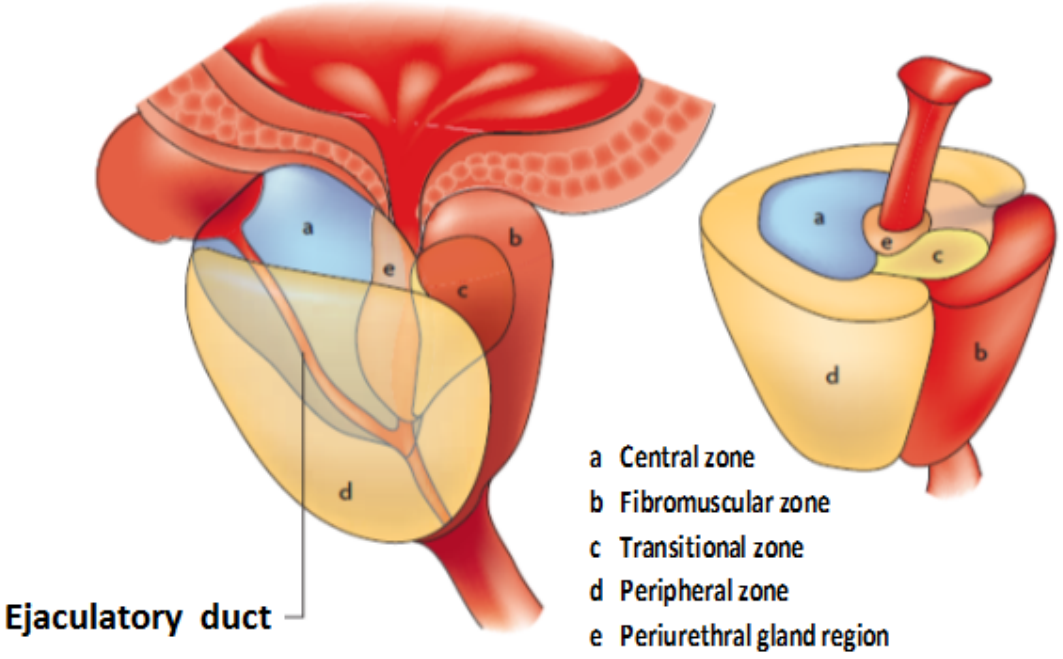

	Prostate zone		
	Peripheral	Transition	Central
Focal atrophy			
Acute inflammation			
Chronic inflamation			
Benign prostatic hyperplasia			
High-grade PIN			
Carcinoma			

High prevalence | Medium-high prevalence | Low prevalence | None

Figure 2. Predisposition to prostate diseases and association with specific zones in the gland. Zones of the prostate that are susceptible to chronic illnesses that could result in cancer development, adapted from.[18]

Other subtypes of PCa such as ductal adenocarcinoma, mucinous carcinoma, signet carcinoma and neuroendocrine PCa can be defined molecularly and genetically, however, they are uncommon and have similar prognosis.[28] Neuroendocrine PCa shows the most differentiated histological pattern of all, and is generally classified as small cell carcinoma or a carcinoid tumour.[28] The peripheral zone occupies the largest volume (Fig. 2), and harbours the majority of prostate carcinomas. In contrast, benign prostatic hyperplasia (BPH), a common non-malignant condition found in older men, arises from the transition zone (Fig. 2).[16]

1.1.3 Development of prostate cancer

1.1.3.a Molecular Pathogenesis

It is well known that PCa cells have numerous mutations, but the development of its molecular pathogenesis is still unclear. The disruption of the prostate homeostasis, due to genetic and molecular alterations, leads to the dedifferentiation of prostatic smooth muscle and enhanced proliferation of vascular endothelial and epithelial cells during the transition from low to high grade PCa.[27] Molecular mechanisms triggered by inflammatory events induced by highly reactive chemical compounds can also affect prostate epithelial cells undergoing DNA synthesis, increasing the risk of PCa development.[18]

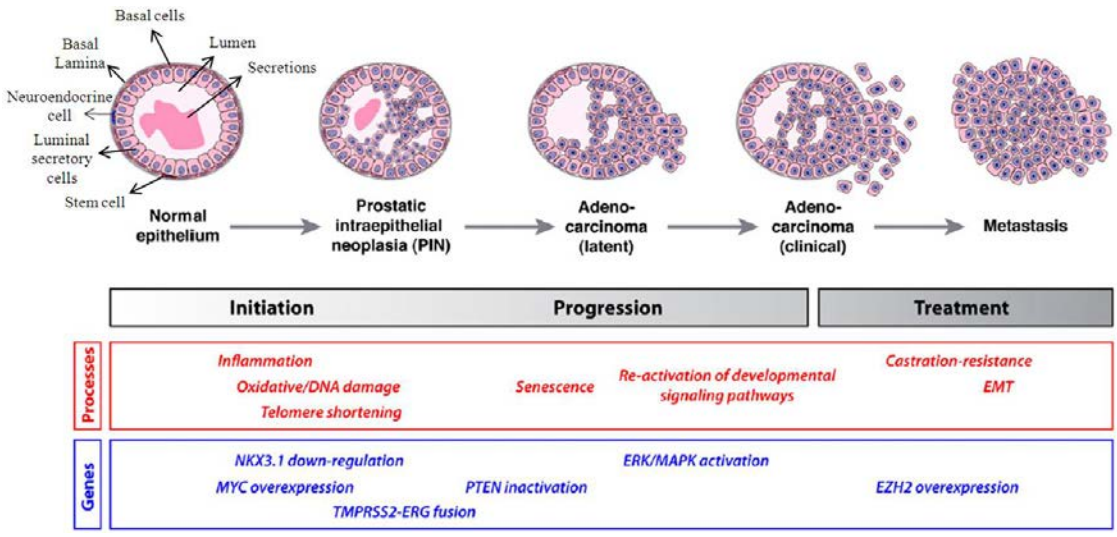

Figure 3. Prostate Cancer progression. Histology of the normal prostate epithelium and the genetic events altered within the progression from a normal to a metastatic prostate phenotype. The luminal secretory cells that attach to the basal cells and extend to the acinar lumen express the androgen receptor and synthesize and secrete distinct prostate differentiation markers (e.g. PSA) into the acinar lumen.[16] EMT; epithelial to mesenchymal transition, NKX3.1; transcription factor NK (named after Niremberg and Kim),[32] homeobox family 3 locus-1, MYC; myelocytomatosis viral oncogene homologue, TMPRSS2-ERG; trans-membrane protease serine 2-Ets-related-gene, PTEN; phosphatase and tensin homolog, ERK/MAPK; mitogen-activated protein kinase and EZH2; enhancer of zeste homolog 2 (Drosophila). Figure modified from.[28]

Inflammation can contribute to PCa progression and the development of high prostatic intraepithelial neoplasia (PIN) that is considered as the only clearly defined precursor of prostatic adenocarcinoma (Fig. 2-3). PIN has an intermediate phenotype and genotype between benign prostatic epithelium and cancer, and is histologically characterized by the enlargement of nuclei and nucleoli, appearance of luminal epithelial hyperplasia, cytoplasmic hyperchromasia, reduction in basal cells and nuclear atypia. In addition, PIN is confirmed in biopsies by the elevation of cellular proliferation markers, the absence of p63 and cytokeratin 5/14 immunostaining and elevated immunostaining of the luminal marker α-methylacyl-CoA-race-mase (AMACR).[28,33]

1.1.3.a.I Gene alterations in Prostate Cancer

Genetic alterations (Fig. 3) in the normal prostate glandular epithelium induce gradual alterations leading to an oncogenic phenotype, initially as a localized androgen-dependent disease.[27] Many phenotypic modifications in PCa are due to enhanced expression of several oncogenes and a decreased expression of tumour suppressor genes induced through gene amplification, somatic mutations, chromosomal aberrations and deletions.[34 27]

Several chromosomal abnormalities have been reported in prostate cancer patients such as the insertion of genetic material in the chromosomes 7p, 7q, 8q and IX or deletions such as in chromosomes 10q, 13q and 16q.[34,35] Other chromosomal alterations include the translocation of the TMPRSS2 and members of the E-twenty-six (ETS) family of transcription factors (ERG and ETS-translocation variant1-4-ETV1,

ETV4, or ETV5) mainly ERG (Fig. 3). The translocation and fusion (by an interstitial deletion) of the TMPRSS2 promoter/enhancer and the coding region of ERG has been identified in 60% of prostate cancer tissue in almost seventeen regions within the chromosome 21q22 where both are localized, and has been shown to be promoted by androgens.[34,36] Of the identified fusions, nine code for functional products (two ERG or six truncated ERG or a new protein combining TMPRSS2 and ERG), and eight do not encode functional proteins because of a premature stop codon.[34] Other common chromosomal alterations present on prostate cancer include the loss of heterozygosity of 8p21.2 in nearly 85% of PCa and of chromosome 12q12-13 in 20% of localized and 50% of metastatic prostate cancer, additionally chromosome 8q24 shows amplifications.[34]

Several genes such as ribonuclease-L (2',5'-oligoisoadenylate synthetase-dependent) (RNASEL), hereditary prostate cancer protein-2 (ELAC2/HPC2), macrophage scavenger receptor-1 (MSR1), androgen receptor (AR), cytochrome P450 17(CYP17) and steroid 5-α-reductase type-2 (SRD5A2), have being identified as susceptibility genes in PCa (Fig. 3).[16] Furthermore, oncogenes and tumour suppressors that regulate cell cycle and apoptosis pathways, such as p53, p21, Rb, also have been implicated in the pathogenesis of PCa.[16] Other genes that have been observed to be deregulated in PCa progression are NKX3.1 (8p21.2), PTEN (10q23.31), c-MYC (8q24), and p27 (Fig. 3).[34] The transcription factor NKX3.1, regulated by AR is involved in the terminal differentiation of prostate epithelial cells, and when downregulated by loss of heterozygosity, tumour progression is facilitated.[34] In contrast, the amplification of MYC by amplification of chromosome 8q24 results in tumour progression and is frequently observed in localized and metastatic PCa.[34] The downregulation of the cell cycle inhibitor p27 has been associated with poor prognosis.[34] In addition, the tumour suppressor gene TP53 (17p13.1) involved in the regulation of apoptosis, cell cycle arrest and senescence has been found to be mutated or downregulated in around 50% of advanced PCa.[18] Moreover, single nucleotide polymorphisms (SNP) in key genes have been suggested to be associated with PCa risk such as the cytochrome P450 17 (CYP17) gene where the SNP rs743572 has been associated with high risk of prostate cancer.[34] PTEN, an inhibitor of the PI3K/Akt/mTOR pathway has been shown to be downregulated in 23-52% of PCas depending on the stage of

cancer progression. The lack of PTEN results in activation of the Akt/mTOR pathway.[34,37] The stimulation of Akt can also be induced by NF-kB through IKK and by cholesterol[28]. The activation of Akt1 or the isoform p110β of PI3K cause activation of the PI3K/Akt/mTOR pathway, inducing tumour progression and resistance to hormone depletion.[28] Other mutations that have been identified in PCa include the genes Forkhead box protein A1/O3 (FOXA1/O3; 6q21)) affecting cell proliferation and accumulation of DNA damage inducing cancer development and progression. In addition, other mutations include the mediator complex subunit 12 (MED12), thrombospondin, type-I, domain containing 7B (THSD7B), sodium channel, voltage-gated, type XI, α subunit (SCN11A), speckle-type POZ protein (SPOP) that increases invasion and zinc finger protein 595 (ZNF595)[38]. Mutations and loss of heterozygosity that leads to pRb inactivation have been linked to the development and progression of PCa in clinical samples and in a mouse model[39].

1.1.3.a.II Hormonal and growth factors

Evidence suggest that hormones and growth factors are implicated in PCa development; high levels of testosterone and Insulin like Growth Factor (IGF-1) are associated with higher incidence and early development.[16] Other growth factors, for example Epidermal Growth Factor (EGF), Fibroblast Growth Factor (FGF), Hepatocyte Growth Factor (HGF), Vascular Endothelial Growth Factor (VEGF) and Transforming Growth Factor Beta (TFG-β) also have been reported to be involved.[16,27] Several hormone and growth factor receptors are also altered in PCa, perhaps the best known is the androgen receptor (AR). AR is a nuclear receptor of 120kDa,[27] and a member of the steroid-thyroid-retinoid superfamily of nuclear receptors, and it is localized on chromosome X and contains eight exons.[29,34] When the AR is activated by ligand-binding, the receptor acts as a transcription factor by inducing the expression of gene products involved in proliferation and development of normal and neoplastic tissue in the prostate.[27] AR is composed of the N-terminal domain (NTD), a carboxy-terminal ligand binding domain (LBD), a DNA-binding domain (DBD) in the mid region and a hinge region (Fig.4).[29,40] There are two activating functions

(AF1 and AF2) localized in NTD and LBD (Fig. 4).[41] Inactive AR is bound to heat-shock proteins and other proteins in the cytoplasm to prevent DNA transcription, while binding of ligand to AR activates the receptor through conformational changes that releases the bound proteins and enables AR phosphorylation, followed by nuclear translocation and binding to androgen response elements (AREs) in target genes.[29]

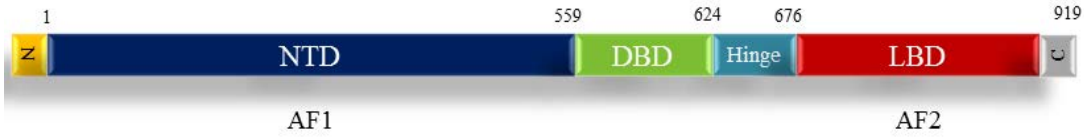

Figure 4. The human androgen receptor (AR). AR contains ~ 919 amino acids. NTD – N-terminal domain; DBD – DNA binding domain; LBD – ligand binding domain; Hinge – hinge region between the DBD and LBD. The activation function 1 (AF1) within the NTD and activation function 2(AF2) resides within the LBD. N; amino terminal end and C; carboxy terminal end.

Activation of AR signalling pathways has been demonstrated to play an essential role in the development of HRPC.[42] Germline variations in the AR gene have been demonstrated as a predictor of cancer aggressiveness.[16] There are 1029 different mutations reported for the AR with most of them not causing malignancy, while 159 mutations, most of which have single base substitutions due to somatic mutations have been associated with PCa.[43] Genetic modifications within the AR coding region include point mutations, gene amplification and deletions which, can lead to AR overexpression, androgen hypersensitivity, AR-polymorphism and promiscuous binding to non-androgens (Table 1).[29] Cancer related mutations in AR are more common in androgen independent PCa, most of which occur in the conserved domains (DBD and LBD) (Fig. 4).[44] Mutations can also generate an AR that is hypersensitive to androgenic hormones, for example products of the dihydrotestosterone (DHT) metabolism. The mutations Val715Met and Val730Met in the AR-LBD are examples of substitutions that were identified in a metastatic tumour and a confined tumour respectively.[44] Other examples of AR-LBD include the somatic mutations Leu701His and in LNCaP cells Thr778Ala which induce prostate cancer cell growth and cell survival.[34]

Table 1. Mechanisms for development of hormone-refractory metastatic prostate cancer.

Type	Pathway	Ligand dependence	AR dependence	Mechanism
1	Hypersensitive AR	Androgen dependent	AR dependent	Amplified AR Sensitive AR Increased DHT
2	Promiscuous AR	Pseudo-androgens Androgen antagonists Corticosteroids Co-regulator mutations	Dependent on a mutant AR in LNCaP cells and ARcortisol responsive cells	Widened AR specificity Illicit stimulation by non-androgens Flutamide withdrawal' (antagonists acting as agonists)
3	Outlaw AR	Androgen independent Ligand independent	AR dependent	Mutant PTEN Amplified HER-2/neu Activated PI3K Activated MAPK Mutant co-regulators
4	Bypass AR	Androgen independent	AR independent	Parallel or alternative survival pathways: Overexpression of BCL2 Activation of other oncogenes Inactivation of tumour suppressor genes
5	Lurker cells	Androgen independent	AR independent	Malignant epithelial stem cells

Modified from [29].

1.1.3.b Prostate Cancer metastasis

Advanced PCa shows bone and lymph node metastasis in almost 80% of cases. Osteoblastic lesions occur in vertebral bodies, pelvic bones, sternum, ribs, and the femurs.[16] These lesions are the main cause of death in most patients, however the cancer cell tropism is not well understood.[28] Metastatic prostate tumour cells in the circulation show multiple chromosomal rearrangements and typical genomic instability.[28] Findings suggest that metastatic PCa arises from a monoclonal cell source, selected as a result of treatment with chemo- or radiation-therapy killing most cancer cells, but not prostate cancer stem cells that have accumulated multiple mutations and epigenetic changes.[45] Inflammation also creates a selective environment that triggers this carcinogenic progression.[45]

1.1.4 Diagnosis of Prostate Cancer

During the last 20 years more patients have been diagnosed at earlier stages, mainly because of increased screening in men. Screening is aimed at reducing PCa mortality. The choice of screening method is dependent on local health care regulations. To

increase the rate and accuracy of PCa detection it is necessary to combine different screening methods such as digital rectal examination (DRE), prostate specific antigen (PSA), and transrectal ultrasound (TRUS). However, to confirm PCa histological evidence is also needed in all cases and is obtained by biopsy sampling.

1.1.4.a Digital rectal exam (DRE)

The DRE has the potential advantage of detecting abnormal growth of the prostate and consequently both benign and malignant tumours and to limit overdiagnosis.[46] DRE has a 50% predictive accuracy, although it is only accurate and reproducible if executed by an expert.[47] A disadvantage of DRE is that it is relatively insensitive and several cancers are not detected due to the inability to palpate the entire prostate gland and to detect tumours elsewhere in the prostatic capsule or at a more advanced pathological stage.[46] Patients diagnosed by DRE alone have a poor survival rate, in which 75% of the patients eventually die.[47] The effectiveness of DRE increases if used in combination with other diagnostic methods.

1.1.4.b Prostate-specific antigen (PSA)

PSA is a serine protease produced by the prostatic epithelium and periurethral glands.[47] Although elevated PSA levels are a good diagnostic factor for PCa, changes in PSA levels could also be caused by other events such as prostate infection, prostatitis, urinary tract infection or recent ejaculation. In addition, PSA is not elevated in some patients with PCa.[48] The PSA values recommended for use for diagnosis are determined by age range and ethnicity (Table 2).[49] The widespread use of PSA testing has increased the diagnosis of patients with clinically localized low-grade carcinomas that may not require treatment and could be managed by watchful waiting.[28] The absence of a non-invasive prognostic method that distinguishes between a low-grade and an aggressive tumour has led to overtreatment of patients that otherwise would not require active treatment. The over-diagnosis and treatment of PCa reduces the overall impact and benefits in survival rates.[28] Recent studies have revealed that PSA doubling time (PSADT) rather than absolute PSA

levels is a better predictor to determine the risk of metastatic disease and further progression of PCa.[48] In a multi-ethnic older-men study a PSADT of less than 9 months was associated with poorer overall survival and a worse prognosis than PSADT of more than 9 months after radical prostatectomy.[50]

Table 2. Recommended age-specific PSA reference ranges for diagnosis among different ethnicities. PSA values above the indicated ranges suggest potential higher risk for developing PCa.

Prostate Specific Antigen				
Age Range	White	Black	Asian	
40-49	0-2.5	0-2	0-2	ng/ml
50-59	0-3.5	0-4	0-3	
60-69	0-4.5	0-4.5	0-4	
70-79	0-6.5	0-5.5	0-5	

Modified from [49].

1.1.4.c Transrectal ultrasound (TRUS)

TRUS is currently the most common imaging tool for PCa and is used as a guide for needle biopsies.[51] TRUS gives an image of the prostate and seminal vesicles by using a biplane intra rectal probe.[47] By convention TRUS is not considered a suitable single diagnostic and staging tool for PCa, due to low sensitivity and accuracy of non-palpable cancers where 50% are missed.[47,51] In addition, during TRUS-guided biopsies events such as infection, bleeding and pain can appear during the procedure.[46] However, TRUS is a reliable method to identify cyst, abscesses and calcifications within the prostate, and can be used to measure the volume of the prostate.[16] A method derived from TRUS termed transrectal elastosonography (TRES) appears as a better diagnostic tool in terms of accuracy, however current analysis evaluating the efficacy of TRES are not conclusive since the studies did not use a standardized procedure that could be comparable.[52]

1.1.4.d Biopsies

A biopsy comprises the collection of 10 to 12 needle core samples for mapping the prostate, and involves taking samples from the parasagittal base, the mid-gland, the

apex from each side and from the far lateral peripheral zones.[47] In biopsies, diagnosis of prostate adenocarcinoma can be confirmed by the absence of immunostaining using p63 and cytokeratin 5/14 antibodies and an elevated immunostaining of a-mehtylacyl-CoA racemase (AMACR), a luminal marker overexpressed in carcinomas.[28] Common complications of this invasive procedure include urinary tract infections, bleeding, haemospermia and pain in some cases requiring hospitalization. Unfortunately, a negative biopsy does not exclude the possibility of prostate cancer.[47] In summary, currently there is no single diagnostic method that could be considered as 100% accurate, thus it is recommended to be evaluated with more than one diagnostic tool is in all cases.

1.1.5 Grading and Staging of PCa

1.1.5.a Gleason grade

According to the degree of histological differentiation, prostate adenocarcinomas are classified based on the patterns of gland formation. The most accepted grading system was developed in 1966 by Gleason.[53] This system is based on two levels of scoring due to heterogeneous differentiation patterns and determines the aggressiveness of the tumour.

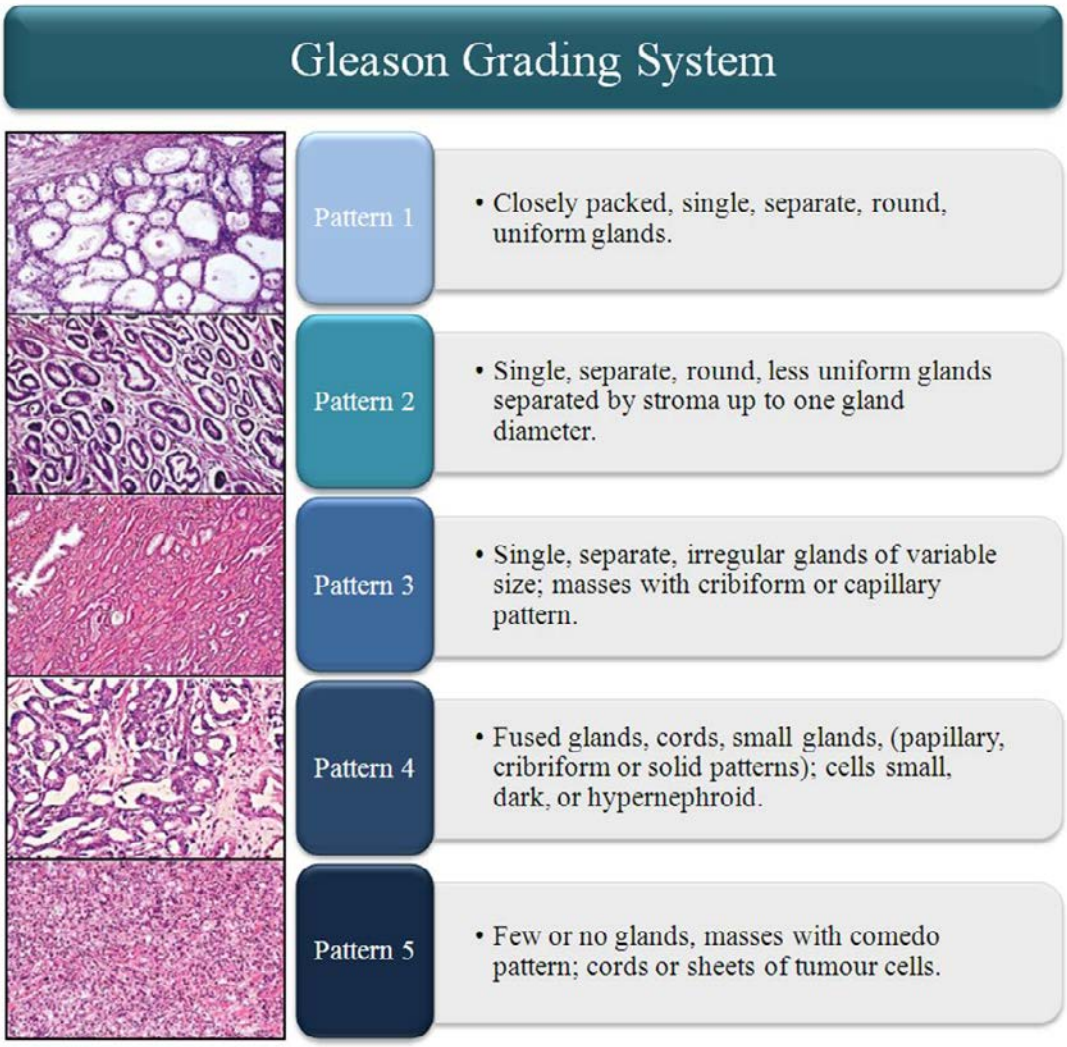

Figure 5. Gleason Grading System. Histological grading for adenocarcinomas of the prostate. The main pattern in the glands is graded on a score from 1 (least aggressive) to 5 (most aggressive) on the largest available histological specimen. The two most common Gleason patterns are added to give a total score ranging from 2 (1 + 1) to 10 (5 + 5). Where there is no secondary grade, the primary grade is designated as both the primary and the secondary grade (e.g., 3 + 3),[47] modified from .[16,54]

The primary pattern is assigned with a Gleason grade of 1 (less aggressive) to 5 (more aggressive) based on morphology and its differentiated progression from normal appearance (Fig. 5). The second pattern is also assigned with a score resulting in a two digit scores i.e. 3 + 4 = 7.[47] This scoring has been criticized for the complexity in determining the secondary pattern and an adequate distinction between good and poor prognosis in the majority of patients with scores from 5 to 7.[16] However, the Gleason grading is highly reliable and reproducible, and it has been demonstrated that a higher Gleason score is a marker for higher mortality.[16]

1.1.6.b Tumour, Nodes and Metastases Staging System (TNM)

The TNM system according to the Classification for Adenocarcinoma of the Prostate is the predominant method for staging PCa.[47] According to the TNM categories, the T category refers to the primary tumour and is based on clinical examination, imaging, endoscopy, biopsy and biochemical tests (Fig. 6).

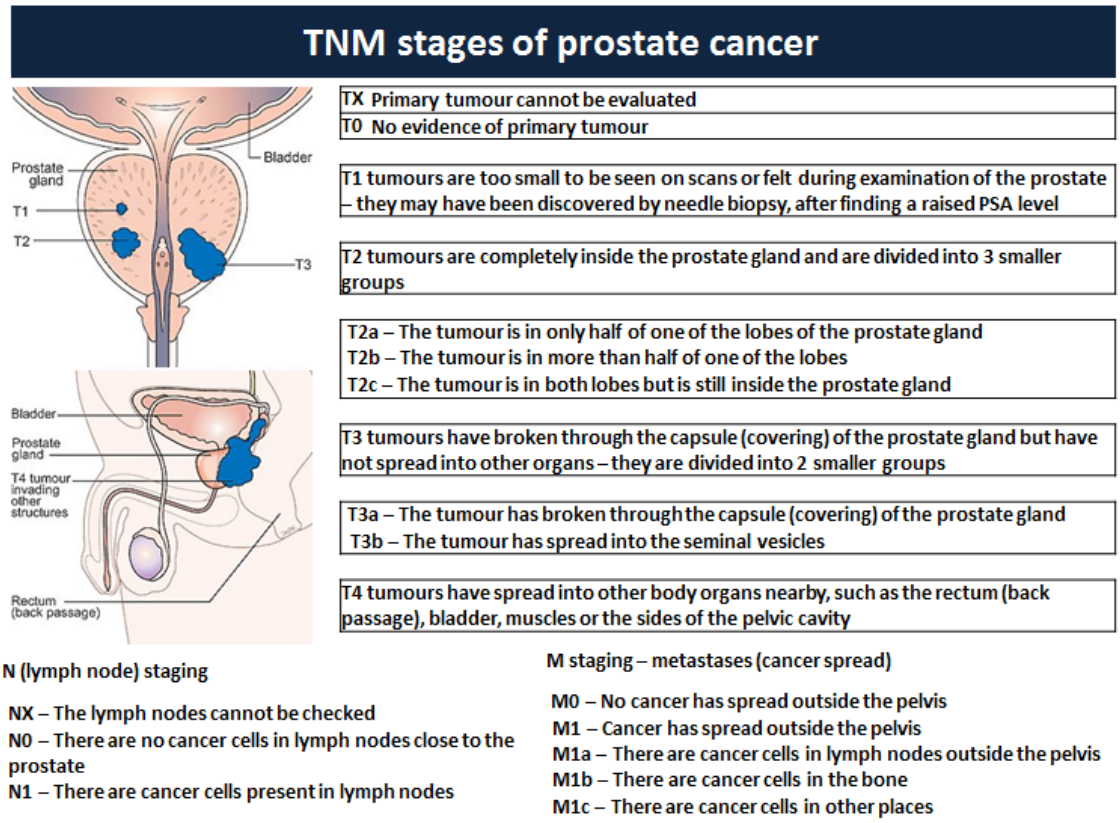

Figure 6. Staging of prostate cancer according to the TNM system. The TNM system evaluates the location and size of a tumour in the prostate. T= local tumour growth, N= the lymph nodes, M= distant metastases,[55] adapted from.[15]

The grading and staging of PCa are important in determining which treatment is the most adequate for the patient. Therefore the combination of Gleason score, the TNM system and the PSA levels (Table 2) are determinants for the prognosis and treatment procedure. PCa can be divided in four stages where stage 1 is considered as low risk prognosis and stage 4 high risk with poor prognosis (Table 3).[15]

Table 3. Prostate cancer staging for prognosis.

Stage	T	N	M	PSA (ng/ml)	Gleason score
I	T1a–c	N0	M0	<10	≤ 6
	T2a	N0	M0	<10	≤ 7
	T1–2a	N0	M0	X	X
IIA	T1a–c	N0	M0	<20	7
	T1a–c	N0	M0	≥10 and <20	≤ 6
	T2a	N0	M0	<20	7
	T2b	N0	M0	<20	≤ 7
	T2b	N0	M0	X	X
IIB	T2c	N0	M0	Any PSA	Any Gleason
	T1–2	N0	M0	≥20	Any Gleason
	T1–2	N0	M0	Any PSA	≥8
III	T3a–b	N0	M0	Any PSA	Any Gleason
IV	T4	N0	M0	Any PSA	Any Gleason
	Any T	N1	M0	Any PSA	Any Gleason
	Any T	Any N	M1	Any PSA	Any Gleason

M, Metastasis; N, node; PSA, prostate-specific antigen; T, tumour; X, unknown, modified from [56].

1.1.6 Treatment

1.1.6.a Surgery and radiation therapy

Radical prostatectomy (RP) is surgical removal of the prostate for patients with localized PCa, however it is not the preferred option for most patients.[57] This procedure removes the prostate gland and some surrounding tissue.[27] The survival rate for patients with favourable preoperative characteristics treated by RP is 5 to 9 years without biochemical relapse.[27] Recent studies have shown that RP is associated with a reduction in the rate of death from PCa.[58] Radiation therapy by external beam radiation or brachytherapy (internal radiation) is used to treat localized PCa at early stages, low grade and low volume or with localized metastasis (when metastasis are close to normal tissues).[27]

Radiation doses for cancer treatment are measured in Gray units (Gy), which measures the amount of radiation energy absorbed by 1kg of human tissue, thus different doses of radiation are needed to kill different types of cancer cells.[59] The standard of care for patients in most countries is of 1.8-2.2Gy administered in 16-20

fractions.[60] Studies have shown that biochemical progression-free survival and local control can be significantly improved with post-operative radiation therapy using 60Gy.[61] However, there is no clinical evidence that doses above 70Gy are beneficial for patients with previous long-term hormonal therapy.[60] Radiotherapy, on average, results in 12 years of survival before recurrence.[27]

1.1.6.b Hormonal therapy

Androgen deprivation therapy is accepted as a standard treatment for advanced PCa.[57] The most used current treatment comprises luteinizing hormone-releasing hormone (LHRH) agonist drugs (e.g. buserelin, goserelin, histrelin, leuprorelin and triptorelin) where testosterone production is ultimately inhibited by suppression of luteinizing hormone (LH) secretion. Alternatively LHRH antagonists drugs including abarelix, cetrorelix and degarelix directly inhibit LHRH with no agonist properties.[62] Other current treatments include steroidal antiandrogen monotherapy (e.g. megesterol acetate, medroxyprogesterone and cyproterone acetate) where the pituitary and hypothalamus are inhibited, supressing testosterone production.[62] In addition, non-steroidal anti-androgens such as bicatulamide, flutamide and nilutamide where androgen binding to the AR is inhibited in target tissues.[62] The aim of anti-androgen therapy is to block androgen effects within or beyond the prostate tissue; it is often used in combination with surgery. After a few years of successful treatment, patients develop resistance to the treatment and acquire an androgen independent state with poor prognosis.[27] Other androgen antagonists (e.g. ketoconazole and dilutamideor) target the cytochrome P450 hydroxylase and an anti-androgen in combination with the 5-α-reductase inhibitor finasteride prevents synthesis of androgens.[62,63] Abiraterone acetate, a pro-drug of abiraterone, is a selective inhibitor of androgen biosynthesis that potently blocks cytochrome P450 c17 (CYP17), an enzyme in testosterone synthesis, thereby blocking androgen synthesis by the adrenal glands and testes and within the prostate tumour.[64] Recent studies have shown that the inhibition of androgen biosynthesis by abiraterone acetate prolonged overall survival among patients with metastatic castration-resistant PCa who previously received chemotherapy and was approved for

treatment by the FDA, in April 2011.[64,65] Currently, there are several new drugs in clinical trials and on the market with similar mechanism of action.[59]

1.1.6.c Chemotherapy

Chemotherapy is the preferred treatment for some patients that do not respond to androgen ablation and is also used as an alternative for patients with HRPC.[27] However, the overall survival benefits are low, while chemodrug combinations have shown a palliative response to improve the quality of life for patients with pain.[66] Clinical trials data suggest that for locally advanced PCa the administration of cytotoxic drugs before surgery or as an adjuvant therapy is helpful in combination with anti-androgen therapy after surgery.[27] Current chemotherapeutic regimes include the combination of agents such as mitoxantrone, taxols (docetaxel or paclitaxel), prednisone, estramustine, suramin, etoposide, vinblastine and platinum compounds (satraplatin, platinum IV, cisplatin or carboplatin).[27] The chemotherapeutic regimes are effective in early stages of PCa but ineffective in most advanced hormone refractory and metastatic PCas, due to dose-limiting toxicities and treatment resistance.[27] Therefore, it is essential to improve current treatment regimens and improve the development of alternative treatments that could be used in combination with conventional chemotherapeutic drugs.

1.1.6.c.I Mitoxantrone

Mitoxantrone is the most active compound in the anthracenedione series, and is an amino anthracenedione (Fig. 7)[16] that induces inter- and intra-strand crosslinking and double-strand DNA breaks by inhibition of topoisomerase II ultimately resulting in apoptotic cell death.[67] Mitoxantrone in combination with prednisone was considered as the gold standard for HRPC treatment before the introduction of docetaxel.[16] Mitoxantrone is administered intravenously at a dose of 12 - 14 mg/m^2 once every 3 weeks in patients with solid tumours, and is rapidly cleared from plasma.[16] The drug binds tightly to DNA and resistance develops through alterations in topoisomerase II. Mitoxantrone is not specific for any phase of the cell cycle.[67] The limiting factors for

mitoxantrone treatment are neutropenia, nausea, vomiting, alopecia and cardiac toxicity, at cumulative doses above 160 mg/m^2.[16]

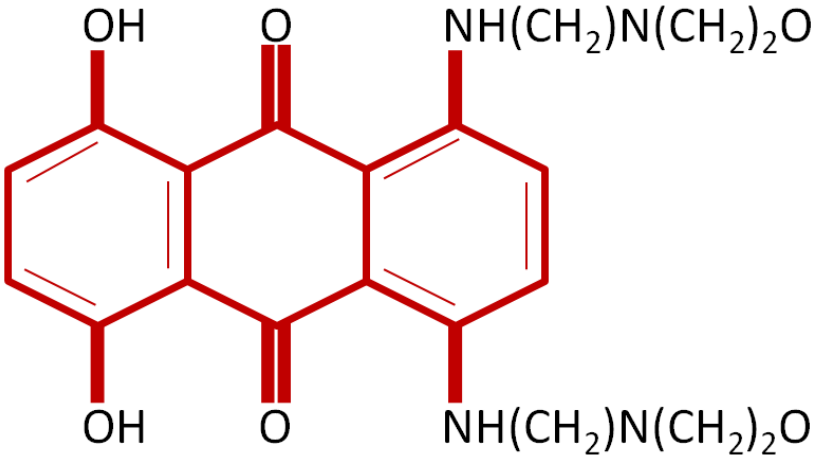

Figure 7. Structure of mitoxantrone, adapted from.[16]

1.1.6.c.II Docetaxel

The taxane docetaxel is the current therapy of choice for HRPC in the UK. It is a semisynthetic analogue of paclitaxel with antimitotic activities and inhibits microtubule depolymerisation resulting in cell cycle arrest (Fig. 8).[66] In phase III clinical trials docetaxel was shown to significantly decrease disease progression, decrease/stabilize PSA, prolong survival and to have palliative effects in patients with HRCP.[66] Docetaxel is administered every 21 days at a dose of 75mg/m^2 intravenously.[68] Prolonged treatment with taxanes such as docetaxel can result in resistance and induce neutropenia as the main toxic side effect. Docetaxel is a wide spectrum drug that binds to the N-terminal 31 amino acids of the β-tubulin subunit of tubulin polymers and has a 1.9-fold higher affinity than paclitaxel.[16]

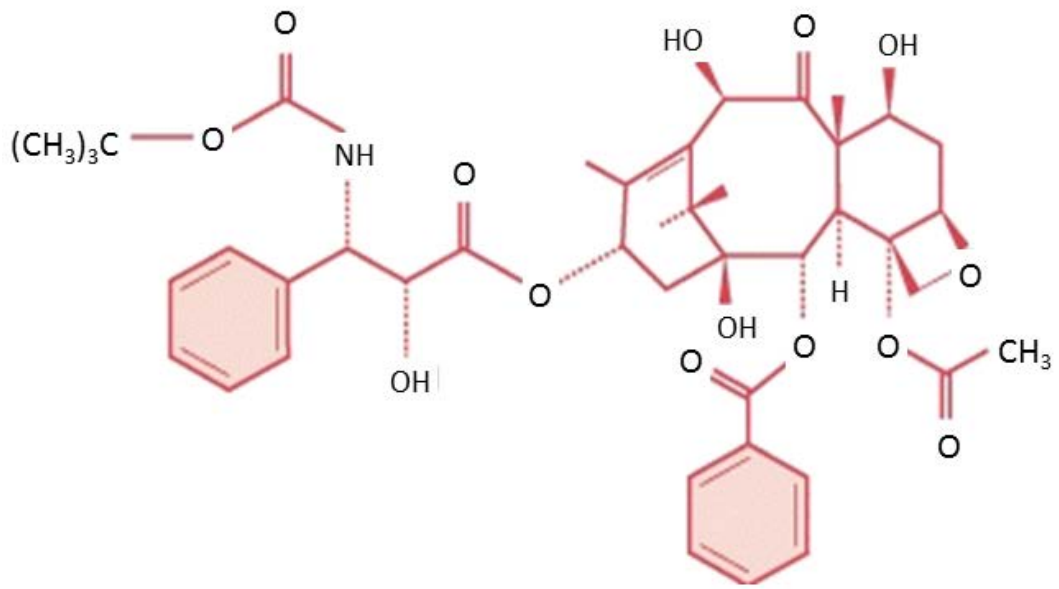

Figure 8. Structure of docetaxel, adapted from [16].

Docetaxel, like other taxanes alters the tubulin dissociation rate at both ends of the microtubules by reducing the tubulin concentration required for microtubule assembly, promoting nucleation and elongation phases of the polymerization reaction.[16] Thus, stabilizing the microtubules against depolymerisation and enhancing polymerization thereby increasing the levels of microtubules and their stability in turn preventing cell cycle progression and inhibiting cell proliferation by sustained mitotic block at the metaphase/anaphase boundary. Moreover, it is known that disruption of microtubule reorganization induces the tumour suppressor gene *p53* and inhibits the cyclin dependant kinase inhibitor 1a Cdkn1a (p21/Waf-1) and several protein kinases inducing G2/M-phase arrest and apoptosis. However, the exact taxane-dependent cell killing mechanisms are still not completely understood.[16]

1.2 Adenovirus

1.2.1 Types of human Adenoviruses

Adenoviruses were first identified during the 1950's in tonsils and adenoid tissue, and were named according to the original tissue in which they were discovered (Adenoid) and are classified under *Adenoviridae* family.[69] The strains infecting humans belong to the Mastadenovirus genera. Human adenoviruses are grouped in 56 serotypes and seven species (A-G) (Table 4).[70,71] The classification is based on their ability to agglutinate red blood cells, the genome sequences and phylogenomics, protein characteristics and biological properties (Table 4).[69,71,72] Adenoviruses can cause genitourinary infections, epidemic conjunctivitis and acute respiratory tract infections, being responsible for up to 5 to 10% of respiratory illness in children. In addition, adenoviruses are associated with a wide variety of clinical syndromes, with infantile gastroenteritis as the most common disease. [69,70]

Table. 4. Human Adenoviruses.

Had Subgroups	Types	Predominant natural tropism	Known receptors
A	12, 18, 31.	Gastrointestinal	CAR
B1	3, 7, 16, 21, 50.	Respiratory	CD46, CD80/86. Receptor X, HSPG
B2	11, 14, 34, 35, 55.	Renal	CD46, CD80/86. Receptor X, HSPG
C	1, 2, 5, 6.	Respiratory	CAR, HSPG, MHC-I, VCAM-I, Integrins
D	8, 9, 10, 13, 15, 17, 19, 20, 22-30, 32, 33, 36-39, 42-49, 51, 53, 54, 55, 56.	Ocular	CAR, Sialic acid, CD46
E	4	Respiratory, Ocular	CAR
F	40, 41.	Gastrointestinal	CAR
G	52	Gastrointestinal	Not described

CAR; Coxsackie virus and adenovirus receptor, HSPG; Cell surface heparan sulfates proteoglycans, VCAM-I; vascular cell adhesion molecule 1, MHC-I; major histocompatibility complex 1. Table generated from published information in [70-72].

1.2.2 Adenovirus Structure

Adenoviruses are non-enveloped viruses and have a linear double-stranded DNA genome encapsulated in an icosahedral protein shell of about 70 to 100nm in diameter called the capsid.[69] Structurally the capsid consists of seven polypeptides; hexon (protein II), penton base (protein III), fibre (protein IV), proteins IIIa, VI, VIII, and IX.[73] The main components of the capsid are 252 subunits called capsomeres, of which 240 are homotrimeric hexons of 105 kDa localized on each face of the capsid and 12 pentones of 63 kDa (Fig.9).[73,74] Each pentameric pentone is associated with a trimeric fibre of 62 kDa forming a complex of 12 vertices extending from the icosahedrons.[73,74] Minor components of the capsid comprise protein IIIa (63 kDa) that is associated with the hexons and protein VI that is localized below the penton base (Fig. 9).[74] The polypeptide VI (23 kDa) is also associated with the hexons and is thought to be involved in the early stages of infection as a lytic factor.[73] Protein VIII (15 kDa) binds hexons and the rest of the capsid.[73,74]

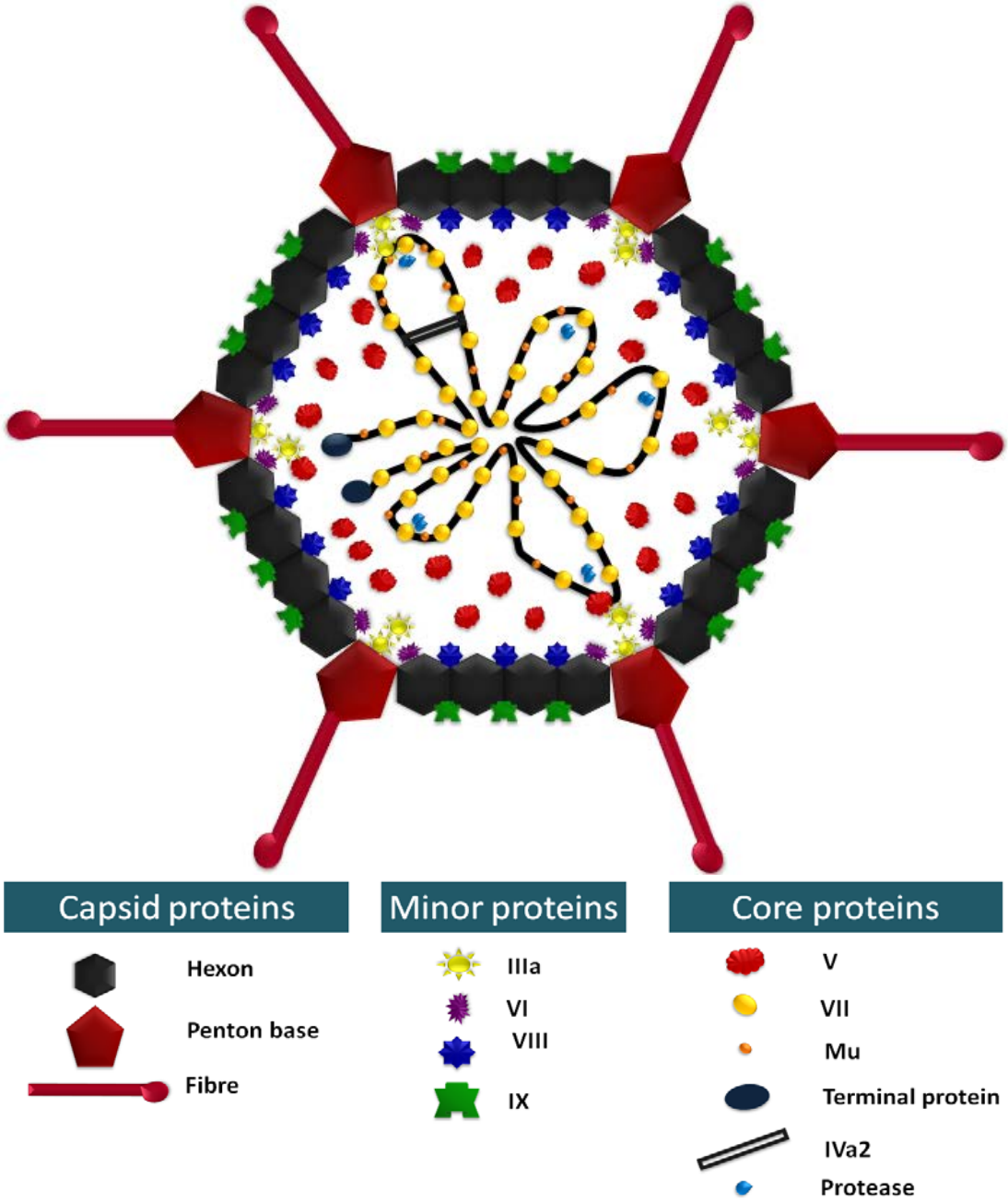

Figure 9. Adenoviral structure. Representation of the proteins involved in the adenoviral structure and function.[74]

Protein IX (14 kDa) is a structural protein that stabilises the capsid by interacting with hexon.[73] Other structural proteins of adenovirus are localized in the virus core and are associated with the viral genome. These proteins named V, VII, X (Mu), terminal protein (TP), form nucleosome-like structures protecting the genome. Other proteins that are also located in the core are IVa2 and the viral protease (Fig. 9).[73,74]

1.2.3 Genome Organization

The linear genome of 34-36 kb for human adenoviruses contains two origins for DNA replication.[75] The genome also includes a cis-acting packaging sequence that drives the interaction between the viral DNA and the proteins of the capsid.[69] The viral genome has five early transcription units (E1A, E1B, E2, E3 and E4) (Fig.10), involved in the regulation of viral gene expression and DNA replication; two delayed early units (IX and IVa2), and one late unit (major late) that is processed to generate five families of late mRNAs (L1-L5) (Fig.10), all viral genes are transcribed by the host cell RNA polymerase II.[69] The viral genome also carries two virus associated (VA) RNAs transcribed by RNA polymerase III.[69] The adenoviral genome has two reading strands, the transcription of the rightward strand codes for E1B, IX, major late, VA, E3 and E1A that is drawn by convention at the left end; the leftward codes for the E4 gene localised at the right extreme, before E2, and IVa2 genes.[69,75] The E1A gene encodes proteins that activate transcription and induce the host cell to enter the S-phase of the cell cycle (described in section 1.2.4).[69]

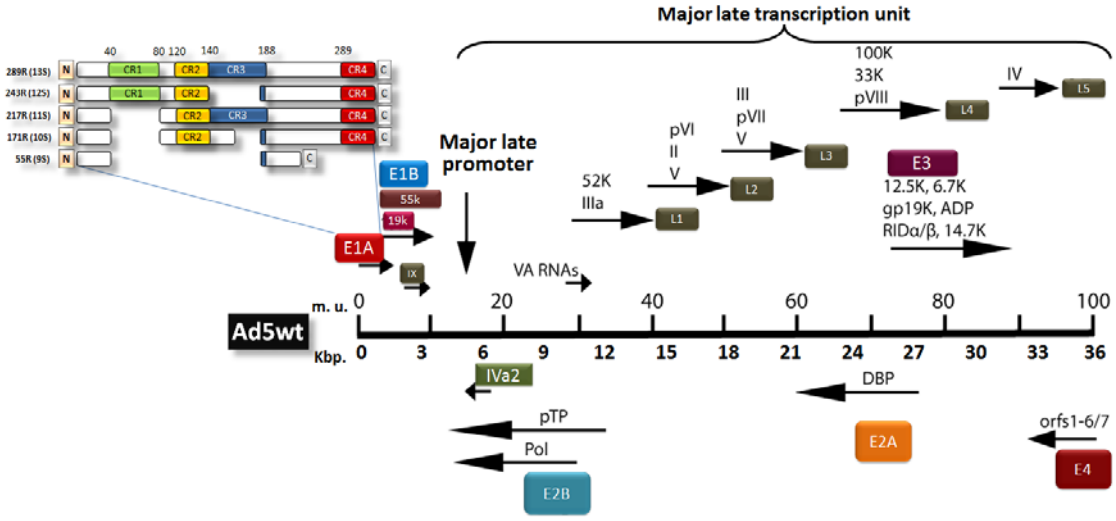

Figure 10. Genomic organization and protein products of the serotype 5 adenoviral genome (Ad5). Ad5 genome structure indicating location of viral genes and the respective proteins expressed that are involved in the viral replication machinery. Splice variants are also indicated. The central genome is presented in both map units and kilobase pairs (Kbp) bottom. Coding regions are shown as shaded boxes and RNAs are represented by single lines with small arrowheads and base pairs indicated. The direction of the transcription is shown by arrows.[75]

1.2.3.a Early region genes

The early region 1B (E1B) is located on the right of E1A within the viral genome. The E1B gene encodes 5 mRNAs that are processed by alternative splicing (Fig. 10).[75] The most abundantly expressed are E1B19kD and E1B55kD which both block apoptosis.[69] E1B19kD is a member of the Bcl-2 anti-apoptotic family of proteins and is a functional Bcl-2 homologue.[75] The E1B19kD protein inhibits apoptosis by sequestering the Bcl-2 homologous antagonist killer (BAK) and Bcl-2 associated X protein (Bax).[76] The E1B55kD protein forms a complex with the E4ORF6 product and inhibits p53 activity by direct binding and facilitates the transport of late viral RNAs for translation from the nucleus to the ribosomes.[75,76] The E2 gene encodes three proteins that function directly in viral DNA replication.[69] The gene is divided in two regions; E2A that transcribes a 59 kDa DNA-binding protein, E2B expressing a 135.6 kDa DNA polymerase and a 74.5 kDa terminal protein precursor.[77] The E3 genes encode nine proteins with nine open reading frames (ORFs), 12.5, 14.7, the heterodimer 10.4/14.5, 3.6, 7.1, 11.6, 7.5kDa and the glycosylated gp19kDa proteins (Fig. 10) that modulate the immune response of the host to the viral infection.[75] The E314.7 kDa can also inhibit apoptosis induced by TNF-α. The three E3-proteins 14.7, 10.4 and 14.5kDa forms the E3B region that is essential to avoid rapid immune system-mediated clearance of the virus during infection, two of the genes 10.4kDa and 14.5kDa form the receptor internalization and degradation (RID) complex.[78,79] The E4 region has seven open reading frames (ORFs) that are transcribed leftward with five of the ORFs having their own start codons (Fig. 10).[75] Each reading frame gives specific products due to alternative splicing of mRNA; these products are involved in mRNA transport, in the modulation of viral DNA synthesis, in inhibiting cellular protein synthesis, cell death and inhibition of cellular DNA-damage repair.[69,75] E4ORF4 regulates protein phosphorylation in infected cells, down-regulates genes activated by E1A and cyclic adenosine monophosphate (cAMP) and regulates alternative splicing of adenoviral mRNAs.[75,77] In addition, E4ORF4 can cause cell death mediated through binding to protein phosphatase 2A (PP2A).[75] E4ORF6 regulates late viral gene expression, viral DNA replication and transformation (Fig. 11), can form a complex with E1B55kD to target p53 for degradation by

ubiquitination thereby inhibiting p53-dependent cell death.[75] The E4orf6 protein can also bind to p53 in the carboxy-terminal region and block its transcriptional activation function, inhibiting its interaction with a subunit of TFIID called TAF31.[69] E4orf6 also inhibits the translocation of cytochrome c from the mitochondria to the cytoplasm.[69] E4ORF6/7 enhances E2 transcription thus inducing cell growth arrest and cell death (Fig. 11).[75]

The proteins IX and IVa2 are transcribed by gene products expressed from the delayed early region or intermediate region. Protein IX is a structural protein involved in DNA packaging and a transcriptional activator for the major late promoter (MLP). The IVa2 protein is also a transcription factor for the major late genes.[77]

A)

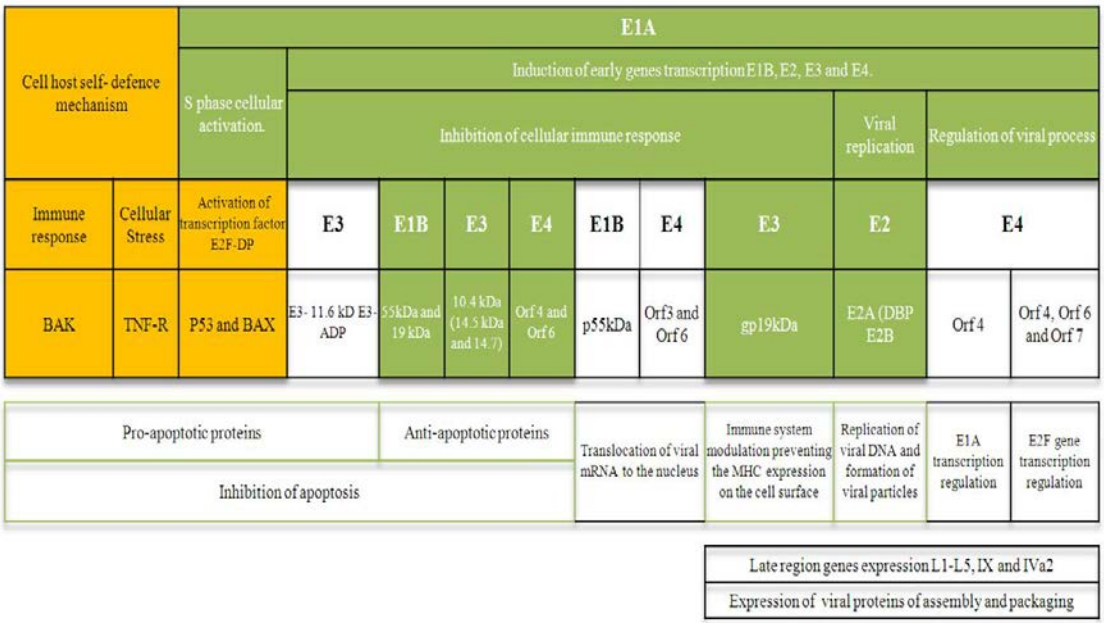

B)

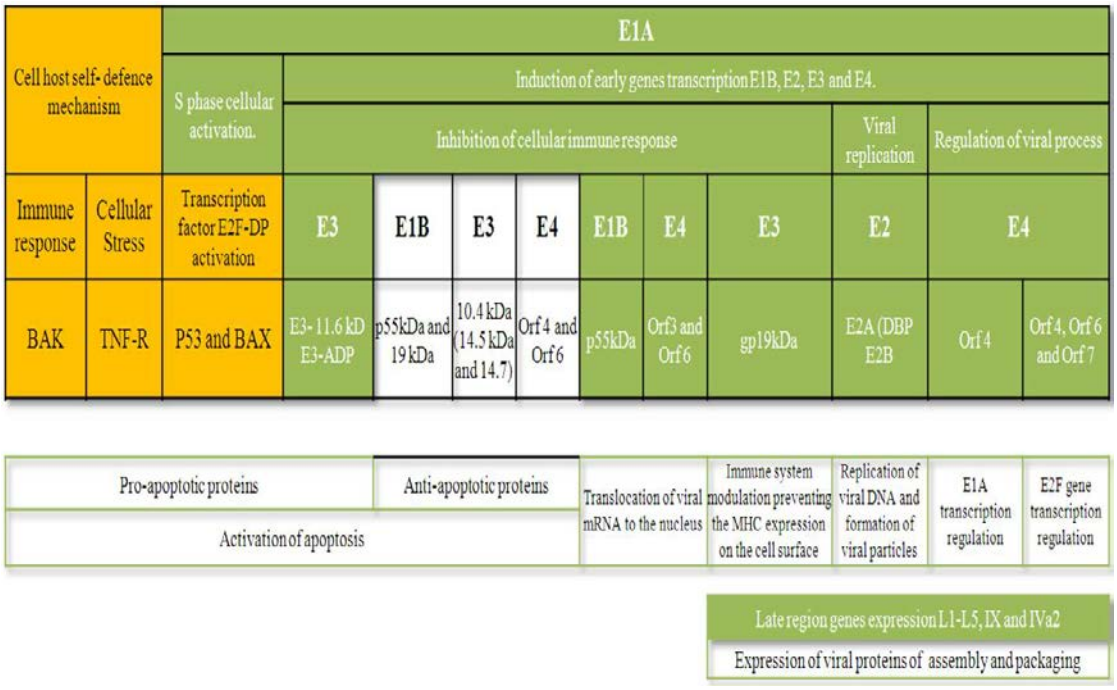

C)

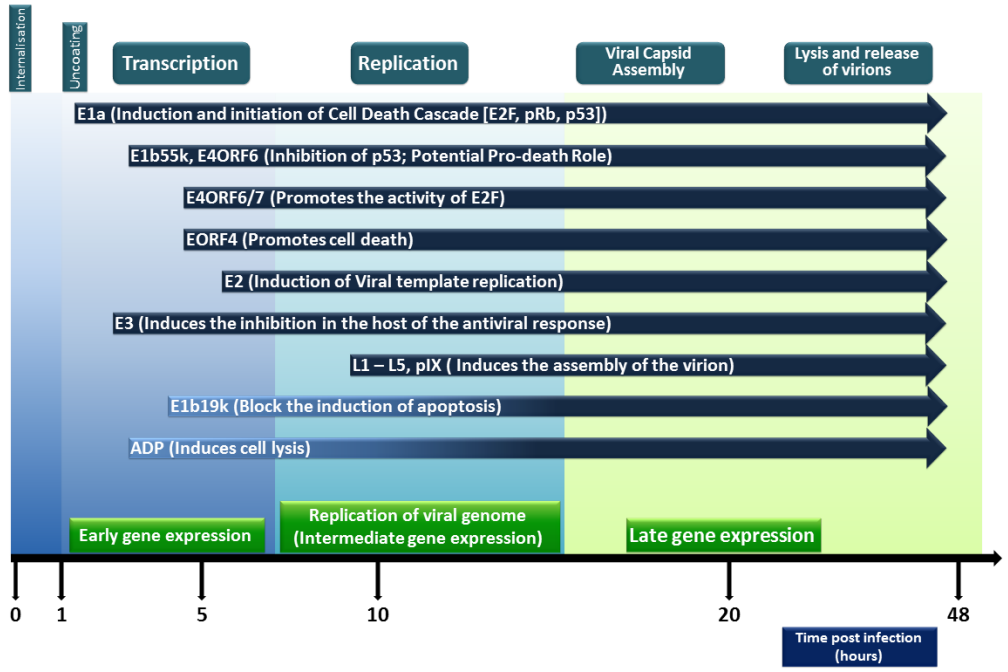

Figure 11. Sequential expression of genes during infection with Ad5. A) Early gene expression. **B)** Late gene expression. **C)** Sequential events during viral infection and the time lapse of the process. (A and B) Green Boxes represent genes expressed by the virus, yellow boxes represent cellular genes, and white boxes indicate genes that are not active at that moment. Modified from [75] and IMGT® The International imMunoGeneTics information system; http://www.imgt.org, Gamrot, E, 2009.[80]

1.2.3.b Late region genes

The late family genes are involved in the production and assembly of components of the capsid and are named in sequence from II to IX (Fig. 9).[69] They are transcribed from the major late promoter (MLP) as a single primary transcript (Fig. 10). The late genes are grouped in five families (L1-L5), each one with a distinct polyA signal.[77] The L1 gene codes for two proteins, the 52 kDa protein that acts as a scaffold for capsid assembly and protein IIIa located in the outer surface of the capsid for structural support.[77] The L2 sequence codes for four polypeptides, including the penton base protein that is part of the 12 pentagonal vertices protruding from the capsid. These vertices facilitate the viral internalization via integrins, in particular $\alpha_v\beta5$ and $\alpha_v\beta3$ mediated by the amino acid sequence arg-gly-asp (RGD) in the penton (Fig.12).[69,77]

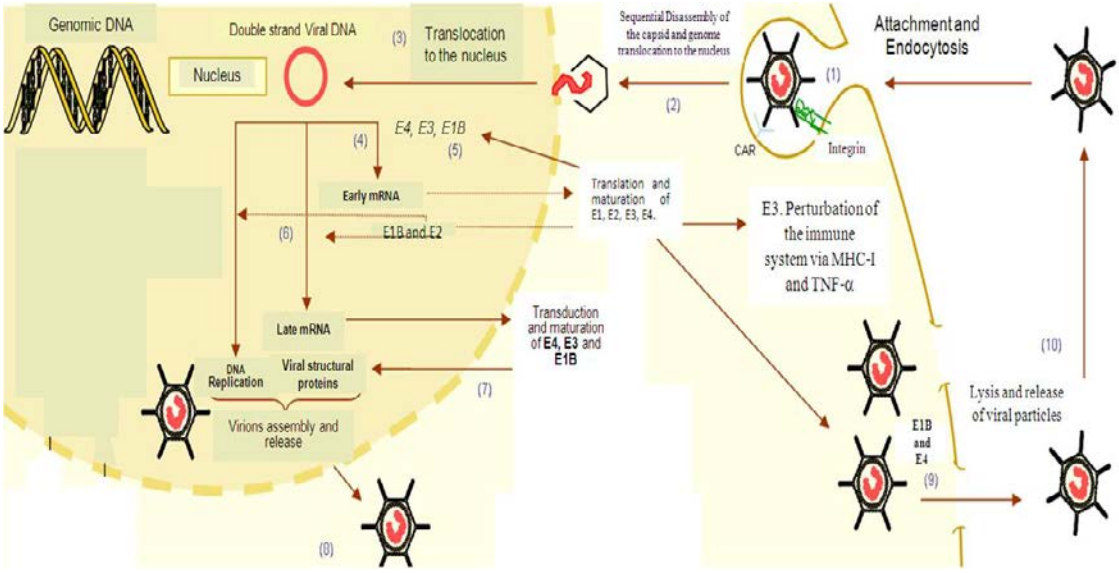

Figure 12. The Adenoviral infectious cycle. **1)** There are two steps for viral entry into the cells, mainly triggered by fiber knob attachment to CAR and endocytosis through clathrin and caveolae/lipid raft-mediated internalization.[73] The clathrin-mediated classical model of virus uptake is induced by interactions between arginine-glycin-aspartic acid (RGD) motifs present within the surface loops of penton base and cell surface $\alpha_v\beta_1$, $\alpha_v\beta_3$, $\alpha_v\beta_5$, or $\alpha_3\beta_1$ integrins.[73] In addition to endocytosis another mechanism utilised by the virus might be micropinocytosis.[73] **2)** The internalization triggers the activation of dynamin and phosphatidylinositide-3 OH kinase (PI3K),[73,81] which can then activate downstream targets like protein kinase C (PKC) and the Rab5 GTPase. PKC activation induces the reorganization of actin filaments and Rab5, a marker and determinant of the endosomal vesicular trafficking and maturation.[73,81] Disassembly begins with the release of fibres during the early stages of entry. Endosomal acidification triggers a conformational change in the viral capsid resulting

in endosomolysis and release of the virion into the cytoplasm.[73] Protein VI contains a N-terminal amphipathic α-helical lytic domain that is responsible for the disruption of the endosomal membrane and escape.[73] Free in the cytoplasm the partially dismantled capsid interacts with dynein, in a process facilitated by the hexons and the virions translocate along microtubules towards the microtubule organizing centre (MTOC) near the nucleus.[73,81] The cellular nuclear export factor CRM1 has recently been implicated in the release of virions from the MTOC to the host cell nucleus.[73] **3)** The virus binds to the CAN/Nup214 protein of the nuclear pore complex (NPC), this association and interactions between virions and the histone H1, leads to further disassembly and eventual import of adenoviral genome in the nucleus.[73] **4-5)** The replication cycle can be divided into two phases, an early phase that starts as soon as the viral genome is transported to the nucleus, followed by the transcription and translation of early viral genes. **6-7)** These events modulate the functions of the host cell to facilitate the replication of the late genes. **8-10)** The second phase starts with expression of the late genes, leading to the assembly in the nucleus of the structural proteins and the maturation of infectious viruses.[82] Modified from IMGT® The International imMunoGeneTics information system; http://www.imgt.org, Gamrot, E, 2009.[80]

Protein X (mu) and the viral core proteins VII and V are also located within the L2 gene.[77] L3 transcribes the capsid proteins VI, the major structural component of the capsid hexon, and a viral protease.[77] L4 codes for protein VIII and L5 the fibre protein that binds via the knob domain to the coxsackievirus and adenovirus receptor (CAR), a member of the immunoglobulin superfamily (Fig. 12).[77,81] CAR is a high affinity receptor for human adenoviruses from subgroups A, C, D, E and F, but not for subgroup B.[81] The class I major histocompatibility complex (MHC) α2 domain has also been reported to serve as a receptor for Ad5.[81] Additional receptors that have been suggested to bind adenoviruses are listed in Table 4.

1.2.4. E1A

1.2.4.a Structure and functions

The first viral transcription unit to be expressed in the nucleus after viral infection is the early region 1A (E1A) gene.[81] E1A has a high amount of proline residues within its sequence and is phosphorylated at serine residues 89, 96, 132 and 219.[83] E1A expression is under control of a constitutively active promoter[81] and is required for expression of other viral genes to promote virus replication and regulate cellular

gene expression.[77] E1A can bind to transcription factors such as TATA-binding protein (TBP), TBP-associated factors (TAF), ATF-2, c-Jun, CBP/p300, YY1 and CDK8 and the nuclear receptors for thyroid hormone and retinoic acid (Fig. 13).[83,84] In the cytoplasm E1A targets Sug1 and S4 components of the proteasome, and RACK1.[83] E1A also binds to P300/CBP-associated factor (PCAF) that can acetylate p53 in response to DNA-damage inducing the transcription of p53 target genes including p21, however, E1A can also inhibit p53-dependent activation of p21 and G1 arrest independently of its interaction with pRb.[76]

The E1A gene encodes five proteins generated by alternative splicing; a protein of 243 amino acids termed 12S, a 289 amino acids protein termed 13S, 11S, 10S and the 9S proteins (Fig. 13B). During replication E1A13S is the first protein to be produced and is essential for viral replication due to its trans-activating activity; subsequently E1A12S is generated inducing cell to progress through s-phase.[85] Moreover, 9S is expressed late and is able to induce the expression of viral genes during infection in a process that requires the S8 component of the proteasome.[85] The 11S and 10S are similar to the 13S and 12S proteins respectively but lack the amino acid sequence 27-98 and are expressed late, there are no known specific functions identified for this proteins (Fig. 13B).[75,85] The E1A gene is located at the left end of the viral genome and has four highly conserved regions (CR1-CR4) (Fig. 13B).[84] CR1 and CR2 are essential for S-phase induction by E1A.[83] Either CR1 and CR2 can stimulate cell cycle progression from G_0 to S-phase, while both CR1 and 2 are essential for progression into mitosis.[76]

A)

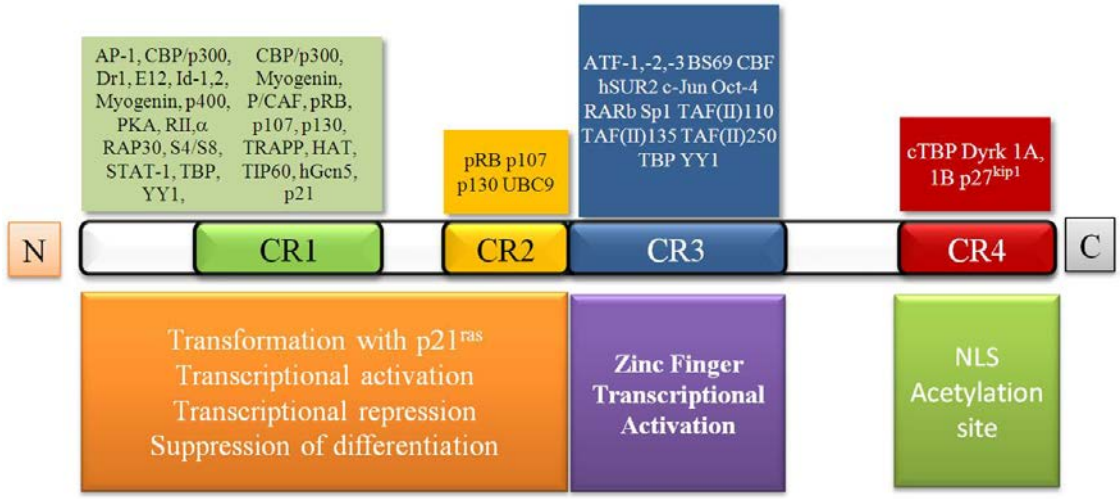

B)

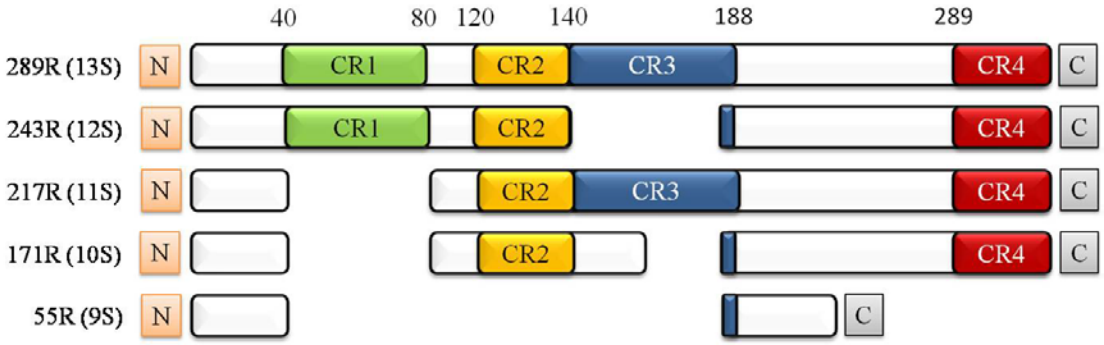

Figure 13. E1A gene structure with cellular proteins indicated at the specific E1A-binding regions. A) Cellular E1A-binding proteins and their binding region within the E1A gene. B) E1A proteins derived from alternative splicing of the E1A gene. The names are indicated at the left of each transcript. The numbers above refer to the respective amino acid at the beginning and end of each constant region (CR). The carboxy-terminal and amino-terminal are indicated with C and N respectively.[83,84]

The E1ACR1 region can bind and inhibit the transcriptional co-activator p300/CREB binding protein (CBP).[76] Previous work demonstrated that the deletion of the pRb or p300-binding domains within the E1A gene preferentially induced selective cytopathic effects in tumour cells *in vitro* and inhibited tumour growth *in vivo.*[86-88] Furthermore, p300 was originally identified using protein-interaction assays with the adenoviral E1A.[89] p300 has been implicated in a number of diverse biological functions including cell proliferation, cell cycle regulation, apoptosis, cell differentiation and DNA damage response.[89-91] p300 is highly homologous to the cyclic AMP response element-binding (CREB) protein (CBP), and transcriptional co-

activation is mediated by p300/CBP acting as a bridge linking DNA-binding transcription factors to the basal transcriptional machinery.[76]

The protein complex p300/CBP has acetyltransferase activity, that induces the acetylation of histone tails and lysines of transcription factors.[76] The binding of E1A with p300/CBP blocks its acetyltransferase activity inducing S-phase through Myc activation antagonizing the inhibitory activity of $p27^{kip1}$ preventing G1 arrest that can be induced by the transforming growth factor-β (TGF- β).[76,81,92] In PCa, p300 is essential for regulating androgen-induced genes required for PCa progression.[93] The binding of E1A to p300 promotes apoptosis induction, although the exact mechanism remains unknown, p53 can be stabilized and its degradation impaired through the binding of E1A and p300, therefore contributing to apoptosis induction.[76,94,95] E1ACR1 can interact with components of the proteasome to stabilize p53, unless it is blocked by E1B55K or E1B19K.[76] E1ACR1 also binds to proteins involved in chromatin structure control, and binds to p400, TRAPP, HAT PCAF, TIP60, hGcn5 and p21 also inducing cell cycle progression (Fig. 13A).[76] The 400kDa protein doublet p400 is part of the nucleosome acetyltransferase of H4 (NuA4) complex that is involved in transcriptional activation by acetylation of the nucleosomal histones H2A and H4.[76] E1A binds p400 in a region overlapping p300-binding-region inducing ATP-dependent chromatin remodelling and cell cycle regulation and promotes cell death in fibroblast cells, although requiring pRb simultaneous association.[92,96] The E1ACR2 region binds to retinoblastoma proteins (Rb) and p107 and p130 Rb-related proteins that regulate the E2F family of transcriptional factors.[76] The physical interaction of E1A with pRb displaces E2F from the pRb–E2F complex, through binding of its high affinity motif LxCxE to the Rb proteins, thus increasing the cellular concentration of free E2F.[76,97] Free E2F then activates both the Ad5 E2 gene (viral polymerase) promoter and cell cycle regulatory genes such as cyclin E, cyclin A, cdc2, cdk2, cdc6, orc1, Mcm 2-6, and DNA polymerase,[76,86,97,98] inducing cell cycle progression to S-phase and preventing senescence.[76] In a variety of human cancers, however, the *Rb* gene is inactivated or the pRb pathway is deregulated such that E1ACR2 deletion mutants can readily replicate and lyse cells as efficiently as wild-type Ad (Adwt). E1ACR3 is the most conserved region of the E1A gene and is a globular protein domain.[76,99] The E1ACR3 region is only present in the 13S protein.[76] E1ACR3 functions as an activation domain

that is essential for early viral promoters; this region can bind to MED23 that leads to the stimulation of viral transcription initiation and re-initiation.[76] E1ACR3 can induce transcriptional activation by binding p300 independently of the CR1 binding site.[100] E1ACR4 is a nuclear localization signal and a transcriptional regulatory region. E1ACR4 is the C-terminal region of E1A that binds to the cellular E1A C-terminal binding protein (CtBP), a transcriptional regulatory protein that inhibits transcription through histone deacetylases. In addition, the only known target genes of CtBP include CDH1 (E-Cadherin), CDKN2A (p16), Sirtuin 1 and BRCA1.[76,101] E1A inhibits CtBP and can sensitize tumour cells to anoikis by binding to the repressor-binding site of CtBP.[76]

1.2.5. Replication-selective adenoviral mutants

The development of replication-selective oncolytic adenoviruses represents a promising anticancer approach with proven efficacy in cancer cells and tumour xenografts *in vivo* without cross-resistance to conventional clinical therapies.[102,103] The characteristics that make adenoviruses attractive as vectors are their broad organ tropism, the relatively easy genetic engineering and production and the potential of inserting large genes and for generating selectively oncolytic mutants.[104] One of the earliest engineered oncolytic viruses used in clinical trials is *dl*1520 (ONYX-015).[105-107] ONYX-015 is a modified adenovirus lacking the E1B55K protein, which typically causes p53 repression and degradation.[105-107] ONYX-015 has been used in various clinical trials (phase I, II and III) for pancreatic, liver, and head and neck cancers and has been approved by the Chinese FDA for treatment of head and neck cancers. [102,108,109] p53, the so-called guardian of the genome, is responsible for several cellular functions, including apoptosis induction in DNA damaged cells, and cell cycle arrest, both of which need to be prevented for successful viral replication.[105-107] Wild-type adenoviruses suppress p53 activity by expressing E1B and E4 genes. Since many tumours have deletions or mutations in the p53 pathway, E1B is not necessary for the virus to replicate in these cells.[105-107] However, in normal, quiescent cells, viruses lacking E1B are unable to replicate because the cells have

wild-type p53 expression, which inhibits viral propagation and prevents cell cycle progression.[106] ONYX-015 has been used successfully to treat tumour cells *in vitro* and tumour xenografts in animals, but it has been less successful in treating human cancers as single agent.[102,108] Eventually, it was established that p53 status was not the critically restrictive factor, but rather complementation in tumour cells of the mRNA nuclear export functions of E1B55K and the lack of protection against the host immune response to viral infection because of the deletion in the E3B genes.[110,111] Both genes contributed to the attenuated efficacy of the virus. The *dl*1520 mutant, H101, was licensed for anticancer therapy in China in 2005 (Shanghai Sunway Biotech).[109] Whereas tumour selectivity was shown for both ONYX-015 and H101, efficacy was only reported in combination with cytotoxic drugs.[109,112,113] To date, safety has been demonstrated in clinical trials with these mutants in thousands of patients.

Recently, more potent oncolytic mutants than the *dl*1520 mutants have been developed that retain functions essential for the viral life cycle by deletion of smaller gene regions and by modifying tropism to target tumours specifically to enable viral gene expression and amplification at the tumour site with minimal toxicity to normal cells.[102,112] One example is the E1ACR2-deleted *dl*922-947 virus, that in combination with cytotoxic drugs such as 5-fluorouracil (5-FU) or gemcitabine enhanced cell killing in both *in vitro* and *in vivo* models of pancreatic cancer.[114] Another example is the Ad$\Delta\Delta$ mutant (E1ACR2- and E1B19K-deleted) virus, which was shown to be more potent and efficacious in enhancing cell killing, than both wild type (Ad5tg) and *dl*922-947 viruses in combination with the cytotoxic drugs gemcitabine, irinotecan and cisplatin in preclinical pancreatic cancer models.[115] Moreover, normal cells were not sensitized by the Ad$\Delta\Delta$ virus.[115] In an ovarian cancer study, enhanced cell killing was induced in response to treatment with a chimeric mutant, Ad5/3-Δ24 with the serotype-3 knob domain insertion in the fibre and the CR2-pRB binding region deleted, in combination with gemcitabine *in vivo* and *in vitro*.[116] A study in medulloblastoma cells, showed that the replication-selective Ad5-Δ-24-virus effectively reduced cell viability, although the virus was slightly less efficacious than wild type.[117] These and several other reports demonstrate the need of combining

even the most potent oncolytic adenoviral mutants with other cytotoxic drugs and factors to improve anti-cancer efficacy. The potent oncolytic adenoviral mutant AdΔΔ (AdΔE1ACR2 and AdΔE1B19K-deleted) was engineered to synergise with cytotoxic drugs by deletion of the E1B19K, resulting in a virus that enhanced chemotherapeutic drug-induced apoptotic cell death.[118] AdΔΔ interacted synergistically with the chemotherapeutic drugs docetaxel and mitoxantrone in PCa models both *in vivo* and *in vitro* and with gemcitabine and irinotecan in pancreatic cancer models,[115] whereas cell killing and viral replication were attenuated in normal cells.[118] Moreover, AdΔΔ also showed high specificity and potency in killing cancer cells in culture when administered alone. Other approaches to improve on viral specificity and potentially efficacy are the incorporation of selective promoters to drive viral replication and/or cytotoxic transgene expression targeting prostate[119-121] and other solid tumours.[84,122-125]

There is substantial evidence of the successful application of oncolytic adenovirus in combination with chemotherapeutic drugs as shown in different clinical trials.[126] Clinical trials with encouraging results using oncolytic adenoviruses include a Phase-I study with the CG7060 virus, which was engineered to have the PSA promoter driving viral replication. CG7060 induced a decrease in circulating levels of PSA and showed anti-tumour activity in PCa.[120] A mutant expressing the prodrug-coverting chimeric CD-TK enzyme, Ad5-CD/TKrep (E1B-55K and E3-deleted), was combined with 5-fluorocytosine (5-FC), intensity-modulated radiotherapy (IMRT) and ganciclovir in clinical trials resulting in anti-cancer efficacy for up to 4 years in prostate cancer patients.[121] In addition, other Ad5-CD/TK-derived viral mutants and more recently the CG7870 virus (where E1A and E1B are under control of the rat probasin promoter and the PSA promoter-enhancer respectively), have been successfully evaluated in PCa clinical trials in combination with cytotoxic drugs and/or radiation-therapy.[126,127] Recently the first Phase I clinical trials with AdΔ24RGD (that includes AdΔ24 an 8-amino-acid deletion in the CR-2 region of E1A and the insertion of an RGD-4C motif in the HI loop of the fiber protein) viral mutants were completed for recurrent ovarian cancer and malignant gliomas (NCT00562003 and NCT01582516) with promising results; they showed tumour-selectivity and no

serious side-effects.[128] In summary, numerous oncolytic adenoviral mutants are being developed pre-clinically to improve efficacy in the treatment of late-stage PCa.

1.2.6 Sensitisation to chemotherapeutics by adenovirus E1A-gene expression

In cancer cells and tumour xenografts, and in particular in prostate cancer models it has been demonstrated that E1A enhances the sensitization of cells to chemotherapeutic drugs through synergistic interactions to induce apoptosis and cell death, which is independent of but further enhanced by viral replication.[95,118,129-131] The E1A gene is spliced generating five proteins, of which E1A13S and E1A12S have been implicated in the chemosensitization.[95,132-134] Although the E1ACR3-region does not seem to be essential to mediate the sensitization of cells.[95,135] In a mouse model of embryonic fibroblast E1A was observed to induce sensitization to ionizing radiation enhancing apoptosis in a p53-dependent fashion.[130]

In pancreatic cancer cells, gemcitabine-induced cell death was greatly enhanced when used in combination with the AdΔE1B19K virus *in vitro*, the virus showed more efficiency in inducing apoptotic cell death than with the wild type.[136] The combination of gemcitabine with AdΔE1B19K induced tumour suppression in a pancreatic tumour xenograft model but had no effect in normal cells.[136] Furthermore, infection with the oncolytic virus *dl*922–947 of mitoxantrone- and docetaxel-treated cells has been shown to synergistically enhance cell killing of PCa cells both xenograft *in vivo* studies and *in vitro*.[131] The AdΔΔ virus was also demonstrated to be highly potent in PCa cells lines in combination with mitoxantrone and docetaxel.[118] Moreover, the AdΔΔ virus in combination with gemcitabine showed enhanced apoptotic cell-death in models of pancreatic cancer, cell killing was induced by synergy between AdΔΔ and gemcitabine and not by viral replication.[115] Interestingly, both AdΔΔ and Ad5-wild type viruses enhanced cell killing through synergistic effects when combines with several dietary phytochemicals in PCa cell lines and in xenografts in vivo PCa.[137] The highest efficacy was demonstrated for the AdΔΔ mutant in combination with equol and resveratrol, inducing caspase-dependent cell-death in PCa cells but not in normal cells.[137]

Furthermore, gemcitabine, equol and resveratrol attenuated viral replication, while E1A remained strongly induced promoting cell death.[137] In another study, using glioma cells the Ad-Δ-24 virus was observed to induce topoisomerase-I and enhance the sensitization to irinotecan (a topoisomerase-I inhibitor) *in vitro* and prolonged animal survival *in vivo*.[138] However, the exact mechanism of E1A-dependent enhancement of sensitization to chemotherapeutic drugs remains elusive because of the great number of factors that may intervene by binding to E1A, the different genetic backgrounds of cells lines and the mechanism of action for specific chemotherapeutic drugs.[95]

1.2.7 Alternative oncolytic viruses

There are many oncolytic viruses that have been used in different clinical trials in combination with other therapies such as chemodrugs with promising results. Currently, viruses being used in clinical trials apart from adenovirus include reovirus, herpes simplex virus (HSV), measles virus (MV), vaccinia virus (VV), New castle disease virus (NDV), Coxsackie virus, Vesicular stomatitis virus (VSV), and Parvoviruses.[139,140] Reovirus, NDV and VSV are small viruses with fast replicative cycles. Larger viruses that have been genetically modified include vaccinia virus, the Edmonton strain of measles virus, HSV or poliovirus.[139] However, despite the promising results obtained with these viruses in reducing tumour growth and demonstrated safety, most of the clinical trials were not conclusive mainly because only small numbers of patients could be evaluated.

1.2.7.a Herpes Simplex Virus (HSV)

The HSV is a human pathogen that causes latent infections by hiding in neuronal tissue avoiding the host immune system. Although, HVS can be limited by pre-existing immunity and hepatic elimination, HSV has wide tropism and large regions of the genome can be replaced. HSV has a 152kbp double-stranded DNA that can be

engineered by removing genes that are not required for replication, such as the neurovirulence factor genes that are deleted in all therapeutic HSV vectors.[139] In a glioma phase I clinical trial a modified HSV virus, the G207 virus proved to be safe with positive responses to the treatment. The HSV G207 has the γ-34.5 and ICP6 genes deleted. The normal function of the γ-34.5 gene is to downregulate the cellular antiviral response by blocking the double stranded RNA-dependent protein kinase (PKR), while the ICP6 gene encodes a viral ribonucleotide reductase (RR).[141] The deletion of γ-34.5 inhibits the capacity of HSV to replicate in neural cells and the viral latency properties. Another study, in glioma cells, with a γ-34.5-deleted oncolytic HSV was shown to enhance efficacy both *in vitro* and *in vivo* in combination with temozolomide that induces a DNA damage repair response.[140] Furthermore, another HSV mutant used in clinical trials is the NV1020 virus that has the γ-34.5, ICP0, ICP4 genes and the latency-associated transcripts (LAT) deleted. Moreover, NV1020 has an insertion of an exogenous HSV thymidine kinase gene (TK) in the region where γ-34.5, ICP0 and ICP4 were deleted, called the $U_{L/S}$ junction.[142] The insertion of a TK gene was because of clinical safety reasons (the lack of TK expression makes the virus irresponsive to antiviral treatments).[139,142] The NV1020 has been used in phase I clinical trials in patients with colorectal cancer and liver metastasis, and proved to be safe with no major toxicity in combination with chemotherapy.[142-144] Additionally, the HSV oncolytic virus VEXGM-CSF (OncoVEX^{GM-CSF}) with deletions in the ICP6 and γ-34.5 genes and insertion of a CMV-promoter and a human granulocyte macrophage-colony stimulating factor (GMCSF) instead of the γ-34.5 gene sequence, has been evaluated in phase I/II clinical trials in patients with cutaneous melanoma, breast cancer, head and neck cancer, and gastrointestinal cancer. OncoVEX^{GM-CSF} proved to be safe and showed anti-tumour efficacy with the best results in melanoma patients.[139,145] However, the trials were carried out with small numbers of patients. Other strategies have also been tested using modified HSV mutants such as the HSV-G47Δ virus that has the antiangiogenic protein platelet factor-4 inserted instead of the ICP6 gene region or the βG47Δ-dnFGFR virus with the dominant-negative fibroblast growth factor receptor inserted also instead of the ICP6 gene.[146,147] These viruses significantly reduced tumour vasculature and enhanced therapeutic efficacy.

Also, simultaneous treatment of oncolytic HSV and metalloproteinases-1,8 (MMP-1,8), enhanced HSV spread.[140] Another study showed that a Us3-deleted HSV virus synergises with inhibitors of the PI3K/Akt pathway *in vitro* and showed high efficacy and low toxicity *in vivo*.[140] One group showed that the histone deacetylase inhibitor trichostatin-A in combination with HSV enhanced efficacy *in vivo* and synergistic cell killing *in vitro* in brain and colon cancer cells.[148] Moreover, cells overexpressing mitogen-activated protein (MAP) kinase or extracellular signal-regulated kinase (ERK) showed enhanced viral replication of γ-34.5-deleted HSV.[140] Furthermore, the G207, HSV-1 and NV1020 mutants have been reported to cause cytolytic effects in the prostate cancer cell lines PC-3, DU145, LNCaP, and C4-2 *in vitro*.[149] More recently, talimogene laherparepvec (T-VEC), previously known as OncoVEX^{GM-CSF}, was proven to have anti-tumour efficacy in melanoma patients in a worldwide phase III clinical trial (NCT00769704) being the first oncolytic virus with demonstrated efficacy.[150] In this trial T-VEC proved to be safe with only mild side effects and showed anti-tumour efficacy locally and systemically (distant metastases) by boosting a systemic immune response against tumour cells.[150]

1.2.7.b Vaccinia Virus (VV)

Vaccinia virus has been widely used as the vaccine for smallpox and has also become an attractive vector in oncolytic therapy. VV has a 190kbp double-stranded DNA encapsulated within a host cell-derived envelope and can harbour large transgenes.[139] Moreover, VV is easy to modify genetically, easy to produce and replicates and spreads rapidly due to its motile characteristics, without the risk of genomic integration into host DNA.[151] Modified VV has been shown, in several studies, to be highly efficient and safe even when administered systemically.[151,152] JX-594, is a Wyeth strain vaccinia virus that was evaluated in phase I clinical trials with a deleted TK gene, required for viral replication in normal but not tumour cells, and a GM-CSF insertion into the TK region, was shown to effectively spread intravenously to target tumours. JX-594 is currently being evaluated in trials targeting lung, renal and prostate cancers.[153-155] In another study, murine cytokine-induced killer cells (CIK) that naturally target tumour cells were infected with a Western Reserve strain

of oncolytic vaccinia virus and re-administered to mice. The mutant was deleted in the TK and viral growth factor (VGF) genes, enabling viral replication in cells with deregulated cell cycle and EGF-R/Ras signaling pathways.[156] Moreover, in a glioma study a double-deleted VV (TK and VGF deleted) in combination with rapamycin or cyclophosphamide was shown to enhance anti-tumour efficacy human glioma cell lines *in vitro* and administered systemically *in vivo* reducing tumour growth and prolonging survival in mice and rats.[151] Moreover, the double-deleted VV also have shown efficacy in reducing tumour growth and prolong cell survival in xenograft models of paediatric neuroblastoma and sarcoma.[157] Furthermore, this mutant Western Reserve VV expressed either GFP or firefly luciferase to monitor viral distribution. Vaccinia-infected CIK cells (CIK cells obtained from human peripheral blood) administered systemically in mice were shown to effectively deliver the virus to tumours and preventing an anti-viral immune response. This combination of vaccinia and CIK cells resulted in synergistic cell killing of colorectal tumour cells.[156] However, the potential application of this method in human patients has the limitation of harvesting patient cells *ex vivo* and to redeliver these cells to the patients which implies more expenses and extra-manipulation of samples. Additionally, the Western Reserve mutant JX-795 had increased efficacy and tissue selectivity in many cancer cells with deregulated IFN pathway. The JX-795 (WR-delB18R) has the TK and B18R genes deleted, the B18R gene was removed since neutralizes type I interferon. Moreover, the JX-795 virus has an IFN-β inserted in the TK region. The JX-795 was shown to have increased tumour selectivity for cells with deregulated IFN pathway both *in vitro* in human ovarian cell lines and intravenous efficacy in *in vivo* in tumour mouse models derived from murine JC and colorectal CMT93 cells.[140,158]

1.2.7.c Reovirus

The non-pathogenic double-stranded RNA virus, Reovirus (*r*espiratory *e*nteric *o*rphan virus) has a genome size that ranges from 16-27kbp with high potential when delivered systemically. The Dearing strain type 3 (RT3D) and other reoviral strains can only replicate in cells with overexpressed Ras (about 40% of all cancers), which

inhibits PKR-mediated antiviral mechanisms.[139] The RT3D virus has been used in phase I clinical trials and only mild toxicity was reported.[139] Currently, an oncolytic wild type reovirus (Reolysin) is under clinical development. Phase I/II clinical trials with Reolysin including patients with advanced prostate, ovarian, pancreatic, melanoma and lung cancers have shown that the virus had both antitumour activity and overall safety.[155,159,160] Furthermore, recently Reolysin in combination with paclitaxel and carboplatin were evaluated for efficacy and overall survival in a phase III clinical trial for squamous cell carcinoma of the head and neck (NCT01166542), however the results of the study are still not published.[161] In a phase II clinical trial for squamous cell lung cancer, Reolysin was combined with carboplatin and paclitaxel, and was proved to be safe. [161] Furthermore, promising results were reported demonstrating a reduction in tumour size in 92% of patients (NCT00998192).

1.2.7.d Measles Virus (MV)

Another viral vaccine strains that have been used for cancer therapy is the attenuated or modified MV; a 16kbp single-stranded RNA virus. The MV targets deregulated cell membrane receptors including CD46, folate receptor-α (FR-α) and signalling lymphocytic activation molecule (SLAM) family receptors in cancer cells.[139,162] Moreover, MV strains have been modified to target cells with upregulated CD46 (a complement regulator) in the cancer cell membranes to, facilitate selective infection and lysis.[139] A MV targeted receptor nectin-4 (active only during foetal development and not in fully developed tissue) that is abnormally expressed in tumour cells has been targeted in many types of cancers including breast, lung and ovarian tumour cells.[163-166] However, the main disadvantage of MV is the pre-existent neutralizing antibodies against measles virus in around 95% of the western population and the subsequently suboptimal replication in the host.[139] Although, in a phase I clinical trial treatment with a modified MV with a human carcinoembryonic antigen (CEA) inserted upstream of the nucleoprotein (N) gene, the median overall survival of 12 months was twice as high as the median survival for untreated (6 months) patients with refractory ovarian cancer.[167] Moreover, induction

of MV-induced oncolysis of mesothelioma cells co-cultured with dendritic cells (DC) caused *in vitro* maturation of specific $CD8^+$ T-cells, when mature DC where co-cultured with purified $CD8^+$ T cells.[168] In two phase I clinical trials with mesothelioma and myeloma patients treated with MV expressing the sodium iodide symporter (NIS) allowing for tracing of MV after systemic administration to monitored its viral replication. However, the virus had to be administered in combination with the immunosuppressant cyclophosphamide to avoid clearance by the immunesystem.[139] Additionally, murine T-cells infected with MV were shown to protect MV from low concentrations of anti-measles neutralizing antibodies. However, the efficiency of the infection was only 1-2% of cells.[169] Therefore, more studies are required to improve the efficacy, infectivity and delivery of MV.

1.2.7.e Vesicular Stomatitis Virus (VSV)

Another virus vector that has been used to target tumour cells is the vesicular stomatitis virus (VSV); a single-stranded RNA of 11kbp. The approach with this virus consists of carrying the vector to the target cells in pre-infected cells (carrier cells).[140] Carrier cells that have been efficiently used include leukaemia cell lines, mesenchymal stem cells, endothelial and T-cells to target tumour-derived cells.[170] Additionally, enhanced viral replication of VSV has been observed in cancer cells with defective Ras-ERK and IFN pathways.[171] However, the efficacy of VSV has been shown to be highly dependent on the type of cells. In PCa cell lines different sensitivity to VSV-infection was shown in LNCaP cells being more sensitive than PC-3 cells.[172]

1.2.7.f Myxoma Virus, Coxsackievirus and Newcastle Disease Virus (NDV)

Additional studies showed that treatment with myxoma virus (a rabbit poxvirus), a double-stranded DNA of 160kbp is dependent on the overexpression of Akt for efficient propagation.[140] Moreover, myxoma virus in combination with rapamycin enhanced viral replication in tumour cells but not in normal cells.[173] In PCa cells,

various modified coxsackievirus strains, a 7kbp single stranded RNA virus, have also been effectively used. The coxsackievirus viruses A21 (CV A21) and the A21-expressing the decay-accelerating factor (CV A21-DAFv) virus were used for systemic delivery *in vivo*, in PCa model with PC-3 and LNCaP xenograft tumour and were reported to cause tumour reduction, both viruses require the intercellular cell adhesion molecule 1 (ICAM-1) to infect cells.[174] The A21-DAFv strain was generated from serial passages of CV-A21 strain in negative rhabdomyosarcoma (RD) cells negative for ICAM-1 and expressing DAF.[174] The use of the non-pathogenic NDV as a therapeutic strategy was first reported in 1964 in patients with acute myelogenous leukaemia. NDV is an avian virus with a 16kbp single-stranded RNA genome that is highly limited systemically by immune-mediated clearance in humans.[175] The oncolytic activity of the virus is thought to arise from the NDV-induced enhancement of systemic TNF-α secretion and the induction of sensitivity to TNF-α in neoplastic cells but not in normal tissue.[155] The NDV tumour selectivity and viral replication derives from the interferon (IFN) defective pathway found in many tumours but not in normal cells.[176] A deficient IFN pathway impairs tumour cell mechanisms of defence against viral agents causing these cells to be targeted for viral infection.[176] A NDV virus with promising efficacy and proven safe is the 73-T virus, this virus was derived from a NDV strain that has been attenuated by 73 passages *in vitro* and 13 passages *in vivo* in murine Ehrlich ascites tumour cells.[177] The 73-T has shown efficacy inhibiting tumour growth in prostate (PC-3), epidermoid (KB8-5-11), colon (SW620, HT29 and MM17387), large cell lung (NCIH460) and breast (SKBR3) carcinoma xenografts.[178] Another NDV strain, the PV701 that derives from the attenuated NDV MK107 strain, has been used in phase I clinical trials for squamous cell carcinoma, peritoneal cancer, lung and liver solid tumours in which the virus showed only mild toxicity, where an antitumour response was observed only at high doses via intravenous.[155,176,179] However, there are no current prostate cancer clinical trials with these virus strains.

1.3 MicroRNAs (miRNAs)

1.3.1 Discovery of miRNAs

There are many types of small RNAs including endogenous small interfering RNAs (siRNAs, Piwi-interacting RNAs (piRNAs) and microRNAs (miRNAs), that have been identified in many organism including plants, fungi and animals, where the main function is gene regulation through silencing and post-transcriptional regulation.[180] The main difference between miRNAs and other small RNAs is that miRNAs are derived from a distinctive hairpin structure.[180] MicroRNAs are short non-protein-coding RNA molecules of approximately 19 to 22 nucleotides that regulate genes at the translational level and are highly evolutionary conserved molecules.[181] MicroRNAs modulate important processes such as cell cycle, apoptosis, autophagy, cancer, diseases, metabolism, differentiation and development, tissue patterning and aging.[182-184] MiRNAs were initially identified in *Caenorhabditis elegans*; the first ones discovered lin-4 (in 1993) and let-7 (in 2000).[185,186] miRNAs account for approximately 1% of the mammalian genome regulating 30% of mammalian genes, and half of the known mammalian miRNAs are localized to highly conserved regions within introns of host genes and are co-expressed with these genes.[187-190] Around 80% of conserved vertebrate miRNAs are tissue specific, therefore, different patterns of miRNA expression can allow the identification of tumours of different origins and also to differentiate between tumours and normal tissue.[191]

1.3.2 Biogenesis of miRNAs

The miRNAs can be processed from transcripts either from independent genes or from introns of protein-coding genes (Fig. 14).[192]

The miRNA biogenesis is a multi-step process where the miRNA genes are initially transcribed by the RNA polymerase II into a long transcript called primary miRNA or pri-miRNA (Fig.14).[193] Pri-miRNAs can consist of hundreds to thousands of bases and are usually capped at the 5'-end and polyadenylated at the 3' end. [194] Pri-miRNAs can have one or more secondary structures consisting of stem-loop structures, most

probably intermediates resulting from the process of maturation.[195] Some miRNAs are produced individually from separate transcription units (mono-cistronic) while most miRNAs are produced from transcription units that generate more than one product (poly-cistronic) by transcribing clusters of distinct miRNAs.[196]

Regardless of its mono- or poly-cistronic origin the transcription of pri-miRNAs is effectuated in the nucleus by the microprocessor complex (500-600 kDa) formed by Drosha (RNAase III endonuclease) and the cofactor DiGeorge syndrome critical region 8 (DGCR8 or Pasha in flies and nematodes) (Fig. 14).[197-200] The complex processes the pri-miRNAs into 70 to 80 nucleotide precursors miRNAs (pre-miRNAs) with a 5'-phosphate and a 3' two nucleotide overhang, which folds into a mini-helical structure recognized by Exportin 5 (Exp5, member of the Ran transport receptor family) that allows pre-miRNA trafficking from the nucleus to the cytoplasm (Fig.14).[201] In addition, pri-miRNAs can be processed independently of the microprocessor complex by the spliceosome from very short introns called Mirtrons and are originated from a single processed miRNA precursor although are not common (Fig.14).[202]

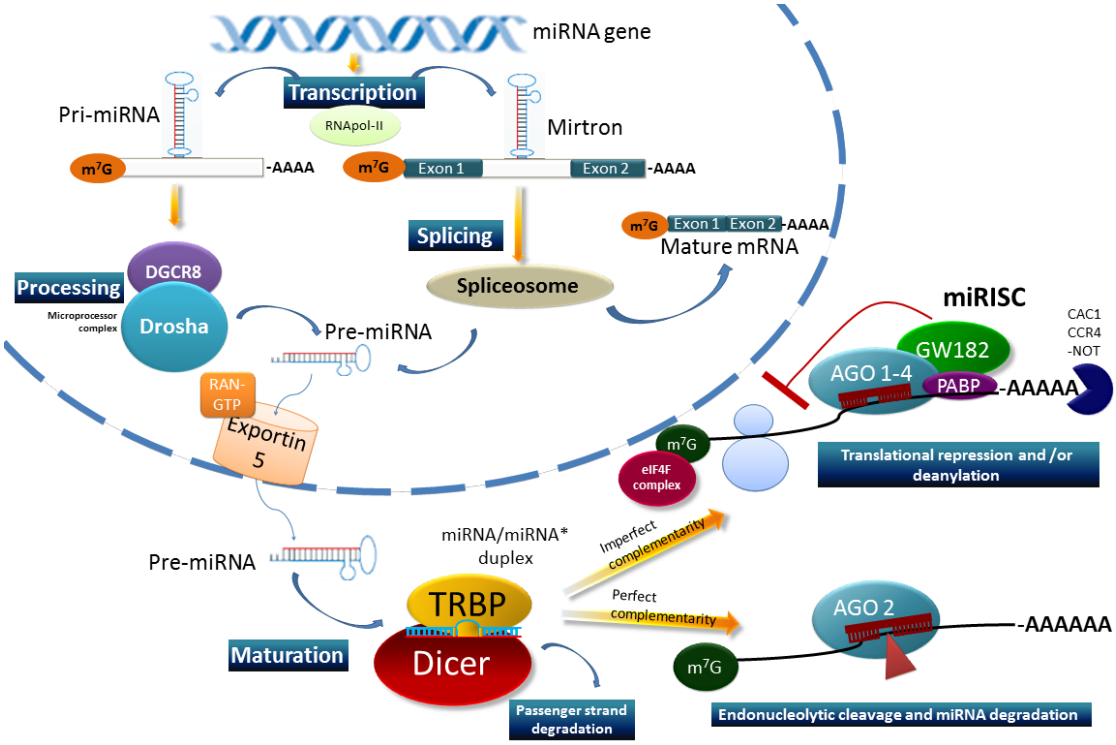

Figure. 14. MicroRNA biogenesis. See text for explanation, modified from [203].

In the cytoplasm pre-miRNAs are processed by Dicer1 (an RNase III-like endonuclease; Dicer2 is only active in the cleavage of siRNAs) that recognizes at the Piwi/Argonaute/Zwille (PAZ) domain in the 3'-terminus of the pre-miRNA hairpin structure.[204-206] Dicer1 forms a complex with the human immunodeficiency virus trans-activating response RNA-binding protein (TRBP or TARBP2) which is required to stabilize the interaction of Dicer1 with the pre-miRNA.[207] The complex Dicer1-TRBP cuts the pre-miRNA structure at the end of the loop generating a duplex of 22 nucleotides consisting of the mature strand miRNA and a passenger strand indicated by miRNA* (miRNA-miRNA* duplex)(Fig. 14).[204-206] The miRNA duplex is then incorporated into the microRNA- or RNA-induced silencing complex (miRISC or RISC).[208] The RISC complex is composed by Argonaute protein (Ago, also called EIF2C1-EIF2C14 or Ago1-Ago4 [209]), the core protein within the complex in association with Dicer1 and TRBP, although Gemin3, Gemin4, Mov10, Imp8 and the glycine-tryptophan protein of 182kDa (GW182) are also known to be part of this complex.[196] In RISC, the miRNA duplex is loaded onto an Ago protein where the two strands are separated.[196] In RISC, the miRNA with less stable base pairing at the 5'-end remains associated with the Ago protein while miRNA* is unwound and degraded, the remaining mature miRNA is then guided by RISC to their targets.[208,210]

1.3.3 Regulation of target genes by miRNAs

The miRNAs regulatory mechanisms are very complex due to their capacity to regulate multiple gene targets, thus a single miRNA can target as many as 200 genes and multiple regulatory pathways.[211] These miRNAs properties are a consequence of their imperfect complementarity to mRNA targets, which is a characteristic of their structure (Fig.14). Moreover, another miRNA recognition factor of mRNAs involves the Watson-Crick base pairing of the highly conserved nucleotides 2-8 in miRNAs, a region called the seed region or sequence that allows the miRNAs to bind to many potential targets.[212]

The pairing of miRNA-mRNA is mostly imperfect at the 3'-untranslated region (UTR), facilitating the translational repression of the gene, although the exact mechanism is still elusive. It is known that translational repression occurs during the ribosomal scanning of the 43S subunit and requires the poly(A) binding protein and eIF4G although physical interaction is not essential (Fig. 14).[213,214] The pairing of nucleotides, although less common in mammals than plants, can also be perfect, in which case the mRNA is cleaved by Ago 2. There are four Ago proteins in mammals but only Ago 2 has cleavage activity in humans (Fig. 14).[210,215]

The regulation of translation by miRISC starts with the recognition of the mRNA 5'-terminal cap by eIF4E a subunit of the eIF4F complex. The subunits eIF4A and eIF4G are also part of the eIF4F complex.[216] Another factor required for the initiation of repression is the eIF3 protein that interacts with eIF4G (through the eIF3e subunit), to recruit the 40S ribosomal subunit to the 5'-end, forming the 40S pre-initiation complex.[212,216] The pre-initiation complex binds afterwards to the 60S ribosomal subunit to begin elongation at the AUG codon. The subunit eIF4g also interacts with the polyA-binding protein PABP1 that interacts with the 3'-end.[217,218] The ability of eIF4G to interact with eIF4E and PABP1 causes the mRNA molecule to circularize.[216] The circularization of the mRNA molecule increases translational efficacy.[219] Processing bodies (P-bodies or glycin-tryptophan or GW-bodies in mammals) that are cytoplasmic structures involved in the storage and degradation of mRNA are also thought to be involved in miRNA regulation. The targeted gene (mRNA) and the miRNAs are guided in combination with RISC to the GW-bodies structure (Fig.14).[220] At miRISC translation is inhibited at the post-initiation stage by inhibition of the ribosome elongation.[216] The mRNA then decays after the inhibition of ribosome elongation in a sequential process initiated by the interaction of miRISC with CCR4-NOT complex facilitating the poly(A) tail deadenylation by PAN2-PAN3 denyalases (Fig 14), afterwards, m7G is removed and degradation of mRNA is effectuated by Xrn1 5'-3' exonuclease.[216]

However, the outcome of the miRISC regulatory mechanism is downregulation of protein expression but not necessarily the downregulation of mRNA levels.[221]

1.3.4 The roles of miRNAs in cancer

MicroRNAs are involved in key regulatory mechanisms within cellular pathways.[184] Therefore, it has been suggested that miRNAs can be involved in the regulation and development of tumourigenesis.[182] Since the role of miRNAs is regulation of protein expression, changes in miRNA levels have been associated with cancer. For example, chromosomal localization of miRNAs at fragile chromosome sites or regions of frequent chromosomal instability (e.g. amplification, translocation or deletions) that have been associated with cancer account for nearly 52% of miRNA genes.[222] Among the miRNAs whose deregulation have been implicated in human malignancies, the deletion of hsa-let-7 family has been associated with breast, lung and ovarian cancer.[222] Moreover, amplification and translocation of the hsa-miR-17-92 cluster has been associated with lymphoma and T-cell acute lymphoblastic leukaemia, respectively.[223] The amplification of hsa-miR-26a has been associated with glioblastoma.[223] miRNAs can be divided according to the respective functions in cancer, as tumour suppressors (hsa-let-7 family and hsa-miR-15a/16),[224,225] or oncogenes (hsa-miR-17-92 cluster and hsa-miR-hsa-miR-21 [226,227]) or both depending on the type of cancer.[228]

Other potential mechanisms that directly contribute to a role of miRNAs in cancer are mutations in miRNA-containing genes and/or in the 3'UTR binding sites, and/or in pathways that regulate their expression during biogenesis and/or alterations of the number of copies of miRNAs that are expressed.[228,229] Alterations in the miRNA expression patterns also have been demonstrated to define each specific type of cancer.[191] Functional studies of individual miRNAs demonstrated that they can act both as oncogenes (oncomiRs) or tumour suppressors.[230]

The miRNA signatures for tumours derived from different cellular origins seems to be unique, enabling the classification and matching of expression profiles to specific human cancers, and possibly to the grade of malignancy.[231] Therefore patterns of miRNA expression can be an important ontogenetic source of information for tumours in addition to the expression profiling from mRNA microarray analysis.[191] Unique patters of expression of miRNAs offer information-rich signatures for cancer diagnosis, disease prognosis, treatment-responses and survival, prediction of

responses to therapy, and will potentially generate tools to delineate cellular pathways for more efficient targeting of novel cancer therapeutics.[232,233]

1.3.5 The role of miRNAs in prostate cancer

The roles of miRNAs in prostate cancer were first evaluated by Porkka in 2007, since then other studies have verified the implications of miRNAs in tumour progression or inhibition.[234-238] In prostate cancer many miRNAs are differentially expressed, frequently those miRNAs are involved in the deregulation of anti- or pro-carcinogenic pathways. Many miRNAs studied in PCa were reported to exhibit a different expression pattern dependent on the study. Those inaccuracies were due to the type of study carried out, the cell lines, the type of tissue and the sample size.[239]

As in other types of cancer, the deregulation of miRNA expression levels can trigger prostate cancer. Dicer, one of the miRNA processing regulators, has been shown to be upregulated in PCa in a direct correlation with the clinical stage of Gleason score.[240] There are many deregulated miRNAs that have been implicated in prostate cancer either as oncogenes including hsa-miR-221/-222, hsa-miR-21, and hsa-miR-125b or tumour suppressors including hsa-miR-101, hsa-miR-126, hsa-miR-146a, hsa-miR-330, hsa-miR-34, and hsa-miR-200 (Table 5).[241] It is known that the expression-profiles of miRNAs are highly tissue specific, although miRNAs can also be differentially deregulated within the same tissue, which is the case for the PC-3, LNCaP and DU145 cells that are all derived from prostate cancer tissue. While LNCaP and DU145 cells express hsa-miR-200c and hsa-miR-141, PC-3 cells have lost the expression of these miRNAs.[242] One miRNA that is implicated in PCa progression and resistance to hormone ablation treatment is the AR-induced overexpression of hsa-miR-21, although the mechanism is not clear in glioblastoma cells it has been shown that p53, TGF-β and mitochondrial apoptosis tumour suppressor genes are targeted by hsa-miR-21 inducing proliferation.[243,244] The androgen-dependent- overexpression of hsa-miR-125b in PCa cells induces proliferation and inhibition of apoptosis by targeting Bak.[245] The screening of the expression of miRNAs in prostate cancer might aid in elucidating the mechanisms behind treatment resistance, to more specifically

target factors that are important regulators of this mechanisms and for developing biomarkers for prognosis and treatment outcomes. For example, LNCaP cells treated with resveratrol showed that commonly overexpressed miRNAs in prostate cancer such as the hsa-miR-17-92 cluster and hsa-miR-106a were downregulated.[246] These miRNAs have been shown to have a strong anti-apoptotic activity when overexpressed, by interfering in MYC, PTEN and p21 pathways.[247,248]

Table 5. Selected deregulated miRNAs identified in various cancers.

miRNA	Function	Cancer
let-7 family	TS	CLL, lymphoma, gastric, lung, prostate, breast, ovarian, colon, leiomyoma, melanoma
mir-15/16	TS	CLL, lymphoma, multiple, myeloma, pituitary adenoma, prostate, pancreatic
mir-17-92	OG	Lymphoma, multiple myeloma, lung, colon, medulloblastoma, breast, prostate
mir-21	OG	Lymphoma, breast, lung, prostate, gastric, cervical, head and neck, colorectal, glioblastoma
mir-26a	TS/OG	Lymphoma, hepatocellular carcinoma, thyroid carcinoma, Glioblastoma
mir-34a/b/c	TS	CLL, lymphoma, Pancreatic, colon, neuroblastoma, Glioblastoma
mir-155	OG	Lymphoma (ie. Burkitt's, Hodgkin's, non-Hodgkin's), CLL, breast, lung, colon, pancreatic
mir-200/141	TS/OG	Breast, renal clear cell carcinoma, gastric, bladder, Ovarian
mir-205	TS	Prostate, bladder, breast, oesophageal, Ovarian
mir-206	TS	Rhabdomyosarcoma, breast
mir-9	TS/OG	Medulloblastoma, ovarian, Breast
mir-143/145	TS	Colorectal cancer, breast, prostate, cervical, lymphoid cancer.

Tumour suppressor (TS), oncogenic (OG); chronic lymphoid leukaemia (CLL).[203,228]

1.4 Apoptosis

The term apoptosis was first introduced in 1972[249] to describe a well regulated evolutionary conserved type of programmed cell death distinct from necrosis. Both processes can occur sequentially, independently or simultaneously.[250] It is important to distinguish the different mechanisms of programmed cell death since cytotoxic stimulus at certain doses can induce apoptosis but at higher doses can induce necrosis.[251] The characteristics of apoptotic cell death are defined by cell shrinkage, membrane blebbing, nuclear condensation and fragmentation, the dispersion of

cellular components into apoptotic bodies, caspase activation and phosphatidylserine redistribution to the extracellular surface.[252] [249,253] Most of the current knowledge of apoptosis in mammalian cells is derived from the initial findings in the nematode *Caenorhabditis elegans.*[254] Apoptosis is a homeostatic mechanism that serves to maintain cells and tissue during aging, development and as a defence to preserve the integrity of tissues with damaged cells caused by extrinsic factors such as infection of cytotoxic agents.[255] Apoptosis occurs through two main pathways, the extrinsic pathway that involves the activation of cell surface receptors by external signals and the intrinsic pathway that is activated by death signals within the cell however, both pathways converge in the activation of caspases. [256]

1.4.1 Regulation of Apoptosis: extrinsic and intrinsic pathways

1.4.1.a Extrinsic Pathway

The extrinsic pathway is triggered by the activation of death receptors including the tumour necrosis factor receptor (TNFR) superfamily members CD95/FasR, TNFR1 and TNF-related apoptosis-inducing ligand-1 and 2 (TRAILR1 and TRAILR2) by the respective death ligands CD95L/Fas ligand (FasL), TNF-α, lymphotoxin-α and TRAIL.[257,258] The common characteristics of the TNFR superfamily members are the cysteine-rich extracellular domain and an intracellular cytoplasmic death domain. [259] The binding of ligands to their receptors induces the clustering of receptors and the trimerisation of ligands, triggers the recruitment of adaptor molecules in the cytoplasm to form the death-inducing signalling complex (DISC) (Fig. 15).[182,183] The formation of DISC involves the activation and recruitment of pro-caspase-8 that by auto-cleavage forms caspase-8 (Fig. 15).[260,261] Furthermore, cell death activation via Fas, TRAILR1 and TRAILR2, requires the recruitment of FAS-associated death domain (FADD) to DISC in addition to caspase-8.[258,262] However, TNFR1-induced cell death causes the recruitment of TNFR-associated death domain (TRADD) and TNFR-associated factor-2 (TRAF2).[257,258,262] The formed DISC then induces three separate cell death pathways. The first pathway is induced by caspase-8 by proteolytic cleavage of the Bcl2 homology-3 (BH3)-only protein (Bid), subsequently Bid is

translocated to the mitochondria where it activates the mitochondria outer membrane permeabilisation (MOMP) process (Fig. 15).[261,263] The second pathway is induced by direct activation of caspases where the effector caspases 3, 7 or caspase-6 are targeted leading to cell death (Fig. 15).[258,263] The third pathway is activated only in T cells and involves the activation of the receptor-interacting protein kinase-1 (RIPK1).[264]

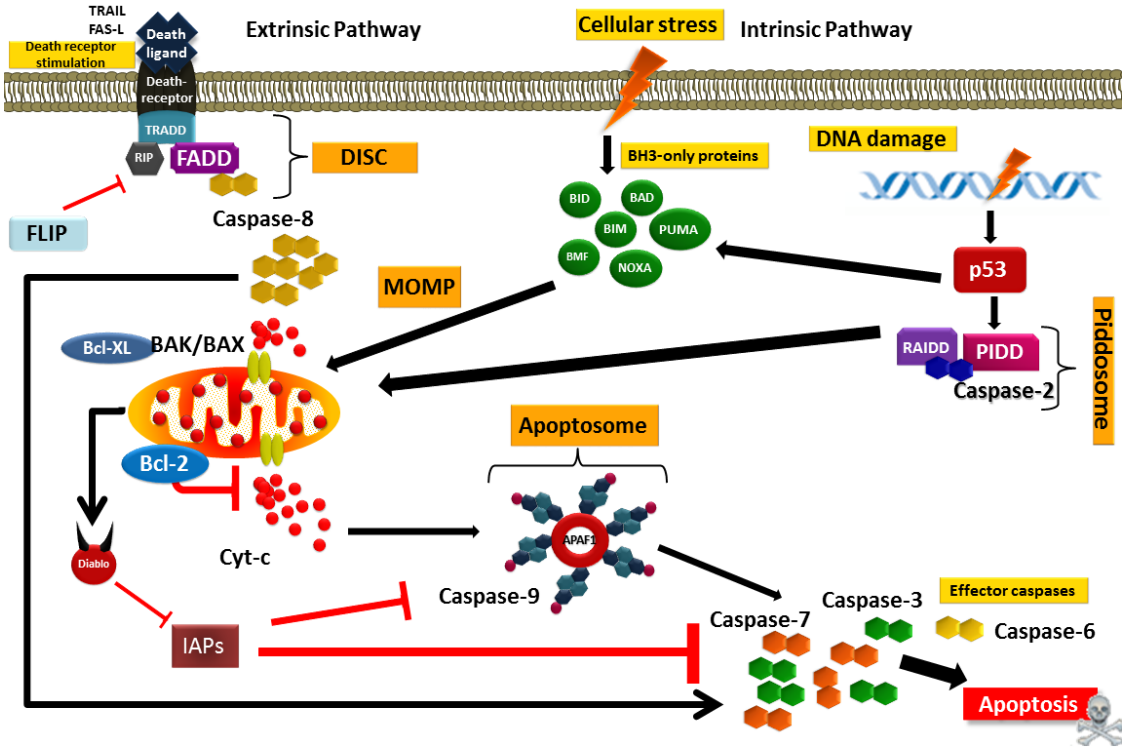

Figure 15. Apoptosis: Extrinsic and intrinsic pathways. Apoptosis is led by the action of two pathways: The extrinsic and the intrinsic pathways. The extrinsic pathway involves the stimulation of death receptors of the tumour necrosis factor receptor superfamily by their respective ligands such as CD95/Fas, TNFR or TRAILR. The stimulation of death receptors induces the recruitment and activation of caspase-8 by FADD and TRADD to form DISC. Moreover, DISC in consequence can led to the proteolysis of BID inducing the translocation of truncated BID to the mitochondria triggering MOMP, or directly induced down-stream effector caspases. The intrinsic pathway involves the activation of MOMP and in consequence the release of cyt-c, resulting in the assembly of the apoptosome, a complex formed by caspase-9 and APAF1 that induces the down-stream effector caspases. Moreover, MOMP can be induced by BH3-only proteins in response to cell stress and DNA damage. The BH3-only proteins induce the oligomerization of Bax and/or Bak enabling the release of mitochondrial from the intermembrane space resulting in the activation of down-stream effector caspases. In the DNA damage response p53 is stabilize resulting in the activation of PUMA and NOXA to promote MOMP. Alternatively, the DNA damage response can also induce MOMP through the activation of caspase-2 that in association with PIDD and RAIDD form the piddosome, in consequence the piddosome activates MOMP. However, caspase-2 can directly induce the activation of down-stream effector caspases. Modified from [265].

1.4.1.b Intrinsic Apoptotic Pathway

The intrinsic pathway is triggered by intracellular stimuli, in response to oxidative stress and DNA damage, radiation, toxins, hypoxia, hyperthermia, viral infections.[266] These cell insults induce the activation of MOMP which comprises the loss of mitochondrial-trans-membrane potential, by opening the membrane permeability transition (MPT) pores.[267] Thus, MOMP triggers the release of mitochondrial cytochrome-c (cyt-c), activating the apoptotic downstream machinery resulting in the assembly of the caspase activating complex called apoptosome (Fig. 15). The apoptosome composed by cyt-c and the apoptotic-protease-activating-factor-1 (Apaf-1) recruits and activates caspase-9 (Fig. 15).[266,268] The activation of caspase-9 in consequence cleaves and prompts caspase-3, -6 or-7 leading to the cleavage of other cellular targets including the poly-adenosine diphosphate ribose (ADP)-polymerase (PARP) and the inhibitor of caspase-activated DNAse (ICAD).[269] The breaking of ICAD releases CAD favouring the degradation of DNA fragments; meanwhile, the cleavage of laminin takes place by caspase-6, ultimately leading to cell dismantling and nuclear collapse.[270] In addition to cyt-c, other factors are released from the mitochondria during MOMP such as the second mitochondria-derived activator of caspase (Smac)/direct inhibitor of apoptosis protein (IAP)-binding protein with low isoelectric point (DIABLO) and high temperature requirement protein A2 (HTRA2/OMI), these factors shield caspase activity by attenuating caspase inhibitors such as X-linked inhibitor of apoptosis protein (XIAP).[271-273]

MOMP is regulated by the interaction of pro- and anti-apoptotic members of the B-cell Lymphoma 2 (Bcl-2) family that are classified according to their Bcl-2 homology (BH) domain.[267] The members of the Bcl-2 family that have the BH1-BH3 domains such as Bcl-2-antagonist killer (Bak), Bcl-2–associated X protein (Bax) and BCL2-related ovarian killer (Bok), are the pro-apoptotic effectors of MOMP. In contrast, BH1-BH4 members Bcl-2, B cell lymphoma-2-like X isoform L (Bcl-XL) and Bcl-w bind to Bax and Bak inhibiting their function, therefore blocking apoptosis and inducing cell survival.[267,274] BH3-only family members such as Bid, Bad, Bim, Bik, BNIP3, BMF, HRK, Noxa and Puma can be phosphorylated, cleaved or relocated to promote MOMP (Fig. 15). BH3-only proteins induce MOMP by promoting the oligomerization

of Bax and/or Bak in the outer mitochondrial membrane generating channels to allow the release of mitochondrial proteins and proceed with apoptosis in response to cell stress or infection.[267,274,275] BH-3 family members can also induce MOMP by inhibiting anti-apoptotic effectors such as Bcl-2 within a pro-apoptotic response.[267] Alternatively, p53-stabilization in response to DNA-damage induces the activation of Puma and Noxa triggering MOMP and inducing apoptosis.[276] In addition, the formation of the complex termed piddosome composed by p53-induced-protein with a death domain (PIDD) and RIP-associated protein with a death domain (RAIDD) in response to DNA-damage induces the activation of caspase-2 consequently promoting MOMP or direct caspase activation.[277] Although the extrinsic and the intrinsic apoptotic pathways are clearly defined, they are not mutually exclusive processes.[278]

1.4.2 Apoptosis and cancer

One of the main factors that enable cancer progression is the deregulation of the apoptotic pathways. The link between apoptosis and cancer was first established by the induction of apoptotic cell death in response to radiotherapy in 1972 and was reinforced by the recognition of Bcl-2 as a proto-oncogene as part of the t(14:18) chromosome translocation in B- cell lymphoma that enabled prolonged survival of B-cells by inhibition of apoptosis.[249,279-281] There are many key apoptotic factors that can be deregulated during cancer progression like overexpression of Bcl-Xl and the downregulation of Bax and Bak, although these alterations may not be enough to promote cancer by its own and might require additional genetic alterations. [282-285]

One main regulator within the apoptotic pathway is the transcription factor p53 that regulates cell cycle arrest, apoptosis and DNA-damage repair functions. p53 induces apoptosis through transactivation of BH-3 family members including Bax, Bid, Puma and Noxa that induce MOMP and the release of apoptotic mitochondrial factors from the inter-membrane space and also by trans-repressing Bcl-2.[275,286,287]

1.4.3 MicroRNA regulation of apoptosis

How miRNAs regulate apoptosis is still under investigation. However some evidence indicates that miRNA regulation of apoptosis depend on the cell environment and context.[288] The regulation of apoptotic pathways by a single miRNA can induce two opposite responses depending on the cell type and tissue, for example, the inhibition of hsa-miR-24 increased cell growth in HeLa cells (cervical carcinoma) and in contrast decreased cell growth in A549 cells (lung carcinoma).[184] In addition, several miRNAs are regulators of key apoptotic factors such as caspase-3, where hsa-miR-1d, hsa-miR-148, hsa-miR-204, hsa-miR-210, hsa-miR-216 and hsa-miR-296 induce an increases in caspase-3 activity. In contrast, hsa-miR-214 inhibits capsase-3 activity.[184] Other factors include Bcl-2 activity which is post-transcriptionally regulated by hsa-miR-15 and hsa-miR-16, most probably by direct binding to Bcl-2 mRNA. Inhibition of hsa-miR-15 and hsa-miR-16 resulted in increased Bcl-2 levels inducing proliferation evading, additionally, the c-Myc-regulated hsa-miR-17-cluster can induce cell proliferation and evade the apoptotic response.[248,289] Furthermore, the miRNAs hsa-miR-221/222 have been implicated in the reduction of caspase-3 and caspase-8 in TRAIL-sensitive cells favouring cell survival, in addition to the proto-oncogene Kit and tumour suppressor p27kip.[289-291] Other studies have shown regulation of Pro-apoptotic Programmed Cell Death 4 (PDCD4) by hsa-miR-21 in colorectal and breast cancer.[292] In response to DNA-damage p53 can up-regulate hsa-miR-34 promoting cell death.[230] The regulation of apoptosis by miRNAs and their de-regulation during cancer progression makes them interesting targets for investigating the mechanisms of cancer progression and therapy resistance.

1.5 Autophagy

Eukaryotic cells have developed throughout evolution a well conserved homeostatic and catabolic process named autophagy (self-eating)[293] that enables cells to degrade their own cellular organelles and proteins allowing cellular biosynthesis under conditions of nutrient deprivation or metabolic stress.[294] There are three autophagic

processes that have been described and characterized: macroautophagy, microautophagy and chaperone-mediated autophagy.[295] Microautophagy is referred as the process where the cytoplasm is sequestered by invagination of the lysosomal or vacuolar membranes and is the least characterized of the three.[295] The chaperone-mediated autophagy is considered as a secondary response to starvation involving the direct translocation of target proteins through the lysosomal membrane.[295] Macroautophagy (hereafter referred to as autophagy), is the most studied of the autophagy mechanisms and involves sequestration of cytoplasm and intracellular organelles by cytosolic double- or multi-membrane autophagic vacuoles (autophagosomes). Autophagosomes fuse with lysosomes and the content is degraded.[265,295]

1.5.1 Initiation and regulation of Autophagy

The regulation of autophagic flux (the complete process of autophagy) is performed by a set of genes called autophagy-related genes (ATG) that were initially identified in yeast.[296,297] The genes have been shown to be highly conserved among organisms and many homologues of these genes have been identified in higher eukaryotes including *Caenorhabditis elegans*, *Drosophila melanogaster*, mouse and man.[297] Autophagy is a multi-step process that can be divided into initiation, formation of autophagosomes (where the vesicle nucleation, elongation and completion are carried out), maturation and degradation.[298]

In mammalian cells the initial autophagic steps are regulated by a Serine/threonine-protein kinase complex, which consist of the human orthologues of ATG1 or ULK1/2 (Unc-51-like kinase), ATG13 and the scaffold protein FIP200/RB1CC1 (Focal adhesion kinase family interacting protein of 200kDa; human orthologue of Atg17) (Fig. 16).[297,298] In addition to ULK1/2-ATG13-FIP200-complex, a second complementary regulatory conglomerate is formed by the human orthologues of vacuolar protein sorting 34 (hVps34) that is a class III phosphatidylinositol-3-kinase (PI3K-III) and by ATG6/ Bcl-2-interacting myosin- like coiled-coil protein-1 (Beclin-1; 60kDa) (FIG. 16).[299] The ULK1/2-ATG13-FIP200-complex collects stress signals that come from the

nutrient-sensing mammalian target of rapamycin Ser/Thr kinase complex 1 (mTOR Ser/Thr kinase complex 1 or mTORC1) (Fig. 16).[298,300] The serine/threonine kinase protein mTOR of nearly 300kDa is part of the phosphatidylinositol kinase-related kinase (PIKK) family.[301] mTOR was first described in 1991 as a target protein of the immunosuppressant and fungicidal drug rapamycin.[302] mTOR forms two complexes, where mTOR is associated with the regulatory-associated protein of mTOR (Raptor;KOG1 ortholog), GbL/mLst8, PRAS40 and DEPTOR to form the mTORC1. Alternatively mTOR binds to the rapamycin-insensitive companion of mTOR (Rictor; Avo3 ortholog), GbL/mLst8, Sin1 (Avo1 ortholog), PRR5/protor and DEPTOR to form mTORC2.[301,303]

The mTORC1 can be activated by growth signalling pathways like the insulin/insulin-like growth factor (IGF-1)-PI3K-I (phosphatidylinositol 3-kinase class I)-Akt pathway and by high nutrient status. The protein kinase Akt and sufficient nutrient conditions positively regulates mTORC1, inducing phosphorylation and inhibition of ATG13 and ULK1/2, inhibiting autophagy.[301] In addition, inhibition of mTORC1 by PTEN and TSC2 or under starvation conditions, mTOR dissociates from ULK1.[301] The inhibition of mTORC1 blocks the mTORC1-dependent phosphorylation of ATG13 and ULK1/2, inducing the activation of ULK1/2 (Fig. 16).[304] Autophagy is induced by ULK1/2-dependent phosphorylation of ATG13, FIP200/RB1CC1 and ULK1/2 auto-phosphorylation.[298,300,304] The auto-phosphorylation of ULK complex induces its accumulation, triggering vesicle formation by the formation of the isolation membrane or phagophore (Fig. 16).[304]

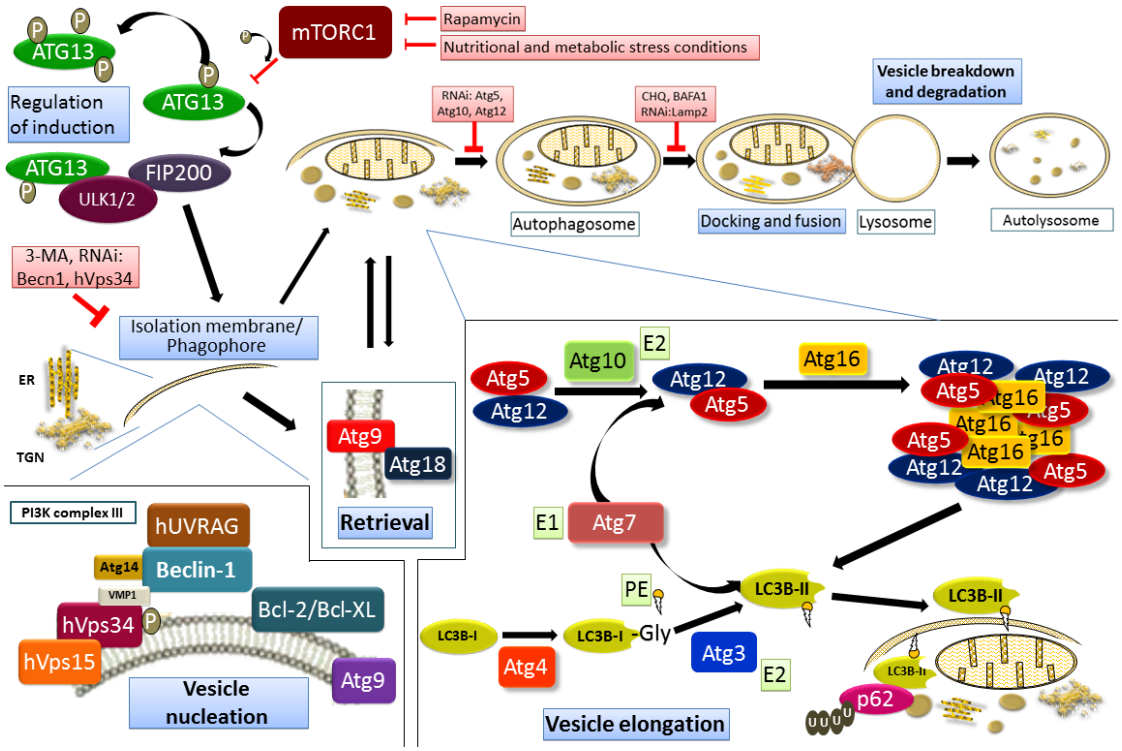

Figure 16. Autophagy flux. Autophagy starts with the de-repression of the mTOR Ser/Thr kinase, which inhibits autophagy by phosphorylating Atg13. The phosphorylation dissociates Atg13 from the ULK1/2 and FIP200 protein complex attenuating ULK1/2 kinase activity. In contrast, the inhibition of mTOR triggers the de-phosphorylation of Atg13, enabling the reconstitution of the Atg13-ULK1/2-FIP200 complex. Moreover, autophagy continues with vesicle nucleation where hVps34 is activated forming a multi-protein complex with Beclin-1, UVRAG and Vps15. There are two pathways involve in vesicle elongation. In one, Atg12 to Atg5 are conjugated in a process mediated by the E1-like enzyme Atg7 and the E2-like enzyme Atg10. The second involves the conjugation of PE to LC3B-I by the sequential action of Atg4, the E1-like enzyme Atg7 and the E2-like enzyme Atg3. The lipid conjugation of LC3B-I causes the conversion of LC3-I to the autophagic-vesicle-associated form LC3-II. The mechanism of retrieval mediated by the Atg9 complex is poorly understood. The maturation of the autophagosomes involves the fusion with lysosomes to create autolysosomes. In the autolysosomes, the content is degraded by lysosomal enzymes that required acidic conditions. The sites of inhibition and autophagy-flux inhibitors are marked by red arrows. Endoplasmic reticulum (ER), trans-golgi-network (TGN). Modified from [265]

1.5.2 Formation, maturation and degradation of the Autophagic vesicles

The formation of autophagosomes occurs by the interaction of four groups of assembled proteins: the Atg1/Unc-51-like kinase (ULK) complex; the conjugation system composed of two ubiquitin-like proteins (Atg12 and LC3); the class III phosphatidylinositol 3-kinase (PI3K)/hVps34 complex; and two trans-membrane

proteins Atg9 associated and Atg18.[305] The protein complexes are recruited at the phagophore assembly site (PAS) in the cytoplasm.[305] The development of the isolation membrane or phagophore depends on the activation of hVps34 or PI3K-III, to generate phosphatidylinositol-3-phosphate (PI3P).[298,306] The activation of hVps34 depends on the formation of another complex that contains beclin-1, UV irradiated resistance-associated tumour suppressor gene (UVRAG) and the myristylated kinase hVps15 (p150/; PIK3R4; yeast Vps15).[298,307] Beclin-1 initially discovered as a Bcl-2 direct interacting protein is a protein linked to the *trans*-Golgi network (TGN) that provides the phagophore with membrane sources in addition to the endoplasmic reticulum.[308,309] The release of beclin-1 from Bcl-2 is driven by the mammalian vacuole-membrane-protein-1 (VMP1), the binding of beclin-1 and VMP1 in addition to hVps34 is essential for the integration of the PI3K-III complex and where VMP1 is essential in subsequent steps of the vesicle elongation.[310] However, Beclin-1 is also involved in other cellular functions including endocytic trafficking, phagocytosis, cytokinesis and in development. The regulation of gene expression of Beclin-1 is driven by FOXO3 and HIF1α.[309] The vesicle elongation process that generates the autophagosomes is mediated by the Atg12-5-16 complex.[298] Throughout the formation of the complex the ubiquitin-like protein ATG12 is activated by ATG7 (an E1-like enzyme) and binds to the E2-like enzyme ATG10, before being transported to ATG5 (Fig. 16). Furthermore, ATG5 binds directly to the membrane, however, this binding is negatively regulated by ATG12 and activated by ATG16 (Fig. 16).[311] Furthermore, the interaction of ATG16 with ATG5 induces oligomerization to form ATG16L that associates to form the ATG12-5-16 complex (Fig. 16).[312] The second system involves the conjugation of ATG8 or microtubule-associated protein 1A/1B-light chain 3 (LC3 or GATE16 and GABARAPL1 mammalian orthologues of yeast Atg8) by an action in cascade of proteases ATG4, the E1-enzyme-like Atg7 and the E2-enzyme-like Atg3 (Fig. 16).[265,298] The microtubule-associated protein 1A/1B-light chain 3 (LC3) was initially described as a microtubule-associated protein 1A and 1B in rat brain, LC3B is present in two forms identified as LC3B-I and LC3B-II at 18 and 16 kDa respectively.[313] LC3B-II has increased electrophoretic mobility that causes the apparent size of 16kDa on SDS-PAGE gel while the molecular weight is higher than that of LC3-I.[313,314] Following synthesis, LC3B is immediately processed by ATG4 from

the precursor protein proLC3 by cleavage at the C-terminal Gly-120 amino acid.[315] During autophagic flux the cytosolic soluble form LC3B-I is further processed by ATG3 and ATG7 inducing a reversible lipid conjugation with phosphatidylethanolamine (PE) to generate the autophagy-vesicle associated form LC3B-II.[305] The ATG12–ATG5–ATG16 complex targets LC3B-II to the phagophore membrane and is essential for the formation of autophagosomes.[311] Moreover, the site of autophagosomes formation is conducted at the endoplasmic reticulum (ER)-mitochondria contact site in mammalian cells.[316] The ER-mitochondrial contact sites regulate mitochondrial biogenesis and intracellular trafficking.[317] The regulation of the phagophore-elongation process to form the autophagosomes is tightly regulated by LC3B-II, therefore, the amount of LC3-II is directly correlated with the extent of autophagosome formation.[265,298,314] The process of autophagosome maturation involves fusion of the autophagosomes with the lysosome in a multistep process.[297] The maturation process starts with the fusion of early endosomes vesicles forming multi-vesicular endosomes that successively fuses with autophagosomes generating amphisomes that finally merges with lysosomes.[297] The maturation of the autophagosomes and subsequent fusion to lysosomes occurs only in the presence of the lysosomal proteins LAMP1 and LAMP2, the small GTPase Rab7 (RAB7A).[297] The UVRAG protein targets RAB7 to the autophagosomal membrane facilitating the maturation events of the autophagosomes.[318] The autophagosomes when formed have the same pH as the surrounding cytoplasmic environment although while merging to the lysosomes the internal pH of the autolysosomes becomes acidic, due to the presence of proton pumps rather than lysosomal enzymes.[297] Prior to the fusion of autophagosomes to lysosomes the conjugated LC3B-II is removed from the outer membrane of the autophagosomes.[319] Furthermore, LC3B binds to the protein p62/SQSTM1. The protein p62/SQSTM1 regulates the packing and delivering of polyubiquitinated unfolded proteins as part of the ubiquitination process of cargo proteins. Also is responsible for the clearance through autophagy of aggregated proteins, dysfunctional organelles and of toxic aggregates.[320] The binding of p62/SQSTM1 with LC3B induces the formation of p62 aggregates which are sequestered into autophagosomes (Fig. 16). The formation of the autolysosome induces the degradation of the cargo and p62/SQSTM1 aggregates, however when

autophagy is impaired the p62/SQSTM1 aggregates and other ubiquitin-positive aggregates accumulate, making p62/SQSTM1 a suitable marker for autophagy-flux.[321] Within the autolysosomes the intracellular content is degraded by cathepsins (lysosomal hydrolases) that act optimally within the acidic compartment. The catabolically generated molecules (amino acids and other materials) are released from the autolysosome and incorporated into anabolic pathway.[322,323] The inner membrane as well as the luminal content of the acidic vesicle then is degraded by lysosomal enzymes completing the autophagy flux.[324]

Depending on the conditions autophagy can be either a pro-survival or a cell death mechanism, suggesting that autophagy is tightly connected to cell death and survival pathways and that the balance of homeostasis can be disrupted depending on stimulus. Moreover, experimental conditions can also induce or prevent autophagy, frequently resulting in contradictory reports which indicate that autophagy is a far more complex process than previously appreciated.

1.5.3 Autophagy in cancer

1.5.3.a The role of autophagy in promotion of tumourigenesis

In normal human cells autophagy is a conserved process that is activated in order to maintain homeostasis within the cellular environment in response to metabolic stress to promote cell survival. It has been suggested that in cancer cells autophagy inhibits cell death pathways acting as an environmental adaptor enabling cancer cell proliferation.[265] The evidence of the autophagy-induced stress tolerance within a tumour environment are considerable in both *in vivo* and *in vitro* models.[298] Within the tumour environment unfavourable conditions such as nutrient deprivation and hypoxia may lead to autophagy activation and cellular survival by increased biosynthesis or catabolism and removal of high-energy consuming organelles.[265] Under hypoxic conditions autophagy can be induced by HIF-1α-dependent or independent activation, leading to mitochondrial degradation (mitophagy).[325] Mitophagy can induce cell survival either by reducing energy consumption or by

reducing the susceptibility of cells to mitochondrial outer membrane permeabilisation (MOMP) that induces apoptosis, a mechanism where ATG7 and ATG1 seem to be essential.[265,326] Increased basal levels of autophagy have been described in several types of cancer cell lines and tumour tissue from breast, renal and pancreatic cancers.[327-331] The first evidence of the involvement of autophagy in cancer progression and development was the observation that incidence of a mono-allelic deletion of Beclin-1 (Becn1) was near 50% in breast, leukaemia, lymphomas, lung and liver tumours, and that complete deletion induced the impairment of autophagy.[332] Moreover, in a breast cancer model with impaired autophagy due to the deletion of one allele of Beclin-1 was shown to induce cytoprotective mechanism that was overcome by reintroducing normal Beclin-1 restoring autophagy and Beclin-1 tumour-suppressor activity.[298,333] Other studies have shown that tumour promotion, genomic instability and aneuploidy are induced by the loss of autophagy.[333] Furthermore, homozygous depletion of $ATG7^{-/-}$ and $ATG5^{-/-}$ is sufficient for tumour initiation however, not for tumour progression.[334,335] Tumour formation has been observed in models of impaired autophagy and p62/SQSTM1 overexpression and is inhibited by re-established autophagic flux and p62/SQSTM1 degradation.[336] Additionally, increased tumourigenesis was observed when BIF1 and UVRAG failed to bind Beclin-1 induced either by abrogation or allele deletion, inducing downregulating of autophagy.[298] Furthermore, necrosis-induced inflammation causes the secretion of growth factors to the tumour microenvironment promoting tumour-proliferation; this mechanism of cell survival was triggered in response to Akt-dependent inhibition of autophagy and the blockage-apoptosis-induced necrosis.[337] However, autophagy also induces cell death (ACD, autophagic cell death).[265]

1.5.4 Autophagy induces cancer cell death: Crosstalk between autophagy and apoptosis

There are two cell death mechanism induced by autophagy, the less common self-destructive autophagy or type-II programmed cell death where massive autophagy degrades the cytosol and organelles, inducing irreversible atrophy, damage and

consequently cell death. Type-I programmed cell death, where autophagy induces necrosis or apoptosis.[265]

Type-II autophagic cell death or massive autophagy is a cell death mechanism which is not well understood.[265] However, it has been reported that a Bax and Bak double-knockout murine model the inhibition of apoptosis induced by DNA-damage triggered massive autophagy in embryonic fibroblasts, therefore inducing cell death.[338] Nonetheless, the induction of massive autophagy was only shown when DNA-damage was induced, and no other apoptotic stimulus induced massive autophagy.[338] In contrast, the knockout of the essential autophagic genes Atg5 and beclin-1 reduced cell death.[338]

In type-I programmed cell death, autophagy causes cell death by necrosis or apoptosis dependent on the stimulus.[265] There are many stimuli that induce both autophagy and apoptosis, like reactive oxygen species (ROS) that can induce the pro-apoptotic MOMP and stimulate the proteolysis of ATG4 also stimulating autophagy.[339] Moreover, p53 has been shown to be a linking factor between autophagy and apoptosis. The activation of p53, induced the inhibition of mTOR via the 5'-adenosine-monophosphate-activated protein kinase **(**AMPK) and the tumour suppressor tuberous-sclerosis-1 (TSC1) and TSC2, consequently inducing autophagy.[277] Additionally, induction of autophagy through activation of p53, is mediated by the damage-regulated autophagy modulator (DRAM). Furthermore, it was also demonstrated that DRAM could be trans-activated by p53 and was essential in p53-mediated apoptosis.[278] It was also demonstrated in T-cells, apoptosis was induced after initial stimulation of autophagy.[340] In contrast, inhibition of the autophagic regulators Beclin-1 and ATG-7 resulted in impaired apoptosis.[340] In addition, the apoptosis-inhibitor Bcl-2 inhibits Beclin-1-dependent autophagy in mammalian cells by binding to Beclin-1, showing that Bcl-2 acts as a shared regulator of apoptosis and autophagy.[341] Furthermore, in glioma cells overexpression of Bcl-2 inhibits autophagy through Beclin-1 and the Akt-mTOR pathways.[342] In the context of inflammation, it was shown that the re-establishment of autophagy inhibited by Akt induced apoptosis or autophagic cell death as a consequence of metabolic stress.[337] The autophagy regulator ATG5 has been shown to have a dual role in autophagy and apoptosis, the cleavage of ATG5 by calpains triggers ATG5-pro-apoptotic functions.

Moreover, ATG5 lost its autophagy activity by translocation to the mitochondria where it inhibits Bcl-xL facilitating MOMP and inducing a caspase dependent apoptosis through interacting with Fas-associated via death domain (FADD).[343] Additionally, the overexpression of ATG5 induces autophagy and enhances susceptibility to apoptosis with doxorubicin.[343]

1.5.5 Adenovirus infection and autophagy

Also important, are the implications of viral infection on autophagy where different studies have shown that viral infections induce contrasting outcomes in autophagy. For example, it was reported that infection with wild type adenovirus (Ad5) strongly induced autophagy, seen by an increase in the conversion of LC3B-I to LC3B-II and the formation of the complex ATG12-ATG5 in lung cancer cells.[344] In addition, Ad5 induced autophagy in cervical and colon cancer cells.[344] The inhibition of autophagy in lung cancer cells by the inhibitor 3-methyladenine (3-MA; inhibitor PI3K-III) decreased Ad5 viral replication.[344] Another study in ovarian cancer cells showed that infection with *dl*922-947 induced autophagy as a survival mechanism, in contrast, the combination with cisplatin showed a caspase-3-independent apoptosis-like cell death mechanism.[345] A previous study with glioma cells showed that infection with a replication selective adenovirus expressing the human telomerase reverse transcriptase (hTERT-Ad) induced autophagy-like cell death and no apoptosis; additionally, infection with hTERT-Ad induced autophagy in PCa cells (PC-3).[346] Recently, another study showed that infection of glioma cells with Ad5 and the oncolytic adenovirus Ad-Δ-24-RGD (AdΔ24, CR2-deletion; RGD, Arg-Gly-Asp-motif inserted in the fiber protein gene) induced complete autophagy-flux. Viral induction of autophagy promoted cell lysis. Moreover, inhibition of ATG5 and ATG10 reduced viral-induced cell lysis. Furthermore, it was suggested that cell lysis was also supported by the activation of the extrinsic FADD/caspase-8 pathway although, it was only observed in leukaemia cells.[347] Alternatively, a study of glioma cells infected with wild type adenovirus and Ad-Δ-24-RGD showed an induction of autophagy except with the AdE1BΔ19K virus (E1B19K gene deleted), showing that E1B19K

strongly contributes to autophagy induction.[348] It was suggested, that the binding of E1B19K with the PI3K-III complex and Beclin-1 lead to autophagy induction, were E1B19K competes and antagonizes Bcl-2 protein and its function.[348] However, the binding of E1B19K to Beclin-1 and the PI3K-III complex was only shown in HeLa cells and whether complete autophagic-flux occurred was not reported.[348] The infection of glioma cells with the oncolytic adenovirus *dl*922–947 increased the conversion of LC3B-I to LC3B-II and reduced levels of p62, surprisingly the mutant also induced the activation of the autophagy-inhibitory pathway Akt/mTOR.[349] In contrast, the inhibition of autophagy in infected cells caused increased cytotoxicity due to apoptosis.[349] In a new study with osteosarcoma cells, the oncolytic virus OBP-702 induced the overexpression of p53, leading to an enhanced combination of apoptosis and autophagy-mediated cell death. The viral-enhancement of cell death was shown to be regulated by DRAM and the hsa-miR-93/106b cluster.[350] In summary, the regulation and outcome of autophagy in response to viral infection is dependent on the type of virus and cell, therefore it is important to characterize the cell response to viral infection aiming for the improvement or development of new cancer treatments.

1.5.6 MicroRNA regulation of Autophagy

The regulation of autophagy through microRNAs was observed for the first time in 2009 when Beclin-1 was shown to be post-transcriptionally regulated by hsa-miR-30a.[351] Moreover, hsa-miR-30a caused downregulation of Beclin-1 and thus autophagy, inducing a decrease in the levels of LC3-II levels and double membrane vacuoles despite the treatment with rapamycin.[351] Since then more miRNAs have been identified in autophagic regulation and associated with cancer and other pathologies.[352]

Many miRNAs have been identified to regulate different stages of the autophagic flux that can be either pro- or anti-oncogenic. Within the oncogenic pathway, the miRNA hsa-miR-106a a member of a highly oncogenic miRNA family was found to be highly upregulated in myeloid Leukaemia cells targeting and downregulating ULK1 a

regulator of autophagy at the initial stage. In addition, in cisplatin-sensitive squamous-cell-carcinoma cells ULK2 among other proteins was identified as a direct target of hsa-miR-885-3p, the binding with hsa-miR-885-3p induces ULK2 downregulation.[353,354] Moreover, ATG13, ATG9 and ATG2 also have binding sites for hsa-miR-885-3p.[355] The hsa-miR-181a has been shown to regulate autophagy upon starvation conditions and by the induction of rapamycin by targeting ATG5.[356] In addition, hsa-miR-30a plays an important role in autophagy regulation, by directly targeting Beclin-1 during vesicle nucleation.[351] Moreover, the overexpression of hsa-miR-30a reduces rapamycin-induced autophagy. In contrast, rapamycin-induced autophagy affects endogenous levels of hsa-miR-30a.[351,355] Furthermore, in HeLa cells cisplatin-induced autophagy was impaired by hsa-miR-30a, causing a reduction of tumour size in a liver tumour-xenograft.[357] Furthermore, in leukaemia hsa-miR-30a inhibited autophagy by downregulating the expression of both beclin-1 and ATG5, in contrast the knockdown of ATG5 and beclin-1 inhibited autophagy enhancing imatinib-induced cell death by mitochondria-dependent intrinsic apoptosis.[358,359] In addition, the impairment of hsa-miR-30a increased beclin-1 and ATG5 and reduced the cytotoxicity of the tyrosine kinase inhibitor imatinib.[358,359]

1.6 Rationale for the thesis

Prostate cancer (PCa)is the second most frequently diagnosed cancer in men in the world and the most common cancer in men in the United Kingdom (UK).[1,15] Moreover, PCa is the second leading cause of cancer-related deaths in the UK.[15] Initially, depending upon diagnosis the treatment of PCa involves androgen ablation therapy, however PCa inevitably relapses and results in the development of hormone-refractory metastatic disease (HRPC).[3] There is no cure for HRPC and current treatments are only palliative including the cytotoxic drugs mitoxantrone and docetaxel, and radiotherapy.[66] Therefore, novel therapeutic strategies with different mechanism of action are required for the improvement of PCa treatment.

Replication-selective oncolytic adenoviruses are a promising anticancer strategy with proven efficacy in cancer cell lines and tumour xenografts *in vivo*; anti-tumour efficacy has been shown to be highly improved in combination with

chemotherapeutics in numerous models of cancers including prostate cancer.[360] Several preclinical studies have shown that synergistically enhanced cell killing in response to combinations of oncolytic adenoviral mutants and chemotherapeutic drugs is mainly dependent on the expression of the viral E1A gene. Some examples are the enhancement of drug-induced apoptotic death in combination with AdΔΔ and *dl*922–947.[118,131,360] It has been demonstrated that E1A is essential both for induction of chemosensitization of cancer cells and for viral replication.[95,129,130,361] The E1A gene encodes five proteins generated by alternative splicing, of which the 13S and 12S variants are major forms. Importantly, E1A13S encodes the CR3 domain which is essential for viral induction of S-phase and consequently viral replication while E1A12S alone does not support viral replication.[75] However, both E1A13S and E1A12S can potently interact synergistically with mitoxantrone and docetaxel in PCa cells to enhance cell killing.[95] It has been established that specific regions in the E1A proteins bind to numerous cellular factors to regulate the host cell function and the viral life cycle, including binding to p300, p400 and pRb family proteins. However, the exact mechanisms of cell death induced by the combination of E1A-expression and chemotherapeutic drugs remain elusive.[95] In this thesis I focused on investigating the roles of specific E1A gene regions involved in the sensitization to the cytotoxic drugs mitoxantrone and docetaxel in PCa cell lines by employing non-replicating E1A12S-expressing mutants that were deleted in specific domains to prevent binding of cellular factors including p300, p400 and pRb. We hypothesised that by identifying specific E1A domains and/or cellular factors that are essential for synergistically improved cell killing in combination with the drugs, we would establish key mechanisms that could be explored in future studies to develop improved anti-cancer therapeutics and or biomarkers for disease progression or treatment responses.

1.6.1. Background to project

All E1A-deleted mutants used in my work had been previously constructed by a PhD student in the team (Dr. Miranda-Rota).[362] The mutants had been characterised and

sequenced and a great amount of sensitization and synergy data had also been produced.[362] I initially verified and expanded on these studies that resulted in a publication combining my own and the previous findings.[95] Part of these data are presented below (Section 1.6.2) to give a clear background to my further studies and the additional results leading to the publication are included in the Result (Sections 3.1 and 6.1) together with the data produced during the second part of my project.

1.6.1.a. Adenovirus-mediated sensitization to the cytotoxic drugs docetaxel and mitoxantrone is dependent on regulatory domains in the E1ACR1 gene-region.

Our first approach was to investigate several replicating mutants that were previously demonstrated to be defective in binding to p300/CBP (*dl*1101, *dl*1104), p400/p21 (*dl*1101, *dl*1102), pRb, p130 and p170 (*dl*922–947, *dl*1108), or pRb and p130 (*dl*1107), and determine cytotoxicity in human PCa cells.[95] In brief, we observed higher potency of replicating adenoviral mutants with small deletions in the E1A-region than of the clinically used E1B55K-deleted *dl*1520 mutant in both PC-3 and DU145 PCa cell lines (Fig. 17A). Moreover, in combination with the drugs mitoxantrone and docetaxel we determined that drug-induced cell killing was enhanced by the replicating E1A mutants with some variations between cell lines because of the differences in genetic alterations (Fig. 17C).[95]

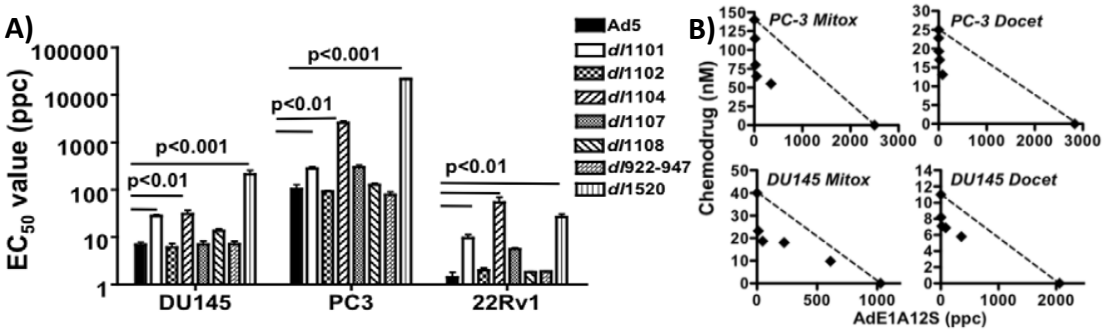

C)

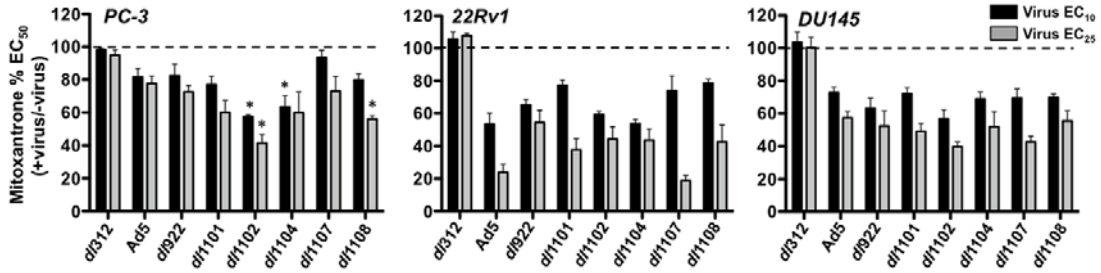

Figure 17. Potent cell killing of prostate cancer cell lines by replicating E1A-deletion mutants in combination with mitoxantrone. **A)**EC_{50} values for the replicating mutants were determined from dose-response curves and presented as averages ± SD, n = 3. Significantly different values compared to Ad5 are indicated. **B)** Isobolograms generated from EC50 values for combinations of the AdE1A12S mutant with mitoxantrone (Mit) or docetaxel (Doc) at four constant ratios (0.5. 2.5, 12.5 and 62.5 ppc/nM drug) in PC-3 and DU145 cells. The straight lines represent the theoretical values for additive effects and points below the line synergistic cell killing, one representative study (n = 3–4) **C)** Sensitization of the human PC-3, 22Rv1 and DU145 cells to mitoxantrone by fixed doses of each virus at EC10 and EC25. Data presented as percentages of mitoxantrone EC_{50} values in each cell line, averages ± SD, n = 3. Statistical analysis by one-way Anova, *p,0.05 for drug EC_{50} values that were significantly lower than the corresponding Ad5 values. The *dl*312 (DE1A) non-replicating virus served as negative control.

Previously, our group demonstrated potent synergistic cell killing with Ad5, *dl*1520 and E1ACR2-deleted mutants (*dl*922-947, AdΔΔ) in combination with mitoxantrone or docetaxel in PCa models.[95,118,131] The combination of cytotoxic drugs with the replicating E1A-deletion mutants effectively enhanced drug-induced cell killing.[95] We speculated that in addition to E1A, additional viral gene products or viral replication might contribute to the sensitization of PCa cells to the chemotherapeutic drugs and therefore, constructed expression plasmids with the small E1A12S under control of the CMV promoter. We found that the expression of E1A12S declined over time in transiently transfected PCa cells. However, we still observed potent synergistic cell killing in combination with both mitoxantrone and docetaxel immediately after transfection (Fig. 17B). These findings demonstrated that the small E1A12S protein was sufficient to promote synergistic cell killing in combination with apoptosis-inducing chemotherapeutic drugs. To enable in depth studies of the mechanism for this interaction we generated non-replicating AdE1A12S-expressing Ad5 mutants deleted in both E1B and E3 genes (to eliminate the transfection step and improve on E1A-expression); AdE1A1102, AdE1A1104 and AdE1A1108 that do not bind to p400,

p300/CBP and pRb, respectively. PCa cells infected with the selected mutants showed that all mutants except for AdE1A1104 were highly cytotoxic even in the absence of viral replication.[95] In combination with mitoxantrone and docetaxel, all mutants except AdE1A1104 caused significant sensitization to both drugs in three PCa cell lines, PC-3, DU145 and 22Rv1 (Fig. 18). Furthermore, studies *in vivo* using PC-3 xenografts and intra-tumoural administration of the replicating E1A-mutants combined with intra-peritoneal administration of docetaxel showed that the p300-binding region in E1A is essential for the synergistic sensitization of PCa cells as suggested by the findings in cultured cells both with the replicating and non-replicating E1A mutants (see Result section 3.1.7).

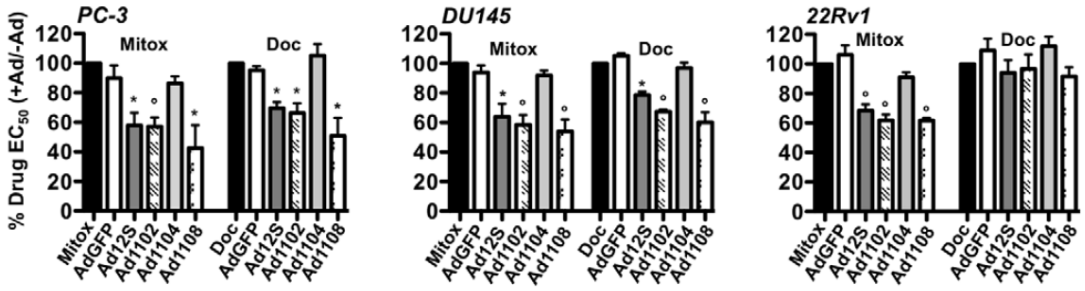

Figure 18. All replication-defective E1A12S mutants sensitize prostate cancer cells to mitoxantrone and docetaxel except the AdE1A1104 virus. Drug dose responses in each cell line were evaluated after infection with AdE1A12S, AdE1A1102, AdE1A1104, and AdE1A1108 mutants with AdGFP as negative control to determine changes in drug EC50 values. All cell lines were infected at doses killing ,10% of cells alone; PC-3 cells at 100 ppc (left panel), DU145 cells at 10 ppc (mid panel) and 22Rv1 cells at 2.5 ppc (right panel). Data represent averages 6SD, n = 4–5 independent experiments analysed by t-test comparing EC50 values for each combination to that of drug alone, expressed as percentages, *p,0.05 and up,0.01.

These findings enabled us to further investigate the mechanisms involved in the synergistic cell killing in PCa cells. Preliminary results indicated that the synergistic interactions resulted from activation of apoptotic pathways. However, we had also observed that both mitoxantrone and docetaxel increased the expression levels of LC3B-II, and indicator of autophagy when LC3B-I levels are decreased. Other members of the team (Adam V, unpublished data and thesis) had previously observed that the replication–selective AdΔΔ mutant could prevent these drug-induced increases in LC3B-II/I ratios. To this end we set out, in the second part of the project, to explore whether there was a link between increased apoptosis and

decreased autophagy that might cause the synergistically, enhanced cell killing in response to virus-drug combinations. In addition to standard molecular and laboratory approaches we also employed a miRNA screen to address this question and also explore a wider network of potential pathway regulators in response to the combination treatments. We performed these studies in the PC3 cell line which demonstrated the highest drug- and virus- resistance and also the greatest degree of synergistically enhanced cell killing in response to the combination treatments. The results from this screen will be described in section 3.2. The findings in this thesis together with additional future studies will aid in delineating the mechanisms responsible for E1A-mediated sensitization in PCa cells. We anticipate that, taken together, the findings will form the basis for future developments of improved therapies for prostate cancer.

1.7 Aims of this thesis

The overall aim of this work was to identify E1A regions that are involved in the sensitisation of prostate cancer cells, firstly to the cytotoxic drug mitoxantrone and secondly to docetaxel, while retaining cancer-selectivity. To further dissect the mechanisms involved in the enhancement of cell killing by the identification of cellular factors that are essential for the synergistic interactions, with the idea to develop improved therapies that target these cellular pathways.

- To determine if the observed effects in response to combination treatments with AdE1A1102 and AdE1A1104 are reproduced by the corresponding replicating mutants *dl*1102 and *dl*1104.
- To determine whether the viral mutants selectively sensitize prostate cancer cells but not normal cells.
- To verify that the deletions in *dl*1104 and AdE1A1104 (p300-binding region) abrogate drug sensitization (e.g. no enhancement of apoptosis).
- To verify the miRNA analysis and investigate the potential effects on cellular signalling pathways under sensitizing/synergistic conditions. For example, by determining changes in cell cycle progression, cell death and survival pathways, and by monitoring changes in protein expression of selected proteins that might be targeted by the identified miRNAs.

2. Materials and Methods

2.1. Cell Culture Conditions

The following human prostate cancer cell lines were used; PC-3 (grade IV adenocarcinoma bone metastasis, epithelioid morphology),[363,364] 22Rv1 (carcinoma epithelial cell line derived from serially propagated xenografts in mice after castration-induced regression and relapse of the parental, androgen-dependent CWR22, epitheloid morphology),[364,365] DU145 (derived from brain metastasis, epithelioid morphology)[364,366] and LNCAP (carcinoma from supraclavicular lymph node metastasis, fibroblastoid morphology).[364,367] All cell lines were obtained from American Type Tissue Culture Collection (ATCC, VA, USA) and Cancer Research UK (CRUK, Clare Hall, London, UK). Human ovarian cell lines Skov3.ip1 and Skov3 (obtained from Prof. Iain McNeish, Centre for Molecular Oncology), Skov3 was originally from CRUK Cell Services and Skov3.ip1 from Dr J Price (University of Texas MD Anderson Cancer Centre, TX, USA). The human embryonic kidney cell line HEK293 and the sub-line JH293 cells were obtained from CRUK Cell Services. All cell lines were cultured in Dulbecco's Modified Eagle Medium (DMEM; CRUK) supplemented with 10% foetal calf serum (FCS; Sigma-Aldrich, Chemie, Germany), at 37°C and 5% CO_2. Normal human bronchial epithelial (NHBE) and prostate epithelial cells (PrEC) cells were cultured following the manufacturer's protocol using the B-ALI™ Bronchial Air Liquid Interface Medium BulletKit™ and PrEGM™ BulletKit™, respectively (Lonza Ltd, Switzerland). All cell lines were authenticated by short tandem repeat (STR) profiling (LGC Standards, Middlesex, UK) during the course of this study and only verified cell stocks were used. The viral infections were performed in serum-free DMEM for 2h in 6-well plates and in 2% FCS in DMEM when cultured in 96-well plates.

Table 6. Expression of proteins in the human prostate cancer cell lines used in this thesis.

Protein	LNCaP	DU-145	PC-3	22RV1
AKT1	+	+	+	+
AR	+	-	-	+
BCL-2	+	-	+	+
CHK2	+	+	+	+
Cyclin D1	+	+	+	+
Cyclin E	+	+	+	+
ERK1	+	+	+	+
ERK2	+	+	+	+
GSK3ß	+	+	+	+
HDM2	+	+	+	+
JNK1	+	+	+	+
JNK2	+	+	+	+
MEK1	+	+	+	+
p21	+	+	+	+
p300	+	+	+	+
p38	+	+	+	+
p53	+	+	-	+
P-AKT	+	-	+	+
P-ERK1	-	+	-	+
P-ERK2	-	+	-	+
P-GSK3ß	+	+	+	+
PKA	+	+	+	+
PKC	+	+	+	+
P-p38	-	-	-	+
P-PKC	+	+	+	+
Pro-caspase-3	+	+	+	+
PSA protein	+	-	-	+
PTEN	-	+	-	+

Information obtained from [363,365,366,368,369].

2.1.a Skov3 and Skov3ip1

The ovarian cancer cell line Skov3 is a hypodiploid human cell line with 43 chromosomes and duplicates every 28h.[364] Moreover, Skov3 has been reported to be more infectible and more sensitive than its derived sub-clone Skov3ip1, in response to adenoviral infection.[370-373] Skov3ip1 were derived from ascitic tumour cells of nude mice bearing a Skov3 tumour. Furthermore, SKOV3ip1 cells were demonstrated to be more invasive and malignant than the parental Skov3 cell line.[373] Additionally, both cell lines are established as p53 null.[374] However, in a cDNA array 1557 genes were differentially expressed.[373] In Skov3ip1 cells 676 genes were upregulated and 881 downregulated compared to Skov3.[373] For example, HER2/neu was shown to be overexpressed in Skov3ip1 compared to Skov3, other genes found as differentially expressed were Pim-2, FGFR1 oncogene partner and Ras gene family members that were also upregulated in Skov3ip1.[373]

2.2 Virus preparation and viral assays

2.2.1 Viruses used in the study

The viruses used in this study and their characteristics are listed in Table 7 and Figure 19. Wild-type adenovirus species C type 5 (Ad5wt or Ad5), was used as control in many assays, Ad5wt virus expresses all adenoviral genes including the complete E1A gene.[81] Generation of the double-deleted mutant AdΔΔ (E1ACR2-region and E1B19K-gene deleted) has been described previously.[118]

The non-replicating, E1A-12S-expressing viruses used for this study do not have transcriptional activity, have the E1B and E3 genes deleted and were generated as described (Fig. 19; see appendix section 6 for characterization of viral mutants). The replicating *dl*1102 and *dl*1104 viruses were used in comparative assays with their non-replicating counterparts. The *dl*1102 and *dl*1104 have a *dl*309 backbone with the E3B genes deleted and express both E1A12S and E1A13S.[375-377]

Table 7. Virus used in this study and their genetic background

Virus	Nucleotide deletion	Amino acid deletion	Description
***d*l1102**	635-664	26-35	Does not bind p400. Express E1A13S and E1A12S
***d*l1104**	701-739	48-60	Does not bind p300. Express E1A13S and E1A12S
AdE1A1102	635-664	26-35	Does not bind p400. Express E1A12S
AdE1A1104	701-739	48-60	Does not bind p300. Express E1A12S
AdE1A1108	929-940	124-127	Does not bind pRb, p130 or p107. Express E1A12S
AdE1A12S	974-1229	140-185	Does not express CR3. Express E1A12S
AdGFP	448-1349	1-289	GFP gene under control of CMV promoter replacing E1A and E1B deleted
AdΔΔ	920-974/ 1,711- 2,236	120-140/ 289-464	CR2- and E1B19K-Deleted. Does not bind pRb, p130, p107and Bax/Bak

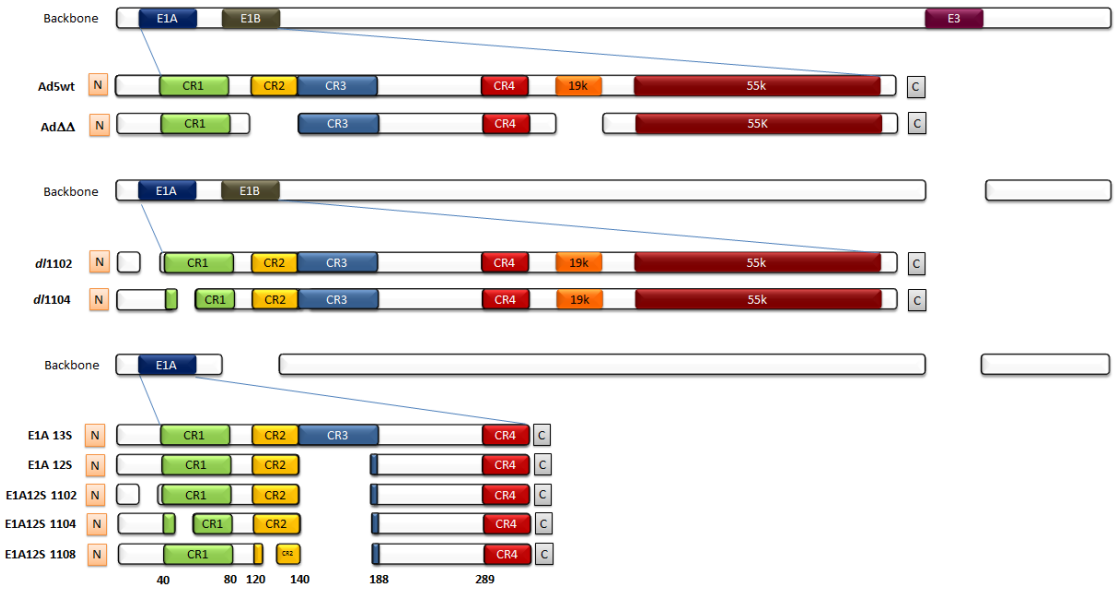

Figure 19. The AdΔΔ and the AdE1A12S replicating- and non-replicating mutants generated for our study. A549 cells were infected with Ad5 at 100ppc. The mRNA was purified from the cells 20h post-infection and was used to synthesise cDNA using Taqman Reverse transcription reagents and oligo-(dT) (Life Technologies Ltd, Applied Biosystems Division, Warrington, UK) for RT-PCR as described by the manufacturer. The reaction mixture was gel purified to separate 13S and 12S cDNA, followed by PCR-amplification of the cDNA corresponding to E1A12S. The pCR2.1-TOPO-12S was generated by insertion of the amplified and purified E1A12S cDNA for further amplification, digestion and isolation of the E1A12S gene that was cloned into a pShuttle-CMV vector (Stratagene, TX, USA). The pShuttle-CMV-E1A12S was linearized and co-transfected with the E1- and E3-deleted pAdEASY plasmid into BJ5183 electrocompetent bacteria (Stratagene), for homologous recombination according to the manufacturer's instructions (Stratagene). Generation of E1A1102, E1A1104 and E1A1108

cDNA was done by gene splicing by overlapping extension PCR (SOEing PCR). Primers were designed to generate the deletions corresponding to E1A1102, E1A1104 and E1A1108 and has been described previously.[95] The generated cDNAs for the E1A12S mutants were cloned into the pCR2.1-TOPO vector and viral mutants were produced as described for AdE1A12S.[95]

2.2.2 Viral production and characterization

2.2.2.a Primary expansion

Human Embryonic Kidney (HEK293) cells were seeded in a T175 flask in DMEM with 10% FCS and infected with 30µl of $CsCl_2$-purified stock-virus in 15 ml of 2% FCS in DMEM when cells were 75% confluent. Once the cells detached or showed cytopathic effect (CPE) approximately 48h post-infection, medium and cells were collected and stored at -80^{o}C.

2.2.2.b Viral Purification

Four T175 flasks with HEK293 cells (~ 30x10^{6} cells/flask) at 80% confluence were trypsinised and harvested for viral production. The HEK293 cells were seeded in a ten-layer Cell Factory (CF-10; Fisher Scientific) and incubated at 37°C and 5% CO_2. A parallel T175 flask was seeded as a reference to monitor cell growth for 48-72h. When cells reached 80% confluence they were infected with the primary expansion (section 6.2.2.1) in 2% FCS in DMEM and 48-72h post-infection, once cells detached, medium and cells were collected. The cell suspension was centrifuged at 2000rpm for 10min using a Sigma 6K15 centrifuge (Sigma, Germany) at 4^{o}C, the pellet was washed in PBS, centrifuged for 10 min at 1000rpm at 4^{o}C and was re-suspended in 12ml of 10mM Tris-HCl (pH 8.0) at 4^{o}C. The virus-containing cell suspension was freeze-thawed 3 times (N_2(l) and 37°C) in order to release viral particles remaining in cells and centrifuged using a Sigma 6K15 centrifuge for 10min at 6000rpm. The supernatant was collected and layered on a $CsCl_2$ gradient, consisting of 10ml of 1.25g/ml $CsCl_2$ and 7.6ml of 1.4g/ml $CsCl_2$ solution, and centrifuged for 2h at 25,000rpm at 15°C (Beckman SW32i swing-out rotor; Optima LE-80K ultracentrifuge). The thick bottom band of the gradient suspension was extracted by piercing the tube

with a 19G needle, and layered on top of a 2.5ml 1.35g/ml $CsCl_2$ solution, centrifuged for 15h at 40,000rpm at 15°C (Beckman SW55ti swing-out rotor; Optima LE-80K ultracentrifuge). The virus band was transferred to a tube and the volume made up to a total of 12ml with TSG buffer (96mM NaCl, 0.5mM Na_2HPO_4, 2.8mM KCl, 0.3mM $MgCl_2$, 0.5mM $CaCl_2$ and 30% (v/v) glycerol, pH7.5). The suspension was dialysed in a Slide-a-Lyser (Pierce Biotechnology, IL, USA) in a buffer containing 10mM Tris-HCl (pH7.5), 1mM $MgCl_2$, 150mM NaCl and 10% (v/v) glycerol) for 24h at 4°C, to remove $CsCl_2$. The purified virus was removed from the dialysis cassette, aliquoted and stored at -80°C.

2.2.2.c Viral particle (vp) determination

Viral particles were determined by measuring the DNA content of the viral preparation using the Quanti-iT Pico Green dsDNA Assay Kit (Invitrogen). Lambda-phage DNA (provided with the kit) was used for standard dilutions starting from 750ng/ml in 5-fold serial dilutions. Viral stocks were undiluted (neat) or diluted in TE buffer (10 mM Tris-HCl, 1 mM EDTA, pH 7.5) at A) 1:2, B) 1:6 and C) 1:10 dilutions, and each sample was assayed in triplicates in 96-well plates. The Pico Green reagent diluted 1:200 (100 μl) was added to each well. The absorbance of the samples was determined at 535nm after excitation at 485nm using the Tecan Infinite F200 plate-reader (Mannedorf, Switzerland) with the Magellan Software version 6.3. The DNA concentrations of the lambda-phage DNA-dilutions were plotted versus fluorescence using the GraphPad Prism software. Viral particle counts (vp/ml) were calculated by linear regression analysis taking the dilution of the samples into account, and assuming that 1 μg DNA = $2.7x10^{10}$ viral particles (vp).

2.2.2.d Determination of infectious units (pfu)

A limiting dilution tissue culture assay, $TCID_{50}$ (tissue culture inhibitory dose 50%), was used to determine viral replication. JH293 cells (a sub-clone of the HEK293 cell line that has better adherence properties in monolayer culture) were seeded at a

density of $1x10^4$ cells/well (96-wells) in 200 μl of 10% FCS in DMEM and incubated at 37°C in 5% CO_2 for 24h in triplicate plates. The purified viral mutants were added to the top row (12 wells) in 20μl aliquots from a pre-diluted sample (diluted in 0% FCS in DMEM), mixed and 20μl transferred to the next row of wells and so on resulting in serial 10-fold dilutions down the plate, leaving the last row of wells uninfected as control cells. Samples were diluted in the range from $1x10^2$ to $1x10^{13}$. A previously characterized Ad5wt control virus (stock) with known activity was always included as a positive control, diluted $1x10^7$ times in 0% FCS in DMEM. The plates were incubated for up to 10 days (minimum 7 days) when each well was scored for cytopathic effects (CPE). The titre of each sample was calculated with a modified Karber-Spearman equation and the results were expressed in plaque-forming units (pfu)/ml [378].

$\text{Log TCID}_{50} = A - D\,(S - 0.5)$

Where,

A = Log of the highest dilution showing CPE in more than 50% of the wells

D = Log of the dilution factor.

S = summation of the proportion of positive wells in each row.

2.2.2.e Identification of viral genomes by PCR

Table 8. Set of primers for viral characterization.

PRIMER SET	5' PRIMER	3' PRIMER	Wt BAND (bp)	MUTANT BAND (bp)	Target sequence
1	5'476	3'853	Ad5=377	*1102=348 1104=339	E1A start
2	5'767	3'1029	Ad5=262	**CR2-deletion = 236	E1A-CR2
3	5'1069	3'1453	Ad5=384	AdE1A12S=224	E1A end
4	5'1554	3'2086	Ad5=532	AdΔΔ=314	E1B-19K
5	5'2073	3'2440	Ad5=367	-	E1B-55K
6	5'2383	3'3434	Ad5=1051	-	E1B-55K
7	5'29915	3'31038	Ad5=1123	dl1102/ dl1104=937	E3B
8	5'28715	3'29135	Ad5=420	-	E3-gp19K
E1A	5'448	3'1349	Ad5= 1Kbp	E1A12S=800	E1A

*Deletion 1102= *dl*1102/AdE1A1102 and 1104= *dl*1104/AdE1A1104
**Deletion in CR2=AdΔΔ and AdE1A1108

To characterize the viral mutants, identity was determined by qualitative PCR. Viral DNA was extracted from 200 µl of purified virus using the DNA Blood Mini Kit (Qiagen, West Sussex, UK) according to the manufacturer's protocol. Eight primer sets specific for Ad5 and one E1A-specific primer set were used for each viral mutant (Table 8). Each sample (30µl of PCR-mix) was incubated with the Advantage 2 PCR Kit (Clontech, CA, USA) and amplified (Gene Amp PCR system 9700; Life Technologies Ltd, Applied Biosystems). Amplified products were analysed together with a Quick-Load® 100 bp DNA Ladder (New England Biolabs) on a 1.5% agarose gel in the presence of Ethidium Bromide (EtBr).

2.2.3 Viral infection of cells and preparation of lysates

Cells were infected with the non-replicating AdE1A12S, AdE1A1102, AdE1A1104, AdE1A1108, and AdGFP (Fig. 19) at 2.5 ppc for 22Rv1 or 100ppc for PC-3, in 1ml/well (6-wells) of 0% FCS in DMEM. After 2h of infection, medium was aspirated and exchanged with 2ml/well of mitoxantrone at 50nM (Onkotrene, Baxter, Norfolk, UK)

in 10% FCS-DMEM was added for 48h. The cells were washed with PBS, trypsinised, centrifuged at 1200rpm in an Allegra X-22 Centrifuge (Beckman Coulter, CA, USA) and the pellet was lysed with 100μl of lysis Buffer (1mM EDTA, 0.01M Na_3PO_4, 0.150M NaCl, 1%NP40 v/v, 1% Sodium Deoxycholate w/v, 0.1% SDS w/v, including a PhosSTOP Phosphatase Inhibitor Cocktail and an EDTA-free Protease Inhibitor Cocktail Tablets (ROCHE diagnostics, West Sussex, UK), placed on ice for 30 min, and stored at -80^{o}C. Total protein was quantified by diluting 2μl of the whole cell extract in 200μl of Bradford Reagent (Bio-Rad, Hertfordshire, UK), diluted 1:5 in distilled H_2O per well in a 96 well plate. A standard curve (0, 1, 2, 2.5, 3, 3.5 and 4 μl), using the 1:5 reagent dilution was prepared with 1μg/μl BSA (Sigma-Aldrich). The absorbance was determined at 595 nm (Beckman DU520 spectrophotometer) and samples were quantified by generating a standard curve and adjusting the values with a linear regression of the standard curve of absorbance *vs* concentration. Samples were diluted to a final concentration of 1μg/μl in NuPAGE 4x lithium dodecylsufate (LDS) sample buffer (Invitrogen) and distilled water.

2.2.4 Immunoblotting (Western blotting)

Polyacrylamide gels were prepared at 10-12% (dependent on protein size) and samples were loaded; 20μg total protein/well for each sample. The samples were separated by electrophoresis at 100-150V for 1h in a Tris-glycine-SDS-PAGE buffer solution. The separated samples were transferred from the gel to a Polyvinylidene Fluoride membrane (PVDF, Millipore) using a Trans-Blot Semi-Dry System (Bio-Rad) for 45 min at 20V. The membranes were incubated for 5 min in methanol and washed in PBS containing 0.01% Tween (PBS-Tween), 6 x 5 min. The membranes where incubated with the primary antibodies (Table 9), in PBS-Tween containing 5% BSA (Sigma-Aldrich) overnight at 4°C, washed, incubated with the respective secondary antibodies (Table 9) at a 1:2000 dilution for 1h in PBS-Tween-BSA, washed and incubated for 1 min with the Amersham ECL Plus™ Western Blotting Detection Reagents reagent. The bands were detected with Super RX Fuji Medical X-Ray Film (Fujifilm; Düsseldorf, Germany), developed at different time points with a Curix 60 Developer (Agfa, Middlesex, UK) or by using the Syngene equipment (Synoptics Ltd,

Cambridge, UK) to scan for chemiluminescence and to quantify protein expression relative to loading controls (Gene Tools version 4.01; Synoptics Ltd, Cambridge, UK).

Table 9. List of antibodies used in this thesis.

MW of target protein in kDa	Antibody	Species	Type	Dilution in 1.5% BSA-TBS-Tween 0.01%	Supplier
43	Actin	goat	primary	1:2000	Santa Cruz Biotechnology, Inc.
39	Ad5 E1A	mouse	primary	1:200	Neomakers, CA USA
60	AKT	rabbit	primary	1:1000	Cell Signaling Technology, Inc.
28	Bcl-2	rabbit	primary	1:500	Cell Signaling Technology, Inc.
35,19,17	caspase3	rabbit	primary	1:500	Cell Signaling Technology, Inc.
54	Cyclin A	rabbit	primary	1:500	Santa Cruz Biotechnology, Inc.
62	Cyclin B	mouse	primary	1:200	Abcam
37-38	Cyclin D	rabbit	primary	1:200	Santa Cruz Biotechnology, Inc.
53	Cyclin E	mouse	primary	1:200	Santa Cruz Biotechnology, Inc.
90	foxo3a/FKHRL1	rabbit	primary	1:1000	UBI
17, 19	LC3B-I/II	rabbit	primary	1:2000	Abcam
21	p21	mouse	primary	1:200	Cell Signaling Technology, Inc.
53	p53	mouse	primary	1:200	Santa Cruz Biotechnology, Inc.
62	p62/SQSTM1	mouse	primary	1:500	Santa Cruz Biotechnology, Inc.
60	p-AKT (ser473)	rabbit	primary	1:1000	Cell Signaling Technology, Inc.
116-89	parp	rabbit	primary	1:500	Cell Signaling Technology, Inc.
53	phospho-p53 (ser15)	rabbit	primary	1:500	Cell Signaling Technology, Inc.
32/cleaved 17-12	Pro-caspase 3	rabbit	primary	1:200	Santa Cruz Biotechnology, Inc.
170	Topoisomerase IIa	mouse	primary	1:200	Santa Cruz Biotechnology, Inc.
55	Tubulin	mouse	primary	1:10000	Abcam
NA	Anti-goat-HRP	rabbit	secondary	1:2000	Dako
NA	Anti-mouse-HRP	rabbit	secondary	1:2000	Dako
NA	Anti-rabbit-HRP	goat	secondary	1:2000	Dako

2.2.5 Cell viability assay

The prostate cancer cell lines PC-3, DU145 ($1x10^4$ cells/well) and 22Rv1 ($2x10^4$ cells/well) were seeded 24h prior to treatment and infection in 96-well plates in triplicates to perform cell viability assays. The cells were infected with 5-fold serial dilutions of viruses and drugs at initial concentrations of 200µM for mitoxantrone and $1x10^5$ppc for each virus. Untreated cells and wells containing medium alone were used as controls, for total viable cells and background (medium) respectively. Six or three days post-treatment, the CellTiter 96$^{(R)}$ AQueous MTS reagent (Promega Southampton, UK) was added to the plates. The tetrazolium salt MTS, [3-(4, 5-dimethylthiazol-2-yl)-5-(3-carboxymethoxyphenyl)-2-(4-sulfophenyl)-2H-tetrazolium, is reduced to a soluble formazan compound by mitochondrial dehydrogenases

present in metabolically active cells, a reaction catalysed by phenazine methosulfate (PMS), an electron coupling reagent. The soluble formazan compound absorbs light at 490nm and the number of living cells is directly proportional to the concentration in the sample. The medium of the treated cells in the 96-well plates was replaced with 100µl per well of the MTS solution (80µl DMEM, 20µl MTS and 1µl PMS per well). After 2-4h of incubation at 37°C and 5% CO_2 absorbance was measured in an OpsysMR plate reader (Dynex Technologies Inc, Chantilly, VA, USA). The absorbance values were processed by subtracting the absorbance values of wells with medium alone (background signal) and expressed as percentages of the absorbance of untreated cells (viable cells = 100%). The data were analysed by generating dose-response curves for each treatment using GraphPad Prism5.01 (GraphPad Software, CA, USA) to generate EC_{50} values (effective dose killing 50% of cells).

2.2.5.a Combination studies

For the combination assays, cells were seeded in 96-well plates and after 24h the cells were treated at selected concentrations based on the results from dose-response curves and EC_{50} values. Concentrations that killed <30% of cells were chosen. PC-3 cells were treated with mitoxantrone from 200 - 2000nM and infected with viruses at 50 - 4000ppc, both alone and in combination. The 22Rv1 cells were treated with mitoxantrone from 50 - 1000nM and infected with viruses at 25 - 500ppc alone and in combination. NHBE and PrEC cells were treated with 200nM mitoxantrone and infected with 5ppc and 10ppc with replicating and non-replicating viruses alone or in combination. Three days post-treatment the MTS assay was performed to determine cell viability. The data was analysed for percentage cell death and plotted as bar graphs for each treatment using GraphPad Prism 5.01. Theoretical additive values were estimated for each combination and dose by adding the averages of viable cells for drug and virus. Statistical significance was determined by Students t test ($p<0.01$).

2.2.6 Synergy Assays

To quantify cell death and determine synergistic interactions, the PC-3 ($1x10^4$ cells/well) and 22Rv1 ($2x10^4$ cells/well) cells were seeded in 96-well plates in triplicates. Viruses (*dl*1102, *dl*1104, AdE1A12S, AdE1A1102 or AdE1A1104) (Fig. 19) and mitoxantrone were added to the cells either alone or in combination at fixed ratios to enable determination of the combination index (CI) using the quantitative isobologram method, as previously described.[361,379-381] Viruses and drugs were diluted five-fold starting at concentrations of 200µM for mitoxantrone and $1x10^5$ppc for each virus (Table 10). The fixed ratios of virus to drug were 62.5, 12.5, 2.5 and 0.5 ppc/nM, based on previous studies in our group.[95] Untreated cells and wells containing medium alone were used as controls, for total viable cells and background (medium) respectively.

Table 10. Full dose ranges of virus and drug in the 96-well plate layout. Combinations of 5-fold dilutions of viral mutants with drug at fixed ratios.

Full dose range used in the experiment														
Virus	V1	V2	V3	V4	V5	V6	V7	V8	V9	V10	V11	V12		
	1.0E+05	2.0E+04	4.0E+03	8.0E+02	1.6E+02	3.2E+01	6.4E+00	1.3E+00	2.6E-01	5.1E-02	1.0E-02	2.0E-03		
Drug	D1	D2	D3	D4	D5	D6	D7	D8	D9	D10	D11	D12	D13	D14
	2.0E+05	4.0E+04	8.0E+03	1.6E+03	3.2E+02	6.4E+01	1.3E+01	2.6E+00	5.1E-01	1.0E-01	2.0E-02	4.1E-03	8.2E-04	1.6E-04

Combination arrangement												
	Col 1	Col 2	Col 3	Col 4	Col 5	Col 6	Col 7	Col 8	Col 9	Col 10	Col 11	Col 12
Row1	medium	control cells	V1	V2	V3	V4	V5	V6	V7	V8	V9	V10
Row2	medium	control cells	D1	D2	D3	D4	D5	D6	D7	D8	D9	D10
Row3	medium	control cells	V3	V4	V5	V6	V7	V8	V9	V10	V11	V12
	medium	control cells	D3	D4	D5	D6	D7	D8	D9	D10	D11	D12
Row4	medium	control cells	V3	V4	V5	V6	V7	V8	V9	V10	V11	V12
	medium	control cells	D4	D5	D6	D7	D8	D9	D10	D11	D12	D13
Row5	medium	control cells	V2	V3	V4	V5	V6	V7	V8	V9	V10	V11
	medium	control cells	D4	D5	D6	D7	D8	D9	D10	D11	D12	D13
Row6	medium	control cells	V2	V3	V4	V5	V6	V7	V8	V9	V10	V11
	medium	control cells	D5	D6	D7	D8	D9	D10	D11	D12	D13	D14

Mixture ratio (Virus ppc/Drug nM)	
Virus alone	
Drug alone	
V3:D3	0.50
V3D4	2.50
V2D4	12.50
V2D5	62.50

Six days post-treatment the MTS reagent was added to the plates to determine cell death. The data were analysed by generating dose-response curves and EC_{50} values for each treatment using the GraphPad Prism software. To determine the nature of the interactions (synergistic, additive or antagonistic effects), isobolograms were generated by plotting the respective EC_{50} value for each agent alone and in combinations. The results were analysed according to Chou and Talalay[379] and as previously described by our team.[380] Virus and drug interactions were considered

synergistic when CI≤0.9, additive for 0.9<CI<1.1 and antagonistic when CI≥1.1.CI values were calculated using a formula modified from:[381]

$$CI = \frac{EC_{50}V_c}{EC_{50}V_a} + \frac{EC_{50}D_c}{EC_{50}D_a},$$

Where

$EC_{50}V_a$ = EC_{50} for the virus alone
$EC_{50}V_c$ = EC_{50} for the virus in combination
$EC_{50}D_a$ = EC_{50} for the drug alone
$EC_{50}D_c$ = EC_{50} for the drug in combination

2.2.7 Infectability assay in cancer cell lines

The prostate cancer cells lines PC-3 and 22Rv1 and the ovarian cancer cell lines Skov3 and Skov3ip.1 were seeded in 6-well plates at a density of $1x10^5$ cells per well. After 24h, cells were infected with the non-replicating AdGFP at a fixed dose of 0, 10 and 100ppc in serum free DMEM for 2h. Medium was replaced with 10% FCS in DMEM after infection and cells were incubated for 48h at 37°C and 5% CO_2. After 48h, cells were harvested for flow cytometry analysis. The cells were washed with cold PBS and detached by trypsinisation, DMEM supplemented with 10% FCS was added to neutralise trypsin, cells were centrifuged at 1700rpm in an Allegra X-22 Centrifuge (Beckman Coulter, CA, USA) for 3min, the pellets were washed with PBS and centrifuged for 1700rpm (Allegra X-22 Centrifuge; Beckman Coulter, CA, USA) for 3min and re-suspended in PBS for FACS analysis. A total of $1x10^4$ events (cells) were acquired for each condition using a FACSCalibur (Becton Dickinson, Cowley, UK) and analysed with Cell Quest Pro Software (Becton Dickinson). The GFP-positive cells were detected and quantified at 525nm using the green fluorescence channel 1 (FL-1).

2.2.8 Reverse transcription quantitative PCR (RT-qPCR)

The PC-3 and 22Rv1 cells were seeded in 6 well plates at $2x10^5$ and $4x10^5$ cells/well, respectively. The cells were infected at 400ppc for PC-3 and 10 ppc for 22Rv1 cells in

serum free DMEM, 2h post-infection medium was changed and cells were treated with mitoxantrone at 50nM in 10% FCS in DMEM for 48h. The cells were trypsinised and processed for RNA extraction according to the RNeasy mini kit handbook protocol for total RNA extraction (**QIAGEN**® West Sussex, UK). RNA samples were treated to remove any DNA contamination with RNAse-free DNase Treatment and Removal Reagent, (DNA-*free*™; Ambion, Life Technologies, CA, USA). RNA concentrations were determined using a Nanodrop® ND-1000 Spectrophotometer (Labtech International Ltd, East Sussex, UK), measuring the absorbance ratio of 260nm/280nm where a ratio close to 2.0 implies RNA purity (DNA free). Generation of cDNA was carried out using the TaqMan® Reverse Transcription kit (Life Technologies, AB) according to the manufacturer's protocol using Oligo$(dt)_{16}$ as primers. The cDNA samples were prepared for RT-qPCR analysis for p21-CDKN1A using the Forward primer: TGGAGACTCTCAGGGTCGAAA (21bp) and the Reverse primer: GGCGTTTGGAGTGGTAGAAATC (22bp) (Life Technologies Ltd, Invitrogen division, Paisley, UK), using *Power* SYBR® Green PCR Master Mix (Life technologies Ltd, AB) according to the manufacturer's protocol. Data were normalized against the respective GAPDH value to obtain ΔCt values. The ΔCt value of each sample was normalized against the control untreated samples to get the ΔΔCt value, used to calculate the fold change that was expressed as percentages of the control.

$\Delta Ct = Ct_{Sample} - Ct_{Control}$

$\Delta\Delta Ct = \Delta Ct_{sample} - \Delta Ct_{control}$

Normalized target gene expression in fold change $= 2^{-\Delta\Delta Ct}$

Where ΔCt_{sample} is the Ct value for any sample normalized to an endogenous housekeeping gene and $\Delta Ct_{control}$ is the Ct value for the calibrator also normalized to the endogenous housekeeping gene.

Fold change percentage $= (2^{-(\Delta\Delta Ct)})x100$

2.2.9 Mitochondrial membrane potential depolarization

PC-3 cells were seeded 24h prior to treatments in 6-well plates at a density of $1x10^5$cells/well. The cells were infected in duplicates with AdE1A12S virus for 2h in

1ml/well of serum-free DMEM. After 2h, the cells medium was changed to 10% FCS in DMEM with or without the addition of mitoxantrone (1000nM). Staurosporine at 1nM (Sigma-Aldrich) and rapamycin 100nM (Sigma-Aldrich) were included as positive controls for apoptosis and autophagy, respectively. A pan-caspase-inhibitor zVAD-fmk (25μM; Calbiochem, CA, USA) was also used as a caspase-cascade control. After 96h, medium was collected from each well; cells were washed with PBS, trypsinised and transferred to 5ml tubes (BD Falcon™, USA). The cells were centrifuged at 1200rpm in an Allegra X-22 Centrifuge (Beckman Coulter, CA, USA), washed with PBS and stained with Tetramethylrhodamine ethyl ester (TMRE; Sigma-Aldrich). TMRE (1mg/ml), 40μl, was added to the cell suspension (500μl of PBS) and incubated for 30min at 37°C in the dark. After 30min the cells were washed with PBS and stained with 1μg/ml of 4',6-diamidino-2-phenylindole (DAPI; Sigma-Aldrich) for 10min at 24°C. The cells were assessed in a BD LSRFortessa™ (Becton Dickinson, Oxford, UK) gated with lasers 585nm versus 445nm and analysed by the BD FACSDiva™ software (Becton Dickinson).

2.2.10 MicroRNA (miRNA) analysis

For the microRNA (miRNA) array analysis PC-3 cells were seeded in 6-well plates. After 24h, cells were infected with AdE1A12S (100ppc) or treated with mitoxantrone at 50nM (concentrations previously shown to sensitize PC-3 cells and enhance cell killing [95]) or a combination of both agents. Duplicate wells were harvested for each condition and the 24h time point was repeated in a second experiment. The cells were harvested at 24h and 48h post-infection and total RNA was extracted. The RNA samples were analysed for changes in miRNA expression by LC Sciences (TX, USA), using a miRNA microarray platform with 850 human miRNAs based on the Sanger miRNA database.[382] From the generated and analysed original data (LC Sciences), we made a selection of miRNAs that had a signal intensity of 500 or higher and that were statistically significant ($p<0.01$; Students t-test). To determine the differences in expression between the various treatments, the results were processed and expressed as a ratio; single agent-treated/untreated, combination-treated/untreated, combination-treated/the sum of the single agents, and the 24h

compared to 48h values. The ratios were converted into log2 scale to assess differential directions and magnitudes.[383] A positive log2 value indicates an up-regulation and a negative log2 value indicates downregulation. Accessible databases and tools such as Ensembl.org, mirbase.org, PubMed, mirTarBase.org, TargetScan Human, miRecords, miRDB, microRNA.org, transmir miR2disease and published reports,[231,233-238,384,385] were used for selection of relevant miRNAs and their targets. We also took into account whether the miRNAs had been previously reported to play a role in specific pathways in cancer cells and tissue with special focus on prostate cancer.

3. Results

3.1 AdE1A12S requires p300 to sensitize prostate cancer cells to chemotherapeutic drugs

We have previously demonstrated that E1A-expression alone was sufficient to cause synergistic cell killing in combination with mitoxantrone and docetaxel.[131,362] To identify specific E1A-regions responsible for the sensitisation of PCa cell lines to cytotoxic drugs, several AdE1A12S non-replicating mutants with various E1A deletions (1102, 1104 and 1108; Fig. 19) and without E1B and E3 genes were previously generated in our group.[362] The absence of the E1A13S, E1B and E3 genes enabled the study of the E1A deletions without interference from additional viral proteins or viral replication.

The mutant AdE1A1102 does not bind p400, a co-transcription factor involved in ATP-dependent chromatin remodelling activity and cell cycle control. AdE1A1104 does not bind p300, a co-transcription factor with intrinsic histone acetyltransferase (HAT) activity. Furtheremore, AdE1A1108 does not bind the tumour suppressor pRb protein which inhibits cell cycle progression.[83] The conclusions from these studies were that AdE1A1104 was unable to sensitize PCa cells to mitoxantrone and docetaxel. In contrast, AdE1A1102 and AdE1A1108 enhanced mitoxantrone and docetaxel induced cell death, both in treatment-sensitive (22Rv1) and more resistant (PC-3) PCa cells.[95]

3.1.1 Mitoxantrone induces cyclins A and B in PC-3 cells but not in 22Rv1 cells.

Previous data demonstrated that the combination of mitoxantrone with non-replicating E1A mutants increased the G2/M cell population, in comparison to treatment with mitoxantrone or virus alone, in both PC-3 and 22Rv1 cells.[95] This increase was only detected when infecting with AdE1A12S, AdE1A1102 and AdE1A1108 that sensitized the cells to mitoxantrone. AdGFP was used as control

virus and did not induce changes in phase distribution, resulting in the same profile as mitoxantrone alone.[95]

In order to further extend these findings, we explored the regulation of cell cycle, by determining the expression levels of cell cycle proteins under similar treatment conditions, in both PCa cell lines (PC-3 and 22Rv1).

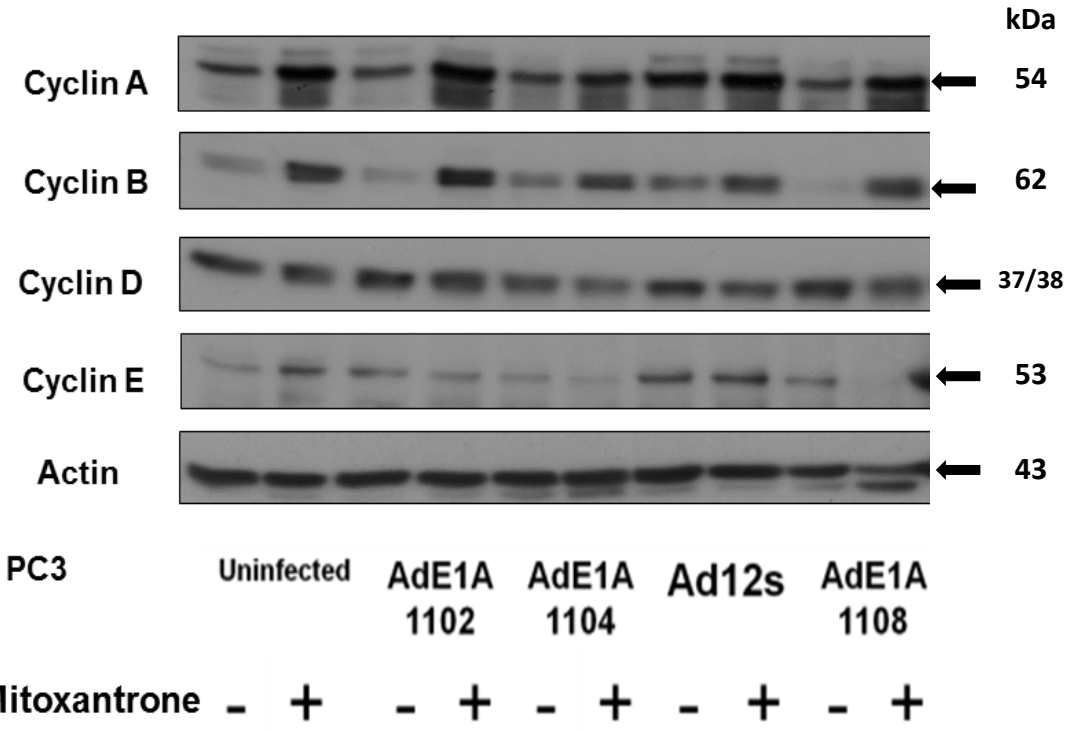

Figure 20. Changes in expression patterns of cell cycle regulatory proteins in PC-3 cells infected with non-replicating E1A12S mutants (100ppc) in combination with Mitoxantrone (50nM) for 48h. SDS-PAGE gel loaded with 20μg total protein/lane per sample. Immunoblot is representative of three experiments.

In PC-3 cells, treatment with mitoxantrone for 48h induced expression of cyclins A and B (Fig. 20). However, this induction of cyclins A and B was not altered in cells infected with all viral mutants. Mitoxantrone slightly attenuated cyclin D expression both alone and in combination with all viral mutants (Fig. 20). The viruses did not induce detectable changes in cyclin D levels. Moreover, Cyclin E was upregulated in cells treated with mitoxantrone alone, but not in combination with the viral mutants (Fig. 20). Only infection with AdE1A12S, AdE1A1102 alone appeared to induce cyclin E (Fig. 20). Moreover, infection with AdE1A1108 in combination with mitoxantrone reduced the levels of cyclin E. These data indicate that the E1A12S mutants had

minor effects on expression levels of cyclins, while mitoxantrone induces cyclin A and B, as expected due to previously generated cell cycle data.[95] In addition, G2/M phase cell cycle arrest has shown to be induced by the overexpression of p21,[386] therefore we investigated changes in the protein-levels of p21 under chemosensitizing conditions. However, the expression of p21 was below the limit of detection in PC-3 cells by immunobloting. In summary, increases in the G2/M cell population in PC-3 cells treated with the combination of the viral mutants and mitoxantrone could not be conclusively explained by observed changes in cell cycle-related proteins. Therefore, further experiments were performed to unravel the mechanisms for synergy.

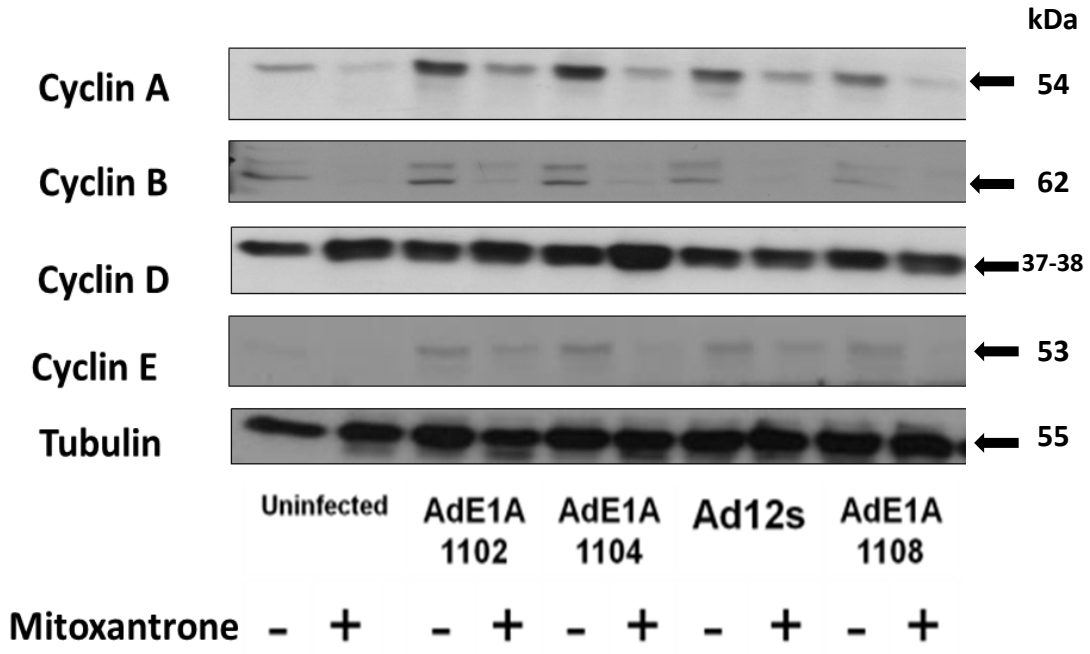

Figure 21. Changes in expression patterns of cell cycle regulatory proteins in 22Rv1 cells infected with non-replicating E1A12S mutants in combination with Mitoxantrone (50nM) for 48h. SDS-PAGE loaded with 20μg total protein/lane per sample. Immunoblot is representative of three experiments.

In contrast to the findings in PC-3 cells, mitoxantrone decreased the expression levels of cyclin A and B in 22Rv1 cells (Fig. 21). All viral mutants induced an increase in expression of cyclin A compared to uninfected cells, but was reduced in combination with mitoxantrone. Moreover, none of the viruses induced cyclin B while mitoxantrone decreased the expression and remained low in the presence of virus (Fig. 21). We did not observe significant changes in expression levels of Cyclin D with viruses alone or in combination with mitoxantrone. Although, a tendency to higher

Cyclin D levels was noted in mitoxantrone-treated cells. Moreover, Cyclin E was slightly induced by infection with all viral mutants and combination with mitoxantrone appeared to attenuate this induction. In summary, viral infection induced cyclins- A and E and D. Moreover, cyclin B was not induced by AdE1A12S and AdE1A1108. Additionally, mitoxantrone strongly attenuated the expression of all cyclins (except possibly Cyclin D). However, these effects were not specific for any of the viral mutants and may reflect cellular changes in response to infection only.

Figure 22. Changes in expression patterns of p21 in 22Rv1 cells infected with non-replicating E1A12S mutants. in combination with Mitoxantrone (50nM) or docetaxel (1nM) for 48h. SDS-PAGE loaded with 20μg total protein/lane per sample. Immunoblot is representative of three experiments.

In addition, we assessed the expression of p21 in 22Rv1 cells. Treatment with mitoxantrone alone and in combination with all mutants induced p21 (Fig.22). Infection with the viral mutants induced p21 to a lesser degree than mitoxantrone, except AdE1A1108 and AdGFP where the expression of p21 was similar to that of the untreated control cells. Additionally, the expression of p21 was induced by docetaxel alone and in combination with the AdE1A12S mutants, except AdE1A1108 and AdGFP, where AdE1A1108 attenuates mitoxantrone-induced p21 expression (Fig. 22). The induction of p21 expression in response to docetaxel treatment was similar to virus-induced expression, although less than levels induced by mitoxantrone. Moreover, no differences were observed for the various mutants in combination with docetaxel or mitoxantrone. In summary, mitoxantrone induces p21 contributing to cell cycle arrest in 22Rv1 cells, although, the involvement of the viral mutants in the expression of p21 was not clear and further studies would be needed for conclusive data.

3.1.2 The AdE1A12S and AdE1A1102 viral mutants enhance mitoxantrone-induced p21 mRNA expression in PC-3 cells but not in 22Rv1 cells.

Since the levels of expression of p21 in PC-3 cells were too low to be detected by immunoblotting, we assessed the expression of p21 mRNA by RT-qPCR in both PC-3 and 22Rv1 cells.

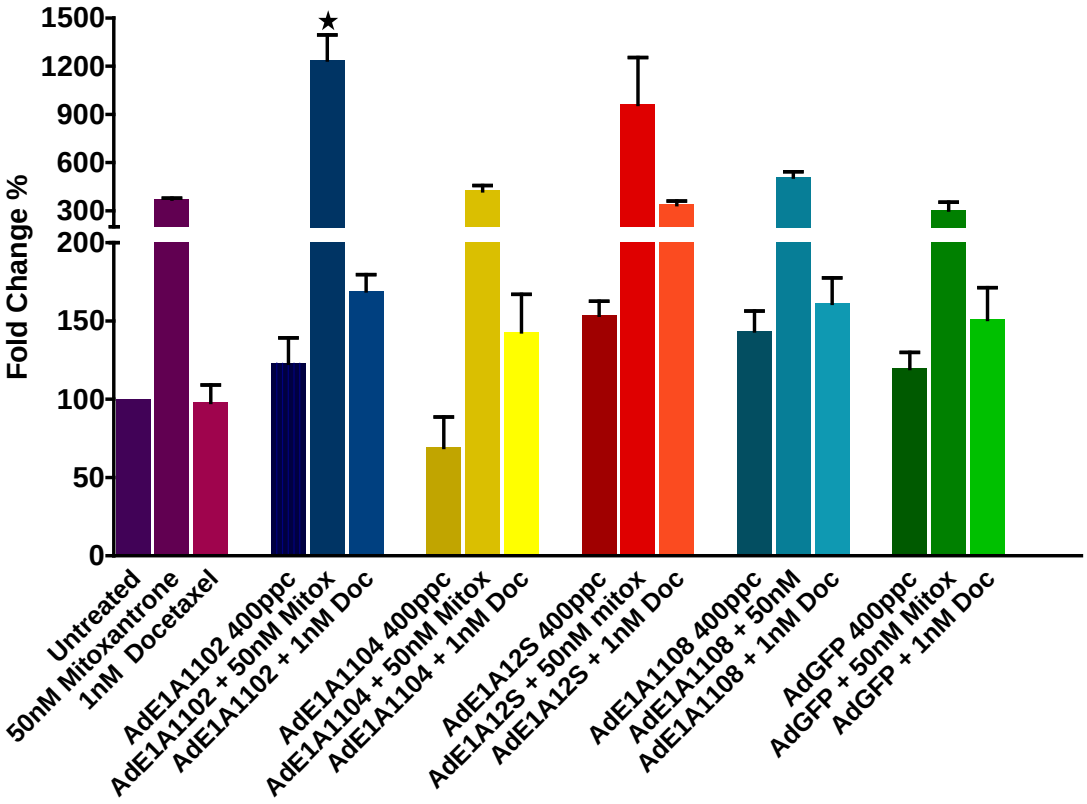

Figure 23. Fold change percentage (FC %) of p21 mRNA expression in PC-3 cells. PC-3 cells infected with AdE1A viral mutants alone and in combination with 50nM of mitoxantrone or 1nM docetaxel for 48h. Data points were normalized as described in section 6.7. n=3. Student t-test, significant compared to mitoxantrone alone *p<0.05 .

PC-3 cells treated with mitoxantrone showed an induction of p21 in both infected and uninfected cells (Fig. 23). The treatment with mitoxantrone induced the expression of p21 by 3-fold compared to untreated cells, the combination with AdE1A1104 showed similar expression as mitoxantrone alone (Fig. 23). The combination of mitoxantrone with AdE1A1102 and AdE1A12S showed an enhancement in p21 expression of 12- and 9-fold respectively in comparison to

untreated cells. The combination of mitoxantrone with AdE1A1102 was significantly increased compared to mitoxantrone alone (Fig. 23). Infection with AdE1A1102, AdE1A1108 and AdE1A12S viruses showed a slight increasing trend in the expression of p21 compared to untreated cells, but not by AdE1A1104. The treatment with docetaxel alone did not induce p21. In contrast, the expression of p21 was enhanced with docetaxel in combination with all viruses. Docetaxel in combination with AdE1A12S showed the highest increase in p21 expression (3-fold increase in comparison to untreated cells) (Fig. 23). These results surprisingly indicate that mitoxantrone (as observed in 22Rv1 cells) induces p21 in PC-3 cells. This might contribute to G2/M cell cycle arrest, although through a p53-independent pathway. Furthermore, the combination of mitoxantrone with the AdE1A1102 and AdE1A12S viruses further increased p21 mRNA expression.

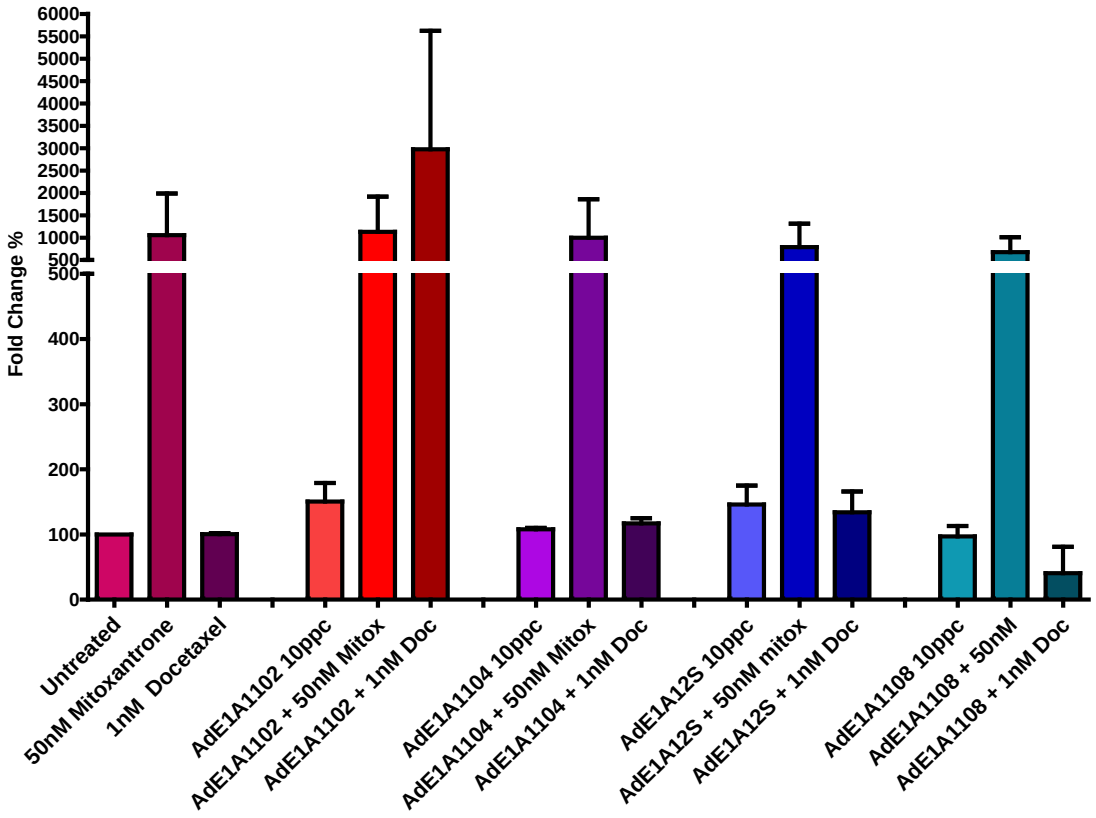

Figure 24. Fold change in percentage (FC %) of p21 mRNA expression of in 22Rv1 cells. 22Rv1 cells were infected with the AdE1A1102 mutant at 10ppc, with and without 50nM of mitoxantrone, for 48h. Data points were normalized as described in section 6.7. n=2.

The expression of p21 mRNA was also assessed in 22Rv1 cells to verify the immunoblot findings. In accordance with the previous data, treatment with

mitoxantrone alone and in combination with all AdE1A12S viral mutants induced a 10-fold increase in p21 mRNA expression compared to untreated cells (Fig. 24). However, only slight changes were observed in mRNA levels of p21 in response to infection with the viral mutants alone (Fig. 24). Treatment with docetaxel did not induce changes in p21, except in combination with AdE1A1102, where p21 increased >20-fold (Fig. 24). In summary, these results indicate that the induction of p21-mRNA by mitoxantrone was higher in 22Rv1 cells than in PC-3 cells. The AdE1A1102 and AdE1A12S mutants further increased the expression of p21 mRNA only in PC-3 cells, while in 22Rv1 cells the viral mutants did not induce any changes in p21-mRNA levels.

3.1.3 Differential sensitivity in response to differential infectivity? Alternative cancer model in ovarian cells.

Previous data have demonstrated different levels of infectivity between the PCa cell lines 22Rv1 and PC-3. Moreover, PC-3 cells showed more resistance to viral infection, while 22Rv1 were more sensitive.[362] Furthermore, I and other members of my group have observed different responses to the various treatments between the two cell lines.[362] These differences complicated the dissection of the pathways underlying the synergy since cell-specific factors might play a role in the synergistic mechanisms. To explore whether the observed differences in PC-3 and 22Rv1 were caused by the different levels of infectivity and viral uptake, we explored a pair of matched ovarian cell lines, Skov3 and Skov3ip1.[371] Skov3 was previously reported to be more sensitive to viral infection and Skov3ip1 less sensitive and also more invasive and metastatic.[371,373] We speculated that these cells may help us identify possible viral and drug targets for further studies.

3.1.3.a Skov3ip1 cells are four times more sensitive to viral infection than Skov3 cells.

We conducted infectivity assays, as well a dose response assays, to determine the differences in sensitivity to viruses alone (Ad5wt, AdΔΔ and AdE1A12S) and in combination with mitoxantrone in Skov3 and Skov3ip1 cells.

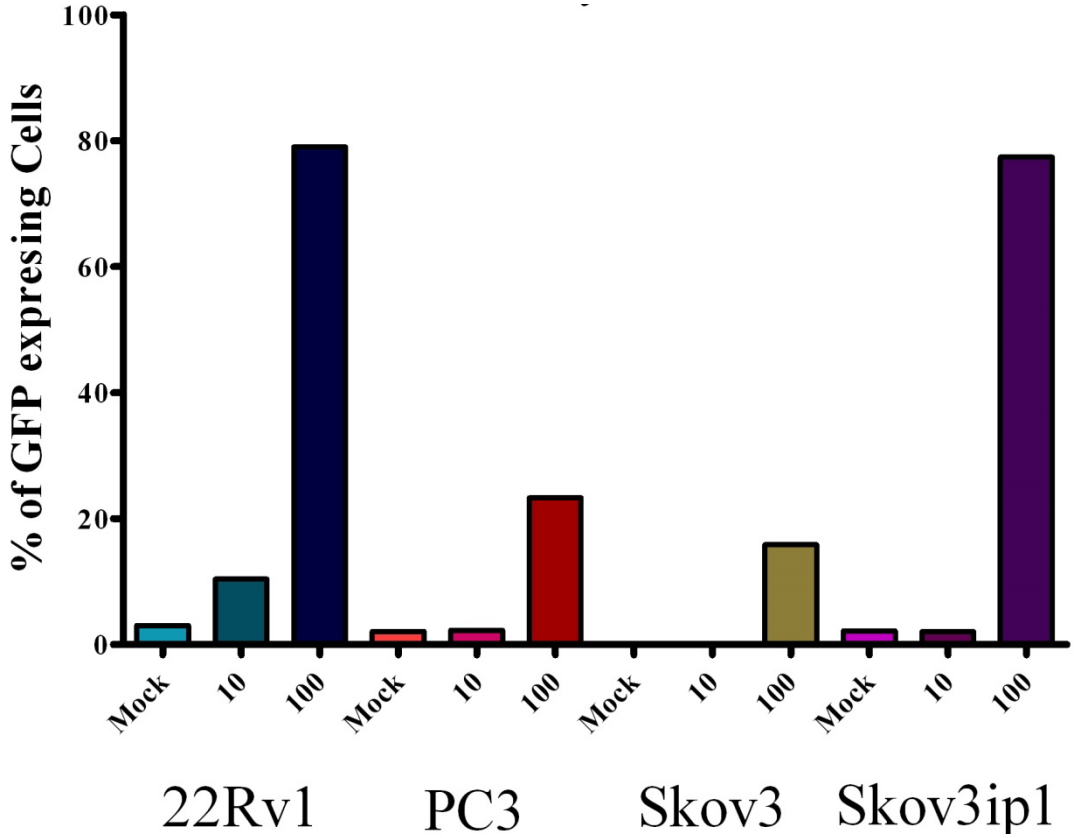

Figure 25. Percentage of cells expressing GFP 48h post-infection with a non-replicating AdGFP mutant. Prostate cancer cell lines 22Rv1, PC-3, and ovarian cancer cell lines Skov3 and Skov3ip1 were infected with a non-replicating AdGFP virus at 10 and 100ppc for 48h and analysed by flow cytometry. Each bar indicates the percentage of GFP^+ cells in $1x10^4$ cells. n=1.

We compared infectivity in prostate and ovarian cancer cell lines to determine the level of viral uptake using a GFP expressing virus (AdGFP). As expected 22Rv1 cells were more infectable than PC-3 cells in a 5:1 ratio at 10 ppc and 3:1 ratio at 100 ppc (Fig.25). However, our results contrasted with previously published data, where Skov3 cells were reported to be more sensitive to viral infection than Skov3ip1.[372] The ovarian cancer cells Skov3 were more resistant to viral infection than Skov3ip1, and were also more resistant than PC-3 cells. In contrast Skov3ip1 cells were more sensitive to infection at a 5:1 ratio compared to Skov3, and showed similar

infectability to 22Rv1 cells at 100 ppc. However, at 10 ppc 22Rv1 were more sensitive to viral infection.

3.1.3.b Skov3ip1 and Skov3 cells have similar sensitivity to AdE1A12S in combination with mitoxantrone

Although our results of cell infectivity were contradictory to previous reports, where Skov3 cells were more sensitive to infection than Skov3ip1 cells, the differences found between these cell lines were comparable to the differences in infectivity of PC-3 and 22Rv1 cells (Fig.25). Therefore, a dose-response assay to virus and mitoxantrone was set up in order to determine whether the differences in infectivity and viral uptake were reflected in sensitivity to cell killing.

The cells were infected using serial dilutions (5-fold) of the viruses Ad5wt, AdΔΔ (E1ACR2-region and E1B19K-gene deleted; replication competent) and AdE1A12S (replication-incompetent with E1B and E3 genes deleted) or treated with mitoxantrone. At 72h post-treatment the cells were analysed and the data were collected to determine the EC_{50} values. Unexpectedly the results showed that Skov3 cells were more sensitive than Skov3ip1 to all the treatments except for AdE1A12S. The Skov3 cells had the highest sensitivity to the AdΔΔ virus (mean EC_{50} of 35.2 ± 9.02), Skov3ip1 cells showed a similar order of sensitivity to Skov3 cells (Fig. 26); being more sensitive to AdΔΔ (mean EC_{50} of 65.10 ± 43.8) and less to Ad12S (mean EC_{50} of 2680 ± 2486) (Fig. 26). The sensitivity of both cell lines to AdE1A12S was significantly different ($p \leq 0.05$) to Ad5wt and AdΔΔ. The relative sensitivity of viruses was similar in both cell lines.

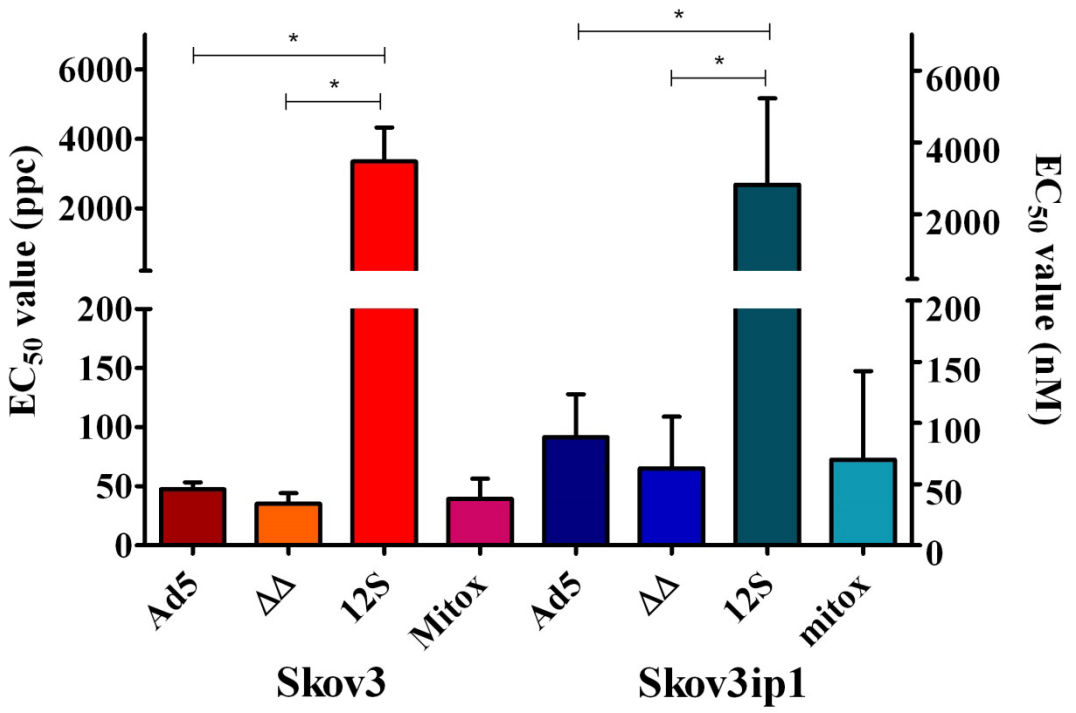

	SKOV3				SKOV3ip1			
	Ad5	AdΔΔ	Ad12S	Mitoxantrone	Ad5	AdΔΔ	Ad12S	Mitoxantrone
EC_{50}	47.44 ± 5.95	35.2 ± 9.02	3346 ± 982	39.4 ± 17	91.5 ± 36.4	65.1 ± 43.8	2680 ± 2486	72.6 ± 74.9

Figure 26. Differences in sensitivity of ovarian cancer cell lines Skov3 and Skov3ip1 cells to viral infection and mitoxantrone treatment. Skov3 and Skov3ip1 cells were treated with serial 5-fold dilutions of mitoxantrone alone or the replicating viruses Ad5wt, and AdΔΔ and the non-replicating AdE1A12S, for 72h. This graph shows the mean EC_{50} values of four independent experiments in triplicates. The mean EC_{50} values are shown in the table (ppc for virus and nM for mitoxantrone), and their correspondant SE. One-way ANOVA, significance *p≤0.05.

The differences in sensitivity to each virus in the two cell lines were not significant. Therefore, these matched cell lines could not be used for our intended studies. Despite having different degrees of viral uptake, the differences in sensitivity to AdE1A12S-mediated or mitoxantrone-mediated cell killing were not significant and consequently would not be a suitable model for mechanistic studies.

3.1.4 Synergistic effects of infection with replicating and non-replicating E1A viral mutants in combination with mitoxantrone in PC-3 and 22Rv1 cells.

During the course of this project we were completing previous sensitization studies that demonstrated that AdE1A12S mutants sensitize PCa cell lines to mitoxantrone enhancing cell killing. To further investigate whether these interactions causing enhanced cell killing were synergistic and comparable between non-replicating and replicating mutants, I set up assays at fixed ratios to determine combination index (CI).[95] Four constant ratios of viruses and drug dose-response curves were selected based on previous preliminary studies in our group where EC_{50} values for each agent were determined.[362] Selected ratios were tested to determine the CIs; additive, antagonistic or synergistic interactions. These experiments were aimed at determining which E1A deletion(s) in oncolytic adenoviral mutants could best sensitize cells and enhance cell killing in combination with mitoxantrone. Additionally, we investigated if the replicating mutants *dl*1102 and *dl*1104 showed similar effects to their respective non-replicative counterparts.

3.1.4.a Mutants with E1A p300-binding region intact induce potent synergy in combination with mitoxantrone in PC-3 cells

I tested the AdE1A12S virus and the replicating *dl*1102 and *dl*1104 and non-replicating AdE1A1102 and AdE1A1104 E1A mutants in combination with mitoxantrone in PC-3 cells. I assessed the percentage of cell death six days post-infection; these data were used to construct dose-response curves in order to determine the EC_{50} values for each treatment. Having determined the EC_{50} values, the CI values were calculated, to determine whether the interactions were synergistic (CI≤0.9), additive (CI 0.9-1.1) or antagonistic (CI≥1.1) (Fig. 27).

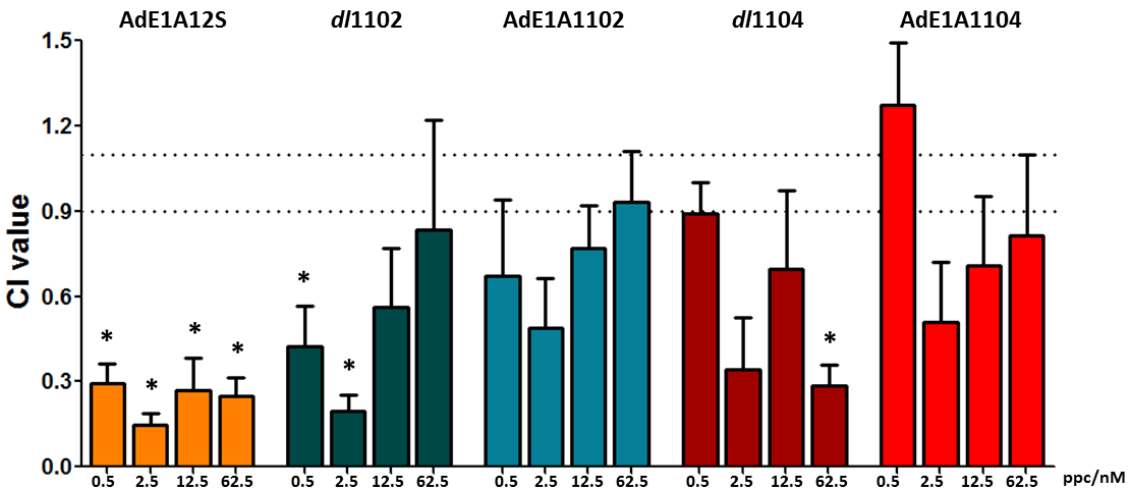

	CI				
Ratio ppc/nM	AdE1A12S	*dl*1102	AdE1A1102	*dl*1104	AdE1A1104
0.5	0.29 ± 0.07	0.43 ± 0.14	0.55 ± 0.23	0.89 ± 0.11	1.27 ± 0.22
2.5	0.15 ± 0.04	0.20 ± 0.06	0.49 ± 0.18	0.34 ± 0.18	0.51 ± 0.21
12.5	0.27 ± 0.11	0.44 ± 0.19	0.77 ± 0.15	0.70 ± 0.27	0.71 ± 0.24
62.5	0.25 ± 0.07	0.83 ± 0.39	0.93 ± 0.18	0.29 ± 0.07	0.81 ± 0.29

Figure 27. Mean CI values of PC-3 cells infected with AdE1A12S virus, the replicating and non-replicating 1102 and 1104 viruses, in combination with mitoxantrone at four different ratios. The ratios 0.5, 2.5, 12.5 and 62.5 ppc/nM were selected based on previous findings, to determine synergistic (CI≤0.9), additive (CI 0.9-1.1; dashed lines) or antagonistic (CI≥1.1) effects. Mean CI values are from five independent experiments in triplicates with the respective SEM. Significance p≤0.05(*) by t-test when compared to the theoretical additive value (0.9-1.1).

The average CI values for the combination treatment of mitoxantrone and AdE1A12S were significantly lower in PC-3 cells than the theoretical additive value (Add) at all ratios (4/4), showing strong synergistic interaction (Fig.27). In addition, *dl*1102 in combination with mitoxantrone showed synergy in 3 out of 4 ratios. The combination of the non-replicating AdE1A1102 with mitoxantrone showed synergy trend in 2 out of 4 ratios (0.5 and 2.5 ppc/nM), whereas 2 out of 4 ratios showed additive effects. These results demonstrate that AdE1A1102 has a similar propensity to *dl*1102 in acting synergistically in combination with mitoxantrone however, *dl*1102 induced synergy more effectively. The *dl*1104 virus acted synergistically in combination with mitoxantrone in 2 out of 4 ratios (2.5 and 62.5ppc/nM) (Fig. 27). Moreover, AdE1A1104 in combination with mitoxantrone acted synergistically in 3 out of 4 ratios and antagonistically in 1 out of 4 (0.5 ppc/nM). These results indicate that in

PC-3 cells the combination of mitoxantrone with *dl*1102 and AdE1A12S viruses caused the most potent synergistic cell death and indicate that the p300-binding region is a determinant factor for this interaction, since the deletion in both *dl*1104 and AdE1A1104 reduced synergistic cell killing. The poor synergistic effects with the AdE1A1104 virus (E1AΔp300 binding region) are consistent with our findings where AdE1A1104 did not seem to improve the efficacy of mitoxantrone in PC-3 cells.[95]

3.1.4.b Combination of the replicating E1A viral mutant *dl*1102 and mitoxantrone act synergistically in 22Rv1 cells.

Additionally, we analysed 22Rv1 cells for synergistic interactions. In these cells, *dl*1102 was the only one that showed a predominantly synergistic effect in 3 out of 4 combination ratios (2.5, 12.5 and 62.5 ppc/nM) (Fig 28) in combination with mitoxantrone, with 1 out of 4 combinations being additive. Similar results were observed in PC-3 cells. In contrast to PC-3 cells, the combination with AdE1A12S showed no synergy, but an antagonistic trend in 2 out of 4 ratios and additive effects in two ratios. Furthermore, the combination with AdE1A1102 resulted in antagonistic interactions at all ratios, in contrast with the synergistic trend in PC-3 cells with this virus. The combination with *dl*1104 showed synergy in 1 out of 4 ratios (0.5ppc/nM, CI=0.75) and 2 out of 4 were above the theoretical additive value indicating antagonism, in contrast to the more synergistic responses observed by these combinations in PC-3 cells. With AdE1A1104, 1 out of 4 ratios was synergistic (2.5ppc/nM, CI=0.33) and one ratio showed an antagonistic trend (Fig. 28).

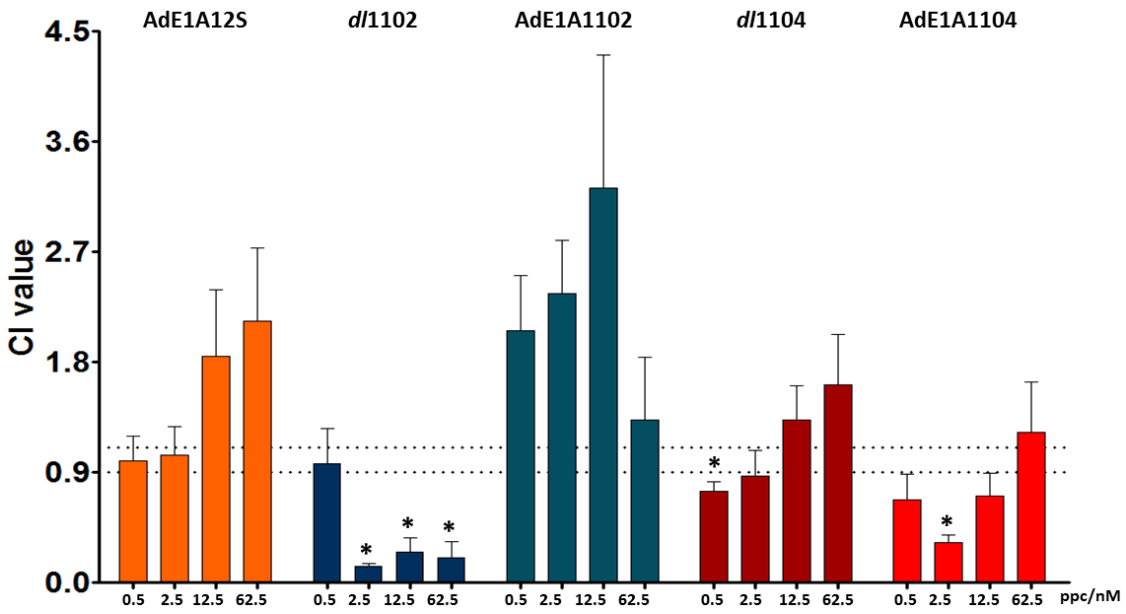

	CI				
Ratio ppc/nM	AdE1A12S	*dl*1102	AdE1A1102	*dl*1104	AdE1A1104
0.5	0.99 ± 0.20	0.97 ± 0.29	2.06 ± 0.45	0.75 ± 0.08	0.67 ± 0.21
2.5	1.04 ± 0.24	0.14 ± 0.02	2.36 ± 0.43	0.87 ± 0.21	0.33 ± 0.06
12.5	1.85 ± 0.54	0.25 ± 0.12	3.22 ± 1.09	1.33 ± 0.27	0.71 ± 0.19
62.5	2.13 ± 0.60	0.20 ± 0.13	1.33 ± 0.51	1.61 ± 0.41	1.23 ± 0.41

Figure 28. Mean CI values of 22Rv1 cells infected with AdE1A12S virus and the replicating and non-replicating 1102 and 1104 viruses, in combination with mitoxantrone at four different ratios. The ratios 0.5, 2.5, 12.5 and 62.5 ppc/nM of viral mutants and mitoxantrone were evaluated to calculate CI values, to determine synergy (CI≤0.9), additive (CI= 0.9-1.1; dashed lines) or antagonistic (CI≥1.1) effects. Average CI values are from 4 experiments measured in triplicates. Significance p≤0.05(*) by t-test, compared to the theoretical additive value (0.9; Dashed line)

In summary, these results showed different interactions in response to the combination of viral mutants and mitoxantrone in PC-3 and 22Rv1 cells, being predominantly synergistic in PC-3 and antagonistic in 22Rv1 cells. However, with the *dl*1102 virus, synergy was observed in both cell lines showing that the virus was highly effective and potent enough to enhance cell killing by mitoxantrone. The combination of AdE1A12S, AdE1A1102, and *dl*1104 with mitoxantrone showed cell-line-dependent synergistic interactions.

3.1.5 The replicating adenoviral mutants do not enhance cell killing in combination with mitoxantrone in normal human cells

Normal human bronchial epithelial cells (NHBE) and normal prostate epithelial cells (PrEC) were used to determine if the deletions in the *dl*1102 or *dl*1104 replicating mutants could potentially be applied to generate more selective oncolytic mutants with minimal effects in normal tissue. Therefore, we assessed their ability to replicate in NHBE cells by determining the viral replication efficacy, measured by $TCID_{50}$ assay over time from 24-72h (Fig. 29).

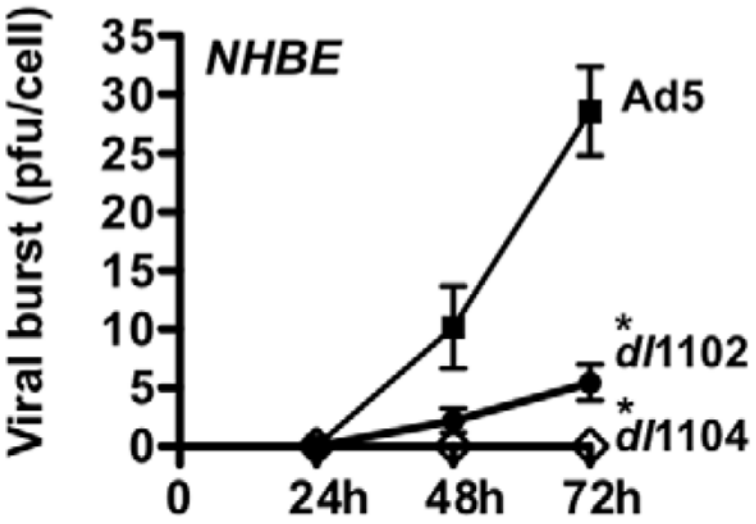

Figure 29. Viral replication in normal human bronchial epithelial cells (NHBE). $TCID_{50}$ assay to determine infective viral particle plaque forming units (pfu). NHBE cells were infected at 100ppc and harvest after 24, 48 and 72h(h.p.i). Cell lysates were titred in the $TCID_{50}$ assay, serially diluted from $1x10^{-3}$ to $1x10^{-9}$ in JH293 cells. Three experiments by duplicate, averaged ± SEM. Student t-test *p<0.005.[95]

NHBE cells infected with both *dl*1102 and *dl*1104 showed significantly less replication than Ad5wt at 48h and 72h. NHBE cells infected with the *dl*1102 showed only 2.30 pfu/cell at 48hpi and 6.1pfu/cell at 72hpi, while no replication was observed for the *dl*1104. Ad5wt virus, showed an increase to 8.41 pfu/cell at 48hpi and 25.1pfu/cell at 72hpi. At 72h the differences in replication were significant when comparing all three viruses. The *dl*1104 infected cells showed poor viral replication compared to both Ad5wt and *dl*1102 at all-time points. The greatly decreased viral replication of both *dl*1102 and *dl*1104 in NHBE cells (Fig. 29), suggested that both mutants have

impaired replication in non-cancerous tissue. In contrast in PCa cells both *dl*1102 and *dl*1104 showed levels of viral replication similar to those of Ad5wt[95]

We also determined the toxicity of the virus and mitoxantrone as single agents and in combination in NHBE cells to further verify that the replicating viruses do not cause more than additive cell death with mitoxantrone in these cells.

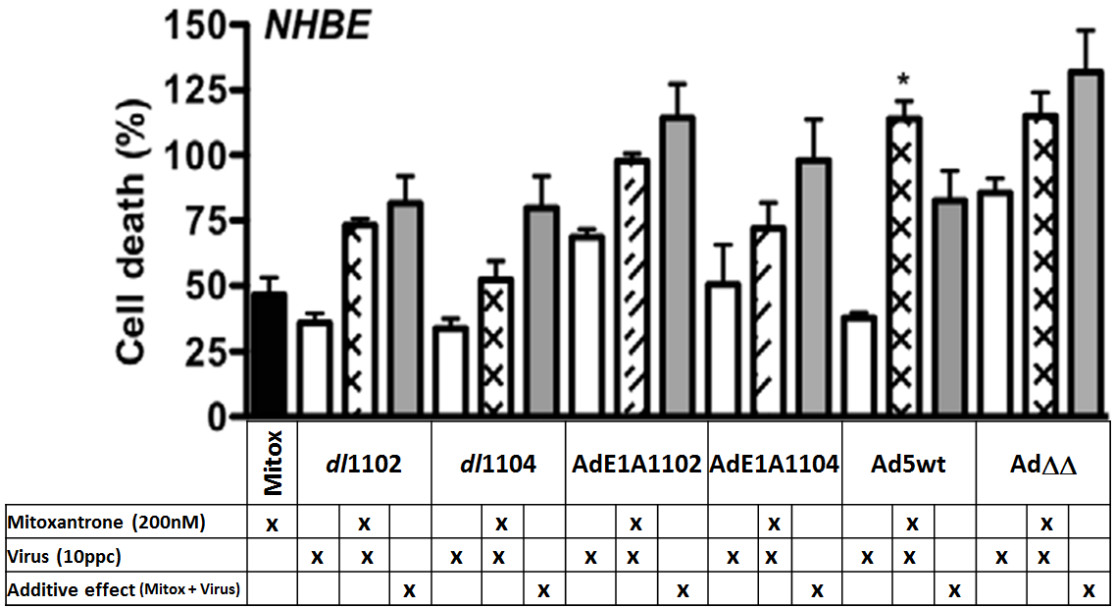

Figure 30. Normal human bronchial epithelial cells (NHBE) treated alone and in combination with adenoviral mutants and mitoxantrone. NHBE cells were infected with the replicating *dl*1102, *dl*1104, Ad5wt, AdΔΔ and the non-replicating AdE1A1102 and AdE1A1104 at 10 ppc alone (white bars), treated with mitoxantrone alone (black bar) at 200nM and in combination (crossed and striped bars). Cell viability was determined by MTS assay 72h post-treatment. The theoretical additive (Additive effect) values are indicated by grey bars, Student t-test *p<0.05 compared to expected additive cell killing, n = 2.[95]

To determine if adenoviral mutants enhance cell killing in combination with mitoxantrone in NHBE cells, the cells were infected with viruses at 10ppc and treated with 200nM mitoxantrone alone and in combination (Fig. 30). The treatment with mitoxantrone alone reduced cell viability to about 50%. The infection with the Ad5wt resulted in more than additive effect in combination with mitoxantrone, demonstrating the non-selectivity of this virus. The combination of mitoxantrone with the non-replicating (AdE1A1102 and AdE1A1104) and replicating (*dl*1102, *dl*1104 and AdΔΔ) adenoviral mutants caused less than additive effects. The infection with the non-replicating AdE1A1102 and AdE1A1104 reduced cell viability to a

slightly higher degree than the replicating counterparts. Moreover, the AdΔΔ showed higher potency compared with *dl*1102 and *dl*1104, although the reduction in cell viability did not sensitize NHBE cells to mitoxantrone. These results demonstrate that the replicating viruses selectively synergize with mitoxantrone in tumour cells but not in normal cells.

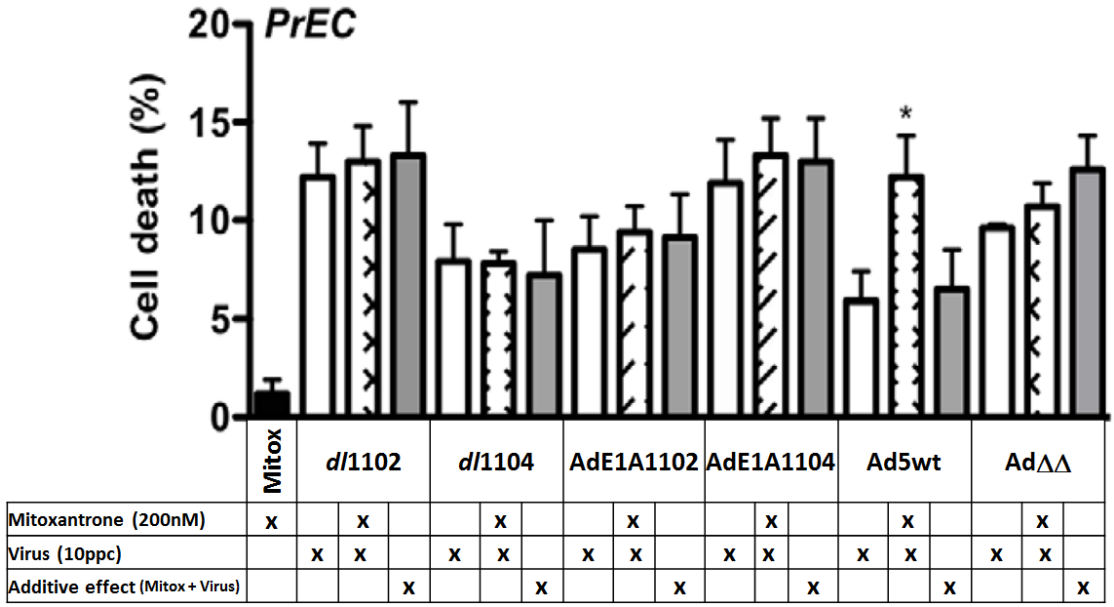

Figure 31. Primary human prostate epithelial cells (PrEC) treated alone and in combination with adenoviral mutants and mitoxantrone. PrEC cells were infected with the replicating *dl*1102, *dl*1104, Ad5wt, AdΔΔ and the non-replicating AdE1A1102 and AdE1A1104 at 10 ppc alone (white bars) and in combination with 200 nM mitoxantrone (M) (crossed and striped bars). Cell viability was determined by MTS assay 72 h later. The theoretical additive (Addit) values are indicated by grey bars, Student t-test *p<0.05 compared to expected additive cell killing, n = 2.[95]

To verify our findings in the NHBE cells we also infected normal human PrEC cells with the replicating and non-replicating viral mutants at 10ppc and treated them with 200nM mitoxantrone alone and in combination (Fig. 31). Treatment with mitoxantrone alone reduced cell viability by less than 5% at this concentration, indicating less sensitivity to the drug than in NHBE cells. In general, PrEC cells were less sensitive to both infection and the drug. Similar to the findings in NHBE cells Ad5wt in combination with mitoxantrone induced more than additive cell killing. Additionally and similarly to NHBE cells, the combination of mitoxantrone with the replicating and non-replicating adenoviral mutants did not induce more than additive effects on cell killing in PrEC cells. In contrast to NHBE cells, PrEC cells were more

sensitive to the infection with the replicating viruses than the non-replicating mutants, with *dl*1102 and AdΔΔ being more potent than AdE1A1102. However, neither *dl*1102 nor AdΔΔ induced more than additive cell killing in combination with mitoxantrone. Surprisingly, AdE1A1104 showed higher potency and reduced cell viability at a higher percentage than its replicating counterpart. Importantly these results show in two normal cell lines, that the viral mutants *dl*1102 and AdΔΔ are as potent as the Ad5wt but do not sensitize the normal cells to chemotherapeutic drugs, validating their tumour selectivity.

3.1.6 The *dl*1102 mutant potently reduces tumour growth in combination with docetaxel in PC-3 xenografts *in vivo*

In order to verify our findings *in vivo*, PC-3 cells were subcutaneously inoculated in athymic mice and infected with the replicating and non-replicating E1A mutants. The non-replicating AdE1A12S, AdE1A1102 and AdE1A1104 mutants were not efficacious in reducing tumour growth alone or in combination with docetaxel.[95] In contrast, the replicating *dl*1102 and *dl*1104 significantly inhibited tumour growth in combination with docetaxel, indicating that the viruses sensitized tumour cells to the drug. However, only *dl*1102 was potent enough to significantly reduce tumour growth alone (Fig. 32).

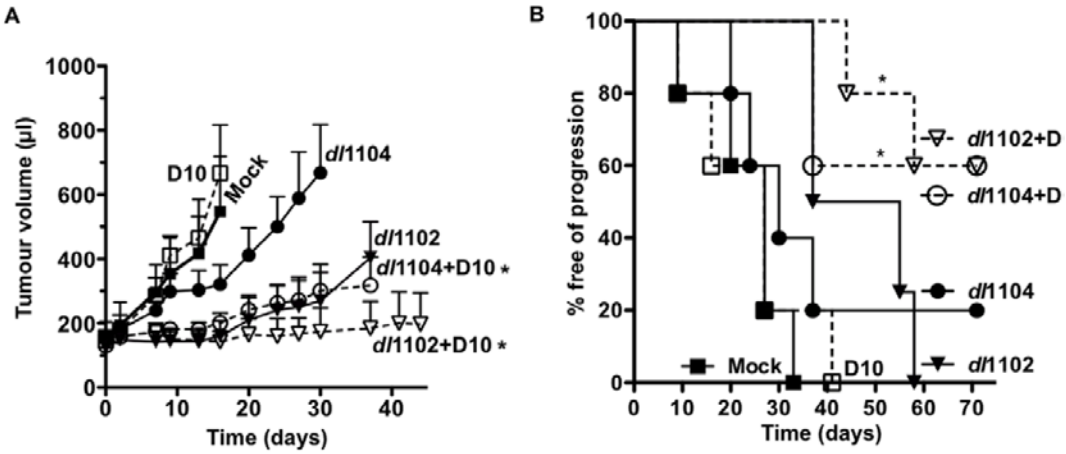

Figure 32. PC-3 xenografts in *vivo* treated with docetaxel alone and in combination with replicating E1A mutants. **A)** Animals with PC-3 subcutaneous tumour xenografts were treated with the *dl*1102 (filled triangle) or *dl*1104 (filled circle) mutants or mock treated with *dl*312 (filled square) at $1x10^9$ vp (i.t. injections on day 1, 3, and 5) with and without docetaxel at 10 mg/kg (D10; i.p. administration on day 2 and 8, open squares), and tumour growth was monitored. *p,0.05, treatments compared with mock and single-agent treatments (one-way

ANOVA), *p<0.05 for dl1102 alone compared to mock, n = 6. **B)** In a second study animals with PC-3 subcutaneous tumour xenografts were treated as above with the indicated suboptimal doses of viral mutants at $1x10^9$vp and docetaxel at 10 mg/kg (D10) or the respective combinations. Median time to tumour progression (tumour volume .500 μl) was determined by Kaplan-Meier survival analysis (8–10 animals per group). *p<0.05, combination-treated compared with docetaxel.[95]

These results verified the *in vitro* findings, where the potent sensitization of prostate cancer cells was induced by the replicating E1A oncolytic mutant *dl*1102, but not *dl*1104. In addition, in a study with C57Bl/6 athymic mice induced with PC-3 subcutaneous tumour xenografts the median time to progression was determined to be 40, 30 and 28 days for animals infected with *dl*1102, *dl*1104 and treated with docetaxel respectively. In contrast, more than half of the animals treated in combination did not show tumour progression at the end of the study, 70 days after treatment. These results showed the potent anti-tumour efficacy *in vivo* of the replicating *dl*1102 and *dl*1104 in combination with docetaxel and verified our previous results *in vitro* where enhanced synergistic cell killing in response to the combination treatments was shown.

3.1.7 In summary

- Mitoxantrone induces cyclins A and B in PC-3 cells but not in 22Rv1 cells.
- The AdE1A12S and AdE1A1102 viral mutants enhance mitoxantrone-induced p21 mRNA expression in PC-3 cells but not in 22Rv1 cells.
- Synergistic effects on cell killing with replicating and non-replicating E1A viral mutants in combination with mitoxantrone in PC-3 and 22Rv1 cells. Mutants with E1A p300-binding region intact induce potent synergy in combination with mitoxantrone in PC-3. Combination of the replicating E1A viral mutant dl1102 and mitoxantrone act synergistically in 22Rv1 cells.
- The replicating adenoviral mutants do not enhance cell killing in combination with mitoxantrone in PrEC and NHBE human normal cells.
- The *dl*1102 mutant potently reduces tumour growth in combination with docetaxel in PC-3 xenografts *in vivo*.

3.2 Analysis of miRNAs that are differentially expressed in PC-3 cells treated with AdE1A12S or mitoxantrone or a combination of both.

Our work demonstrated that the small E1A12S-protein was essential for sensitizing PCa cell lines to the chemotherapeutic drugs mitoxantrone and docetaxel, which are currently used as front line treatments for hormone refractory PCa.[95,362] Previously we demonstrated synergistic cell killing in PC-3 cells (Miranda, 2012[95]; Section 3.1.5), with both drugs in combination with AdE1A12S and AdE1A12S-mutants. Identification of the cellular mechanisms involved in sensitization to E1A has been elusive.[95] Some reasons are that the E1A-protein can bind to a plethora of cellular factors with related functions and that have overlapping binding sites in E1A. Most of these factors are involved in regulation of cell death, survival, and cell cycle pathways. To elucidate the mechanisms and pathways that caused the observed synergistic cell killing requires extensive in depth studies in each cell line. We speculated that a more rational approach including mRNA or miRNA array-screening would enable us to get insights into the cellular pathways that are involved. We chose PC-3 cells because of the insensitivity to each single agent and the significantly synergistic enhancement of cell killing when virus and drug were combined.

We hypothesised that the expression of miRNAs might be affected by either chemotherapeutic drugs and/or expression of E1A12S and that the combination-treated cells would reveal a different pattern of miRNA expression. We anticipated that data from a sensitive and comprehensive miRNA array analysis would guide us towards the cellular pathways and targets that are involved in the sensitization and that these targets could be further exploited in developing improved therapies for PCa.

To this end, a miRNA array analysis was performed using 850 human microRNAs based on the Sanger miRNA database (LC Science, TX, USA). PC-3 cells were infected with AdE1A12S (100ppc) or treated with mitoxantrone (50nM) or a combination of both for 24 and 48h. These doses were demonstrated to cause synergistic cell death in parallel studies.[95] The differences in the expression of miRNAs in response to each agent alone and in combination were quantified and compared to untreated and non-infected cells and to the theoretical combination of both single agents. All

miRNAs with an average signal of intensity of >500 and that were statistically significant ($p<0.01$; Students t-test) were selected for the analysis. In total 73 miRNAs fulfilled these parameters. Moreover, a Log2 positive value indicates upregulation and a negative Log2 value indicates a downregulation.

3.2.1. In PC-3 cells miRNAs are differentially expressed 24h post-infection with the AdE1A12S virus compared to untreated cells.

Highly significant differences ($p<0.001$) in the expression of 29 miRNAs were observed in PC-3 cells infected for 24h with the AdE1A12S virus compared to untreated and uninfected cells. The highly significant miRNAs showed upregulation in 15 out of 29 miRNAs (Log2>0.0; Table 11) whereas 14 out of 29 miRNAs were downregulated (Log2<0.0; Table 11). Interestingly, hsa-miR-16, hsa-miR-19b, hsa-miR-26a, hsa-miR-27a, hsa-mir29a were upregulated by AdE1A12S and have previously been reported to be expressed at low levels in PCa.[231,234-238] Also, hsa-miR-1246 and hsa-miR-574-3p have been reported to be upregulated in PCa, and hsa-miR-483-5p and hsa-miR-574-5p in other cancers, while AdE1A12S significantly downregulated these miRNAs. However the greatest changes (Log2>1.3 and <-1.3) in miRNA levels in response to AdE1A12S was observed for hsa-miR-106a, hsa-miR-106b and hsa-miR-19b, hsa-miR-20a and hsa-miR-29a that had increased expression and hsa-let-7e, hsa-miR-1268, hsa-miR-483-5p, hsa-miR-542-5p, hsa-miR-574-3p/5p, hsa-miR-638 and hsa-miR-923 that had decreased expression, all of which have been validated to be altered in PCa and/or other cancers.[231,234-238]

Table 11. Differentially expressed miRNAs in PC-3 cells 24h post-infection with the AdE1A12S virus (100ppc) compared to uninfected and untreated cells.

	Log2 (AdE1A12S/Untreated)	p value	Regulation in prostate and/or other types of cancer	Validated in Cancer
hsa-let-7e	-1.47	5.59E-03		
hsa-miR-106a	1.56	2.59E-05		
hsa-miR-106b	1.57	6.81E-05		
hsa-miR-1246	-0.35	8.50E-05		
hsa-miR-125a-5p	-0.75	4.04E-03		
hsa-miR-1268	-1.47	5.37E-05		
hsa-miR-1275	-1.2	3.61E-04	NA	
hsa-miR-1280	-0.74	8.76E-04		
hsa-miR-151-3p	0.61	3.68E-04		
hsa-miR-16	0.46	1.27E-03		
hsa-miR-17	1.42	3.41E-05		
hsa-miR-1826	1.31	2.49E-04		
hsa-miR-19b	2.22	6.15E-05		
hsa-miR-20a	1.58	4.88E-05		
hsa-miR-21	0.72	4.81E-03		
hsa-miR-24	0.51	4.15E-04		
hsa-miR-26a	0.86	1.06E-04		
hsa-miR-27a	0.94	2.91E-05		
hsa-miR-29a	1.33	5.30E-07		
hsa-miR-30d	0.73	8.39E-03		
hsa-miR-483-5p	-4.21	1.32E-04		
hsa-miR-542-5p	-5.7	8.25E-03	NA	
hsa-miR-574-3p	-2.58	6.09E-06		
hsa-miR-574-5p	-2.98	1.09E-05		
hsa-miR-638	-2.37	3.09E-05		
hsa-miR-923	-1.43	5.02E-04	NA	
hsa-miR-92b	-0.48	4.28E-04		
hsa-miR-93	1.17	6.36E-06		
hsa-miR-99a	-1.25	1.13E-04		

Up-regulated
Down-regulated
Discrepant results in literature
Highly significant
Deregulation involved in Prostate cancer
Deregulation Involved in other types of cancer
No information available NA
MicroRNAs verified in two experiments

p-values determined by t-test; highly significant p-values ($p<0.001$; yellow).

The information available for the miRNAs hsa-mir1268, hsa-miR-1275, and hsa-miR-542-5p did not allow us to establish a complete profile in terms of their expression in cancer. It is also important to point out that there is no information available for the miRNAs hsa-miR-923 and hsa-miR-1280 since they are not considered as mature miRNA sequences, these miRNAs are likely fragments of the 28S rRNA and of a tRNA respectively.[387] The miRNA hsa-miR-1826 is considered to be a fragment of the 5.8S rRNA and is therefore not a mature miRNA.[387] These findings suggest that at least four miRNAs that are known to be expressed at low levels in PCa (hsa-miR-19b, and

hsa-miR-29a, hsa-let-7e and hsa-miR-638) were significantly up- or downregulated by the E1A12S protein, indicating a role of these miRNAs in cell growth and death.

3.2.2 In PC-3 cells miRNAs are differentially expressed at 24h post-treatment with mitoxantrone compared to untreated cells.

Significant differences ($p<0.001$) in miRNA expression were observed in PC-3 cells treated with mitoxantrone for 24h compared to untreated and uninfected cells. Eleven out of 19 miRNAs were downregulated (red-Log2 column; Table 12) and eight out of 19 upregulated (green-Log2 column; Table 12). The largest differences in the change of expression ($Log2<-2.0$) among downregulated miRNAs were shown by hsa-miR-1268, hsa-miR-638 and hsa-miR-923, although only hsa-miR-1268 and hsa-miR-638 are considered as mature sequences of miRNA.[382] While no information about the miRNA hsa-miR-1268 that could be useful for our purposes was found, this miRNA was downregulated by both AdE1A12S and mitoxantrone. The upregulated miRNA hsa-miR-423-5p showed the largest difference compared to untreated samples ($Log2=1.65$). Interestingly, hsa-miR-100, hsa-miR-16, hsa-miR-200b and hsa-miR-222 were upregulated by mitoxantrone and have previously been reported to be expressed at low levels in PCa. In contrast, hsa-miR-1246 and hsa-miR-99b are known to be overexpressed in PCa and mitoxantrone reduced the expression levels.[231,234-238]

Table 12. Differentially expressed miRNAs in PC-3 cells 24h post-treatment with mitoxantrone (50nM), compared to untreated and uninfected cells.

	Log2 (Mitoxantrone/ Untreated)	p value		Regulation in prostate and/or other types of cancer	Validated in Cancer
hsa-let-7c	-0.75	2.82E-03			
hsa-let-7d	-0.7	6.81E-03			
hsa-let-7e	-1.48	1.85E-03			
hsa-miR-100	0.47	1.30E-03			
hsa-miR-1246	-1.48	2.28E-04			
hsa-miR-125b	-0.59	2.63E-03			
hsa-miR-1268	-2.49	1.03E-03		NA	
hsa-miR-16	0.83	6.80E-05			
hsa-miR-182	0.72	1.44E-03			
hsa-miR-1826	0.67	4.43E-03			
hsa-miR-191	0.51	1.92E-03			
hsa-miR-200b	0.84	2.47E-03			
hsa-miR-222	0.56	2.48E-03			
hsa-miR-423-5p	1.65	6.39E-04		NA	
hsa-miR-638	-2.26	9.33E-03			
hsa-miR-923	-3.32	5.34E-03		NA	
hsa-miR-92a	-0.47	2.08E-04			
hsa-miR-99a	-1.86	8.32E-03			
hsa-miR-99b	-0.78	9.70E-05			

Up-regulated
Down-regulated
Discrepant results in literature
Highly significant
Deregulation involved in Prostate cancer
Deregulation Involved in other types of cancer
No information available NA
MicroRNAs verified in two experiments

p-values determined by t-test; highly significant p-values ($p<0.001$; yellow).

The changes in the expression of miRNAs due to the treatment with mitoxantrone showed fewer regulated miRNAs (total 19) compared to samples infected with the AdE1A12S virus (total 29; Table 11). Moreover, eleven out of nineteen miRNAs hsa-let-7c, hsa-let-7d, hsa-miR-100, hsa-miR-125b, hsa-miR-182, hsa-miR-191, hsa-miR-200b, hsa-miR-222, hsa-miR-423-5p, hsa-miR-92a and hsa-miR-99b were not regulated by the treatment with the virus but changed in response to mitoxantrone alone. Interestingly the expression of the miRNAs hsa-let-7e, hsa-miR-1246, hsa-miR-16 and hsa-miR-1826 (Table 12) showed a similar pattern of expression to miRNAs of samples infected with the AdE1A12S virus (Table 11). The hsa-miR-16, hsa-let-7e and hsa-miR-1826 were upregulated and hsa-miR-1246 was downregulated by both AdE1A12S and mitoxantrone. In contrast, samples infected with the virus alone

showed a change in the expression of twenty different miRNAs (hsa-miR-106a, hsa-miR-106b, hsa-miR-125a-5p, hsa-miR-1275, hsa-miR-1280, hsa-miR-151-3p, hsa-miR-17, hsa-miR-19b, hsa-miR-20a, hsa-miR-21, hsa-miR-24, hsa-miR-26a, hsa-miR-27a, hsa-miR-29a, hsa-miR-30d, hsa-miR-483-5p, hsa-miR-542-5p, hsa-miR-574-3p, hsa-miR-574-5p and hsa-miR-99a) that were not regulated when treated by mitoxantrone as a single agent.

3.2.3 In PC-3 cells miRNAs are differentially expressed at 24h post-treatment with AdE1A12S in combination with mitoxantrone compared to untreated and uninfected cells.

The differences in the expression of miRNAs in PC-3 cells simultaneously treated with mitoxantrone at 50nM and infected with the AdE1A12S virus at 100ppc were compared to untreated and uninfected samples. The expression of 16 out of 37 miRNAs were downregulated (red Log2 column; Table 13) and 21 out of 37 miRNAs were upregulated (green Log2 column; Table 13) in response to the combination. Moreover, 9 out of 16 downregulated miRNAs (hsa-miR-191, hsa-miR-320a, hsa-miR-320c, hsa-miR-320d, hsa-miR-425, hsa-miR-483-5p, hsa-miR-574-3p, hsa-miR-574-5p, hsa-miR-99b; red) and 12 out of 21 upregulated miRNAs (hsa-let-7g, hsa-miR-128, hsa-miR-16, hsa-miR-19b, hsa-miR-23a, hsa-miR-23b, hsa-miR-26a, hsa-miR-26b, hsa-miR-27a, hsa-miR-27b, hsa-miR-29a and hsa-miR-30b; green) have previously been reported to be expressed at higher and lower levels respectively in PCa.[231,234-238]

The largest differences in the expression of downregulated miRNAs (Log2<-2) were shown by the miRNAs hsa-miR-483-5p, hsa-miR-574-3p, hsa-miR-574-5p, hsa-miR-638 and hsa-miR-923. Although they were significantly different, the miRNAs hsa-miR-483-5p, hsa-miR-574-5p hsa-miR-638 and hsa-miR-923 have not been validated in PCa and the latter is not consider a mature miRNA sequence.[387] The largest difference in the expression of upregulated miRNAs (Log2>1.20) was shown (in decreasing order) by the miRNAs hsa-miR-27b, hsa-miR-27a, hsa-miR-20b, hsa-miR-19b, hsa-miR-30b, hsa-miR-20a and hsa-miR-26b (Table 13).

Table 13. Differentially expressed miRNAs in PC-3 cells at 24h post-treatment with the combination of AdE1A12S (100ppc) and mitoxantrone (50nM) compared to untreated and uninfected cells.

	Log2 (Combo/ Untreated)	p value	Regulation in prostate and /or other types of cancer	Validated in Cancer
hsa-let-7b	-0.83	2.21E-03		
hsa-let-7d	-0.66	2.09E-03		
hsa-let-7g	0.71	6.03E-03		
hsa-miR-106a	1.12	3.02E-04		
hsa-miR-106b	0.87	6.27E-04		
hsa-miR-1268	-1.82	1.14E-05	NA	
hsa-miR-128	0.72	9.33E-03		
hsa-miR-1280	-0.57	5.05E-03	NA	
hsa-miR-16	0.97	3.00E-05		
hsa-miR-17	0.95	9.23E-05		
hsa-miR-191	-0.43	8.50E-05		
hsa-miR-19b	1.56	3.78E-04		
hsa-miR-20a	1.27	1.60E-04		
hsa-miR-20b	1.59	3.20E-03		
hsa-miR-21	0.54	2.52E-03		
hsa-miR-23a	0.58	4.08E-04		
hsa-miR-23b	0.61	9.81E-04		
hsa-miR-24	0.46	5.26E-03		
hsa-miR-26a	0.74	1.61E-04		
hsa-miR-26b	1.26	1.76E-04		
hsa-miR-27a	1.70	3.76E-06		
hsa-miR-27b	1.80	5.44E-05		
hsa-miR-29a	1.04	1.36E-06		
hsa-miR-30b	1.34	3.17E-03		
hsa-miR-30c	0.91	9.02E-03		
hsa-miR-320a	-0.67	2.22E-03		
hsa-miR-320c	-0.61	8.17E-03		
hsa-miR-320d	-1.41	3.39E-04		
hsa-miR-425	-0.48	9.59E-03		
hsa-miR-483-5p	-3.66	1.97E-04		
hsa-miR-574-3p	-2.56	2.55E-04		
hsa-miR-574-5p	-2.71	2.48E-04		
hsa-miR-638	-2.09	1.41E-06		
hsa-miR-720	-0.72	1.67E-03	NA	
hsa-miR-923	-2.97	1.16E-04		
hsa-miR-93	0.37	1.94E-03		
hsa-miR-99b	-0.52	6.07E-04		

Up-regulated
Down-regulated
Discrepant results in literature
Highly significant
Deregulation involved in Prostate cancer
Deregulation Involved in other types of cancer
No information available NA
MicroRNAs verified in two experiments

p-values determined by t-test; highly significant p-values ($p<0.001$; yellow).

The number of significantly differentially regulated miRNAs was higher in the combination-treated cells than in cells infected with virus only (37 versus 29) (Table 11 and 13). Additionally, 19 out of 37 miRNAs (hsa-miR-106a, hsa-miR-106b, hsa-miR-1268, hsa-miR-1280, hsa-miR-16, hsa-miR-17, hsa-miR-19b, hsa-miR-20a, hsa-miR-21, hsa-miR-24, hsa-miR-26a, hsa-miR-29a, hsa-miR-483-5p, hsa-miR-574-3p, hsa-miR-574-5p, hsa-miR-638, hsa-miR-923, hsa-miR-93) were regulated both by the virus alone and the combination treatment showing the same pattern of expression

(Table 11 and 13). In contrast, the combination-treated cells compared to mitoxantrone-treated cells, showed that only 7 out of 37 miRNAs (hsa-let-7d, hsa-miR-1268, hsa-miR-16, hsa-miR-191, hsa-miR-638, hsa-miR-923 and hsa-miR-99b) were regulated in both sets (downregulated). Moreover, the intricate complexity of the miRNA regulatory mechanism is shown by hsa-miR-191 that had a different pattern of expression in the combination (downregulated; Table 13) compared to mitoxantrone alone (upregulated; Table 12) and was not modified by the virus alone (Table 11). The regulation of hsa-miR-191 could be induced by mitoxantrone while in the context of viral infection another miRNA might affect its regulation.

3.2.4 In PC-3 cells, simultaneously treated with mitoxantrone and infected with AdE1A12S for 24h, differentially expressed miRNAs show a more than additive deregulation when compared to the theoretical sum of the miRNAs in single agent-treated cells.

The differences in the expression of miRNAs when the combination-treated cells were compared to the sum of the single agent treatment with AdE1A12S and mitoxantrone for 24h (Table 14), were highly significant ($p<0.001$) for 14 miRNAs. Four of these miRNAs (hsa-miR-1826, hsa-miR-191, hsa-miR-320a and hsa-miR-425) were downregulated in the combination-treated cells compared to the sum of the single agents. Ten miRNAs were upregulated (Table 14), (hsa-miR-16, hsa-miR-23a, hsa-miR-23b, hsa-miR-26b, hsa-miR-27a, hsa-miR-27b, hsa-miR-30b and hsa-miR-99a) and nine of these were previously reported as downregulated in PCa.[231,234-238] In addition, hsa-miR-191, hsa-miR-320a and hsa-miR-425 that were downregulated in the combination compared to the sum of the single agents are known to be overexpressed in PCa and other cancers (Table 14).[231,234-238] Table 14 shows that 12 out of 14 deregulated miRNAs in response to the combination treatments compared to the sum of the single agents have been found to be validated and have altered expression in PCa cells and tissue (Table 14; Dark blue).

Table 14. Differentially expressed miRNAs in PC-3 cells simultaneously infected with AdE1A12S (100ppc), and treated with mitoxantrone (50nM) compared to the sum of miRNAs changes in single agent-treated cells.

	Log2 (Combo/ 12S+mitox)	p value		Regulation in prostate and/or other types of cancer	Validated in Cancer
hsa-miR-125a-5p	0.72	8.15E-04			
hsa-miR-16	0.31	3.28E-03			
hsa-miR-1826	-1.01	9.69E-05			
hsa-miR-191	-0.75	3.35E-05			
hsa-miR-23a	0.54	5.52E-05			
hsa-miR-23b	1.16	1.40E-05			
hsa-miR-26b	1.06	4.87E-03			
hsa-miR-27a	0.96	6.79E-04			
hsa-miR-27b	1.16	1.09E-03			
hsa-miR-30b	0.71	4.37E-03			
hsa-miR-30c	0.66	7.49E-03			
hsa-miR-320a	-0.50	5.00E-03			
hsa-miR-425	-0.97	7.49E-03			
hsa-miR-99a	1.22	3.46E-04			

Up-regulated
Down-regulated
Discrepant results in literature
Highly significant
Deregulation involved in Prostate cancer
Deregulation Involved in other types of cancer
No information available — NA
MicroRNAs verified in two experiments

p-values determined by t-test; highly significant p-values ($p<0.001$; yellow).

By comparing the expression of miRNAs in the combination to the sum of single agent treatments shown in Table 14 and the expression of miRNAs in the combination compared to untreated samples shown in Table 13, we observed that the miRNAs hsa-miR-125a-5p, hsa-miR-99a and hsa-miR-1826 only changed when compared to the sum of single agent treatments but not when the expression of the combination was compared to untreated samples. However, the expression of 10 out of 14 miRNAs (hsa-miR-16, hsa-miR-191, hsa-miR-23a, hsa-miR-23b, hsa-miR-26b, hsa-miR-27a, hsa-miR-30b, hsa-miR-30c, hsa-miR-320a, and hsa-miR-425) showed a similar pattern of expression in both analysis (Table 13 and 14).

3.3 Differentially expressed miRNAs in PC-3 cells treated with AdE1A12S, mitoxantrone and the combination of AdE1A12S and mitoxantrone for 48h.

3.3.1 In PC-3 cells, miRNAs are differentially expressed also after 48h when infected with the AdE1A12S virus compared to untreated cells.

The differences in the expression of miRNAs were highly significant 48h post-infection with AdE1A12S in PC-3 cells, resulting in 33 and 27 out of 60 miRNAs being

downregulated and upregulated respectively (Table 15). Fifteen downregulated miRNAs (hsa-let-7i, hsa-miR-106a, hsa-miR-106b, hsa-miR-107, hsa-miR-151-3p, hsa-miR-151-5p, hsa-miR-20a, hsa-miR-21, hsa-miR-17, hsa-miR-182, hsa-miR-24, hsa-miR-25, hsa-miR-30c, hsa-miR-30d and hsa-miR-93), were previously reported to be upregulated in PCa.[231,234-238] Ten of the twenty-seven upregulated miRNAs (hsa-let-7a, hsa-let-7b, hsa-let-7c, hsa-let-7d, hsa-let-7e, hsa-miR-1826, hsa-miR-361-5p, hsa-miR-638, hsa-miR-92a, and hsa-miR-92b) were reported to be downregulated in PCa.[231,234-238] Forty-two of the sixty (Table 15; dark blue) miRNAs have been reported as deregulated in PCa. The differences in the expression (in decreasing order of fold change) of hsa-miR-923, hsa-miR-601, hsa-miR-574-5p, hsa-miR-483-5p, hsa-miR-638, hsa-miR-1280, hsa-miR-1268 and hsa-miR-574-3p were considerably higher (Log2> 2.0) than for other upregulated miRNAs (Table 15). However, the miRNAs hsa-miR-1280 and hsa-miR-923 are not considered to be mature sequences of miRNA,[387] and except for hsa-miR-574-3p all other mature miRNA sequences with Log2>2.0 belong to the 18 out of 60 miRNAs that have not yet been validated in PCa cells or tissue. The differences in the expression of downregulated miRNAs was largest Log2< -2.0 for hsa-miR-21, hsa-miR-26b, hsa-miR-27a, hsa-miR-99a, hsa-miR-29a, hsa-miR-20a and hsa-miR-106a.

Table 15. Differentially expressed miRNAs in PC-3 cells 48h post-infection with the AdE1A12S virus (100ppc) compared to uninfected and untreated cells.

	Log2 (Ad12S/ Untreated)	p value	Regulation in prostate and/or other types of cancer	Validated in Cancer
hsa-let-7a	0.74	1.33E-05		
hsa-let-7b	1.35	2.90E-06		
hsa-let-7c	0.7	9.93E-04		
hsa-let-7d	0.38	4.19E-03		
hsa-let-7e	0.71	3.64E-03		
hsa-let-7g	-1.67	6.24E-04		
hsa-let-7i	-0.78	4.60E-04		
hsa-miR-100	-1.54	1.50E-04		
hsa-miR-103	-0.39	1.59E-03		
hsa-miR-106a	-2.11	1.17E-04		
hsa-miR-106b	-1.85	4.05E-04		
hsa-miR-107	-0.6	4.98E-03		
hsa-miR-125b	-0.46	4.72E-03		
hsa-miR-1268	3.09	1.08E-07	NA	
hsa-miR-1275	2.59	1.17E-06		
hsa-miR-128	-0.49	9.14E-03		
hsa-miR-1280	3.12	1.90E-07	NA	
hsa-miR-1308	1.35	1.83E-05		
hsa-miR-151-3p	-0.86	1.80E-04		
hsa-miR-151-5p	-0.68	6.61E-05		
hsa-miR-16	-1.31	1.29E-04		
hsa-miR-17	-1.9	1.45E-04		
hsa-miR-182	-0.48	1.98E-03		
hsa-miR-1826	0.35	5.13E-03		
hsa-miR-197	1.32	2.76E-03		
hsa-miR-200b	-1.16	2.00E-03		
hsa-miR-20a	-2.35	8.09E-07		
hsa-miR-21	-4.37	2.95E-05		
hsa-miR-221	-0.94	3.66E-08		
hsa-miR-222	-0.17	2.37E-03		

	Log2 (Ad12S/ Untreated)	p value	Regulation in prostate and/or other types of cancer	Validated in Cancer
hsa-miR-23a	-1.46	2.37E-04		
hsa-miR-23b	-1.95	3.64E-06		
hsa-miR-24	-1.46	1.44E-05		
hsa-miR-25	-0.54	7.25E-04		
hsa-miR-26a	-1.25	5.29E-04		
hsa-miR-26b	-3.76	1.66E-05		
hsa-miR-27a	-3.71	3.98E-05		
hsa-miR-29a	-2.88	9.65E-06		
hsa-miR-30b	-1.66	8.07E-07		
hsa-miR-30c	-1.1	4.57E-03		
hsa-miR-30d	-0.72	5.33E-04		
hsa-miR-31	-0.87	8.45E-05		
hsa-miR-320a	1.39	1.47E-07		
hsa-miR-320b	1.45	3.53E-05		
hsa-miR-320c	1.43	1.69E-05		
hsa-miR-320d	1.46	7.75E-05		
hsa-miR-361-5p	0.41	3.78E-04		
hsa-miR-423-5p	1.13	2.32E-06	NA	
hsa-miR-483-5p	4.15	2.13E-03		
hsa-miR-574-3p	2.76	3.15E-04		
hsa-miR-574-5p	4.35	2.92E-05		
hsa-miR-601	5.49	3.62E-03		
hsa-miR-638	4	1.03E-07		
hsa-miR-720	1.87	1.24E-05	NA	
hsa-miR-923	5.7	5.68E-06		
hsa-miR-92a	0.55	2.66E-04		
hsa-miR-92b	0.78	1.55E-03		
hsa-miR-93	-0.72	3.73E-05		
hsa-miR-99a	-3.55	4.73E-03		
hsa-miR-99b	0.78	3.93E-03		

Up-regulated
Down-regulated
Discrepant results in literature
Highly significant

Deregulation Involved in Prostate cancer
Deregulation involved in other types of cancer
No information available
MicroRNAs verified in two experiments

p-values determined by t-test; highly significant p-values (p<0.001; yellow).

The differences in the expression of miRNAs in PC-3 cells at 48h post-infection with the AdE1A12S virus showed an increase in the number of deregulated miRNAs compared to 24h, increasing from 29 to 60 miRNAs (Table 11 and 15). From the 60 significantly deregulated miRNAs, 25 were also deregulated at 24h hsa-let-7e, hsa-miR-106a, hsa-miR-106b, hsa-miR-1268, hsa-miR-1275, hsa-miR-1280, hsa-miR-151-3p, hsa-miR-16, hsa-miR-17, hsa-miR-1826, hsa-miR-20a, hsa-miR-21, hsa-miR-24,

hsa-miR-26a, hsa-miR-27a, hsa-miR-29a, hsa-miR-30d, hsa-miR-483-5p, hsa-miR-574-3p, hsa-miR-574-5p, hsa-miR-638, hsa-miR-923, hsa-miR-92b, hsa-miR-93, hsa-miR-99a) (Tables 11 and 15). Moreover, from the 25 miRNAs only hsa-miR-1826 and hsa-miR-99a were regulated at both time points in the same manner (up- and down-regulated respectively), the remaining 23 miRNAs showed a different regulation after infection (Tables 11 and 15), this implies that changes in the miRNA expression are time-dependent and that secondary regulatory mechanisms are activated at later time points.

3.3.2 In PC-3 cells, miRNAs are differentially expressed also at 48h post-treatment with mitoxantrone compared to untreated cells.

The pattern of expression of highly significant changes in miRNAs in PC-3 cells treated with mitoxantrone for 48h, showed that 20/45 miRNAs were upregulated and 25 out of 45 were downregulated in response to the treatment (Table 16). Moreover, 11/20 upregulated miRNAs (hsa-let-7b, hsa-let-7c, hsa-let-7d, hsa-let-7e, hsa-miR-125a-5p, hsa-miR-15b, hsa-miR-16, hsa-miR-1826, hsa-miR-29c, hsa-miR-92b, and hsa-miR-99a) were reported to be downregulated in PCa or other types of cancer (Table 16). In contrast, 14 out of 25 downregulated miRNAs (hsa-miR-106a, hsa-miR-106b, hsa-miR-107, hsa-miR-151-3p, hsa-miR-151-5p, hsa-miR-17, hsa-miR-191, hsa-miR-20a, hsa-miR-24, hsa-miR-30d, hsa-miR-320a, hsa-miR-425, hsa-miR-93, hsa-miR-99b, were reported to be upregulated in PCa or other types of cancer (Table 16).[231,234-238] The largest difference was for hsa-miR-29c (Log2= 2.04), that has been previously demonstrated to be downregulated in cancer, although it has not been implicated in PCa.[231,234-238] The hsa-miR-29c was not considered for further analysis since, as well as the miRNAs hsa-miR-30d hsa-miR-425, hsa-miR-98 and hsa-miR-99a, were not verified in a second experiment (Section 3.4). And only those miRNAs verified in the second experiment were considered for further analysis.

When results for the treatment with mitoxantrone were compared to those for infection alone at 48h, we observed that 36 out of 45 miRNAs were being regulated by both treatments (Table 16 and 15). From the 36 miRNAs that changed at both time points only 7 miRNAs (upregulated with mitoxantrone green; hsa-miR-16, hsa-

miR-182, hsa-miR-21, hsa-miR-99a; downregulated, red; hsa-miR-320a, hsa-miR-361-5p, and hsa-miR-99b) showed a different pattern of expression, whereas 29 miRNAs showed a similar pattern of expression (Table 16 and 15).

In the analysis we observed that when the miRNAs treated with mitoxantrone for 48h were compared to the 24h samples, there was an increase in the number of miRNAs being deregulated from 19 up to 45 (Table 12 and 16). Moreover, only 13/45 (hsa-let-7c/d/e, hsa-miR-100, hsa-miR-1246, hsa-miR-16, hsa-miR-182, hsa-miR-1826, hsa-miR-191, hsa-miR-222, hsa-miR-423-5p, hsa-miR-99a and hsa-miR-99b) miRNAs were regulated by the treatment at both time points 24h and 48h (Table 12 and 16). The expression of 8/13 miRNAs that were regulated in response to the treatment at both time points showed a different pattern of expression, whereas the miRNAs hsa-let-7c/d/e and hsa-miR-1246 were downregulated at 24h (red) and upregulated at 48h (green) (Table 12 and 16). The miRNAs hsa-miR-191, hsa-miR-222 and hsa-miR-99a and hsa-miR-100 were upregulated at 24h (green) and downregulated at 48h (red) (Table 12 and 16). Only 5 out of 13 miRNAs (upregulated hsa-miR-16, hsa-miR-182, hsa-miR-1826 and hsa-miR-423-5p, green; downregulated hsa-miR-99b red) showed the same pattern of expression at 24h and 48h. However, at 48h most of these miRNAs (except hsa-miR-1826 and hsa-miR-99b) showed almost half Log 2 higher expression in the 24h samples (Table 12 and 16).

Table 16. Differentially expressed miRNAs in PC-3 cells 48h post-treatment with Mitoxantrone (50nM) compared to untreated and uninfected cells.

	Log2 (Mitoxantrone/ Untreated)	p value	Regulation in prostate and/or other types of cancer	Validated in Cancer
hsa-let-7b	0.27	8.58E-03		
hsa-let-7c	0.33	2.06E-03		
hsa-let-7d	0.2	9.44E-03		
hsa-let-7e	1.38	1.35E-04		
hsa-miR-100	-0.43	2.68E-05		
hsa-miR-103	-0.74	1.13E-06		
hsa-miR-106a	-0.54	1.19E-04		
hsa-miR-106b	-0.65	2.27E-06		
hsa-miR-107	-0.55	1.09E-05		
hsa-miR-1246	1.51	3.22E-05		
hsa-miR-125a-5p	0.45	3.88E-03		
hsa-miR-1275	1.19	9.29E-04	NA	
hsa-miR-128	-0.34	3.44E-03		
hsa-miR-1308	0.35	4.21E-03	NA	
hsa-miR-151-3p	-1	1.41E-05		
hsa-miR-151-5p	-0.34	9.22E-05		
hsa-miR-15b	0.31	1.41E-03		
hsa-miR-16	0.2	4.51E-03		
hsa-miR-17	-0.65	5.10E-04		
hsa-miR-182	0.36	5.76E-03		
hsa-miR-1826	1.3	5.88E-07		
hsa-miR-183	0.35	4.05E-03		
hsa-miR-191	-0.41	8.73E-06		

	Log2 (Mitoxantrone/ Untreated)	p value	Regulation in prostate and/or other types of cancer	Validated in Cancer
hsa-miR-20a	-0.58	9.24E-05		
hsa-miR-20b	0.68	3.50E-03		
hsa-miR-21	0.29	4.94E-04		
hsa-miR-221	-0.49	1.11E-03		
hsa-miR-222	-0.63	3.55E-04		
hsa-miR-23a	-0.34	1.05E-03		
hsa-miR-23b	-0.32	4.13E-03		
hsa-miR-24	-0.93	1.63E-04		
hsa-miR-27a	-0.86	4.58E-05		
hsa-miR-29a	-0.63	5.63E-04		
hsa-miR-29c	2.04	5.92E-04		
hsa-miR-30d	-1.04	2.35E-06		
hsa-miR-31	-0.99	4.85E-07		
hsa-miR-320a	-0.28	6.36E-03		
hsa-miR-361-5p	-0.42	1.55E-04		
hsa-miR-423-5p	0.53	2.79E-04	NA	
hsa-miR-425	-0.44	1.11E-03		
hsa-miR-92b	0.39	1.66E-04		
hsa-miR-93	-1.35	5.12E-06		
hsa-miR-98	1.49	2.43E-04		
hsa-miR-99a	1.25	3.28E-04		
hsa-miR-99b	-0.87	1.52E-04		

Up-regulated
Down-regulated
Discrepant results in literature
Highly significant

Deregulation Involved in Prostate cancer
Deregulation Involved in other types of cancer
No information available
NA
MicroRNAs verified in two experiments

p-values determined by t-test; highly significant p-values (p<0.001; yellow).

The changes in the pattern of expression of different miRNAs, such as let-7c/d/e, may reflect that the regulatory pathways of these miRNAs are dependent on the activation or deregulation of other miRNAs or genes. There might be a progressive signalling cascade that changes over time. Moreover, miRNAs such as hsa-miR-16 showed no change in the pattern of expression at 48h compared to 24h, although there was a change in absolute magnitude of the difference, decreasing from 0.83 at 24h to 0.2 at 48h. Although the regulatory mechanisms seem to be far more complex, the differences in the miRNA expression indicate that miRNAs such as hsa-miR-16 or hsa-hsa-miR-100 that might be primary targets and could trigger the

regulation of secondary target miRNAs (such as hsa-let-7c/d/e or has-hsa-miR-99a) that are acting as late effectors within one or more signalling pathways in a time-dependent manner. Moreover, the miRNAs could also be induced at an early stage but repressed at a late stage by other targets. The direct regulation of such miRNAs is not part of this study, but is an interesting point that should be assessed in future studies.

3.3.3 In PC-3 cells, miRNAs are differentially expressed also after 48h when simultaneously infected with AdE1A12S and treated with mitoxantrone compared to untreated cells.

The combination of mitoxantrone (50nM) and AdE1A12S (100ppc), resulted in upregulation of 23 out of 45 and downregulation of 22 out of 45 miRNAs after 48h when compared to the untreated samples (Table 17). The upregulation of 11/23 miRNAs (hsa-let-7a/b/c/d/e/f, hsa-miR-106a, hsa-miR-107, hsa-miR-125a-5p, hsa-miR-15b, hsa-miR-1826, hsa-miR-638 and hsa-miR-92b) is interesting since these miRNAs have been reported to be downregulated in cancer tissues (Table 17). Moreover the expression of 11/22 miRNAs (hsa-miR-106a, hsa-miR-107, hsa-miR-151-3p, hsa-miR-151-5p, hsa-miR-17, hsa-miR-191, hsa-miR-20a, hsa-miR-24, hsa-miR-30d, hsa-miR-425, hsa-miR-93, hsa-miR-99b) that were downregulated by the combination treatments were previously reported to be upregulated in PCa (Table 17).[231,234-238] From the total of 45 miRNAs deregulated by the combination only 9 have not been verified in PCa (Table 17; light blue), whereas in 4 miRNAs the information is not available (Table 17; NA).

The largest differences in the expression of miRNAs were shown by hsa-miR-1246, hsa-miR-1826 and hsa-miR-638 (Log2> 2.0, upregulated; green) and hsa-miR-222, hsa-miR-24, hsa-miR-31 and hsa-miR-93 (Log2< -1.20, downregulated; red) (Table 17).

When compared to the treatments alone, 36 out of 45 miRNAs were deregulated in response to the combination and were also regulated by the virus alone (Table 15). Moreover, 37 of 45 miRNAs were regulated by the combination and with mitoxantrone alone. The expression of 37 of 37 miRNAs in response to mitoxantrone

alone showed a similar pattern of expression when compared to the combination (up- and downregulated samples; Tables 15 and 17). When we compared the infected samples we observed that 36 of 36 miRNAs also showed the same pattern of expression as the combination (Tables 14 and 17). The expression of 30 out of 45 miRNAs (hsa-let-7b/c/d/e, hsa-miR-100, hsa-miR-103, hsa-miR-106a, hsa-miR-107, hsa-miR-1275, hsa-miR-1308, hsa-miR-151-3p, hsa-miR-151-5p, hsa-miR-17, hsa-miR-182, hsa-miR-1826, hsa-miR-20a, hsa-miR-21, hsa-miR-221, hsa-miR-222, hsa-miR-23a, hsa-miR-23b, hsa-miR-24, hsa-miR-27a, hsa-miR-29a, hsa-miR-30d, hsa-miR-31, hsa-miR-423-5p, hsa-miR-92b, hsa-miR-93 and hsa-miR-99b) overlapped with those in the AdE1A12S-infected samples, mitoxantrone-treated samples and the combination-treated samples when compared to the untreated samples. The expression of only 2 out of 45 miRNAs, hsa-let-7f and hsa-miR-125b, were not deregulated by any of the single agents treatments (Tables 14, 15 and 15).

Table 17. Differentially expressed miRNAs in PC-3 cells simultaneously infected with AdE1A12S (100ppc) and treated with mitoxantrone (50nM) compared to untreated cells at 48h after treatment.

	Log2 (Combo/ Untreated)	p value	Regulation in prostate and/or other types of cancer	Validated in Cancer
hsa-let-7a	0.21	3.32E-03		
hsa-let-7b	0.42	4.81E-04		
hsa-let-7c	0.45	6.42E-04		
hsa-let-7d	0.27	4.31E-03		
hsa-let-7e	1.15	1.55E-03		
hsa-let-7f	0.32	7.02E-03		
hsa-miR-100	-1.10	7.19E-04		
hsa-miR-103	-1.04	2.81E-04		
hsa-miR-106a	-0.90	3.40E-03		
hsa-miR-107	-0.86	9.58E-04		
hsa-miR-1246	2.34	1.09E-06		
hsa-miR-125a-5p	0.41	4.49E-03		
hsa-miR-125b	-0.53	4.57E-04		
hsa-miR-1275	1.42	5.63E-03		
hsa-miR-1280	0.93	2.69E-03	NA	
hsa-miR-1308	1.00	3.07E-05		
hsa-miR-151-3p	-1.04	4.41E-05		
hsa-miR-151-5p	-0.50	1.02E-05		
hsa-miR-15b	0.66	4.51E-03		
hsa-miR-17	-1.05	3.36E-04		
hsa-miR-182	0.62	9.89E-04		
hsa-miR-1826	2.14	4.28E-08		
hsa-miR-183	0.74	1.12E-04		

	Log2 (Combo/ Untreated)	p value	Regulation in prostate and /or other types of cancer	Validated in Cancer
hsa-miR-191	-0.61	1.76E-03		
hsa-miR-20a	-0.90	3.63E-05		
hsa-miR-21	0.27	4.71E-03		
hsa-miR-221	-1.08	1.32E-04		
hsa-miR-222	-1.36	6.67E-05		
hsa-miR-23a	-0.55	1.78E-04		
hsa-miR-23b	-0.58	2.48E-04		
hsa-miR-24	-1.24	3.48E-05		
hsa-miR-27a	-1.01	5.83E-07		
hsa-miR-29a	-1.10	8.23E-07		
hsa-miR-30d	-0.44	2.26E-03		
hsa-miR-31	-1.58	5.18E-06		
hsa-miR-320b	0.50	3.00E-03		
hsa-miR-320d	0.59	4.09E-03		
hsa-miR-423-5p	0.60	2.70E-04	NA	
hsa-miR-425	-0.50	4.77E-03		
hsa-miR-638	2.31	1.26E-06		
hsa-miR-923	1.20	1.55E-04	NA	
hsa-miR-92b	0.58	1.99E-04		
hsa-miR-93	-1.25	1.89E-06		
hsa-miR-98	1.17	5.81E-03		
hsa-miR-99b	-1.19	1.30E-03		

Up-regulated
Down-regulated
Discrepant results in literature
Highly significant

Deregulation involved in Prostate cancer
Deregulation Involved in other types of cancer
No information available
MicroRNAs verified in two experiments
NA

p-values determined by t-test; highly significant p-values (p<0.001; yellow).

When the expression of miRNAs in cells treated with mitoxantrone in combination with AdE1A12S-infection at 48h was compared to the same treatment at 24h, an increase was observed from 37 to 45 differentially expressed miRNAs (Tables 13 and 17). The expression of 18/45 miRNAs (hsa-let-7b, hsa-let-7d, hsa-miR-106a, hsa-miR-1280, hsa-miR-17, hsa-miR-191, hsa-miR-20a, hsa-miR-21, hsa-miR-23a, hsa-miR-23b, hsa-miR-24, hsa-miR-29a, hsa-miR-320d, hsa-miR-425, hsa-miR-638, hsa-miR-923,

hsa-miR-93, hsa-miR-99b) changed at both time points compared to the untreated samples. Although, only the expression of hsa-miR-191, hsa-miR-425, hsa-miR-99b (downregulated) and hsa-miR-21 (upregulated) maintained the same pattern of expression as in the 24h samples (Tables 13 and 17).

3.3.4 In PC-3 cells, simultaneously treated with mitoxantrone and infected with AdE1A12S for 48h, differentially expressed miRNAs show a more than additive deregulation when compared to the theoretical sum of the miRNAs in single agent-treated cells.

The expression of miRNAs in PC-3 cells treated with mitoxantrone (50nM) in combination with AdE1A12S (100ppc) for 48h compared to the theoretical sum of the miRNA in single agent-treated cells, showed upregulation in 7 out of 15 miRNAs (hsa-miR-1246, hsa-miR-128, hsa-miR-15b, hsa-miR-182, hsa-miR-1826, hsa-miR-183, and hsa-miR-30d) and downregulation in 8 out of15 miRNAs (hsa-miR-103, hsa-miR-191, hsa-miR-221, hsa-miR-222, hsa-miR-31, hsa-miR-574-5p, hsa-miR-720 and hsa-miR-99b) (Table 18). It has previously been reported that hsa-miR-128, hsa-miR-15b, hsa-miR-1826 were decreased in PCa tissue and we found these miRNAs to be upregulated by the combination treatment. Similarly, hsa-miR-191, hsa-miR-574-5p and hsa-miR-99b were demonstrated as upregulated in PCa while these miRNAs were downregulated by the treatment. The largest differences in expression were for hsa-miR-1246 and hsa-miR-1826 (Log2> 1.20; upregulated) and hsa-miR-574-5p (Log2<-2.0; downregulated) (Table 18).

We demonstrated that the expression of 11 out of 15 miRNAs (hsa-miR-103, hsa-miR-128, hsa-miR-182, hsa-miR-1826, hsa-miR-221, hsa-miR-222, hsa-miR-30d, hsa-miR-31, and hsa-miR-99b), were changed when comparing the combination to the sum of both single agents (AdE1A12S and mitoxantrone). The same miRNAs were also changed when the cells were infected with virus alone. Moreover, the deregulation in the expression of hsa-miR-574-5p and hsa-miR-720 was only significant when comparing the combination to the sum of the single agents (Tables 17 and 18). The expression of 13/15 miRNAs (hsa-miR-103, hsa-miR-1246, hsa-miR-15b, hsa-miR-128, hsa-miR-182, hsa-miR-1826, hsa-miR-191, hsa-miR-221, hsa-miR-222, hsa-miR-30d, hsa-miR-31, and hsa-miR-99b) also changed when cells were

treated with mitoxantrone alone (Tables 16 and 18). When the miRNAs shown in Table 18 were compared to the miRNAs shown in Table 16, all miRNAs were found to be regulated using both analysis, except for hsa-miR-128, hsa-miR-574-5p and hsa-miR-720 (Tables 16 and 18). However, hsa-miR-720 is not considered a mature miRNA sequence.[387] In addition, the pattern of expression was identical except for hsa-miR-30d (upregulated, Table 18; downregulated Table 17).

Table 18. Differentially expressed miRNAs in PC-3 cells simultaneously infected with AdE1A12S (100ppc) and treated with mitoxantrone (50nM) compared to the theoretical sum of miRNA changes in single agent-treated cells.

	Log2 (Combo/12S +mitox)	p value		Regulation in prostate and/or other types of cancer	Validated in Cancer
hsa-miR-103	-0.48	3.81E-04			
hsa-miR-1246	1.37	8.77E-04			
hsa-miR-128	0.50	3.48E-03			
hsa-miR-15b	0.51	1.92E-03			
hsa-miR-182	0.62	4.58E-03			
hsa-miR-1826	1.24	1.85E-04			
hsa-miR-183	0.69	7.82E-04			
hsa-miR-191	-0.57	4.32E-03			
hsa-miR-221	-0.38	4.08E-03			
hsa-miR-222	-0.98	4.11E-06			
hsa-miR-30d	0.43	6.68E-04			
hsa-miR-31	-0.65	2.10E-05			
hsa-miR-574-5p	-2.82	8.35E-03			
hsa-miR-720	-1.20	7.89E-03	NA		
hsa-miR-99b	-1.36	8.39E-03			

Up-regulated
Down-regulated
Discrepant results in literature
Highly significant
Deregulation involved in Prostate cancer
Deregulation Involved in other types of cancer
No information available NA
MicroRNAs verified in two experiments

p-values determined by t-test; highly significant p-values ($p<0.001$; yellow).

The expression of the set of miRNAs shown in Table 18 (48h) compared to the set shown in Table 14 (24h), showed that only hsa-miR-1826 and hsa-miR-191 were deregulated at both time points. The expression of hsa-miR-1826 was downregulated at 24h and was upregulated at 48h (Tables 14 and 18). Hsa-miR-191 was downregulated at both time points, although with a greater decrease at 24h (Log2= -0.75 at 24h and -0.57 at 48h). The regulation of the miRNAs showed that 8 out of 15 where downregulated at 48h compared to 4 out of 14 at 24h. Moreover, except for 191 no other miRNAs were modified at 24h, this may indicate that these miRNAs could be downregulated indirectly as secondary targets by other miRNAs (primary targets) or gene expression changes as a consequence of the treatment.

3.4 Verification of differentially expressed miRNAs in PC-3 cells treated with AdE1A12S, mitoxantrone and the combination for 24h; second experiment.

Subsequently, a second miRNA array experiment was analysed comparing the differences in miRNA expression for the simultaneously treated and infected cells with the theoretical sum of the changes in single agent-treated cells, AdE1A12S (100ppc) and mitoxantrone (50nM). We selected the 24h time point to investigate more direct effects on the changes in miRNA expression in response to the treatments. A total of 73 miRNAs were differentially expressed with all treatments after 24h (average signal-intensities 500 and statistically significant $p<0.01$; Students t-test). From these, 49 were selected based on previous identification in the first array experiments (both 24 and 48h, highlighted in orange in Table 11-18). To identify the potential targets for each miRNA, several accessible databases and tools were used, such as Ensembl.org, mirbase.org, PubMed, mirTarBase.org, TargetScan Human, miRecords, miRDB, microRNA.org, transmir and miR2disease base, in combination with literature searches.[231,234-238] These analyses resulted in identification of 49 miRNAs that were involved in the regulation of cell death and survival pathways.

3.4.1 Up-regulation of miRNAs in PC-3 cells in response to the combination treatment with AdE1A12S and mitoxantrone

The upregulation of miRNAs in PC-3 cells in response to the combination of AdE1A12S and mitoxantrone (combo) compared to the sum of the changes in single-agent-treated cells (AdE1A12S + mitoxantrone) is shown in Table 19. All miRNAs except hsa-let-7e, hsa-miR-1268 and hsa-miR-1275 have been demonstrated to be expressed in PCa cells and tissue.[231,234-238] The differences in the expression of the miRNAs were significant when $log2>0.20$ including hsa-let-7c (0.37), hsa-let-7d (0.30), hsa-let-7e (0.32), hsa-let-7f (0.35), hsa-let-7g (0.38), hsa-miR-1268 (0.54), hsa-miR-23a (0.23), hsa-miR-23b (0.28), with the largest increase for hsa-miR-1246 (0.61). Moreover, hsa-mir125a-5p, hsa-miR-125b, hsa-miR-25, hsa-miR-26a showed

minimal upregulation (log 2=0.01-0.04) and it is questionable whether such a small change is sufficient to induce a response on target genes. The changes in expression of hsa-miR-92b, hsa-miR-27a, hsa-miR-16, hsa -hsa-miR-15b, hsa -hsa-miR-128, hsa -hsa-miR-1275, and hsa -let-7b were intermediate, from 0.1 < log 2 < 0.2. Furthermore, hsa-let-7d, hsa-let-7e, hsa-let-7f, hsa-let-7g are part of the let-7 cluster and hsa-miR-23a and hsa-miR-23b part of the hsa-miR-23 cluster, including hsa-miR-23, -10, -24, -26, -27 and -30,[388,389] and were highly significant (p<.001); this indicates that these clusters are regulated by the same promoter and/or the same transcription factors. Interestingly, the majority (17 out of 21) of the upregulated miRNAs in the combination treated cells has been reported as downregulated in PCa tissue and cell lines, compared to normal tissue, except hsa-miR-1246 and hsa-miR-25.[231,235-239,390]

Table 19. Up-regulated miRNAs in PC-3 cells treated with a combination of AdE1A12S and mitoxantrone compared to the sum of single-agent-treated cells, at 24h post-treatment.

	Log2 (Combo/12 S+M)	p value		Regulation in prostate and/or other types of cancer	Validated in Cancer
hsa-let-7a	0.21	2.55E-02			
hsa-let-7b	0.13	9.15E-02			
hsa-let-7c	0.37	1.06E-02			
hsa-let-7d	0.30	2.00E-03			
hsa-let-7e	0.32	8.65E-03			
hsa-let-7f	0.35	1.24E-03			
hsa-let-7g	0.38	1.50E-04			
hsa-miR-1246	0.61	6.89E-02			
hsa-miR-125a-5p	0.02	2.90E-01			
hsa-miR-125b	0.04	2.12E-01			
hsa-miR-1268	0.54	1.75E-02		NA	
hsa-miR-1275	0.11	9.57E-02			
hsa-miR-128	0.10	1.15E-01			
hsa-miR-15b	0.17	4.64E-02			
hsa-miR-16	0.15	1.27E-01			
hsa-miR-23a	0.23	5.20E-03			
hsa-miR-23b	0.28	9.25E-03			
hsa-miR-25	0.01	2.20E-01			
hsa-miR-26a	0.04	1.22E-01			
hsa-miR-27a	0.11	1.29E-01			
hsa-miR-92b	0.10	5.62E-02			

Up-regulated
Down-regulated
Discrepant results in literature
Highly significant
Deregulation involved in Prostate cancer
Deregulation Involved in other types of cancer
No information available
NA

p-values determined by t-test; highly significant p-values (p<0.001; yellow).

These results suggest that by combining adenoviral E1A12S gene expression with mitoxantrone-treatment, specific miRNAs that are frequently deregulated (downregulated) in PCa, are targeted and their expression is enhanced. It is possible that upregulation of a specific miRNA or cluster of miRNAs thereby prevent further cancer growth and even sensitize the cells to cell killing. The information available in the literature regarding hsa-miR-1268 (Log2= 0.54) and hsa-miR-1275 (Log 2= 0.11) was limited and did not permit complete analysis, thus this work is to my knowledge the first to report on the involvement of these miRNAs in PCa. However, more studies are necessary to validate these data and to explore the functional implications.

3.4.2 Target selection of upregulated miRNAs in PC-3 cells in response to the combination treatment with AdE1A12S and mitoxantrone

To verify the potential implications of the upregulated miRNAs identified under chemosensitizing conditions, a search for potential targets validated in PCa and other types of cancer was performed using available databases and publications. In cases where the miRNA targets have not been validated in cancer, we used the published reports to include other pathologies to complement our data (Table 20).

Most of the miRNAs that were upregulated in response to our treatment combination have been reported to be downregulated in PCa (17 out of 21; Table 20). Interestingly, 15 out of those 17 (miRNAs hsa-let-7a/b/c/d/e/f/g, hsa-miR-125a-5p, hsa-miR-125b, hsa-miR-128, hsa-miR-15b, hsa-miR-16, hsa-miR-23a, hsa-miR-23b and hsa-miR-27a) have been implicated in the induction of apoptosis by increasing or inhibiting the expression of their respective target genes (including p53, casp3 and Bcl-2), or regulating the autophagic pathway through the PI3K/Akt/mTOR. Consequently, when those miRNAs are downregulated cell survival and proliferation are promoted.[374,389-398]

For example, the hsa-miR-125b has been shown to target and down-regulate Mcl-1, Bcl-w and interleukin (IL)-6R levels resulting in apoptosis-induction.[391] Moreover, hsa-miR-125b was shown to reduce the mitochondrial membrane potential and

induce pro-caspase-3 cleavage, indicating that the induction of apoptosis by hsa-miR-125b was mainly by the inhibition of members of the Bcl-2 family. In contrast, the downregulation of hsa-miR-125b contributes to chemo-resistance and tumour development in hepatocellular carcinoma.[391]

Table 20. Cellular genes reported as targets for upregulated miRNAs in this study. Validated gene targets for each miRNA.

miRNA	Target
hsa-let-7a	CASP3
hsa-let-7b	CCND1, CDC25a, CDC34, CDK6, CRDBP,DICER, HMGA2, HOXA9, IMP-1, ITGB3, MYC, RAS, TLR4
hsa-let-7c	
hsa-let-7d	
hsa-let-7e	
hsa-let-7f	
hsa-let-7g	
hsa-miR-1246	DYRK1A
hsa-miR-125a-5p	ERBB2, ERBB3, LIN28, LIN41, TNFSF4
hsa-miR-125b	p53, BAK1, BBC3, Mcl-1, Bcl-w, IL-6R
hsa-miR-128	PDK1/2, mTOR, PDE3 A/B, FOXO1, AKT
hsa-miR-15b	BCL2, CAPRIN1,CARD10, CCND1, CDK6, CDC27, CGI-38, CYCE, DMTF1,HMGA2, MCL1, MYB, NGN2, VEGF, WNT3A, CDKN1A, PDE3 A/B, CHUK, FOXO1
hsa-miR-16	
hsa-miR-23a	CXCL12, FLJ13258
hsa-miR-23b	Notch1, Src Kinase, AKT, PTEN PI3K
hsa-miR-25	E2F1, PI3K, PTEN, PDK1/2, PDE3 A/B
hsa-miR-26a	PLAG1, PTEN, MDM2, GSK3B, FOXO1
hsa-miR-27a	FOXO1, APC
hsa-miR-92b	PI3K, PTEN, PDK1/2, PDE3 A/B

The overexpression of the hsa-miR23b has been shown to target Src kinase and Akt, decreasing tumour growth in nude mice.[393] In renal cancer the reduction of hsa-miR-23b was associated with increased expression of PTEN and a reduction of PI3K and total Akt was also observed.[399] Another miRNA that targets the apoptotic pathway is the hsa-miR-128 that when overexpressed inhibits PCa cell invasion.[400] An example of miRNA regulation is the hsa-let-7a that induces cell cycle arrest at the G1/S- phase when it is upregulated by direct binding to the mRNAs of E2F2 and CCND2 in PCa.[395] Furthermore, the overexpression of let-7c inhibits cell proliferation and clonogenicity

by targeting IL-6, Myc, Lin-28 and AR in PCa cells.[396] The hsa-miR-15/16 cluster has been shown to induce tumour suppression by targeting Bcl-2, CCND1 and WNT3A in PCa, inhibiting cell survival and proliferation.[397] The overexpression of hsa-miR-1246, a target of the p53 family (H1299 cells), was shown to induce apoptosis by targeting and downregulating DYRK1A (Down-syndrome marker) in U2OS cells.[374] The overexpression of hsa-miR-23a/27a/24-2 cluster has been shown to trigger endoplasmic reticulum stress (ER stress) inducing apoptosis in HEK293T cells.[389] Moreover, cell proliferation induce by Myc is regulated through the repression of hsa-miR-miR-23a and hsa-miR-miR-23b.[401]

3.4.3 Down-regulation of miRNAs in PC-3 cells in response to the combination treatment with AdE1A12S and mitoxantrone, after 24h.

Table 21 illustrates the miRNAs that were downregulated by the combination treatment (combo) compared to the sum of changes in miRNA expression in the single agent-treated cells (AdE1A12S + mitoxantrone; 12S+M). The identified hsa-miR-361-5p, hsa-miR-423-5p, hsa-miR-1826 and hsa-miR-107 are known as deregulated in different types of cancer, although none of them has been reported and validated in PCa. Even though, hsa-miR-107 has not been identified specifically in PCa, it has been demonstrated to belong to a group of miRNAs located next to the hsa-miR-15/16 gene cluster which is frequently downregulated in PCa.[225] The hsa-miR-107 has high homology with hsa-miR-103 with differences only in one nucleotide.[402] Hsa-miR-103 has been validated as deregulated in PCa.[385] In contrast to the upregulated miRNAs, only a few miRNAs exhibited large log2 differences (Table 20 and 21). Most of the downregulated miRNAs had log2 values <-0.20 (21 out of 28), with hsa-miR-21 having the greatest negative log 2 value of -1.13. Other highly different miRNAs were hsa-miR-100 (-0.31), hsa-miR-103 (-0.40), hsa-miR-106a (-0.27), hsa-miR-107 (-0.46), hsa-miR-151-3p (-0.30), hsa-miR-151-5p (-0.25), hsa-miR-17 (-0.28), hsa-miR-1826 (-0.23), hsa-miR-191 (-0.41), hsa-miR-20a (-0.21), hsa-miR-222 (-0.28), hsa-miR-31 (-0.37), hsa-miR-320a (-0.38), hsa-miR-320b (-0.22), hsa-miR-320c (-0.32), hsa-miR-320d (-0.20), hsa-miR-93 (-0.30) and hsa-miR-99b (-0.20).

The miRNAs that had lesser changes in expression (log2 value > -0.10) were hsa-let-7i, hsa-miR-361-5p, hsa-miR-92a, hsa-miR-29a, hsa-miR-182. These small changes imply limited involvement in the response to the treatment and may not be part of the regulatory mechanisms of chemosensitization. However, miRNAs such as hsa-let-7i, hsa-miR-92a and hsa-miR-182 are known to be activated as clusters such as the hsa-let-7 family, hsa-miR-17-92 and hsa-miR-183-96-182 clusters. Thus, despite the lesser changes in expression levels they might still be involved in the regulatory machinery triggering the chemosensitization of the cells.

Table 21. Down-regulated miRNAs in PC-3 cells treated with a combination of AdE1A12S and mitoxantrone under synergistic conditions compared to single agent-treated cells, after 24h of treatment.

	Log2 (Combo/12S+M)	p value	Regulation in prostate and/or other types of cancer	Validated in Cancer
hsa-let-7i	-0.06	3.88E-01		
hsa-miR-100	-0.31	4.29E-02		
hsa-miR-103	-0.40	1.11E-02		
hsa-miR-106a	-0.27	1.07E-01		
hsa-miR-107	-0.46	4.96E-03		
hsa-miR-151-3p	-0.30	4.80E-02		
hsa-miR-151-5p	-0.25	9.79E-02		
hsa-miR-17	-0.28	5.88E-02		
hsa-miR-182	-0.05	4.54E-01		
hsa-miR-1826	-0.23	2.39E-01		
hsa-miR-183	-0.04	4.82E-01		
hsa-miR-191	-0.41	1.88E-02		
hsa-miR-20a	-0.21	1.93E-01		
hsa-miR-21	-1.13	6.76E-02		
hsa-miR-221	-0.15	3.16E-01		
hsa-miR-222	-0.28	7.72E-02		
hsa-miR-24	-0.16	2.68E-01		
hsa-miR-29a	-0.07	4.08E-01		
hsa-miR-31	-0.37	2.57E-02		
hsa-miR-320a	-0.38	4.97E-02		
hsa-miR-320b	-0.22	1.87E-01		
hsa-miR-320c	-0.32	6.11E-02		
hsa-miR-320d	-0.20	3.16E-01		
hsa-miR-361-5p	-0.09	4.31E-01		
hsa-miR-423-5p	-0.16	2.94E-01	NA	
hsa-miR-92a	-0.08	4.59E-01		
hsa-miR-93	-0.30	5.54E-02		
hsa-miR-99b	-0.20	2.09E-01		

Up-regulated	
Down-regulated	
Discrepant results in literature	
Highly significant	
Deregulation involved in Prostate cancer	
Deregulation Involved in other types of cancer	
No information available	NA

p-values determined by t-test; highly significant p-values (p<0.001; yellow).

The hsa-miR-107 had the most significant difference (p=4.96E-3; Log2= -0.46). Most of the miRNAs (18 out of 28) that were downregulated by the combination treatment have been reported as upregulated in cancer. Hsa-miR-100, hsa-miR-103, hsa-miR-1826, hsa-miR-221, hsa-miR-222, hsa-miR-29a, hsa-miR-31, hsa-miR-361-5p, hsa-miR-92a, were downregulated by the treatment and it was previously reported that these miRNAs were typically upregulated in cancer.[231,234-238] However, there are several contradictory reports suggesting that hsa-miR-221, hsa-miR-222, hsa-miR-29, hsa-miR-31, hsa-miR-92 are also upregulated in cancer. In this study, we considered miRNAs as up- or downregulated according to the published data of their regulation in PCa cells or cancerous tissue and reported in two or more studies. Contradictory results also have been reported for hsa-let-7i, hsa-miR-191, hsa-miR-24 and hsa-miR-99 but are predominantly indicated as upregulated. It is likely that hsa-miR-29a and hsa-miR-92a do not play significant roles in the response to treatment since the log2 values are close to zero, although more experiments and validation are required prior to this conclusion. The hsa-miR-1826 was downregulated (Log2= -0.23), and it was recently identified as a tumour suppressor in renal cancer cells.[403] However, hsa-miR-1826 has also been identified as a fragment of the 5.8S rRNA[387] and is thus not considered as a true miRNA and was not included in further analysis. These results demonstrate that the cancer-dependent upregulation of these miRNAs could be attenuated in response to the combination treatment.

3.4.4 Target selection of downregulated miRNAs in PC-3 cells in response to the combination treatment with AdE1A12S and mitoxantrone

We searched for the targets of downregulated miRNAs in response to the combination treatments, using the same criteria of selection as mentioned in section 3.4.2 for the upregulated miRNAs.

Table 22 includes miRNAs that typically are upregulated in cancer cells; the mitoxantrone and AdE1A12S combination induced downregulation of these miRNAs. Thus it is important to consider the mechanistic implications in the downregulation of some of this miRNAs in response to the treatments.

Table 22. Cellular genes reported as targets for the miRNAs identified as downregulated in this study.

miRNA	Target
hsa-let-7i	CCND1, CDC25a, CDC34, CDK6, CRDBP,DICER, HMGA2, HOXA9, IMP-1, ITGB3, MYC, RAS, TLR4
hsa-miR-100	mTOR, ATM, PLK1, FGFR3
hsa-miR-103	CDK5R1
hsa-miR-106a	RB1, p21, PI3K, PTEN, AKT, ULK1
hsa-miR-107	p53
hsa-miR-151-3p	RhoGDIA
hsa-miR-151-5p	
hsa-miR-17	AIB1, AML1, BIM1, CTGF, CDKN1A, E2F1, E2F2, E2F3, HIF-1A, PTEN, TGFBR2, TSP1, Rb2/P130, p62
hsa-miR-182	Casp9, FOXO1/3
hsa-miR-1826	beta-catenin (CTNNB1) and MEK1 (MAP2K1)
hsa-miR-183	PTEN, AKT, FOXO1, LC3B1
hsa-miR-191	SOX4, IL1A,TMC7
hsa-miR-20a	AIB1, AML1, BIM1, CTGF, CDKN1A, E2F1, E2F2, E2F3, HIF-1A, PTEN, TGFBR2, TSP1, Rb2/P130, p62
hsa-miR-21	BCL2, MASPIN, PDCD4, PTEN, TPM1, RECK, RASA1, PDE3 A/B, CHUK, FOXO1, AKT
hsa-miR-221	c-KIT, P27, CDKN1B, P57, CDKN1C, ESR1, MDM2, FOXO1, AKT
hsa-miR-222	
hsa-miR-24	Notch1, MAPK14, FAF1
hsa-miR-29a	CDC42,DNMT3A, B, MCL1, PIK3R1, TCL1, PTEN
hsa-miR-31	PDK 1/2, NOS3
hsa-miR-320a	ETS2,ET-1, VEGF, and FN through ERK 1/2, CD71
hsa-miR-320b	
hsa-miR-320c	
hsa-miR-320d	
hsa-miR-361-5p	VEGFA
hsa-miR-423-5p	PR, IGSF1
hsa-miR-92a	PI3K, PTEN, PDK1/2, PDE3 A/B, p62
hsa-miR-93	integrin-β8,ERBB2, p21 and VEGF, CCNB1
hsa-miR-99b	SMARCA5, SMARCD1, and mTOR.

For example, the regulation of the cell cycle is inhibited by the hsa-miR-106 family by targeting p21 to facilitate cell proliferation.[404] Moreover, the overexpression of the hsa-miR-106b-25 and hsa-miR-17-92 clusters have been shown to regulate the TGFβ signalling by preventing cell cycle arrest and apoptosis in gastrointestinal cells.[405] In addition, a correlation was found in the impairment of PTEN in PCa progression and the overexpression of hsa-miR-22 and the hsa-miR-106b/25 cluster that targets PTEN.[212] Another highly expressed miRNA in cancer progression is the hsa-miR-21; its overexpression has been shown to induce cell proliferation induced by an androgen-stimulus in PCa. In contrast, the inhibition the hsa-miR-21 facilitates the induction of apoptosis triggered by FOXO3a by repressing hsa-miR-21.[406,407] Another example is the amplification of the hsa-miR-17 cluster that is associated with malignant lymphomas.[288] In A549 it has been shown that the downregulation of hsa-miR-24 inhibits cell growth.[288] In melanoma, the transcription factor FOXO3 inhibits cell migration by downregulating the hsa-miR-182, in contrast FOXO3 is impaired when

the hsa-miR-182 is overexpressed.[408] In an orthotopic xenograft mouse model of hepatocellular carcinoma the inhibition of the hsa-miR-191 reduced tumour size while *in vitro* cell proliferation was inhibited and apoptosis was induced.[409] The hsa-miR-221/222 has been shown to target and inhibit the tumour suppressor p27, inducing cell proliferation in PC-3 cells, while the knock-down of hsa-miR-221/222 increased clonogenicity.[291] In addition, the overexpression of hsa-miR-221/222 and the downregulation of hsa-miR-23b/-27b can be considered a poor prognosis marker in metastatic castrate-resistant PCa.[384] Another miRNA that can inhibit apoptosis via the inhibition of PTEN is the hsa-miR-17-92 cluster through the hsa-miR-19 component, inducing tumour progression.[410] Recently the induction of apoptosis and autophagy by p53 has been shown to be enhanced by hsa-miR-93/106b which inhibits p21.[350] The hsa-miR-93/106b has been shown to be regulated by adenoviral E1A and E2F1 in human osteosarcoma.[350]

3.4.5. Summary

Taking all data from the miRNA analysis into consideration I found, as could be expected, a trend that cell death and survival pathways appeared to play major roles in the response to the combination treatment. Therefore, we selected potential key regulators that were indicated as targets for the AdE1A12S and mitoxantrone combination, to investigate the corresponding pathways further by determining changes in the expression levels of selected proteins. Most of the indicated targets are known to be involved in regulation of the cell cycle, cell proliferation, apoptosis and autophagy networks and include p53, Akt, Bcl-2, p62, LC3B-I/II, mTOR, Caspase3, FOXO1/3, PTEN and E2F1.

Further validation of changes in miRNA and/or the corresponding mRNA levels would be necessary to delineate the specific regulation by the treatments and the respective pathways. These extensive investigations are planned for future projects and were beyond the scope of my PhD project due to time-limitations. In the next part of the project, I therefore focused on verifying changes in expression of proteins that are representative of these pathways and are typical key factors in the regulation of cell death and survival.

3.4.5. a In Summary

- Most identified miRNAs have previously been reported to be deregulated in PCa
- The majority of upregulated miRNAs in response to the combination treatments have been previously reported to be downregulated in PCa. In addition, downregulated miRNAs in response to the combination treatments have been previously reported to be upregulated in PCa
- Regulation of cell death and survival pathways (apoptosis, autophagy and proliferation) have been reported for the identified miRNAs that were differentially expressed in response to the combination treatments. Some of the key regulatory factors that were indicated as targets include Akt, Bcl-2, p62, LC3B and p53.
- Most of the differentially expressed miRNAs in response to the combination treatments were previously reported to be regulated either by the MYC or E2F1 transcription factors.
- The miRNAs hsa-miR-1268 and hsa-miR-1275 modulated in response to the combination treatments have not been previously reported to be involved in the progression of PCa.

3.5 Validation of changes in expression of selected miRNA targets

The miRNA analysis predicted the role of regulatory factors implicated in cell death and survival pathways, including autophagy and apoptosis, which might be involved in the enhancement of cell death in response to the combination treatments (virus and mitoxantrone). To address the role of selected factors that were indicated to be altered in response to the combination treatment, we determined changes in expression levels of the corresponding proteins. The selection was based on the miRNA analysis, previous findings in the laboratory and with established functions in cell death and survival pathways reported in the literature. Initially, we assessed the ratio of LC3B-II to LC3B-I, the degradation of p62/SQSTM1, the expression of Bcl-2 and the phosphorylation of Akt by immunoblotting in PCa cells under synergistic

conditions. These key factors are typical markers of autophagic flux (LC3B and p62/SQSTM1), deregulated apoptosis (Bcl-2) and protein translation and survival signalling (Akt).

To validate that the observed differential changes in the expression of miRNAs were reflected in changes in potential downstream target proteins, I investigated the expression-changes of these proteins by immunoblotting. Due to differences in virus and drug batches compared to the earlier preparations of samples for the miRNA analysis (performed in 2009) we conducted a broad screen of virus and drug dose-responses by cell viability assays (section 6.2; Fig. 53) and immunoblotting. The PCa cell lines PC-3 (AR^-p53^-) and 22Rv1 (AR^+p53^+), were treated and screened at different concentrations of mitoxantrone (50-2000nM) alone or infected with the AdE1A12S (50-4000ppc). I also included the replication-selective mutant Ad$\Delta\Delta$ (50-2000ppc) and Ad5wt (50-2000ppc) to explore whether similar factors were involved in the enhancement of cell killing previously reported for Ad$\Delta\Delta$ and Ad5wt.[118]

To monitor autophagic activity in PCa cells lines, we assessed the expression ratio of LC3B-II to LC3B-I. The microtubule-associated protein 1A/1B-light chain 3 (LC3/Atg8), is a 17 kDa cytosolic protein.[411] During autophagy initiation, as part of the autophagosome membrane elongation, the cytosolic form of LC3-I becomes conjugated with phosphatidylethanolamine (PE) to form LC3-II. [411] The conjugated LC3-II is then recruited by the autophagosomes where it accumulates in the membrane until it is degraded by lysosomal hydrolases in the autolysosomal lumen when autophagy is completed (Autophagy flux).[411] Therefore, an increase in the ratio of LC3B-II to LC3B-I is considered as an indicator of autophagosome accumulation, or autophagic activity.[313] Despite that the molecular weight of LC3B-II is larger by its conjugation with PE than LC3B-I, LC3B-II migrates faster than LC3B-I in SDS-PAGE; detection of LC3B-II and LC3B-I is at 17kDa and 15kDa, respectively.[313]

In addition, we investigated the changes in expression of the polyubiquitin-binding protein p62/SQSTM1 as a second autophagic marker. The p62/SQSTM1 can polymerise and form protein bodies within the autophagosomes and lysosomal structures and bind to LC3-II.[412] The levels of p62 are dependent on autophagic activity; whereas inhibition of autophagic flux favours p62 accumulation, complete autophagy flux causes p62 degradation.[313,412] Importantly, p62 levels can also be

modified by autophagy-independent mechanisms including oxidative stress, apoptosis and proteasomal degradation.[313,413]

3.5.1 Autophagic activity is increased in response to mitoxantrone but decreased when simultaneously infected with AdE1A12S for 24h.

To assess the expression of LC3B and p62, PC-3 cells were treated with increasing concentrations of mitoxantrone ranging from 50nM to 2000nM or/and infected with AdE1A12S in a range from 50ppc to 4000ppc, for 24h and 48h (Fig. 33 and 34). The cells were treated with staurosporine (1nM) and rapamycin (100nM), as apoptotic and autophagic inducers, respectively. The concentrations of viruses and mitoxantrone alone were selected according to viral and drug concentrations that killed less than 20% of cells, (50-500nM and 250-1000ppc), and also more extreme doses above that range killing more than 20% of cells (mitoxantrone at 2000nM; virus at 2000ppc and 4000ppc) to include a wider range of doses. The results are expressed as fold change (small changes of 1.0 ± 0.10 were not considered to represent significant changes).[313]

In this experiment, the ratio of LC3B-II to LC3B-I in PC-3 cells treated with mitoxantrone for 24h, showed a 1.27-fold-increase with 50nM and no change with 250nM compared to untreated control. Moreover, the highest difference in the ratio were shown at higher concentrations of mitoxantrone with 500nM, 1000nM and 2000nM were 1.7, 2.15 and 2.19-fold-increases were observed respectively, compared to untreated control. The changes in the ratio of LC3B-II to LC3B-I induced by increasing doses of mitoxantrone were dose dependent (Fig. 33A). Furthermore, in order to complement the LC3B data, we assessed the expression of p62/SQSTM1, observing decreased expression with increasing concentrations of mitoxantrone showing a 0.65-fold decrease with 50nM, and 0.24, 0.27 and 0.21-fold with 500nM, 1000nM and 2000nM, respectively, compared to untreated control. In contrast, there was a 2.11-fold increase with 250nM mitoxantrone (this remarkable increase with 250nM was not observed at other time points). This experiment, showed a predominantly decreasing trend in the expression p62/SQSTM1 with increasing

concentrations of mitoxantrone (except at 250nM) compared to untreated control cells.

The infection with the AdE1A12S virus induced small decreases in the ratio of LC3B-II to LC3B-I at 50ppc, 250ppc and 500ppc at 0.89, 0.82 and 0.85, respectively. Higher concentrations of the virus showed no changes in the ratio of LC3B-II to LC3B-I (with 1000ppc, 2000ppc and 4000ppc) compared to untreated control. The changes in the ratio of LC3B-II to LC3B-I in response to AdE1A12S were not significant, in contrast, the changes induced by mitoxantrone increased more than 2-fold with the highest concentrations (Fig 33A). These results indicate that mitoxantrone induces the accumulation of autophagosomes, whilst the AdE1A12S virus might slightly counteract or inhibit the process.

Furthermore, the infection with AdE1A12S decreased the expression of p62/SQSTM1, similarly to mitoxantrone although to a lesser extent. The infection with 50ppc, 250ppc, 500ppc and 1000ppc caused 0.67, 0.79, 0.61 and 0.58-fold changes compared to untreated control. Moreover, at higher concentrations the reduction was greater with 2000ppc and 4000ppc causing 0.38 and 0.30-fold changes compared with the untreated control, indicating that increasing viral particles strongly reduces the levels of p62/SQSTM1. The decreases in the levels of p62/SQSTM1 might indicate that in response to either agent p62/SQSTM1 might be degraded. Moreover, the degradation of p62/SQSTM1 in combination with an increase in the ratio of LC3B-II to LC3B-I is frequently associated with increased autophagic flux.[313] Therefore, summarizing the data with the single agents in PC-3 cells at 24h, the increases in the ratio of LC3B-II to LC3B-I and the reduction in the levels of p62/SQSTM1 indicates that the treatment with mitoxantrone might be inducing higher autophagic activity with increasing concentrations of the drug. However, the infection with the AdE1A12S virus, might also contribute to the degradation of p62/SQSTM1 despite the absence of elevated LC3B-II to LC3B-I ratios. We suggest that AdE1A12S might reduce p62/SQSTM1 in the absence of autophagosome formation, which is likely caused by non-autophagic processes such as apoptosis-induction as observed for staurosporine. Thus, more conclusive assays would be needed to complement and verify these data.

A)

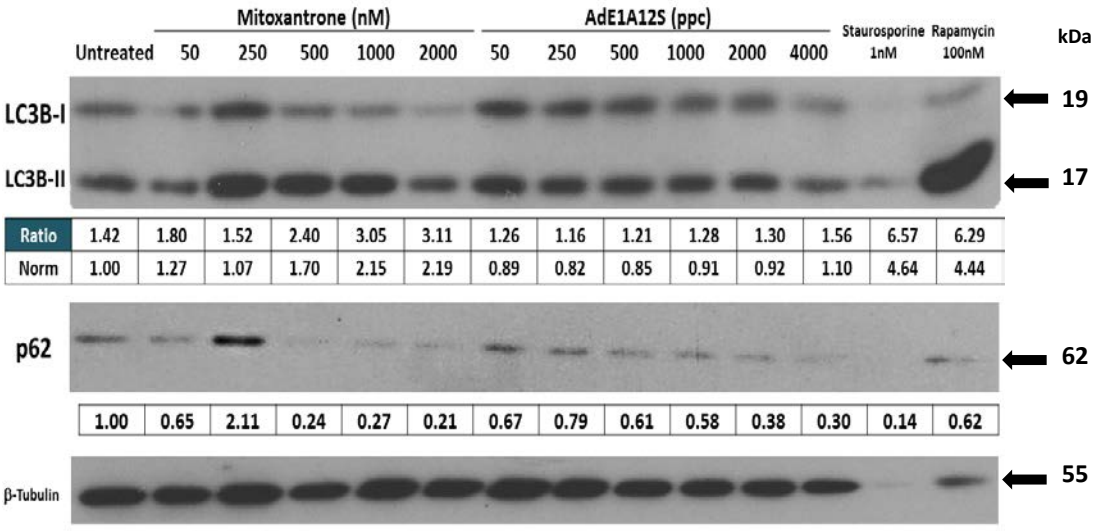

B)

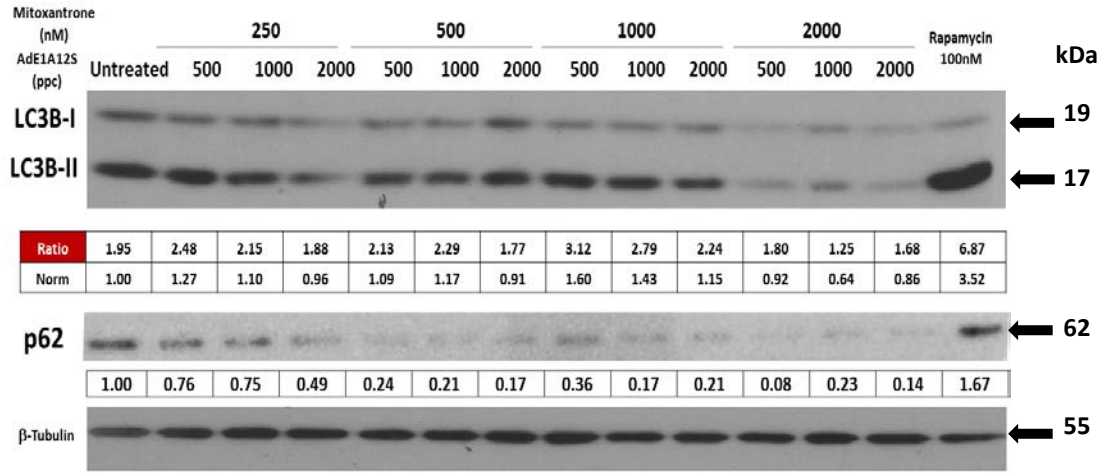

Figure 33. Changes in the ratio of LC3B-II to LC3B-I and expression of p62/SQSTM1 in PC-3 cells at 24h post-treatment with mitoxantrone and/or infection with the AdE1A12S virus. **A)** PC-3 cells treated with mitoxantrone at increasing concentrations, 50nM - 2000nM, or infected with the AdE1A12S virus, at 50ppc - 4000ppc. Cells were also treated with staurosporine at 1nM and rapamycin at 100nM as indicators of apoptotic and autophagic activity. **B)** PC-3 cells treated with mitoxantrone for 24h at 250nM, 500nM, 1000nM and 2000nM in combination with the AdE1A12S virus at 500ppc, 1000ppc and 2000ppc. **A-B)** The intensity of the bands was quantified using Gene Tools version 4.01 (Synoptics. Ltd, Cambridge, UK). The variation in the ratio of LC3B-II to I was calculated after normalizing the intensity of each band to the loading control, β-tubulin (Ratio; red)**. Norm:** indicates the fold change (FC) of each sample compared to untreated control, for LC3B indicates the ratio of LC3B II/I of each sample compared to the ratio of LC3B II/I of the untreated control. Fold changes of untreated samples is 1.00. One experiment, representative of three repetitions.

The combination of mitoxantrone at 250nM in combination with AdE1A12S at 500ppc showed a 1.27 fold increase compared to untreated sample, whereas with

1000ppc and 2000ppc no changes were seen (1.10 and 0.96-fold respectively) compared to untreated cells (Fig. 33B). Moreover, compared to the single treatments the combination of 250nM with 500ppc enhanced the drug-induced increases in the ratios of LC3B-II/I, whilst high concentrations of the virus had no influence. In contrast, the treatment with 500nM mitoxantrone in combination with AdE1A12S at 500ppc, 1000ppc and 2000ppc resulted in no changes in the ratio of LC3B-II to LC3B-I compared to untreated control while mitoxantrone-induced increases in LC3BII/I were reduced by AdE1A12S. Thus, the increases in the LC3B-II to LC3B-I ratios in response to mitoxantrone alone, were prevented by the virus independent of the viral dose. At 1000nM mitoxantrone in combination with AdE1A12S increases in the LC3B-II to LC3B-I ratio of 1.60, 1.43 and 1.15-fold were observed with 500ppc, 1000ppc and 2000ppc viral particles, respectively, compared to 2.15-fold with mitoxantrone alone (Fig. 33B). Interestingly, the combination with 1000nM mitoxantrone and all viral concentrations (500ppc, 1000ppc and 2000ppc) prevented (dose-dependent) full activation of LC3B-II in response to mitoxantrone. However, the ratios were slightly elevated when compared to untreated or virus infected cells. Perhaps, these doses of mitoxantrone were potent enough to partially overcome the viral inhibitory effects. Moreover, the treatment with 2000nM mitoxantrone and infected with 500ppc, 1000ppc and 2000ppc of AdE1A12S showed no increases in the LC3B-II to LC3B-I ratios compared to control or single infected cells. The strongest decrease was observed with 2000nM in combination with 1000ppc (0.64-fold-decrease). Interestingly, mitoxantrone seemed to induce the conjugation of LC3B-I to form LC3B-II (autophagosome formation) in a dose range of 250nM to 1000nM, while the AdE1A12S virus counteracted this induction. The expression of p62/SQSTM1 showed a decrease in response to the treatment with mitoxantrone at 250nM in combination with AdE1A12S at 500ppc, 1000ppc and 2000ppc, 0.76, 0.75 and 0.49-fold decreases respectively, compared to untreated control. These results contrast with the induction of p62/SQSTM1 observed with mitoxantrone alone at 250nM, suggesting that the virus contributes to downregulation of p62/SQSTM1 in these combinations. However, it is important to point out that the values of mitoxantrone at 250nM do not correspond with those at other concentrations of mitoxantrone. Cells treated with 500nM mitoxantrone showed a potent decrease in

p62/SQSTM1 expression when infected with AdE1A12S at 500ppc, 1000ppc and 2000ppc, 0.24, 0.21 and 0.17-fold, compared to untreated control. Additionally, these results showed that in these combination treatments, the low levels of p62/SQSTM1 are caused by mitoxantrone. Moreover, all combinations of virus with 1000nM mitoxantrone showed potent decreases of p62/SQSTM1 expression, with 500ppc, 1000ppc and 2000ppc of AdE1A12S, 0.36, 0.17 and 0.21-fold-decrease respectively, most likely induced by mitoxantrone (Fig. 33). The treatment with 2000nM mitoxantrone in combination with AdE1A12S showed the greatest decrease in p62/SQSTM1 at this time point, when infected at 500ppc, 1000ppc and 2000ppc decreases of 0.08, 0.23 and 0.14, respectively, were noted compared to untreated samples. The low levels of p62/SQSTM1 and LC3B-II in response to mitoxantrone at 2000nM in combination with AdE1A12S at all doses are most likely due to cell death; inducing the degradation of both p62/SQSTM1 and LC3B-II as observed with staurosporine (Fig. 33).

In summary, the results in PC-3 cells at 24h in response to the treatment combinations, suggest that mitoxantrone promotes autophagy-activity at increasing concentrations of the drug observed by increased levels of LC3B-II/-I and reduced p62/SQSTM1 levels whilst AdE1A12S blocks drug-induced autophagy initiation. Moreover, the inhibition of autophagy by the virus was overcome in combination with high concentrations of mitoxantrone.

3.5.2 Autophagic activity is increased in response to mitoxantrone but decreased when simultaneously infected with AdE1A12S for 48h.

The levels of expression of LC3B-II and p62/SQSTM1 were also examined at 48h to determine autophagic activity in response to each agent alone and in combination.

To assess changes in LC3B-II/I ratios at 48h, we treated PC-3 cells with increasing concentrations of mitoxantrone or the AdE1A12S virus (Fig. 34A). We observed great increases in LC3B-II induction at all concentrations of mitoxantrone. PC-3 cells treated with 50nM, 250nM, 500nM, 1000nM and 2000nM mitoxantrone showed 2.20-, 3.19-, 8.46-, 14.21- and 7.38-fold increases in the ratio of LC3B-II to LC3B-I compared to untreated control. In addition, the LC3B-II/I ratio with 2000nM was less

than that of 500nM and 1000nM mitoxantrone, while at 1000nM we observed the highest LC3B-II/I ratio. Taken together, mitoxantrone induced an increase in the levels of expression of LC3B-II compared to LC3B-I (as observed at 24h), indicating formation or accumulation of autophagosomes. In addition, the differences in the LC3B-II/I ratio were greater at 48h than at 24h, as well as the decline in the ratio at the highest concentration of mitoxantrone (2000nM). The expression of p62/SQSTM1 was also assessed at 48h post-treatment in PC-3 cells. Interestingly, the treatment with 50nM and 250nM mitoxantrone induced 1.99 and 2.09-fold increases in the expression of p62/SQSTM1 compared to untreated control. In contrast, decreases were observed at 500nM, 1000nM and 2000nM mitoxantrone showing 0.88, 0.23 and 0.40-fold changes, respectively. Therefore, the treatment with low doses of mitoxantrone increased the levels of p62/SQSTM1, while higher doses appeared to contribute to the degradation of p62. Furthermore, these results showed that in PC-3 cells mitoxantrone treatment for 24h and 48h induces the formation or accumulation of autophagosomes in a dose-response manner. Additionally, when considering the levels of p62/SQSTM1, our data indicate that mitoxantrone induces autophagic flux at all doses after 24h and at the higher doses after 48h.

The infection of PC-3 cells with AdE1A12S for 48h caused increases in the ratios of LC3B-II to LC3B-I with 50ppc, 250ppc, 2000ppc and 4000ppc resulting in 1.57, 1.54, 1.68, 1.71 and 1.7-fold respectively, compared to untreated control (Fig. 34B). When infected with 1000ppc a reduction was observed (0.85-fold decrease). At all viral concentrations (except at 1000ppc) there was an increase in the ratio of LC3B-II to LC3B-I compared to untreated control, although the increases were notably less than with mitoxantrone. These increases in the ratios were not dose-dependent as observed by the small increases in LC3B-II/I ratios between low and high viral doses.

In addition, the infection with AdE1A12S resulted in increased levels of p62/SQSTM1 at 250ppc, 1000ppc, 2000ppc and 4000ppc; 1.21, 1.86, 3.28 and 2.72-fold increases compared to untreated control. In contrast, there were no changes when infected with 50ppc and 500ppc of AdE1A12S. The increase in the ratio of LC3B-II/LC3B-I in addition to the accumulation of p62/SQSTM1 indicate that AdE1A12S might impair autophagic-activity at 24h and 48h employing slightly different mechanism;

prevention of LC3B-II/I increases at 24h and prevention of p62 degradation at 48h (Fig. 34A).

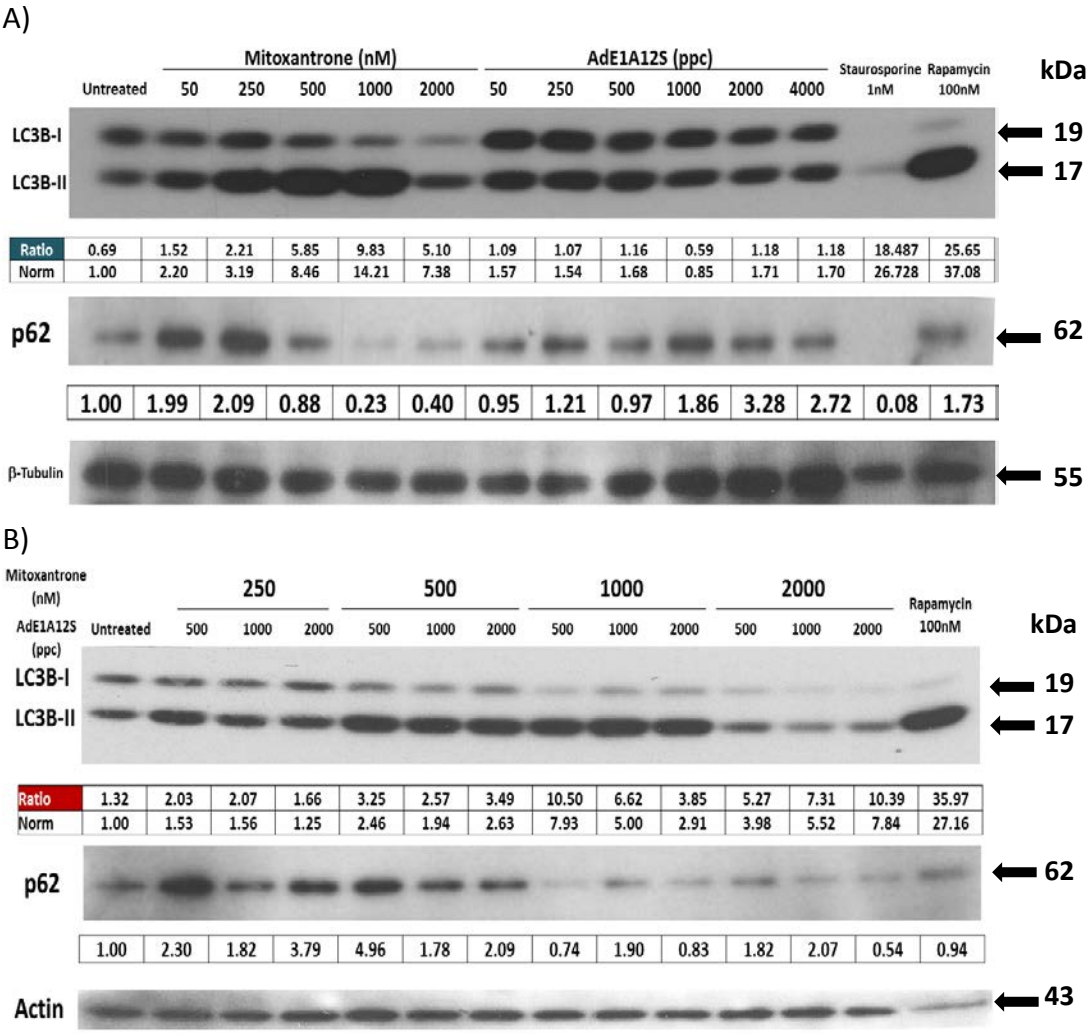

Figure 34. Differences in the ratios of LC3B-II to LC3B-I and expression of p62/SQSTM1 in PC-3 cells at 48h post-treatment with mitoxantrone and/or infection with the AdE1A12S virus. **A)** PC-3 cells treated with mitoxantrone at increasing concentrations, 50nM - 2000nM or infected with the AdE1A12S virus, at 50ppc - 4000ppc. Cells were also treated with staurosporine at 1nM and rapamycin 100nM as indicators of apoptotic and autophagic activity respectively. **B)** PC-3 cells treated with mitoxantrone for 48h at 250nM, 500nM, 1000nM and 2000nM in combination with the AdE1A12S virus at 500ppc, 1000ppc and 2000ppc. A-B) The intensity of the bands where quantified using Gene Tools version 4.01 (Synoptics Ltd, Cambridge, UK). The variation in the ratio of LC3B-II to -I after normalizing the intensity of each band to the loading control (β-tubulin)**. Norm:** indicates the fold change (FC) of each sample compared to untreated control, for LC3B indicates the ratio of LC3B II/I of each sample compared to the ratio of LC3B II/I of the untreated control. Fold changes of untreated samples is 1.00. One experiment, blot representative of three repetitions.

Cells treated in combination with 250nM mitoxantrone and infected with AdE1A12S virus at 500ppc, 1000ppc, and 2000ppc resulted in 1.53, 1.56, 1.25-fold increases in

LC3B-II to LC3B-I ratio compared to untreated samples (Fig. 34B), indicating a strong inhibition of autophagy initiation in response to mitoxantrone (3.19-fold increase for drug alone). Moreover, the treatment with 500nM mitoxantrone and infection with 500ppc, 1000ppc and 2000ppc resulted in 2.46, 1.94 and 2.63-fold increases respectively, compared to untreated control, although, less than with mitoxantrone alone at this concentration (8.44-fold). The treatment with 1000nM mitoxantrone showed a more potent increase in LC3B-II to LC3B-I ratio when combined with AdE1A12S at 500ppc, 1000ppc and 2000ppc showing 7.93, 5.0 and 2.91-fold increases. Despite the increased ratios, the combination with the virus reduced, by half, the levels of LC3B-II induced by mitoxantrone alone (14.21-fold). The combination with 2000nM mitoxantrone and 500ppc, 1000ppc and 2000ppc showed 3.98, 5.52 and 7.84-fold increases, respectively, when compared to untreated control, lower or similar ratios to those obtained by mitoxantrone alone (7.4-fold) (Fig. 34B). Interestingly, the combination of virus with 1000nM and 2000nM mitoxantrone induced different patterns in the ratio of LC3B-II to LC3B-I; treatment with 1000nM showed a trend towards decreased LC3B-II/LC3B-I ratios with increasing concentrations of the virus, whilst in the combination with 2000nM an increased trend was observed with increasing concentrations of the virus.

The LC3B-II to LC3B-I ratios clearly demonstrated that at 48h, mitoxantrone induced the accumulation of LC3B-II, similarly to the results observed at 24h. The combination with the virus resulted in decreases in the ratios of LC3-II/I, indicating that the virus impairs mitoxantrone-induced autophagic activity; although, mitoxantrone is potent enough to partially overcome viral inhibition at higher drug doses also at the 48h time-point.

The accumulation of the polyubiquitin-binding protein p62/SQSTM1 was also assessed in response to the combination treatments at 48h. Treatment with 250nM mitoxantrone in combination with 500ppc, 1000ppc and 2000ppc showed 2.30, 1.82 and 3.79-fold increases respectively, in the expression of p62/SQSTM1 when compared to untreated control. Moreover, the treatment of PC-3 cells with mitoxantrone at 500nM in combination with 500ppc, 1000ppc and 2000ppc of the virus showed 4.96, 1.78 and 2.09-fold increases respectively, in the expression of p62/SQSTM1 when compared to untreated control. The combination of 1000nM

mitoxantrone with 1000ppc of the virus showed 1.90-fold increase when compared to untreated control. In contrast, mitoxantrone at 1000nM in combination with 500ppc and 2000ppc decreased p62/SQSTM1 to 0.79- and 0.83-fold compared to untreated control. The treatment of PC-3 cells with 2000nM mitoxantrone in combination with 500ppc and 1000ppc of the virus showed a 1.82 and 2.07-fold increase in the expression of p62/SQSTM1 compared to untreated control. Moreover, a decrease in the expression of p62/SQSTM1 was observed when 2000nM mitoxantrone was combined with 2000ppc of the virus showing a 0.54 fold change compared to untreated control. The increased accumulation of p62/SQSTM1 in response to the combination treatments compared to mitoxantrone alone showed that at 48h, the virus might impair the mitoxantrone-induced autophagic activity/flux. In addition, despite the accumulation of autophagosomes indicated by the increased ratio of LC3B-II/I, contrary to the induction observed at 24h, these results indicate that mitoxantrone was unable to overcome the viral inhibition of autophagic flux at 48h at the majority of tested concentrations.

3.5.3 Mitoxantrone inhibits p-Akt but not in combination with AdE1A12S in PC-3 cells at 24h.

From the miRNA analysis we identified the protein kinase Akt as one of the most common targets (hsa-miR-23b, hsa-miR-128, hsa-miR-21 and hsa-miR-183; Tables 20 and 22). The protein kinase Akt has been reported as a key regulatory factor of both autophagy and apoptosis.[414-417] When Akt is upregulated and fully activated cell survival and proliferation was induced; Akt can be fully activated only by phosphorylation at Ser-473 by phosphoinositide-dependent kinase 2 (PDK2) of the mTORC2 inducing the activation of mTORC1 that blocks autophagy.[414] Thus, we investigated the expression of phosphorylated-Akt (p-Akt) in response to the combination treatments.

Cells were treated at increasing concentrations of mitoxantrone and infected with AdE1A12S for 24h, to determine changes in the phosphorylation at serine-473 on Akt (Fig. 35A). A dose-dependent decrease in p-Akt was observed in PC-3 cells treated for 24h with increasing concentrations of mitoxantrone. The treatment with 1000nM

and 2000nM mitoxantrone resulted in 0.72 and 0.40-fold, respectively, when compared to untreated control (Fig. 35A). Infection with AdE1A12S at 50ppc and 250ppc caused strong decreases in p-Akt resulting in 0.38 and 0.23-fold compared to untreated control. In contrast, increased doses of AdE1A12S at 500ppc, 1000ppc, 2000ppc and 4000ppc increased p-Akt showing 1.26, 1.60, 2.34 and 2.97-fold changes, respectively, compared to untreated control. We observed that in cells treated for 24h with increasing concentrations of mitoxantrone there was a constant decrease in p-Akt while infection with AdE1A12S despite an initial inhibition of p-Akt at low doses, increasing concentrations strongly induced the levels of p-Akt.

A)

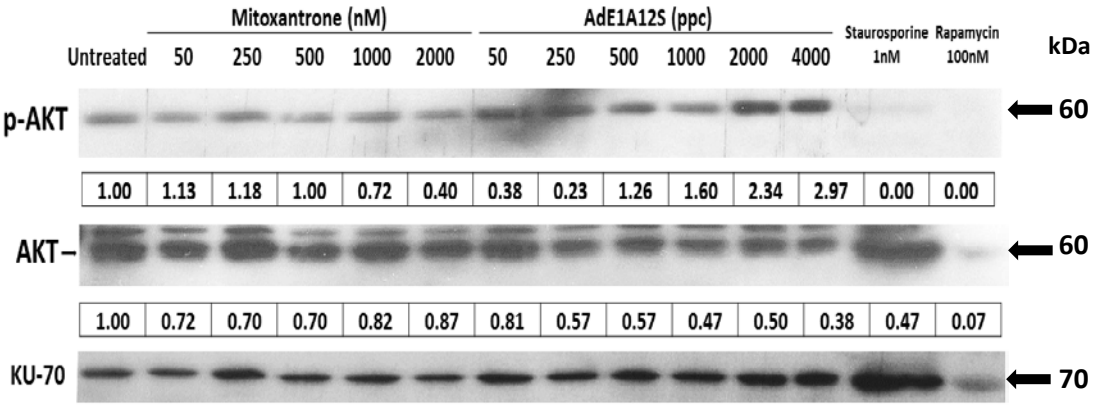

B)

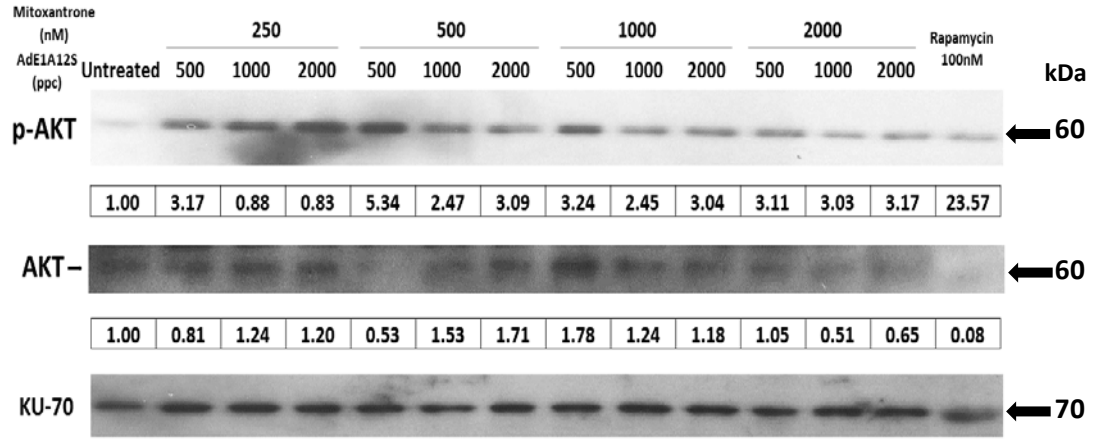

Figure 35. Changes in expression of phosphorylated Akt (Ser-473) and total Akt in PC-3 cells at 24h post-treatment with mitoxantrone and/or infection with the AdE1A12S virus. **A)** PC-3 cells treated with mitoxantrone at increasing concentrations, 50nM - 2000nM or infected with the AdE1A12S virus, at 50ppc - 4000ppc. Cells were also treated with staurosporine at 1nM and rapamycin 100nM as indicators of apoptotic and autophagic activity. **B)** PC-3 cells treated with mitoxantrone for 24h at 250nM, 500nM, 1000nM and 2000nM in combination with the AdE1A12S virus at 500ppc, 1000ppc and 2000ppc. A-B) The intensity of the bands where quantified using Gene Tools version 4.01 (Synoptics. Ltd, Cambridge, UK). Bands were normalized for p-Akt as the intensity of each band to Akt, and Akt to the loading control (KU-70)**.** Fold change of each sample after being compared to untreated control, were the change of the untreated samples is 1.00. One experiment, blot representative of three repetitions.

At 24h post-treatment we also assessed p-Akt in PC-3 cells treated in combination with mitoxantrone and infected with AdE1A12S. The combination of 250nM mitoxantrone with 1000ppc and 2000ppc of AdE1A12S showed slight reductions in p-Akt; 0.88- and 0.83-fold changes, respectively. In contrast when treated with mitoxantrone at 500nM, 1000nM and 2000nM there were strong increases of p-Akt in combination with the virus at all doses compared to untreated samples. In summary, in contrast to the inhibition of p-Akt observed with mitoxantrone alone, all the combinations of AdE1A12S with mitoxantrone (except for some combinations with 250nM) induced strong increases in p-Akt at 24h post-treatment. These results indicate that AdE1A12S blocks mitoxantrone-induced inhibition of p-Akt promoting increases in p-Akt accumulation. The induction of p-Akt by the combination may contribute to the partial inhibition of autophagy initiation at this time point.

3.5.4 Mitoxantrone potently inhibits p-Akt in combination with AdE1A12S at 48h.

Treatment with mitoxantrone at all concentrations induced decreases in the expression of p-Akt compared to untreated control at 48h (Fig. 36A). The treatment with 50nM and 2000nM mitoxantrone caused 0.74- and 0.83-fold, respectively, compared to untreated control. Moreover, the strongest decrease occurred with 250nM and 1000nM mitoxantrone with 0.66 and 0.63-fold changes respectively, compared to untreated control. Despite that p-Akt levels were reduced by mitoxantrone both at 24 and 48h after treatment, the decreases were strongest after 48h, indicating that mitoxantrone-dependent inhibition of p-Akt increases over time.

In contrast, infection with AdE1A12S increased the expression of p-Akt at 500ppc, 1000ppc, 2000ppc and 4000ppc inducing 1.13-, 1.52-, 1.28- and 1.23-fold changes, compared to untreated control (Fig. 36A). Interestingly, the highest increases with the virus in p-Akt were when infected at 1000ppc, this may indicate that the induction of p-Akt by the virus is dose-dependent only to a certain threshold. These results suggest that virus-induced p-Akt might be triggered at early stages and increase over time. We also investigated p-Akt in cells treated with mitoxantrone in combination with AdE1A12S and the drug at 48h post-treatment (Fig. 36B).

Treatment with 250nM mitoxantrone in combination with 500ppc and 1000ppc AdE1A12S resulted in 1.31 and 1.60-fold increases, compared to untreated control. These increases are slightly lower than observed for the same combinations at 24h (Fig. 35B).

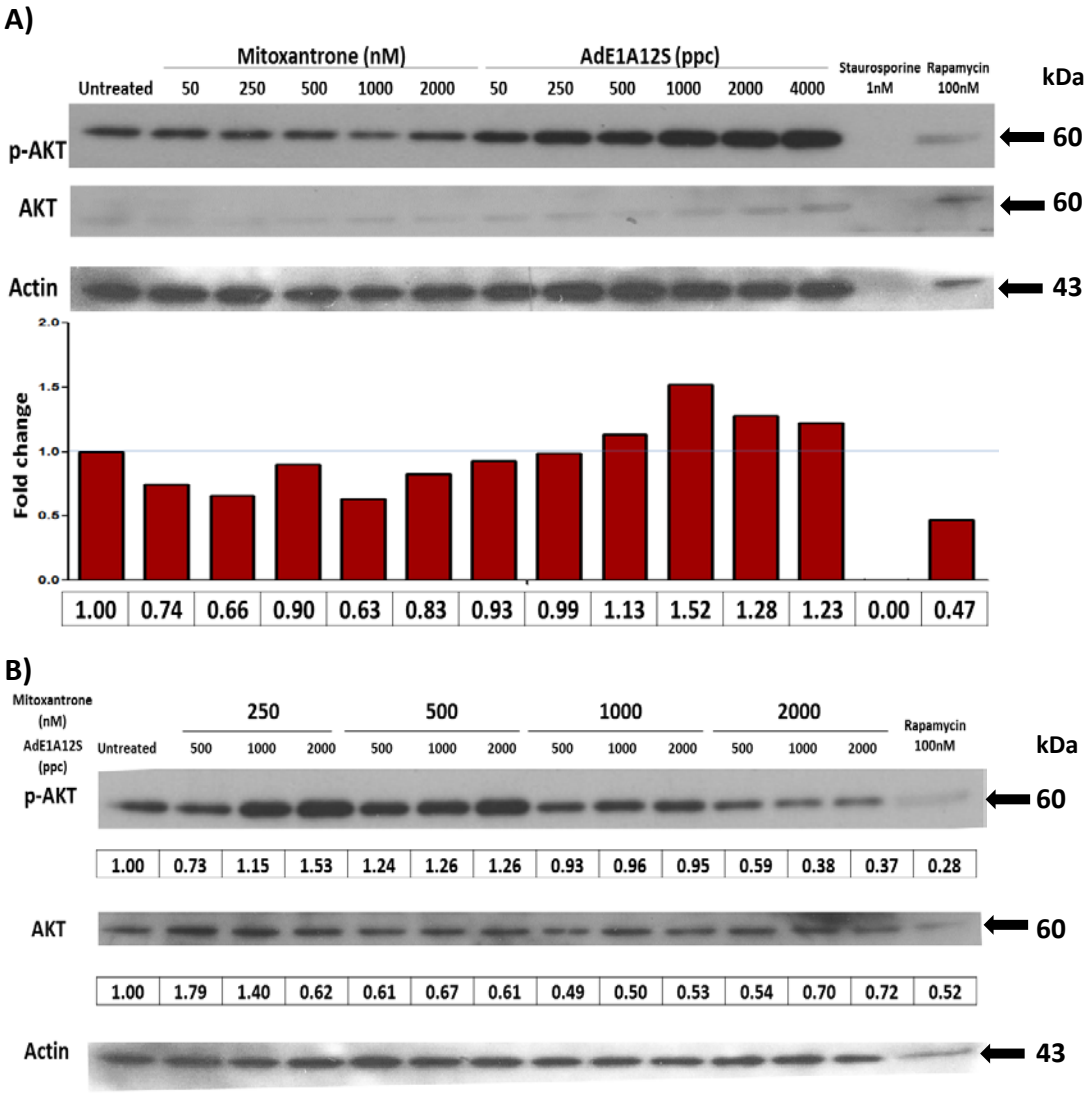

Figure 36. Changes in expression of the phosphorylated Akt (Ser-473) and total Akt in PC-3 cells at 48h post-treatment with mitoxantrone and/or infection with the AdE1A12S virus. **A)** PC-3 cells treated with mitoxantrone at increasing concentrations, 50nM - 2000nM or infected with the AdE1A12S virus, at 50ppc - 4000ppc. Cells were also treated with staurosporine at 1nM and rapamycin 100nM as indicators of apoptotic and autophagic activity. **B)** PC-3 cells treated with mitoxantrone for 48h at 250nM, 500nM, 1000nM and 2000nM in combination with the AdE1A12S virus at 500ppc, 1000ppc and 2000ppc. A-B) The intensity of the bands where quantified using Gene Tools version 4.01 (Synoptics Ltd, Cambridge, UK). A) Bands were normalized as the intensity of each band to the loading control (Actin)**. B)** Bands were normalized for p-Akt as the intensity of each band to Akt, and Akt to the loading control (KU-70)**. F**old change of each sample after being compared to

untreated control, were the change of the untreated samples is 1.00. One experiment, blot representative of three repetitions.

Treatment with 500nM mitoxantrone slightly induced p-Akt when combined with 500ppc, 1000ppc and 2000ppc of the virus to 1.24, 1.26 and 1.26-fold respectively, compared to untreated control and was higher than with mitoxantrone alone (0.90-fold decrease compared to control). When treated with 1000nM in combination with 500ppc, 1000ppc and 2000ppc of virus, basal levels of p-Akt were re-established at 0.93-, 0.96- and 0.95-fold changes. Moreover, with 2000nM mitoxantrone in combination with 500ppc, 1000ppc and 2000ppc of the virus, the strongest decreases in the levels of p-Akt were noted at 0.59, 0.38 and 0.37-fold respectively, when compared to untreated control. Thus, treatment with mitoxantrone abrogated virus-induced p-Akt in a dose-dependent manner at 48h post-treatment. However, although the p-Akt levels were lower in the combination-treated cells than in the AdE1A12S-infected cells, p-Akt levels were still higher than in cells treated with mitoxantrone alone. Furthermore, contrary the results from the 24h time-point in the combination-treated cells (p-Akt was induced; Fig. 35B), the combination treatments at 48h caused decreases in p-Akt compared to virus-only treated cells, suggesting that at this time point mitoxantrone-dependent decreases dominated. It is possible that, the virus-induced cell proliferative signalling through p-Akt to promote cell survival is impeded by mitoxantrone after >24h of treatment.

3.5.5 Mitoxantrone in combination with AdE1A12S induces Bcl-2 in PC-3 cells at 24h.

The upregulation of the miRNAs hsa-miR-15/16 has been shown to target and inhibit Bcl-2 inducing pro-apoptotic signalling (Table 20). Moreover, the expression of Bcl-2 acts as a pro-survival regulator by inhibiting apoptosis by direct binding to Bax. Bcl-2 also blocks autophagy driven by the activation of Beclin-1, making Bcl-2 a key regulatory factor of both pathways.[274,418] Therefore we assessed the expression of Bcl-2 to determine its role under chemosensitizing conditions. The expression of Bcl-2 was assessed in cells treated at increasing concentrations of mitoxantrone (50nM-

2000nM) for 24h (Fig. 37A). Treatment with 250nM mitoxantrone increased the expression of Bcl-2 1.30-fold compared to untreated control cells. In contrast, the expression of Bcl-2 was decreased in cells treated with 1000nM and 2000nM mitoxantrone; 0.80 and 0.77-fold respectively, compared to untreated control. Furthermore, increased concentrations of mitoxantrone decreased (except at 250nM) Bcl-2expression. The expression of Bcl-2 was also assessed in response to AdE1A12S infection (Fig. 37A). Cells infected with 250ppc showed a slight decrease in Bcl-2 levels (0.86-fold) compared to untreated control. In contrast, the infection with 500ppc, 1000ppc and 2000ppc slightly increased in Bcl-2 expression compared to untreated control. Moreover, infection with 4000ppc caused a 1.60-fold increase, the largest difference compared to untreated control (Fig. 37A). Taken together, Bcl-2 expression showed a trend towards dose-dependent decreases with mitoxantrone and a trend towards increased levels with increasing doses of virus at this time point.

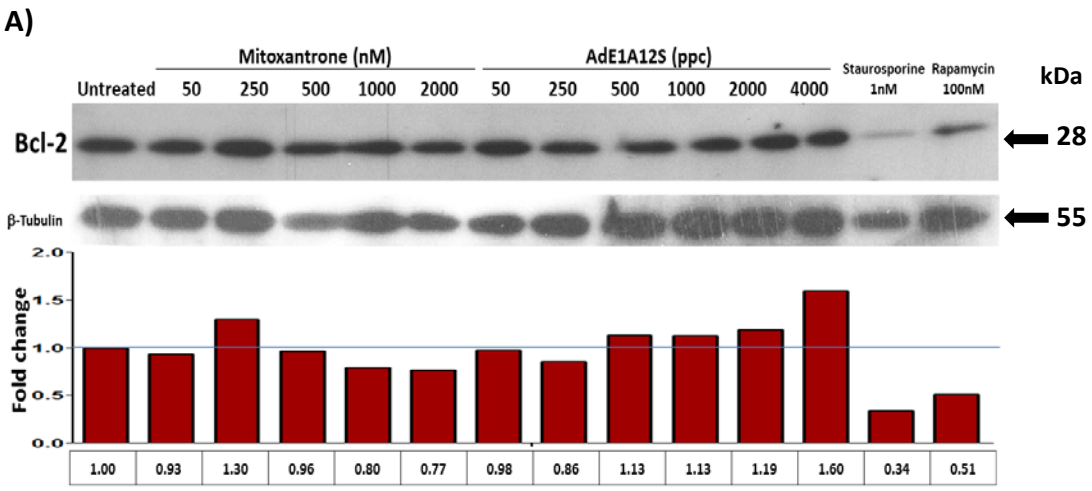

B)

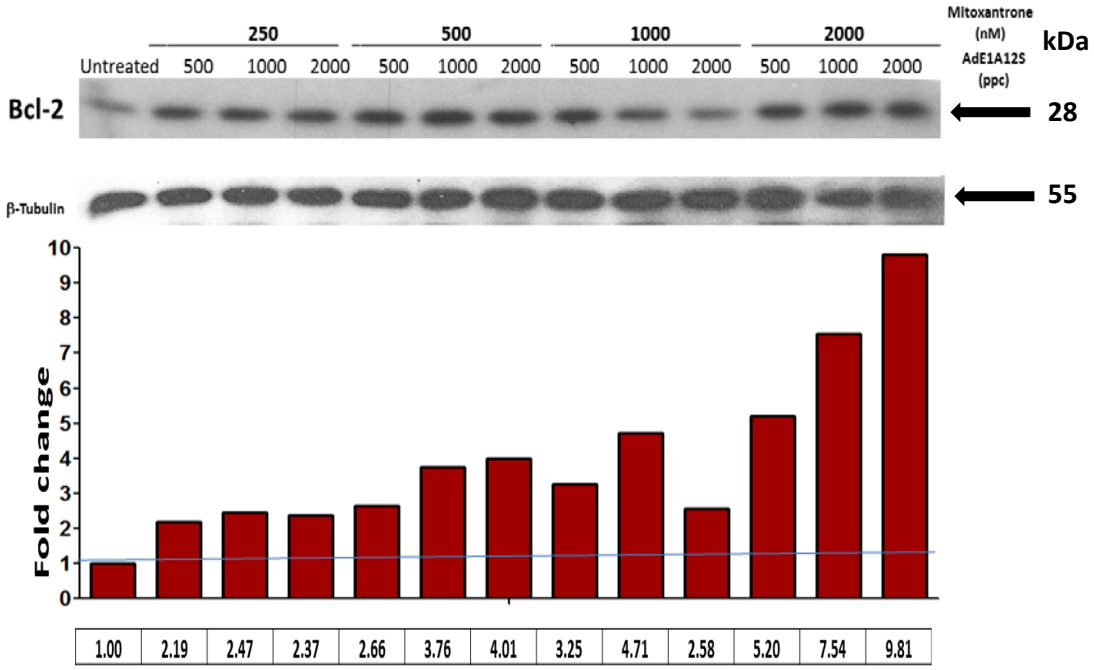

Figure 37. Changes in expression of Bcl-2 in PC-3 cells at 24h post-treatment with mitoxantrone and/or infection with the AdE1A12S virus. **A)** PC-3 cells treated with mitoxantrone at increasing concentrations, 50nM - 2000nM or infected with the AdE1A12S virus, at 50ppc - 4000ppc. Cells were also treated with staurosporine at 1nM and rapamycin 100nM as indicators of apoptotic and autophagic activity. **B)** PC-3 cells treated with mitoxantrone for 24h at 250nM, 500nM, 1000nM and 2000nM in combination with the AdE1A12S virus at 500ppc, 1000ppc and 2000ppc. A-B) The intensity of the bands where quantified using Gene Tools version 4.01 (Synoptics Ltd, Cambridge, UK). Bands were normalized as the intensity of each band to the loading control (β-Tubulin)**. F**old change of each sample after being compared to untreated control, where the change of the untreated samples is 1.00. Blot representative of three repetitions.

The expression of Bcl-2 was also assessed by the treatments in combination. Unexpectedly, Bcl-2 expression was strongly increased when treated at all combinations (Fig. 37B). The strongest was shown with 2000nM mitoxantrone in combination with the virus at 500ppc, 1000ppc and 2000ppc showing 5.2-, 7.54- and 9.81-fold increases, respectively, compared to untreated control. These results showed that mitoxantrone induced a dose-dependent increases in Bcl-2 expression in combination with AdE1A12S. Additionally, the levels of expression of Bcl-2 in the combinations were not impacted by virus doses. In summary, at this time point the combination treatments appear to, unexpectedly, induce an initial cell survival mechanism in contrast to the miRNA data but in agreement with the results observed with p-Akt at this time point.

3.5.6 The combination of mitoxantrone with AdE1A12S decreases the levels of Bcl-2 in PC-3 cells after 48h.

The expression of Bcl-2 was assessed in cells treated with mitoxantrone or infected with AdE1A12S for 48h. Bcl-2 expression was increased by mitoxantrone at 50nM, 250nM and 1000nM showing 1.15, 1.35 and 1.25-fold, respectively, compared to untreated control (Fig. 38A). Additionally, treatment with 1000nM and 2000nM mitoxantrone reduced Bcl-2 levels to 0.88-fold and 0.72-fold when compared to the untreated sample. Thus, low doses of mitoxantrone induced Bcl-2 expression, whilst high concentrations reduced Bcl-2 levels. Infection with AdE1A12S slightly induced Bcl-2 expression at 250ppc by 1.12-fold. In contrast, infection with 500ppc, 2000ppc and 4000ppc decreased Bcl-2 levels to 0.85, 0.74 and 0.64-fold, respectively, compared to untreated control. In summary, infection with AdE1A12S slightly decreased Bcl-2 levels 48h after infection and induced the expression after 24h of infection (Fig. 37 and 38).

A)

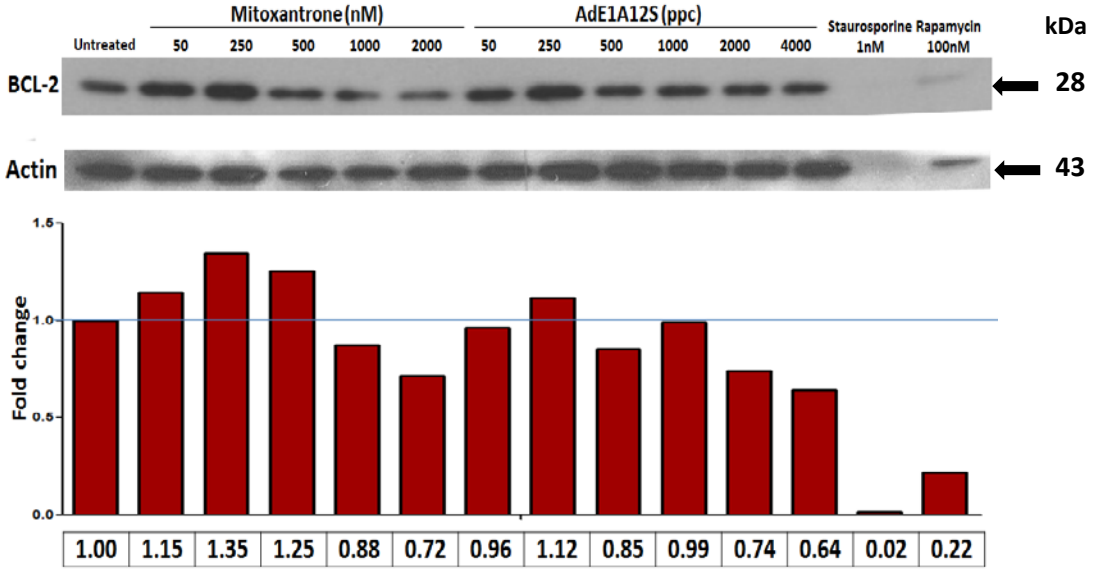

B)

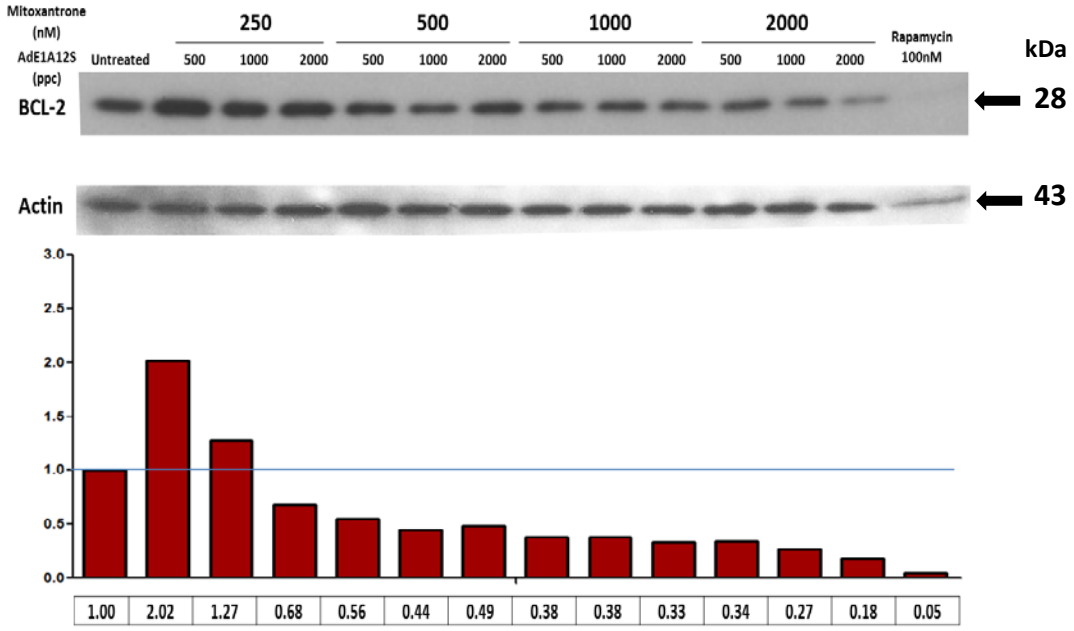

Figure 38. Changes in expression of Bcl-2 in PC-3 cells at 48h post-treatment with mitoxantrone and/or infection with the AdE1A12S virus. **A)** PC-3 cells treated with mitoxantrone at increasing concentrations, 50nM - 2000nM or infected with the AdE1A12S virus, at 50ppc - 4000ppc. Cells were also treated with staurosporine at 1nM and rapamycin 100nM as indicators of apoptotic and autophagic activity. **B)** PC-3 cells treated with mitoxantrone for 48h at 250nM, 500nM, 1000nM and 2000nM in combination with the AdE1A12S virus at 500ppc, 1000ppc and 2000ppc. A-B) The intensity of the bands where quantified using Gene Tools version 4.01 (Synoptics Ltd, Cambridge, UK). Bands were normalized as the intensity of each band to the loading control (Actin). Fold change of each sample after being compared to untreated control, were the change of the untreated samples is 1.00.Blot representative of three repetitions.

The expression of Bcl-2 was also assessed in cells treated in combination for 48h (Fig. 38B). The combination of 250nM mitoxantrone with AdE1A12S at 500 and 1000ppc induced 2.02- and 1.27-fold increases, respectively, compared to untreated samples. In contrast, all other combinations decreased Bcl-2 expression, the largest decrease was observed with 2000nM mitoxantrone and 2000ppc; 0.18 fold. The combination of AdE1A12S and mitoxantrone, in contrast to the effects when added as single agents, reduced Bcl-2 levels in a dose-dependent manner at this time point (48h). Moreover, these results are in contrast with the increased Bcl-2 levels at 24h in response to the combination treatments (Fig. 37B-38B) but are in agreement with the miRNA data (has-miR-15/16; Table 19).

3.5.6.a. Summary of immunoblotting data in PC-3 cells infected with AdE1A12S and/or treated with mitoxantrone:

- Infection with AdE1A12S represses the autophagy flux in PC-3 cells at both 24 and 48h over a range of doses, while mitoxantrone induces the autophagy flux compared to basal levels.
- Infection with AdE1A12S in combination with mitoxantrone greatly decreases mitoxantrone-induced autophagy flux at 24h and 48h compared to mitoxantrone alone and basal levels.
- Infection with AdE1A12S induces p-Akt at 24h and 48h. In contrast, mitoxantrone inhibits p-Akt at both time points compared to untreated samples.
- The combination treatments increase the levels of p-Akt at 24h however, at 48h the combination treatments decreased the levels of p-Akt compared to basal levels and each single agent treatment.
- The combinations of AdE1A12S and mitoxantrone increase the levels of Bcl-2 at 24h. In contrast, at 48h the combinations induce strong dose-dependent inhibition of Bcl-2 compare to basal levels.

3.5.7 AdΔΔ impairs mitoxantrone-induced autophagy in PC-3 cells at 48h.

We previously demonstrated that the oncolytic adenoviral mutant AdΔΔ potentiates apoptotic cell death induced by drugs, including mitoxantrone and docetaxel, by selectively targeting tumours with deregulated cell cycle and apoptosis pathways.[118] Therefore, the replicating mutant AdΔΔ could provide us, within a replicating context, with more insights of the mechanisms causing viral-induced sensitization of PCa cells to chemotherapeutic drugs, and if these were similar to the observed changes in protein expression levels in response to E1A12S combinations with drugs.

To this end we assessed changes in expression of LC3B and p62 in PC-3 cells treated with the replication-selective AdΔΔ oncolytic mutant with and without mitoxantrone, for 48h (Fig. 39A). Treatment with mitoxantrone verified our previous observations that increasing concentrations of mitoxantrone (250nM, 500nM, 1000nM and 2000nM) induced higher ratios of LC3B-II to LC3B-I at 48h post-

treatment. Infection with AdΔΔ did not result in changes in the LC3B-II/I ratios at 50ppc, 250ppc and 500ppc; a slight increase of 1.22 was observed in cells infected with 1000ppc.

Interestingly, p62/SQSTM1 levels increased to 2.08- and 2.30-fold when infected with 250ppc and 500ppc of AdΔΔ, respectively, compared to untreated control. In contrast, slight decreases (0.87 and 0.78-fold) were observed at 50 and 1000ppc. As expected and previously shown (Section 3.5.5), mitoxantrone caused decreases in the expression of p62/SQSTM1 with 250nM, 500nM, 1000nM and 2000nM; 0.59-, 0.44-, 0.56- and 0.20-fold changes respectively.

A)

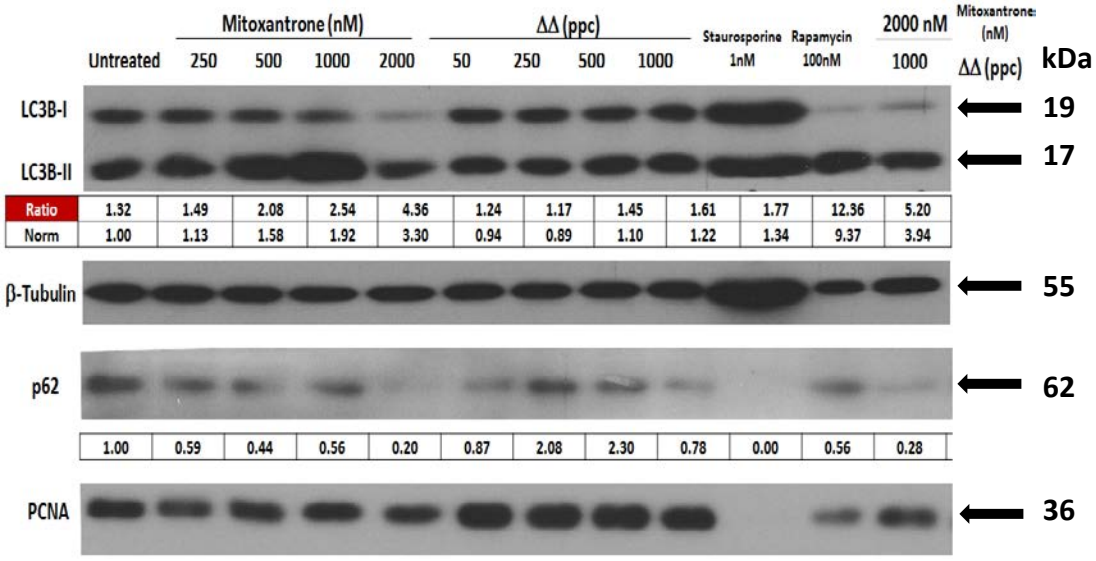

B)

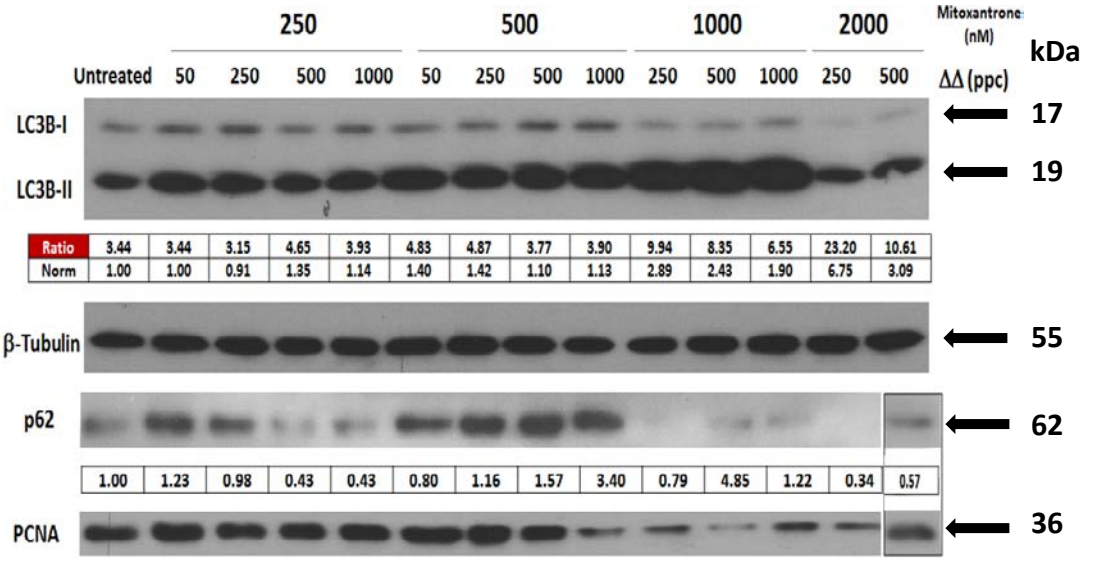

Figure 39. Differences in the ratio of LC3B-II to LC3B-I and expression of p62/SQSTM1 in PC-3 cells at 48h post-treatment with mitoxantrone and/or infection with the AdΔΔ virus. **A)** PC-3 cells treated with mitoxantrone at increasing concentrations, 250nM - 2000nM or infected with the AdΔΔ virus, at 50ppc - 1000ppc and treated in combination with 2000nM mitoxantrone with AdΔΔ at 1000ppc. Cells were also treated with staurosporine at 1nM and rapamycin 100nM as indicators of apoptotic and autophagic activity. **B)** PC-3 cells treated with mitoxantrone for 48h at 250nM, 500nM, 1000nM in combination with the AdΔΔ virus at 50ppc, 250ppc, 500ppc and 1000ppc; 2000nM in combination with the AdΔΔ virus at 250ppc and 500ppc. **A-B)** The intensity of the bands where quantified using Gene Tools version 4.01 (Synoptics Ltd, Cambridge, UK). The variation in the ratio of LC3B-II to -I after normalizing the intensity of each band to the loading control (β-tubulin/PCNA)**. Norm:** indicates the fold change (FC) of each sample compared to untreated control, for LC3B indicates the ratio of LC3B II/I of each sample compared to the ratio of LC3B II/I of the untreated control. Fold changes of untreated samples is 1.00. Blot representative of three repetitions.

In cells treated with 250nM mitoxantrone, the combination with AdΔΔ at 500ppc induced a 1.35-fold increase in the ratio of LC3B-II/I, compared to untreated control while lower viral doses prevented the mitoxantrone-induced increases and higher doses did not seem to have an effect (Fig 39B). Treatment with 500nM mitoxantrone increased the ratio of LC3B-II/I only in combination with 50ppc and 250ppc to 1.40- and 1.42-fold, respectively, compared to untreated samples but these ratios were lower than with mitoxantrone alone. At higher viral doses there was a clear dose dependent decrease in the mitoxantrone-induced LC3II/I ratios down to basal levels. Cells treated with 1000nM mitoxantrone and infected with AdΔΔ at 250ppc and 500ppc induced 2.89-, and 2.43-fold increases, respectively, compared to untreated control and were also higher than with mitoxantrone alone (1.92-fold). In contrast, when 1000nM mitoxantrone was combined with 1000ppc the drug-induced LC3II/I ratio was maintained at the same level. Treatment with 2000nM mitoxantrone increased the ratio of LC3B-II to LC3B-I inducing 6.75, 3.09 and 3.94-fold, respectively, compared to untreated control. In summary, mitoxantrone (as previously observed in Section 3.5.2 with AdE1A12S) induced the accumulation of LC3B-II levels, whilst AdΔΔ counteracted mitoxantrone-induced accumulation at high viral doses.

In cells treated with 250nM mitoxantrone in combination with AdΔΔ at 500ppc and 1000ppc decreased the levels of p62/SQSTM1 to 0.43 and 0.43-fold, respectively, compared to the untreated control. Cells treated with 500nM mitoxantrone in

combination with AdΔΔ at 500ppc and 1000ppc showed 1.57- and 3.40-fold increases of p62/SQSTM1 compared to untreated control. In addition, the treatments with mitoxantrone at 1000nM and 2000nM reduced the levels of p62/SQSTM1 (except for 1000nM mitoxantrone with AdΔΔ at 500ppc and 1000ppc). These results suggest that AdΔΔ in combination-treated cells prevented the mitoxantrone-dependent p62/SQSTM1 degradation. However, this AdΔΔ-induced effect appeared to be limited to a certain dose-range of mitoxantrone (Fig. 39B). In summary, as observed previously, mitoxantrone induces autophagy activity/flux, while AdΔΔ potently inhibits autophagy flux similar to AdE1A12 but only at certain doses of mitoxantrone in PC-3 cells after 48h. Perhaps the observed differences between the viruses are a reflection of AdΔΔ replication that may generate new viral particles at this time point and induce high levels of cell killing masking potential anti-autophagic activities.

3.5.8 AdΔΔ induced activation of Akt is downregulated in combination with high doses of mitoxantrone in PC-3 cells at 48h.

Phosphorylation of Akt in cells infected with AdΔΔ at 50ppc, 250ppc, 500ppc and 1000ppc resulted in 0.65, 0.78, 1.25 and 1.37-fold changes, respectively after 48h, compared with the untreated control, and appeared to be dose-dependent (Fig. 41A). These findings were similar to those in AdE1A12S infected cells (Section 3.5.3). The levels of p-Akt decreased in cells treated with mitoxantrone at 1000nM and 2000nM to 0.08- and 0.15-fold, compared to untreated control. The reduction in p-Akt levels with high concentrations of mitoxantrone was consistent with previous findings (sections 3.5.3 and 3.5.4). The levels of p-Akt were increased in cells treated with 250nM mitoxantrone in combination with AdΔΔ virus at 50ppc, 250ppc, 500ppc and 1000ppc to 1.20-, 1.73-, 1.54- and 1.27-fold, respectively, compared to untreated control and were higher than either agent alone (Fig. 41A-B). Treatment with 500nM mitoxantrone in combination with AdΔΔ at 250ppc and 500ppc showed 1.77- and 1.29-fold increases, of p-Akt compared to untreated control and were higher than either agent alone. In contrast, treatment with 1000nM and 2000nM mitoxantrone at all combinations with AdΔΔ strongly reduced the levels of p-Akt

compared to untreated cells. While the reduction of p-Akt was independent on the virus dose, the p-Akt levels were still higher than with mitoxantrone alone. In summary, increasing doses of mitoxantrone impaired AdΔΔ-induced increases in p-Akt levels, similarly to mitoxantrone in combination with AdE1A12S at 48h. The inhibition of p-Akt by mitoxantrone might contribute to mitoxantrone-induced autophagy activity in agreement with previous results of the autophagic markers at high concentrations of mitoxantrone (Fig. 40)

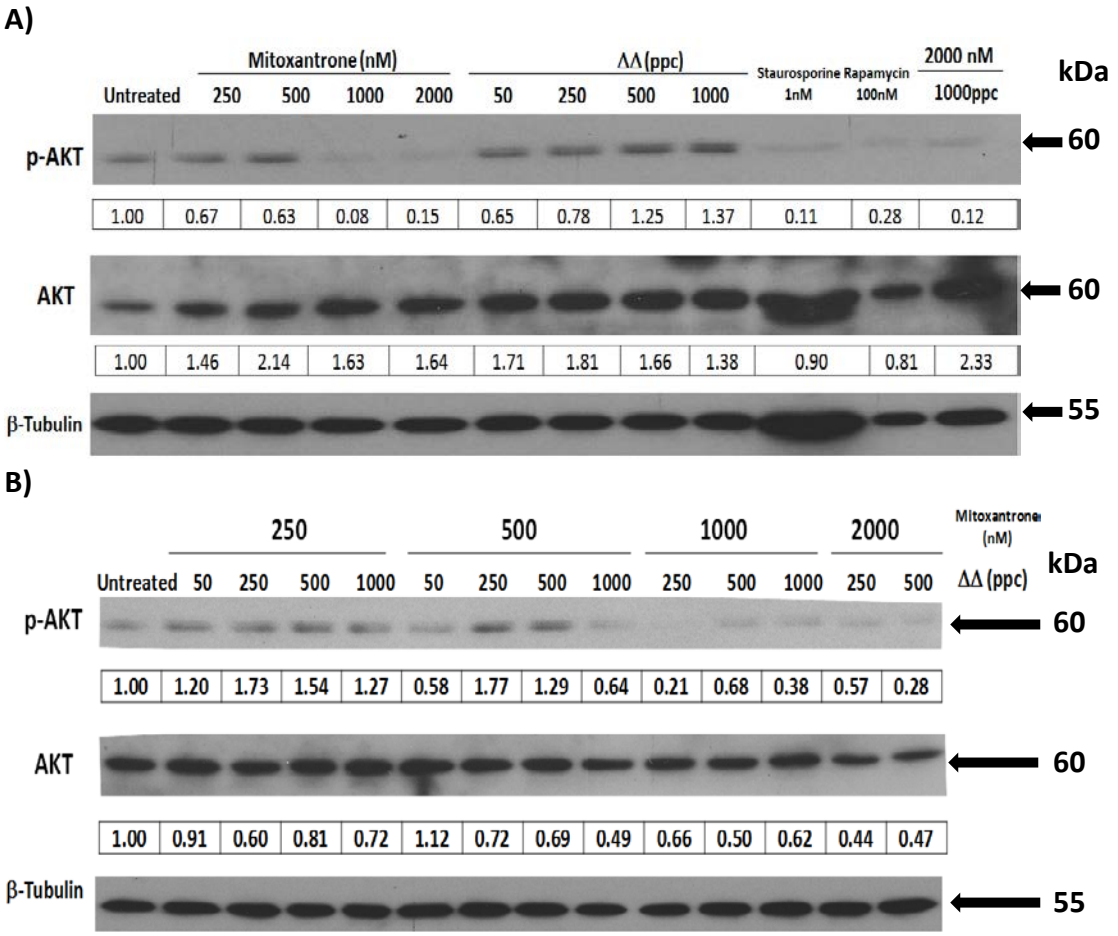

Figure 40. Changes in expression of the phosphorylated Akt (Ser-473) and total Akt in PC-3 cells at 48h post-treatment with mitoxantrone and/or infection with the AdΔΔ **virus**. **A)** PC-3 cells treated with mitoxantrone at increasing concentrations, 250nM - 2000nM or infected with the AdΔΔ virus, at 50ppc - 1000ppc. Cells were also treated with staurosporine at 1nM and rapamycin 100nM as indicators of apoptotic and autophagic activity. **B)** PC-3 cells treated with mitoxantrone for 48h at 250nM, 500nM 1000nM and 2000nM in combination with the AdΔΔ virus at 50ppc, 250ppc, 500ppc and 1000ppc. A-B) The intensity of the bands where quantified using Gene Tools version 4.01 (Synoptics Ltd, Cambridge, UK). Bands were normalized for p-Akt as the intensity of each band to Akt, and Akt to the loading control (KU-70)**.** Fold change of each sample after being compared to untreated control, were the change of the untreated samples is 1.00. One experiment, blot representative of three repetitions

3.5.9 Bcl-2 is induced by mitoxantrone in combination with AdΔΔ inPC-3 cells after 48h of treatment.

PC-3 cells infected with AdΔΔ at 50ppc, 250ppc, 500ppc and 1000ppc showed slight decreased expression of Bcl-2 at 0.86-, 0.85-, 0.84- and 0.73-fold respectively, compared to untreated control. In contrast, treatment with mitoxantrone at 250nM, 500nM, 1000nM and 2000nM induced 1.87-, 1.88-, 1.85- and 1.26-fold increases, respectively, compared to untreated control. However, as shown in previous results (Section 3.5.6), high concentrations of mitoxantrone (2000nM) reduced Bcl-2 expression compared to the lowest concentration (250nM). In summary, infection with AdΔΔ decreased the expression of Bcl-2, but was not dose-dependent. Additionally, mitoxantrone induced Bcl-2 expression at all concentrations, nonetheless, high concentrations of mitoxantrone decreased Bcl-2 expression.

A)

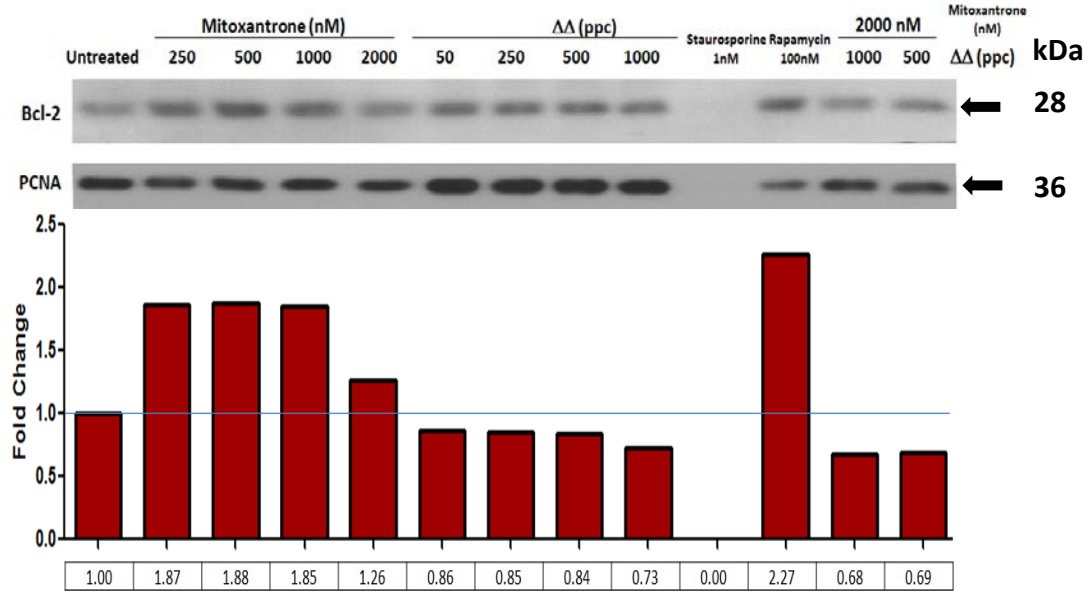

B)

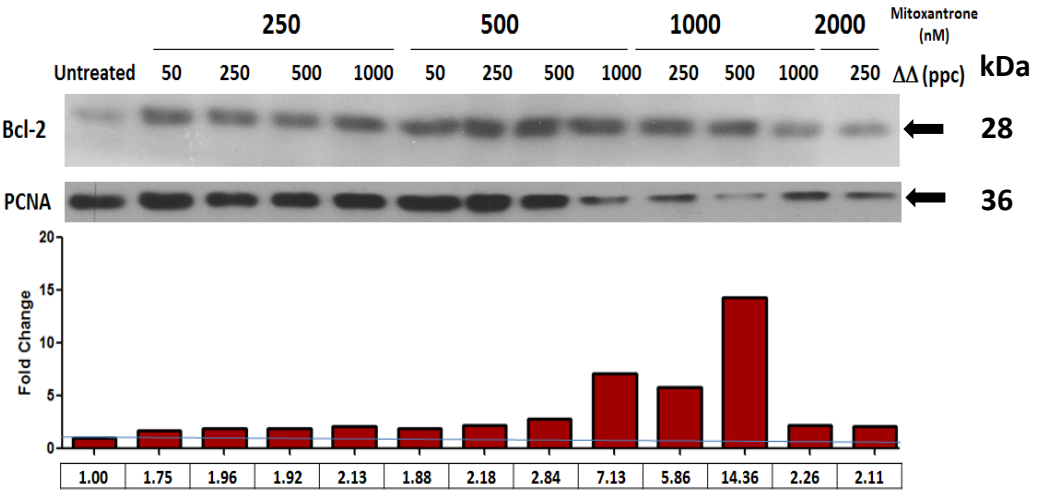

Figure 41. Changes in expression of Bcl-2 in PC-3 cells at 48h post-treatment with mitoxantrone and/or infection with the AdΔΔ virus. **A)** PC-3 cells treated with mitoxantrone at increasing concentrations, 50nM - 2000nM or infected with the AdΔΔ virus, at 50ppc - 1000ppc. Cells were also treated with staurosporine at 1nM and rapamycin 100nM as indicators of apoptotic and autophagic activity. **B)** PC-3 cells treated with mitoxantrone for 48h at 250nM, 500nM, 1000nM and 2000nM in combination with the AdΔΔ virus at 50ppc, 250ppc, 500ppc and 1000ppc. A-B) The intensity of the bands where quantified using Gene Tools version 4.01 (Synoptics Ltd, Cambridge, UK). Bands were normalized as the intensity of each band to the loading control (PCNA). Fold change of each sample after being compared to untreated control, were the change of the untreated samples is 1.00. Blot representative of three repetitions.

Surprisingly, Bcl-2 was increased in cells simultaneously treated with 250nM, 500nM, 1000nM and 2000nM mitoxantrone and infected with AdΔΔ virus at all combinations. The increase corresponded to the increased concentrations of mitoxantrone. In summary, elevated Bcl-2 expression was mitoxantrone-dependent at all concentrations in combination with AdΔΔ in contrast to the findings with mitoxantrone and AdE1A12S at the 48h time point. These differences between viruses might again be explained by the potent replication of the AdΔΔ mutant which could generate a significant amount of new viral particles resulting in high local doses of virus.

3.5.9.a Summary of immunoblotting data in PC-3 cells infected with AdΔΔ and/or treated with mitoxantrone:

- In PC-3 cells infected with AdΔΔ autophagy flux is not affect while in combination with low doses of mitoxantrone (250nM and 500nM) AdΔΔ prevented mitoxantrone-induced autophagy flux and brought LC3I/II ratios back to basal (or below) levels.
- Infection with AdΔΔ induces a dose-dependent increase in p-Akt levels while the combination with mitoxantrone inhibits p-Akt increases similar to the observations with AdE1A12S and brings levels back to basal.
- The levels of Bcl-2 are increased in response to the combination treatments with mitoxantrone and AdΔΔ compared to the untreated control and either single agent. However, the Bcl-2 response appears to be caused mainly mitoxantrone.

3.5.10 Ad5wt-mediated inhibition of autophagy is blocked by high doses of mitoxantrone in PC-3 cells at 48h.

To explore whether Ad5wt infected cells caused similar changes and interacted in similar fashion with mitoxantrone as AdΔΔ, the expression levels of LC3B-II/I and p62/SQSTM1 were determined 48h after treatment. These studies would enable us to identify whether the gene-deletions in AdΔΔ would cause a different response than that induced by the intact Ad5wt virus. For example, it was reported that the E1B19K protein may induce autophagy through interactions with Beclin-1.[348] To assess LC3B-II to LC3B-I ratio, cells were infected for 48h with increasing concentrations of Ad5wt. Infection with Ad5wt strongly decreased the ratio of LC3B-II to LC3B-I at 50ppc and 250ppc showing 0.38- and 0.37-fold changes, respectively, compared to untreated control. Moreover, Ad5wt-infections at 500ppc and 1000ppc resulted in 0.65- and 0.78-fold decreases, respectively, compared to untreated control. In addition, mitoxantrone increased the ratio of LC3B-II to LC3B-I in agreement with my previous results (Sections 3.5.1, 3.5.2 and 3.5.7). In summary, in PC-3 cells Ad5wt clearly reduced LC3B-II to LC3B-I ratios in contrast to the results

with the AdE1A12S non-replicating mutant that caused slight increases but in agreement with the decreases observed in AdΔΔ-infected cells (Fig. 39). Infection with Ad5wt at 250ppc induced a 1.12-fold increase in the levels of p62/SQSTM1 compared to untreated control, whereas 500ppc and 1000ppc increased the levels of p62/SQSTM1 to 1.35 and 2.35-fold, respectively. Thus, Ad5wt increased the levels of p62/SQSTM1 in a dose-dependent manner. These results, suggest that the Ad5wt, similar to the AdΔΔ and AdE1A12S mutants, can impair autophagic flux. In contrast, decreased levels of p62/SQSTM1 were observed in cells treated with mitoxantrone at 500nM, 1000nM and 2000nM, showing 0.31-, 0.04- and 0.17-fold changes respectively. These results indicate as previously shown, that mitoxantrone induced dose-dependent autophagic flux.

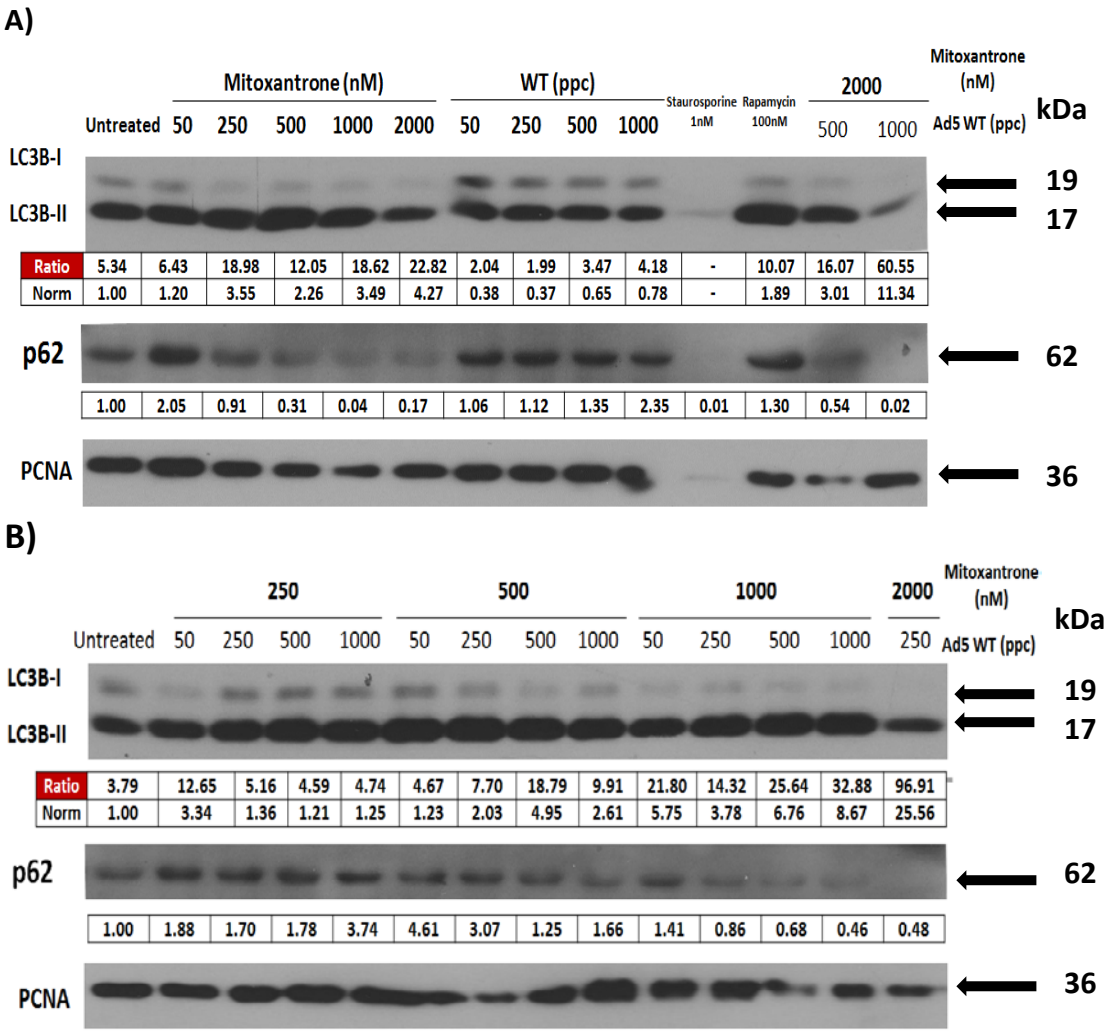

Figure 42. Differences in the ratio of LC3B-II to LC3B-I and expression of p62/SQSTM1 in PC-3 cells at 48h post-treatment with mitoxantrone and/or infection with the Ad5wt virus. A) PC-3 cells treated with mitoxantrone at increasing concentrations, 50nM - 2000nM or

infected with the Ad5wt virus, at 50ppc - 1000ppc. Cells were also treated with staurosporine at 1nM and rapamycin 100nM as indicators of apoptotic and autophagic activity. **B)** PC-3 cells treated with mitoxantrone for 48h at 250nM, 500nM, 1000nM and 2000nM in combination with the Ad5wt virus at 50ppc, 250ppc, 500ppc and 1000ppc. A-B) The intensity of the bands where quantified using Gene Tools version 4.01 (Synoptics Ltd, Cambridge, UK). The variation in the ratio of LC3B-II to I after normalizing the intensity of each band to the loading control (PCNA)**. Norm:** indicates the fold change (FC) of each sample compared to untreated control, for LC3B indicates the ratio of LC3B II/I of each sample compared to the ratio of LC3B II/I of the untreated control. Fold changes of untreated samples is 1.00.Blot representative of three repetitions.

Cells treated with mitoxantrone in combination with Ad5wt increased the ratio of LC3B-II to LC3B-I at all combinations compared to untreated controls. Treatment with 250nM mitoxantrone in combination with Ad5wt at 50ppc, 250ppc, 500ppc and 1000ppc resulted in 3.34-, 1.36-, 1.21- and 1.25-fold increases, respectively, LC3B-II to LC3B-I ratios compared to untreated control. However, compared to mitoxantrone-treatment alone this was a dose-dependent decrease in the LC3B-II/I ratios. Mitoxantrone at 500nM in combination with Ad5wt at 50ppc, 250ppc, 500ppc and 1000ppc showed 1.23-, 2.03-, 4.95- and 2.61-fold increases, respectively, in LC3B-II to LC3B-I ratio compared to untreated control, but except for the two highest virus doses these ratios were lower than with mitoxantrone alone (Fig. 42). Cells treated with 1000nM mitoxantrone in combination with Ad5wt induced 5.75-, 3.78-, 6.76- and 8.67-fold increases, respectively, in LC3B-II to LC3B-I ratios compared to untreated control. Finally, mitoxantrone at 2000nM in combination with Ad5wt at 50ppc, 250ppc, 500ppc and 1000ppc showed 3.01-, 11.34- and 25.56-fold increases, respectively, compared to untreated control (Fig. 42). These results suggest that Ad5wt was unable to supress mitoxantrone-induced accumulation of LC3B-II except at low doses of mitoxantrone (250nM). The levels of p62/SQSTM1 in cells treated with 250nM mitoxantrone in combination with Ad5wt 50ppc, 250ppc, 500ppc and 1000ppc caused 1.88-, 1.70-, 1.78- and 3.74-fold increases, respectively, compared to untreated control and were higher than with drug alone. Moreover, cells treated with 500nM mitoxantrone in combination with Ad5wt at 50ppc, 250ppc, 500ppc and 1000ppc (4.61-, 3.07-, 1.25- and 1.66-fold increases, respectively), strongly increased the levels of p62/SQSTM1 compared to untreated control and drug alone (Fig. 42). Cells treated with 1000nM mitoxantrone in combination with Ad5wt at 50ppc

induced a 1.41-fold increase in p62/SQSTM1 levels compared to untreated control. However, the levels of p62/SQSTM1 were reduced at 1000nM of mitoxantrone in combination with Ad5wt at 250ppc, 500ppc and 1000ppc causing 0.86-, 0.68- and 0.46-fold changes, respectively, compared to untreated control but were still higher than with drug alone. The levels of p62/SQSTM1 potently decreased in cells treated with 2000nM mitoxantrone in combination with Ad5wt at 250ppc, 500ppc and 1000ppc showing 0.48-, 0.54- and 0.02-fold decreases, respectively, compared to untreated control. Taken together, mitoxantrone in combination with Ad5wt caused accumulation of LC3B-II in proportion to LC3B-I, accompanied by decreased levels of p62/SQSTM1 indicating autophagic activity. Although, Ad5wt attenuated the mitoxantrone-induced increases in LC3-II/I and decreases in p62/SQSTM1, the virus did not completely block the mitoxantrone-dependent autophagy induction. However, in the combination-treated cells autophagy activity was only observed at high doses of mitoxantrone (1000nM and 2000nM) and not at lower doses, where the response to Ad5wt dominated and autophagy was impaired.

3.5.11 Both mitoxantrone and Ad5wt can reduce Bcl-2 expression but not in combination in PC-3 cells at48h.

PC-3 cells Infected with Ad5wt at 50ppc, 250ppc, 500ppc and 1000ppc decreased the expression of Bcl-2 to 0.85-, 0.62-, 0.40- and 0.49-fold respectively, compared to untreated control. In addition, treatment with mitoxantrone at 250nM, 500nM, 1000nM and 2000nM decreased the expression of Bcl-2 to 0.73-, 0.63-, 0.73- and 0.56-fold compared to untreated control. In summary, the infection with increasing concentrations of Ad5wt decreased Bcl-2 expression in a dose-dependent manner. Moreover, mitoxantrone reduced the levels of Bcl-2 at all concentrations.

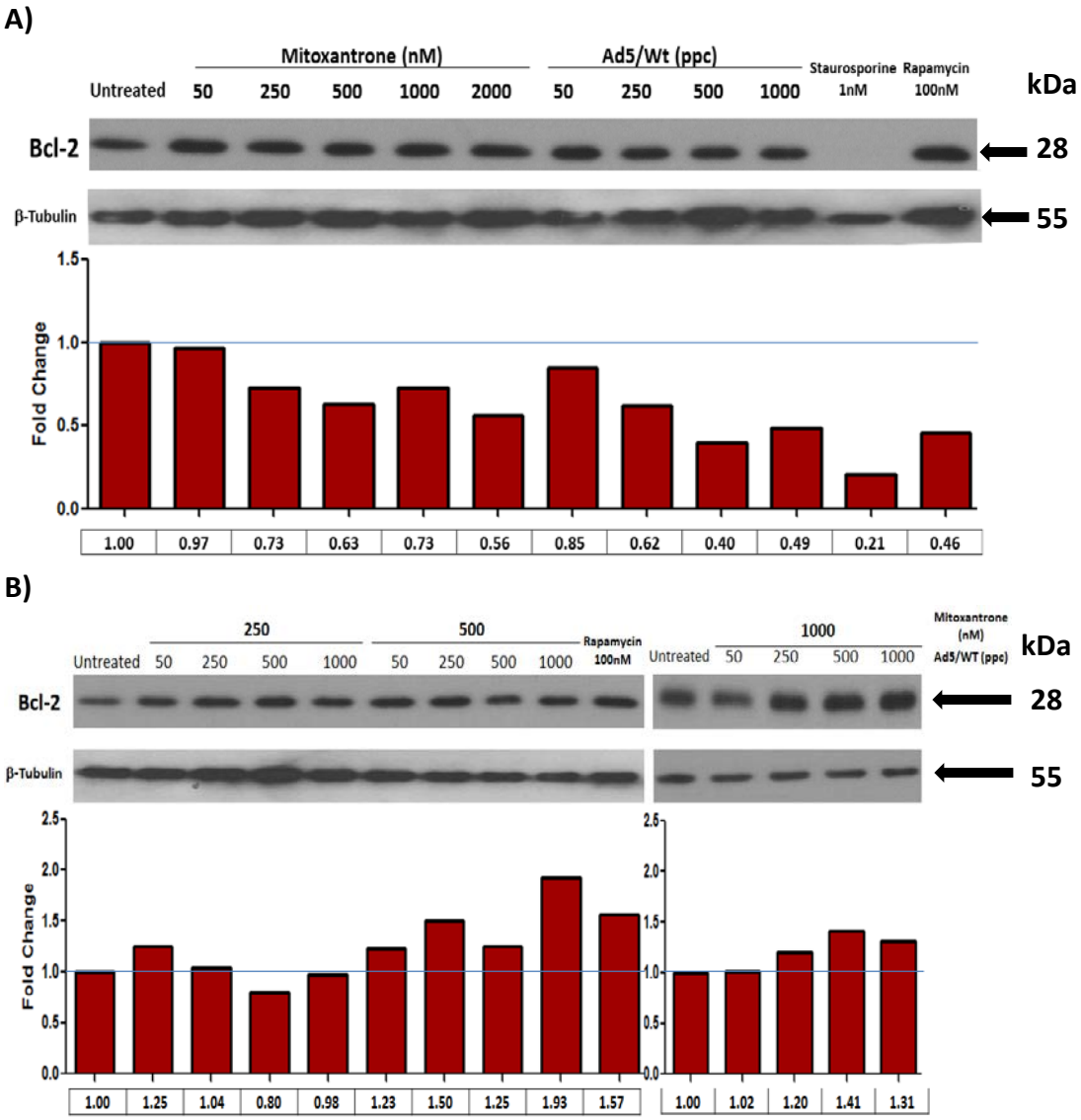

Figure 43. Changes in expression of Bcl-2 in PC-3 cells at 48h post-treatment with mitoxantrone and/or infection with the Ad5wt **virus**. **A)** PC-3 cells treated with mitoxantrone at increasing concentrations, 50nM - 2000nM or infected with the Ad5wt virus, at 50ppc - 1000ppc. Cells were also treated with staurosporine at 1nM and rapamycin 100nM as indicators of apoptotic and autophagic activity. **B)** PC-3 cells treated with mitoxantrone for 48h at 250nM, 500nM and 1000nM in combination with the Ad5wt virus at 50ppc, 250ppc, 500ppc and 1000ppc. A-B) The intensity of the bands where quantified using Gene Tools version 4.01 (Synoptics Ltd, Cambridge, UK). Bands were normalized as the intensity of each band to the loading control (β-Tubulin). Fold change of each sample after being compared to untreated control, were the change of the untreated samples is 1.00. Blot representative of three repetitions.

Cells treated with 250nMmitoxantrone in combination with Ad5wt at 50ppc induced a 1.25-fold increase in Bcl-2 expression, compared to untreated control. In contrast the combination of 250nM with 500ppc decreased the expression of Bcl-2 by 0.80-fold, compared to untreated control (Fig. 43). Cells treated with 500nM

mitoxantrone in combination with Ad5wt at 50ppc, 250ppc, 500ppc and 1000ppc induced 1.23-, 1.50-, 1.25- and 1.93-fold increases, respectively, in the expression of Bcl-2 compared to untreated control (Fig. 43). Treatment of cells with 1000nM mitoxantrone in combination with Ad5wt at 250ppc, 500ppc and 1000ppc resulted in 1.20-, 1.41- and 1.31-fold increases in Bcl-2 expression, respectively, compared to untreated control. In summary, unexpectedly and in contrast to AdE1A12S and similarly to AdΔΔ, the combination of mitoxantrone with Ad5wt re-establishes and in some combinations increased Bcl-2 expression despite the inhibitory activity of both agents when administered alone.

3.5.11.a. Summary of immun0blotting data in PC-3 cells infected with Ad5wt and/or treated with mitoxantrone:

- Infection with Ad5wt inhibits autophagy flux alone and in certain combinations with mitoxantrone (250nM and 500nM), compared to the untreated control and mitoxantrone alone.
- Infection with Ad5wt inhibits increases in Bcl-2 levels at all concentrations similar to mitoxantrone.
- The combination of Ad5wt and mitoxantrone, in contrast to either single agent, increases Bcl-2 levels.

3.5.12 Summary of immunoblotting data in PC-3 cells

In summary, at the 24h time-point, increasing concentrations of mitoxantrone induced autophagy flux observed by the increases in the ratios of LC3B-II/LC3B-I indicating the accumulation of autophagosomes and by the reduction in p62/SQSTM1 levels that are indicative of p62-degradation. In contrast, infection with AdE1A12S maintained basal levels of LC3B-II while p62/SQSTM1-degradation appeared to be promoted. The combination treatments resulted in the promotion of mitoxantrone-dependent autophagy activity, while AdE1A12S counteracted this activity resulting in attenuation of autophagy. The blockage of autophagy by the virus seemed to be overcome by increasing concentrations of the drug.

At the 48h time-point, more potent induction of mitoxantrone-induced autophagy flux was observed, determined as increased LC3B-II/I ratios in a dose-dependent manner and reduced levels of p62/SQSTM1. In contrast, AdE1A12S impaired autophagy flux shown by the decreased ratios of LC3B-II/I and increased levels of p62/SQSTM1. The combinations of mitoxantrone and AdE1A12S also resulted in increased LC3B-II/I ratios but p62/SQSTM1 was accumulated suggesting that the virus impairs mitoxantrone-induced autophagy flux and that mitoxantrone was unable to overcome the viral inhibition.

The infection of PC-3 cells at 48h with AdΔΔ did not induce changes in the ratio of LC3B-II/I. However, AdΔΔ in combination with mitoxantrone, downregulated the levels of LC3B-II/I, although complete suppression to basal levels was not achieved. In addition, AdΔΔ increased the expression of p62/SQSTM1 and in combination with mitoxantrone the virus effect dominated and prevented the mitoxantrone-induced decreases in p62/SQSTM1 (at certain doses). Ad5wt reduced the LC3B-II to LC3B-I ratios, in a dose-dependent manner and increased p62/SQSTM1 levels. In summary, mitoxantrone induced autophagy flux, while AdE1A12S, AdΔΔ and Ad5wt potently inhibited drug-induced autophagy flux but only at certain doses of mitoxantrone at the 48h time-point. Ad5wt and AdΔΔ might have contributed to increased cell killing especially at higher viral doses inhibiting autophagy activity and promoting cell proliferation enabling viral replication. These findings seem to verify some of our results from the miRNA analysis, indicating that in PC-3 cells treatment with mitoxantrone down-regulates the oncomiRs and autophagy inhibitors hsa-miR-17-92, hsa-miR-93/106b/25, hsa-miR-183-96-182 and hsa-miR-21, and consequently, mitoxantrone would be expected to promote autophagy-related events. In addition, AdE1A12S induced upregulation of these miRNAs and would be expected to impair autophagy-related events.

The expression of p-Akt in PC-3 cells treated for 24h with mitoxantrone was decreased. The infection with AdE1A12S inhibited p-Akt at low doses, although, at higher doses the virus strongly induced the levels of p-Akt. Moreover, the combination of AdE1A12S with mitoxantrone strongly increased p-Akt. These results

suggest that mitoxantrone was unable to overcome the induction of p-Akt by AdE1A12S. Furthermore, the blockage of mitoxantrone seemed to potentiate p-Akt contributing to reduce the autophagic activity and possibly promote cell proliferation.

At 48h the treatment with mitoxantrone inhibited p-Akt although, to a lesser extent than at 24h. Additionally infection with AdE1A12S increased the levels of p-Akt. However, the combination of AdE1A12S with increasing concentrations of mitoxantrone reduced p-Akt. The inhibition of p-Akt by the combination might contribute to the initial increase in autophagy activity as observed with increased levels of LC3B-II, however, the accumulation of LC3B-II and p62/SQSTM1 are indicative of impaired autophagy flux and may contribute to increased cell killing. Furthermore, the increase in hsa-miR-128 and the downregulation of p-Akt seemed to correlate with mitoxantrone-dependent abrogation of p-Akt that might lead to increased apoptosis. The infection with AdΔΔ induced a dose-dependent increase of p-Akt. Moreover, mitoxantrone in combination with AdΔΔ impaired the AdΔΔ-induced increases of p-Akt, similarly to mitoxantrone in combination with AdE1A12S.

The protein levels of Bcl-2 resulted in slight increases at 24h in PC-3 cells infected with AdE1A12S, while basal levels were observed in response to mitoxantrone. The combination treatments increased the levels of Bcl-2, as observed with p-Akt at this time point. The combination of mitoxantrone and AdE1A12S may induce cell proliferation, more likely driven by the virus. In contrast, at 48h the levels of Bcl-2 were abrogated by the combination suggesting that, at this time point as observed with p-Akt, the combination treatments might induce cell killing and mitoxantrone might overcome the virus response.

At 48h the results from the combination of mitoxantrone with AdE1A12S suggest that the upregulation of hsa-miR-15/16 contribute to the decreased levels of Bcl-2. Moreover, PC-3 cells infected for 48h with AdΔΔ and Ad5wt in combination with mitoxantrone resulted in increased levels of Bcl-2, with the more potent responses in combination with AdΔΔ. The increased expression of Bcl-2 might be induced in response to the ability of both AdΔΔ and Ad5wt to replicate and strongly promote cell proliferation.

3.5.13 AdE1A12S strongly inhibits autophagic activity in 22Rv1 cells at 48h

We also assessed autophagic activity in response to the treatments alone or in combination in 22Rv1 cells at 48h post-treatment. 22Rv1 cells were treated for 48h with increasing concentrations of mitoxantrone and AdE1A12S alone and in combination. In 22Rv1 cells, the selected concentrations of viruses (10ppc - 1000ppc) and mitoxantrone (5nM - 500nM) were adjusted according to viral and drug concentrations that killed less than 20% of cells, and also including doses above that range. Treatment of 22Rv1 cells with mitoxantrone at 5nM and 25nM induced slight changes in the ratio of LC3B-II to LC3B-I compared to untreated control, whilst no change were observed with 50nM and 250nM mitoxantrone. Moreover, cells treated with 500nM mitoxantrone induced a 1.24-fold increase, in the ratio of LC3B-II to LC3B-I compared to untreated control. These results showing that mitoxantrone might promote autophagy only at very high cytotoxic concentrations, are in contrast to the strong increases in the ratio of LC3B-II to LC3B-I observed in PC-3 cells, suggesting that the differences between PC-3 cells and 22Rv1 cells are most likely due to the different genetic backgrounds in these cells (Table 6).

Treatment of 22Rv1 cells with 5nM and 25nM mitoxantrone decreased the levels of p62/SQSTM1 to 0.81 and 0.72-fold, respectively, compared to untreated control. In addition, treatment with mitoxantrone at 50nM, 250nM and 500nM decreased the levels of p62/SQSTM1 to 0.84, 0.73 and 0.76-fold, respectively, compared to untreated control. In contrast to PC-3 cells where increasing concentrations of mitoxantrone induced dose-dependent decreases in the levels p62/SQSTM1, in 22Rv1 cells, mitoxantrone decreased p62/SQSTM1 independently of the dose. Taken together, in 22Rv1 cells mitoxantrone seemed to induce autophagic flux, although, only at high doses of mitoxantrone, similar to the findings in PC3 cells (Section 3.5.2).

Infection of cells with AdE1A12S at 10ppc increased the ratio of LC3B-II to LC3B-I inducing a 1.26-fold change compared to untreated control. No changes were observed with AdE1A12S at 25ppc and 50ppc (Fig. 44). In contrast, decreased ratios of LC3B-II to LC3B-I were observed in cells infected with AdE1A12S at 250ppc, 500ppc and 1000ppc to 0.79, 0.78 and 0.61-fold, respectively, compared to untreated control (Fig. 44). In summary, in 22Rv1 cells increasing doses of AdE1A12S reduced the ratios

of LC3B-II/-I in a dose-dependent manner. Thus, infection with AdE1A12S in 22Rv1 cells decreases LC3B-II accumulation blocking autophagy.

Infection of 22Rv1 cells with the AdE1A12S virus showed almost no changes in the levels of p62/SQSTM1 at 10ppc and 25ppc compared to untreated control. Increased doses of AdE1A12S decreased the levels of p62/SQSTM1 to 0.79, 0.85, 0.85; 0.64 at 50ppc, 250ppc, 500ppc and 1000ppc, respectively, compared to untreated control (Fig. 44). Interestingly, AdE1A12S reduced the levels of p62/SQSTM1 in contrast to the virus activity in PC-3 cells, indicating a different mechanism of p62/SQSTM1 regulation. However, similar to the findings in PC-3 cells, AdE1A12S did not appear to induce autophagic flux.

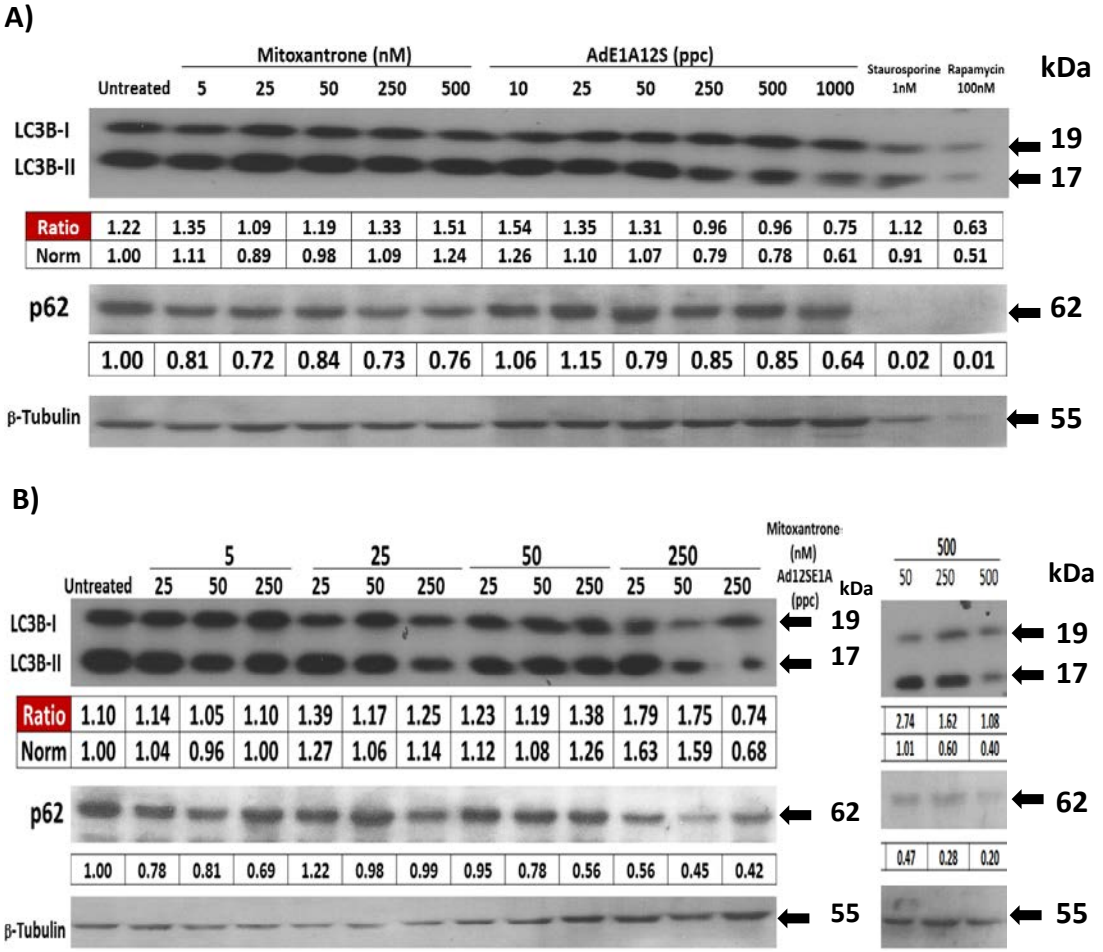

Figure 44. Differences in the ratio of LC3B-II to LC3B-I and expression of p62/SQSTM1 in 22Rv1 cells at 48h post-treatment with mitoxantrone and/or infection with the AdE1A12S virus. **A)** 22Rv1 cells treated with mitoxantrone at increasing concentrations, 5nM - 500nM or infected with the Ad5wt virus, at 10ppc - 1000ppc. Cells were also treated with staurosporine at 1nM and rapamycin 100nM as indicators of apoptotic and autophagic activity. **B)** 22Rv1 cells treated with mitoxantrone for 48h at 5nM, 25nM, 50nM and 250nM

in combination with the AdE1A12S virus at 25ppc, 50ppc and 250ppc; 500nM in combination with the AdE1A12S virus at 50ppc, 250ppc and 500ppc . A-B) The intensity of the bands where quantified using Gene Tools version 4.01 (Synoptics Ltd, Cambridge, UK). The variation in the ratio of LC3B-II to I after normalizing the intensity of each band to the loading control (β-tubulin)**. Norm:** indicates the fold change of each sample compared to untreated control, for LC3B indicates the ratio of LC3B II/I of each sample compared to the ratio of LC3B II/I of the untreated control. Fold changes of untreated samples is 1.00. Blot representative of three repetitions.

In 22Rv1 cells treated for 48h with 5nM mitoxantrone in combination with Ad12SE1A no changes in the ratios of LC3B-II to LC3B-I were observed compared to untreated control and mitoxantrone alone. Moreover, treatment with 25nM mitoxantrone in combination with AdE1A12S at 25ppc and 250ppc slightly increased the ratios to 1.27 and 1.14-fold, respectively, compared to untreated control. 22Rv1 cells treated with 50nM mitoxantrone in combination with AdE1A12S at 25ppc and 250ppc slightly increased the ratio of LC3B-II to LC3B-I compared to untreated control. Cells treated with 250nM mitoxantrone in combination with AdE1A12S at 50ppc and 250ppc increased the ratio of LC3B-II to LC3B-I to 1.63 and 1.59–fold, respectively compared to untreated control. The combination of 500nM mitoxantrone with AdE1A12S at 250ppc and 500ppc decreased the ratio of LC3B-II to LC3B-I to 0.60 and 0.40-fold, respectively, compared to untreated control. No changes were observed in combination with 50ppc. At all combinations (except at 500nM) LC3B-II/I ratios were increased compared to mitoxantrone alone, suggesting that at these doses the combination stimulates the accumulation of LC3-II. These results indicate that in 22Rv1 cells, AdE1A12S may abrogate the accumulation of LC3B-II at higher doses only; furthermore, mitoxantrone appeared to partly induce autophagy in 22Rv1 cells.
The levels of p62/SQSTM1 in 22Rv1 cells were decreased in response to the treatment with 5nM mitoxantrone at all combinations with AdE1A12S to 0.78-, 0.81- and 0.69-fold, compared to untreated control but, remained similar to the levels observed with mitoxantrone alone at this concentration. Moreover, treatment with 25nM mitoxantrone and infected with 25ppc of the virus induced a 1.22-fold increase, of p62/SQSTM1 compared to untreated control, however, the levels of p62/SQSTM1 increased compared to mitoxantrone alone. No other combinations increased the levels of p62. In addition, cells treated with 50nM mitoxantrone in combination with AdE1A12S at 50ppc and 250ppc decreased the levels of

p62/SQSTM1 0.78- and 0.56-fold, respectively, compared to untreated control. Moreover, cells treated with 250nM mitoxantrone in combination with Ad12S at 25ppc, 50ppc, and 250ppc decreased the levels of p62/SQSTM1 to 0.56-, 0.45- and 0.42-fold, respectively, compared to untreated control. Additionally, 500nM mitoxantrone in combination with AdE1A12S at 50ppc, 250ppc and 500ppc decreased the levels of p62/SQSTM1to 0.47, 0.28 and 0.20-fold, respectively, compared to untreated control. Furthermore, the combinations at increasing concentrations of mitoxantrone promoted stronger decreases in the levels of p62/SQSTM1 than mitoxantrone alone.

In summary, the treatment with increasing concentrations of mitoxantrone decreased the expression of p62/SQSTM1 in 22Rv1 cells. In addition, from these results it was not clear if autophagy was induced or might have only been induced by certain combinations. Although, autophagy was not induced at low and high combinations, indicating that at low concentrations the viral-activity might have been more potent than mitoxantrone, whilst at high concentrations of mitoxantrone LC3B-II and p62/SQSTM1 decreases might be the effects of increased cell death.

3.5.14 AdE1A12S potently induces p-Akt in 22Rv1 cells 48h after infection.

Expression of p-Akt (Ser-473) in 22Rv1 cells was assessed in response to increasing doses of mitoxantrone; p-Akt was not induced at any concentrations of drugs (5nM – 500nM). In contrast, there was a strong induction of p-Akt with increasing doses of AdE1A12S. The strongest increases were seen at 50ppc, 250ppc, 500ppc and 1000ppc showing 55.31-, 190.56-, 283.56- and 427.03-fold, respectively, compared to untreated samples. Basal levels of p-Akt were below the limit of detection (Fig. 45).

In addition, 5nM mitoxantrone increased p-Akt in cells infected with AdE1A12S at 25ppc, 50ppc and 250ppc inducing 49.16, 427.58 and 609.61-fold increases, respectively, compared to untreated control and were higher than with virus alone. Treatment with 25nM mitoxantrone in combination with 25ppc, 50ppc and 250ppc induced 148.01, 1873.09 and 292.40-fold increases of p-Akt, respectively, compared to untreated control. Cells treated with 50nM mitoxantrone in combination with

AdE1A12S at 25ppc, 50ppc and 250ppc induced 292.40, 585.07 and 746.90-fold increases, respectively, in the levels of p-Akt compared to untreated control. The treatment with 250nM mitoxantrone in combination with 25ppc, 50ppc and 250ppc showed 165.38, 298.97 and 618.33-fold increases in p-Akt expression compared to untreated control. The levels of p-Akt in cells treated with 500nM mitoxantrone in combination with AdE1A12S at 50ppc, 250ppc and 500ppc increased in 63.61, 164.77 and 120.04-fold, respectively, compared to untreated control. The great increases in the expression levels of p-Akt were normalised to almost non-detectable levels of p-Akt at the basal level (control cells).

A)

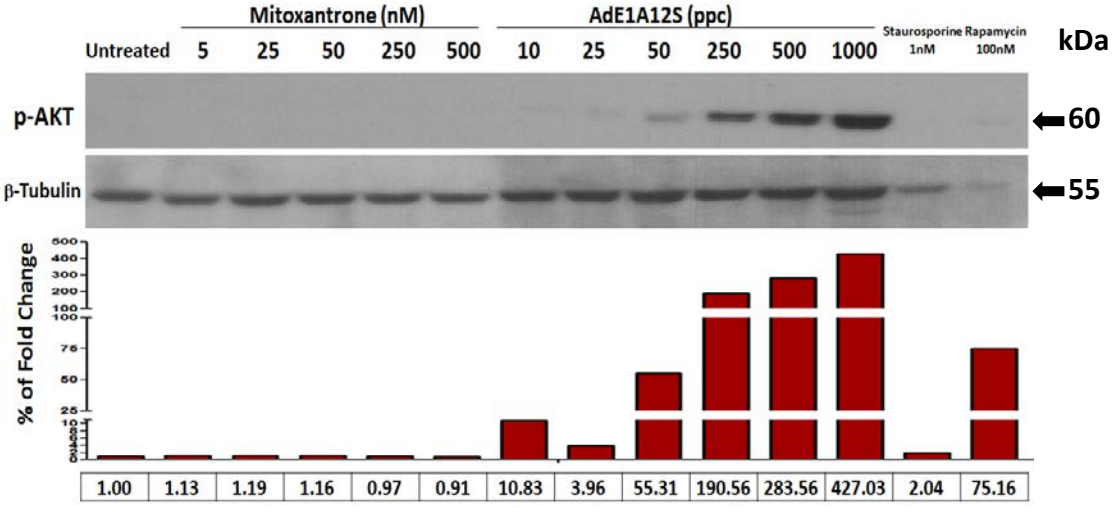

B)

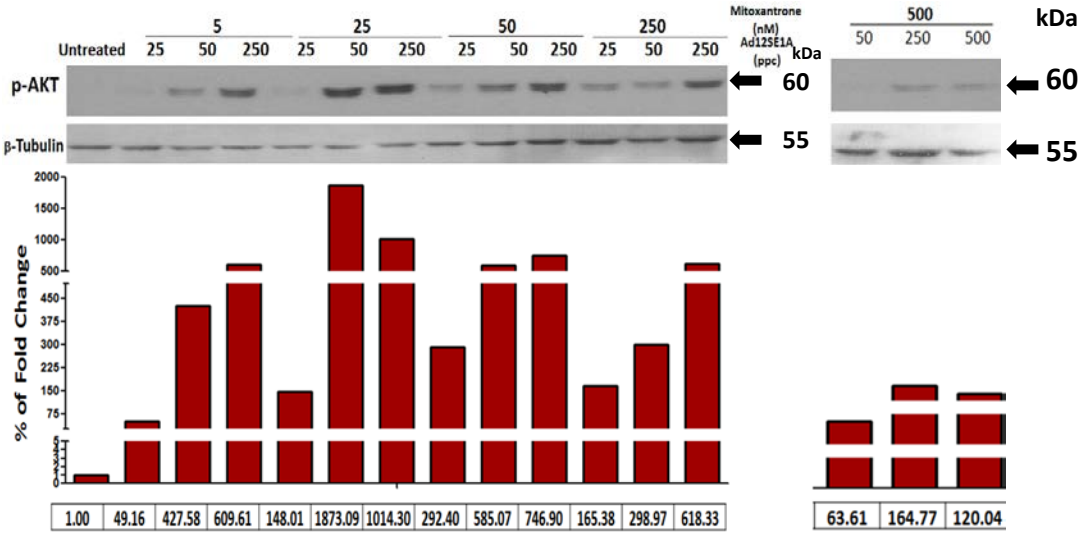

Figure 45. Changes in expression of the phosphorylated Akt in 22Rv1 cells at 48h post-treatment with mitoxantrone and/or infection with the AdE1A12S virus. A) 22Rv1 cells treated with mitoxantrone at increasing concentrations, 5nM - 500nM or infected with the AdE1A12S virus, at 10ppc - 1000ppc. Cells were also treated with staurosporine at 1nM and rapamycin 100nM as indicators of apoptotic and autophagic activity. **B)** 22Rv1 cells treated with mitoxantrone for 48h at 5nM, 25nM, 50nM, and 250nM in combination with the AdE1A12S virus at 25ppc, 50ppc and 250ppc; 500nM in combination with the AdE1A12S virus at 50ppc, 250ppc and 500ppc. A-B) The intensity of the bands where quantified using Gene Tools version 4.01 (Synoptics Ltd, Cambridge, UK). Bands were normalized as the intensity of each band to the loading control (β-Tubulin). Fold change of each sample after being compared to untreated control, were the change of the untreated samples is 1.00. Blot representative of three repetitions

The combination treatments increased the levels of p-Akt at all combinations compared to untreated control and mitoxantrone alone. Moreover, viral-induced increases in p-Akt levels were potentiated by some combinations with mitoxantrone. These findings are in contrast to those in PC-3 cells where p-Akt was decreased by the combinations. These results suggest that in 22Rv1 cells mitoxantrone might not cause Akt phosphorylation at ser-473 at the 48h time-point, although, it might deregulate other factors enabling AdE1A12S to potently induce p-Akt.

3.5.15 Mitoxantrone attenuates the AdE1A12S-dependent inhibition of Bcl-2 in 22Rv1 cells.

Bcl-2 expression slightly increased in 22Rv1 cells treated with 5nM mitoxantrone, inducing a 1.16-fold increase, compared to untreated control. Moreover, with 25nM almost no change was observed compared to untreated control. In addition, mitoxantrone at 50nM, 250nM and 500nM decreased Bcl-2 levels to 0.82, 0.73 and 0.69-fold, respectively, compared to untreated control (Fig. 46A). Infection with AdE1A12S at 10ppc, 25ppc, 50ppc, 250ppc, 500ppc and 1000ppc decreased Bcl-2 expression to 0.32, 0.33, 0.35, 0.31 and 0.25-fold, respectively, compared to untreated control (Fig. 46A).

In summary, increasing concentrations of mitoxantrone induced dose-dependent decreases in Bcl-2 expression in 22Rv1 cells at 48h. Furthermore, infection with AdE1A12S strongly reduced Bcl-2 expression independently of the viral dosage. Interestingly, these results, showed that Bcl-2 in 22Rv1 cells is highly sensitive to

AdE1A12S infection, in contrast to PC-3 cells where only high concentrations of both mitoxantrone and AdE1A12S decreased Bcl-2 expression.

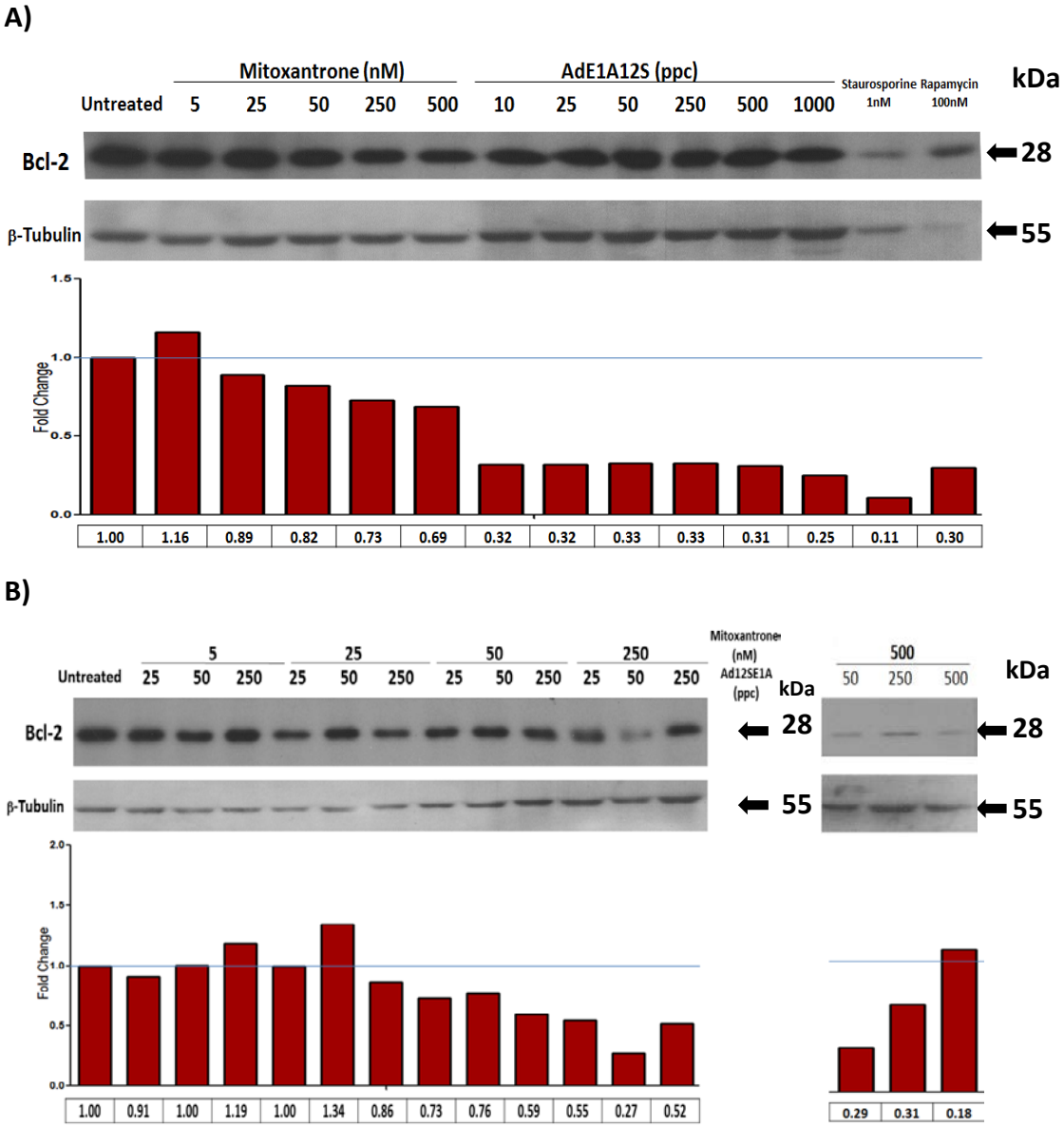

Figure 46. Changes in expression of Bcl-2 in 22Rv1 cells at 48h post-treatment with mitoxantrone and/or infection with the AdE1A12S virus. **A)** 22Rv1 cells treated with mitoxantrone at increasing concentrations, 50nM - 2000nM or infected with the AdE1A12S virus, at 50ppc - 1000ppc. Cells were also treated with staurosporine at 1nM and rapamycin 100nM as indicators of apoptotic and autophagic activity. **B)** 22Rv1 cells treated with mitoxantrone for 48h at 5nM, 25nM, 50nM and 250nM in combination with the AdE1A12S virus at 25ppc, 50ppc and 250ppc; 500nM in combination with the AdE1A12S virus at 50ppc, 250ppc and 500ppc. **A-B)** The intensity of the bands where quantified using Gene Tools version 4.01 (Synoptics Ltd, Cambridge, UK). Bands were normalized as the intensity of each band to the loading control (β-Tubulin)**.** Fold change of each sample after being compared to untreated control, were the change of the untreated samples is 1.00. Blot representative of three repetitions.

While the 22Rv1 cells were highly sensitive to AdE1A12S dependent downregulation of Bcl-2, in combination with 5nM mitoxantrone basal levels of Bcl-2 were re-established. Moreover, Bcl-2 expression in cells treated with 25nM mitoxantrone in combination with AdE1A12S at 50ppc induced a slight increase of 1.34-fold, compared to untreated control (Fig. 46B). The combination of 25nM with 25ppc maintained basal levels of Bcl-2, whereas AdE1A12S at 250ppc slightly reduced the levels of Bcl-2. However, the virus in combination with 25nM showed slight increases compared to mitoxantrone and to the virus alone at similar doses (Fig. 46B). The expression of Bcl-2 decreased in cells treated with 50nM mitoxantrone and AdE1A12S at 25ppc, 50ppc and 250ppc to 0.73-, 0.76- and 0.59-fold, respectively, compared to untreated control. Moreover, the combination when compared to mitoxantrone alone showed similar levels of Bcl-2 except at the highest viral dose, however, these combinations had increased Bcl-2 levels when compared to AdE1A12S alone. Furthermore, 250nM mitoxantrone in combination with AdE1A12S at 25ppc, 50ppc and 250ppc decreased Bcl-2 expression to 0.55-, 0.27- and 0.52-fold, respectively, compared to untreated control (Fig. 46B); the levels of Bcl-2 with the combination were increased (except at 50ppc) compared to AdE1A12S alone. The levels of Bcl-2 with 500nM mitoxantrone in combination with AdE1A12S at 50ppc and 250ppc decreased to 0.34- and 0.67-fold respectively, compared to untreated control (Fig. 46B), the 500nM mitoxantrone in combination with 500ppc regain basal levels; these combinations showed increasing trend compared to the virus alone at those doses. In summary, mitoxantrone abrogates the AdE1A12S-dependent reduction in Bcl-2 levels only at the lower drug doses; in contrast, high doses of mitoxantrone may contribute to Bcl-2 downregulation through cell-death induction.

3.5.15.a. Summary of immunoblotting data in 22Rv1 cells infected with AdE1A12S and/or treated with:

- In 22Rv1 cells infection with AdE1A12S inhibits autophagy flux. In addition, only high doses of mitoxantrone (500nM) induce autophagy slightly. However, the combination of AdE1A12S with mitoxantrone impairs

autophagy flux at low and high doses of mitoxantrone (500nM) compared to untreated control and mitoxantrone alone.

- Treatment with mitoxantrone does not induced p-Akt, while AdE1A12S strongly induces higher levels of p-Akt compared to untreated control. The combination of AdE1A12S with mitoxantrone further potentiates the increases in p-Akt levels compared to single agents.
- Both mitoxantrone and AdE1A12S decreases the levels of Bcl-2 at all concentrations. Bcl-2 expression is increased in response to the combination of both treatments compared to single agent treatment. However, despite that the levels of Bcl-2 are higher the expression levels are still predominantly lower than basal levels.

3.5.16 AdΔΔ potently inhibits autophagy-activity in 22Rv1 cells.

The response to infection with the AdΔΔ virus was assessed in parallel to the infection with AdE1A12S. Levels of the autophagic marker LC3B-II were determined in cells infected with AdΔΔ at 10ppc, 25ppc, 50ppc, 250ppc, 500ppc and 1000ppc showing 0.74-, 0.48-, 0.31-, 0.39-, 0.31- and 0.25-fold decreases, respectively, in the ratio of LC3B-II/LC3B-I compared to untreated samples (Fig. 47A). The expression of p62/SQSTM1 decreased with increasing concentrations of AdΔΔ at 10ppc, 25ppc, 50ppc, 250ppc, 500ppc and 1000ppc to 0.78-, 0.88-, 0.71-, 0.77-, 0.43- and 0.26-fold, respectively, compared to untreated control (Fig.47A). In summary, in 22Rv1 cells AdΔΔ potently impaired autophagy activity similarly to AdE1A12S as indicated by the decreased levels of LC3B-II/I ratios. However, p62/SQSTM1 levels were also decreased, similarly to the effects in PC-3 cells; it is likely that the apparent degradation of p62 is caused by increased cell death in response to the virus and/or viral replication since accumulation of autophagosomes did not occur.

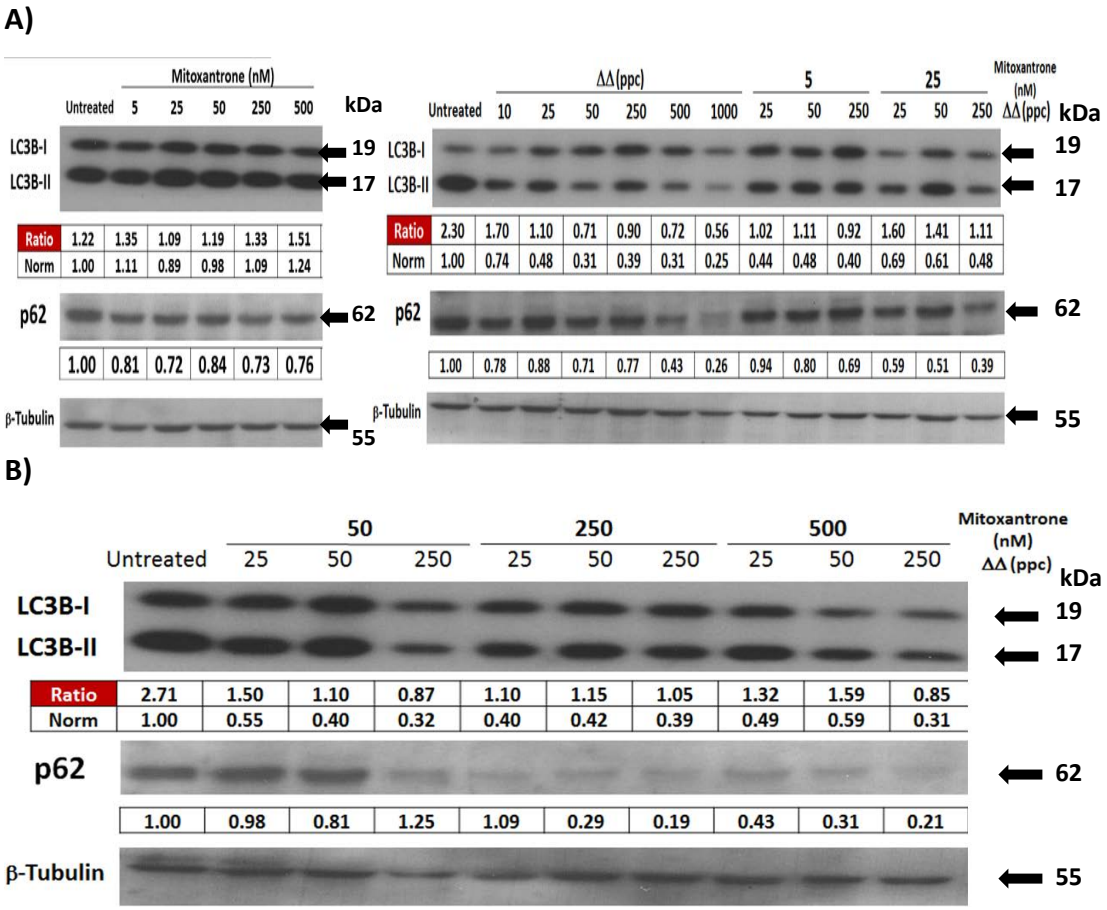

Figure 47. Differences in the ratio of LC3B-II to LC3B-I and expression of p62/SQSTM1 in 22Rv1 cells at 48h post-treatment with mitoxantrone and/or infection with the AdΔΔ virus. **A)** 22Rv1 cells treated with mitoxantrone at increasing concentrations, 5nM - 500nM or infected with the AdΔΔ virus, at 10ppc - 1000ppc. Cells were also treated with staurosporine at 1nM and rapamycin 100nM as indicators of apoptotic and autophagic activity. A/**B)** 22Rv1 cells treated with mitoxantrone for 48h at 5nM, 25nM, 50nM, 250nM and 500nM in combination with the AdΔΔ virus at 25ppc, 50ppc and 250ppc. A-B) The intensity of the bands where quantified using Gene Tools version 4.01 (Synoptics Ltd, Cambridge, UK). The variation in the ratio of LC3B-II to -I after normalizing the intensity of each band to the loading control (β-tubulin)**. Norm:** indicates the fold change of each sample compared to untreated control, for LC3B indicates the ratio of LC3B II/I of each sample compared to the ratio of LC3B II/I of the untreated control. Fold changes of untreated samples is 1.00. One experiment, blot representative of three repetitions.

The combination of 5nM mitoxantrone with AdΔΔ at 25ppc, 50ppc and 250ppc decreased the ratio of LC3B-II to LC3B-I to 0.44-, 0.48- and 0.40-fold, respectively, compared to untreated control (Fig. 47A), the combination ratios were also decreased when compared to mitoxantrone alone but remained similar to AdΔΔ at those doses. Moreover, treatment with 25nM mitoxantrone in combination with AdΔΔ at 25 ppc, 50 ppc and 250ppc caused 0.69-, 0.61- and 0.48-fold decreases, respectively, in LC3B-II to LC3B-I ratios compared to untreated control (Fig. 47A), the

LC3B-II to LC3B-I ratios were also decreased when compared to mitoxantrone alone, but were increased compared to AdΔΔ at those doses. The treatment of 22Rv1 cells with 50nM mitoxantrone also decreased the ratios of LC3B-II to LC3B-I in combination with AdΔΔ at 25ppc, 50ppc and 250ppc to 0.55-, 0.40- and 0.32-fold, respectively compared to untreated control and also to mitoxantrone alone (Fig. 47 A-B) Additionally, 250nM mitoxantrone combined with AdΔΔ at 25ppc, 50ppc, and 250ppc decreased the ratio of LC3B-II/I to 0.40-, 0.42- and 0.39-fold, respectively, compared to untreated control and mitoxantrone alone (Fig. 47 A-B). Finally, cells treated with 500nM mitoxantrone in combination with AdΔΔ at 25ppc, 50ppc and 250ppc caused 0.49-, 0.59- and 0.31-fold decreases, indicating a decrease in the ratio of LC3B-II to LC3B-I compared to untreated control and mitoxantrone alone (Fig. 47 A-B). In summary, all combinations in 22Rv1 cells decreased the accumulation of LC3B-II in respect to LC3B-I. Decreased accumulation of LC3B-II in response to AdΔΔ was dose-independent. Interestingly, AdΔΔ-dependent inhibition of LC3B-II accumulation was stronger than the inhibition induced by AdE1A12S in this cell line.

The decreased p62/SQSTM1 levels in combination-treated cells were dependent on the viral dose; increasing doses of AdΔΔ caused decreasing levels of p62/SQSTM1 (Fig. 47A-B). Cells treated with 5nM mitoxantrone in combination with AdΔΔ at 50ppc and 250ppc showed decreased levels of p62/SQSTM1, 0.80- and 0.69-fold, respectively, when compare to untreated control (Fig. 47), only small variations were observed compared to mitoxantrone alone at 5nM, while, the changes induced by the combination were similar to those observed with AdΔΔ at similar doses. Moreover, the treatment with mitoxantrone at 25nM and infection with AdΔΔ at 25ppc, 50ppc and 250ppc decreased the levels to 0.69-, 0.61- and 0.48-fold, respectively, compared to untreated control and when compared to mitoxantrone and AdΔΔ alone (Fig. 47A-B). In combination with 50nM mitoxantrone and AdΔΔ at 50ppc p62/SQSTM1 levels decreased to 0.81-fold, but not with 250ppc that caused a 1.25-fold increase and 25ppc that caused no change, compared to untreated control, however, the levels of p62/SQSTM1 were increased compared to AdΔΔ and mitoxantrone at 50nM (Fig. 47A-B). Cells treated with mitoxantrone at 250nM also showed decreased levels of p62/SQSTM1 in combination with AdΔΔ at 50ppc and

250ppc at 0.29- and 0.19-fold, respectively, compared to untreated control and mitoxantrone and AdΔΔ. No change was observed in combination with 25ppc compared to untreated control; however, the levels of p62/SQSTM1 were increased compared to both mitoxantrone and AdΔΔ (Fig. 47A-B). Furthermore, cells treated with 500nM mitoxantrone had decreased levels of p62/SQSTM1 in combination with AdΔΔ-infection at 25ppc, 50ppc and 250ppc (0.43-, 0.31- and 0.21-fold respectively), compared to untreated control, mitoxantrone at 500nM and AdΔΔ alone at those doses. Overall, the combination of both agents decreased the levels of p62/SQSTM1. Taken together, mitoxantrone slightly induced autophagy flux, while the oncolytic mutant AdΔΔ attenuated drug-induced autophagosome formation (decreased LC3B-II/I ratios) in all combinations. This attenuation of autophagy-related activities was more potent with AdΔΔ than with AdE1A12S.

3.5.17 Activation of Akt is strongly induced by AdΔΔ and is further increased in combination with mitoxantrone in 22Rv1 cells.

The levels of p-Akt in response to AdΔΔ were assessed in 22Rv1 cells after infection with 10ppc, 25ppc, 50ppc, 250ppc 500ppc and 1000ppc (Fig. 48A). Increases of 15.6-, 37.4-, 32.3-, 58.8-, 47.3- and 22.4-fold respectively, were observed when compared to untreated control. Interestingly, induction of p-Akt was less with 1000ppc compared to 250ppc and 500ppc.

A)

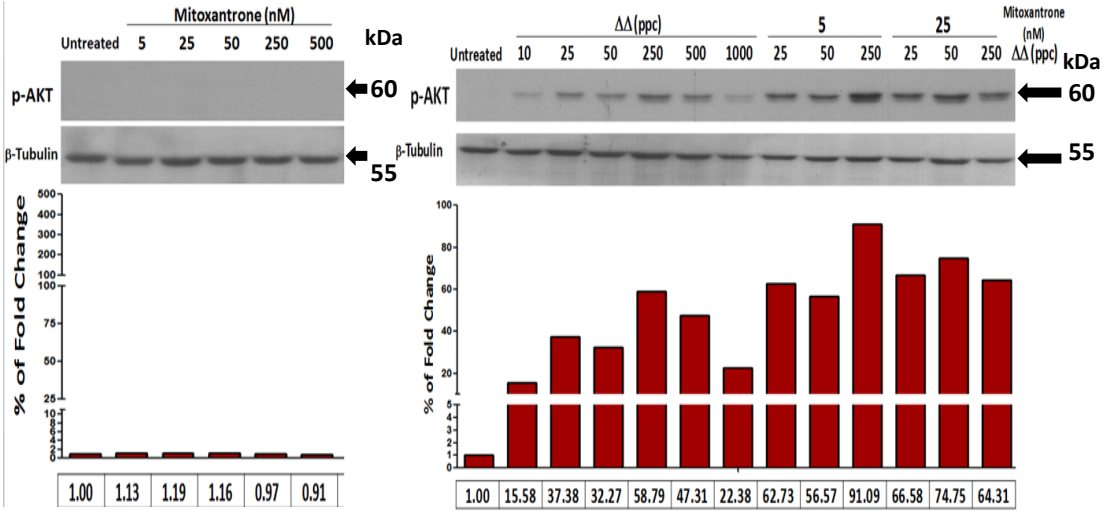

B)

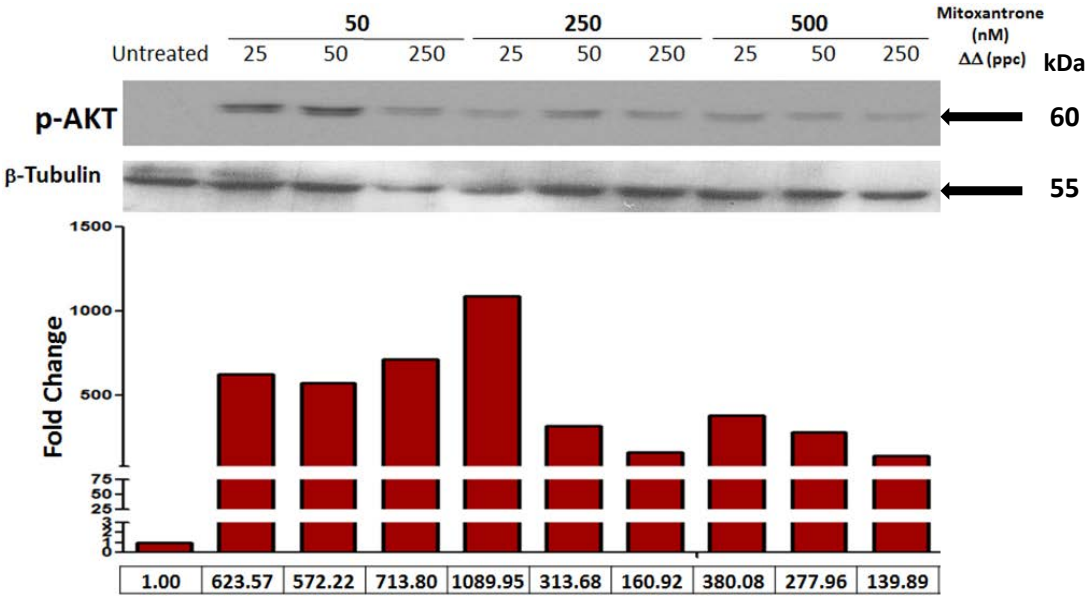

Figure 48. Changes in expression of the phosphorylated Akt in 22Rv1 cells at 48h post-treatment with mitoxantrone and/or infection with the AdΔΔ virus. **A)** 22Rv1 cells treated with mitoxantrone at increasing concentrations, 5nM - 500nM or infected with the AdΔΔ virus, at 10ppc - 1000ppc. Cells were also treated with staurosporine at 1nM and rapamycin 100nM as indicators of apoptotic and autophagic activity. **B)** 22Rv1 cells treated with mitoxantrone for 48h at 5nM, 25nM, 50nM, 250nM and 500nM in combination with the AdΔΔ virus at 25ppc, 50ppc and 250ppc. **A-B)** The intensity of the bands where quantified using Gene Tools version 4.01 (Synoptics Ltd, Cambridge, UK). Bands were normalized as the intensity of each band to the loading control (β-Tubulin). Fold change of each sample after being compared to untreated control, were the change of the untreated samples is 1.00.Blot representative of three repetitions

Although, AdΔΔ increased p-Akt levels it appeared to be less potent than AdE1A12S in activating p-Akt (Fig. 48A-B). The combination of AdΔΔ with mitoxantrone strongly enhanced p-Akt at all combinations compared to the virus alone, indicating that, despite that mitoxantrone does not induce p-Akt, the drug plays a role in potentiating AdΔΔ-induced p-Akt similar to the findings in PC-3 cells.

3.5.18 AdΔΔ and Mitoxantrone downregulated Bcl-2 both alone and in combination in 22Rv1 cells.

22Rv1 cells infected with AdΔΔ at 10ppc, 25ppc, 50ppc, 250ppc, 500ppc and 1000ppc showed decreased levels of Bcl-2; 0.80-, 0.84-, 0.68-, 0.57-, 0.47- and 0.20-fold, respectively, compared to untreated control (Fig. 49A). In addition, infection with AdΔΔ resulted in a dose-dependent decrease in the expression of Bcl-2 in

response to increasing concentrations of the virus. Mitoxantrone also decreased Bcl-2 levels (Fig. 49A).

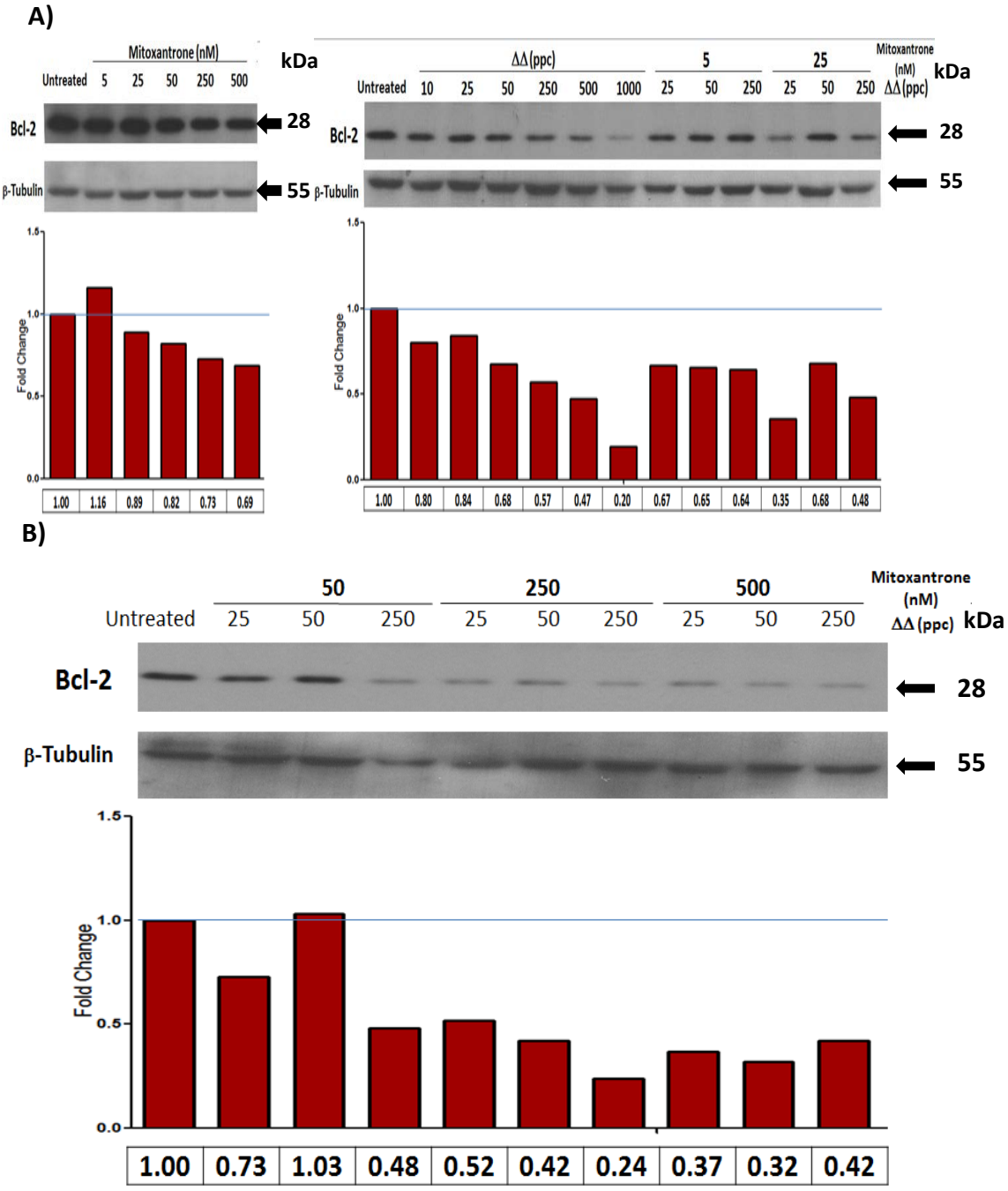

Figure 49. Changes in expression of Bcl-2 in 22Rv1 cells at 48h post-treatment with mitoxantrone and/or infection with the AdΔΔ virus. **A)** 22Rv1 cells treated with mitoxantrone at increasing concentrations, 5nM - 500nM or infected with the AdΔΔ virus, at 10ppc - 1000ppc. Cells were also treated with staurosporine at 1nM and rapamycin 100nM as indicators of apoptotic and autophagic activity. **B)** 22Rv1 cells treated with mitoxantrone for 48h at 5nM, 25nM, 50nM, 250nM and 500nM in combination with the AdΔΔ virus at 25ppc, 50ppc and 250ppc and additionally, with mitoxantrone with 500nM in combination with 50ppc, 250ppc. **A-B)** The intensity of the bands where quantified using Gene Tools version 4.01 (Synoptics Ltd, Cambridge, UK). Bands were normalized as the intensity of each band to the loading control (β-Tubulin)**.** Fold change of each sample after being compared to

untreated control, were the change of the untreated samples is 1.00. Blot representative of three repetitions

Expression of Bcl-2 was decreased in cells treated with 5nM mitoxantrone in combination with AdΔΔ at 25ppc, 50ppc and 250ppc to 0.67-, 0.65- and 0.64-fold, respectively, compared to untreated control and when compared to mitoxantrone alone (Fig. 49A-B). Cells treated with 25nM mitoxantrone in combination with AdΔΔ at 25ppc, 50ppc and 250ppc showed 0.35-, 0.68- and 0.48-fold decreases, respectively, compared to untreated control, mitoxantrone alone and when compared to AdΔΔ at those doses (Fig. 49A-B). Moreover, the expression of Bcl-2 also decreased in cells treated with 50nM mitoxantrone in combination with AdΔΔ at 25ppc and 250ppc showing 0.73- and 0.48-fold changes, respectively, compared to untreated control, and also compared to mitoxantrone alone (Fig. 49A-B). No changes were observed in combination with 50ppc. Furthermore, AdΔΔ at 25ppc, 50ppc and 250ppc combined with 250nM mitoxantrone decreased Bcl-2 levels to 0.52-, 0.42- and 0.24-fold, respectively, compared to untreated control, the values were decreased also when compared to AdΔΔ at those concentrations and to mitoxantrone alone (Fig. 49A-B). Finally, cells treated in combination with 500nM mitoxantrone and AdΔΔ at 25ppc, 50ppc and 250ppc decreased Bcl-2 levels to 0.37-, 0.32- and 0.42-fold, respectively, compared to untreated control (Fig. 49B). The combination at 500nM strongly decreased the levels of Bcl-2 when compared to mitoxantrone alone and AdΔΔ at similar doses. Overall, the expression of Bcl-2 was inhibited both by each agent alone and by the combination treatments. Taken together, both mitoxantrone and AdΔΔ contributed to downregulation of Bcl-2 levels that is likely to play a significant role in driving cell death in these cells.

3.5.18.a. Summary of immunoblotting data in 22Rv1 cells infected with AdΔΔ and/or treated with mitoxantrone:

- Infection with AdΔΔ potently inhibits autophagy flux both alone and in combination with mitoxantrone compared to untreated control.
- The treatment with mitoxantrone alone does not cause changes in the expression levels of p-Akt. In contrast, infection with AdΔΔ strongly increases the expression of p-Akt both alone and in combination with mitoxantrone compared to untreated control and mitoxantrone alone.
- Cells treated with mitoxantrone and/or infected with AdΔΔ show decreased levels of Bcl-2 under all conditions compared to untreated control.

4. Discussion

4.1 The role of the adenoviral early E1A proteins in combination treatments with cytotoxic drugs.

This work was aimed at identifying E1A regions involved in the sensitization of prostate cancer cells to chemotherapeutic drugs and to elucidate the mechanisms involved in the synergistic enhancement of cancer cell killing. The identification of cellular factors that may be responsible for sensitizing the cells could further enable targeting of these cellular pathways by novel drug combinations to improve current therapies for prostate cancer. In summary, through this work we found that the small adenoviral E1A12S protein was sufficient to sensitize both human and murine prostate cancer cells to mitoxantrone. Furthermore, the non-replicating mutants AdE1A12S, AdE1A1102 and AdE1A1108, potently sensitized all tested human PCa cell lines (PC-3, 22Rv1 and DU145) to chemotherapeutic drugs while AdE1A1104 did not. To explore different cellular functions that could uncover the underlying mechanisms of this sensitization, and to give more insight into previous studies on virus-drug interactions causing synergistic cell killing,[95] we investigated changes in the expression of cell cycle regulators. We observed that mitoxantrone induced cyclins A and B in PC-3 cells but not in 22Rv1 cells. In addition, the AdE1A12S and AdE1A1102 viral mutant enhanced mitoxantrone-induced p21 mRNA expression in PC-3 cells but not in 22Rv1 cells. We also demonstrated potent synergistic cell killing with mitoxantrone and mutants with intact E1A p300-binding regions in both PC-3 and 22Rv1 cells. The interaction of mitoxantrone with the replicating mutant *dl*1102 (intact p300-binding) resulted in synergy in both 22Rv1 and PC-3 cells. Furthermore, the replicating adenoviral mutants did not enhance cell killing in combination with mitoxantrone in normal human cells, and the *dl*1102 mutant potently reduced tumour growth in combination with docetaxel in PC-3 xenografts *in vivo*. These results demonstrate that binding of AdE1A12S to p300 is essential for the synergistic sensitisation of prostate cancer cells to mitoxantrone and docetaxel, showing high efficacy and potency in PCa cell killing but being safe to normal tissue. However, these results did not generate in depth mechanistic data and further studies were

necessary to investigate the cellular factors that were involved in the chemosensitization. To better address what cellular pathways might be involved in the sensitization, we employed an extensive miRNA array screen attempting to identify a broader network of potential factors responsible for the sensitization in PCa cells. We first analysed the combination of AdE1A12S with mitoxantrone under synergistic conditions in PC-3 cells and compared to the sum of each single agent treatment. The PC-3 cells were selected because of the high resistance to both virus and drugs when administered as single agents and the potent synergistic cell killing when combined. The miRNA data indicated that pathways regulating cell cycle progression, cell proliferation, survival and death played major roles in the synergistic cell killing. Key factors in these pathways were verified as regulated both by the non-replicating AdE1A12S and the replicating AdΔΔ and Ad5wt viruses in combination with mitoxantrone over time. Interestingly, mitoxantrone induced autophagic flux in both PC-3 and 22Rv1 cells while this induction was prevented in a dose-dependent manner by all viruses and appeared to contribute to the increased cell death.

Our previous results[95] demonstrated that the combinations of mitoxantrone and all tested AdE1A12S mutants (except AdE1A1104) induced changes in cell cycle progression, by increasing the G2/M cell population. In PC-3 cells, the expression of cyclins A and B was induced by mitoxantrone and did not change in combination with any of the AdE1A12S mutants. Both cyclins A and B are highly expressed during the G2/M phase[419,420] and mitoxantrone can induce cell cycle arrest in the G2/M phase because of its DNA-damaging effects.[421] Therefore, increased G2/M phase in PC-3 cells and upregulation of cyclins A and B was likely caused by mitoxantrone alone, since the viral mutants had minor effects alone and showed similar changes as cells infected with AdGFP. However, the variations in the cell cycle profile in response to the combination of mitoxantrone and the different AdE1A12S mutants,[95] specifically AdE1A1104, suggest that E1A-binding to cellular factors contribute to the increase in the G2/M population in the presence of drug. E1A promotes cell proliferation by releasing pRb-bound E2F1.[83] It has also been shown that pRb and CBP/p300 have common binding sites on E2F1; while E2F1-binding to pRb represses E2F1-mediated transcriptional activation, E2F1-binding to CBP/p300 stabilizes and stimulates its

activation.[386] The lack of a CBP/p300 binding to the AdE1A1104 mutant might diminish the role of E1A in cell cycle regulation, perhaps by the inability of this mutant E1A to mediate CBP/p300 interaction with E2F1 and at the same time E1A sequestering pRb. In contrast, the formation of the complex E1A-CBP/p300 (e.g. in AdE1A1102) might enable the binding and transcriptional activation of E2F1, promoting cell cycle.[422] We expected that these mechanisms would be reflected in the levels of cyclin expression. However, the expression patterns of cyclins A, B, E and D in PC-3 and 22Rv1 cells did not give further insights of the cell cycle regulatory mechanisms and the potential roles in chemosensitization in these cells. Even though changes in expression levels were observed, the implication of these changes were less clear and further investigation is required such as determination of the degree of activation (phosphorylation/dephosphorylation) of Cdk1 and Cdk2 proteins.[423]

The role of p21 in G1-arrest is well established, however, overexpression of p21 has also been reported to induce G2/M arrest in both p53-dependent and p53-independent pathways.[386] Therefore, we assessed the expression of this regulatory protein. However, the expression of p21 could not be detected in PC-3 cells by immunoblotting. Previous reports showed that p21 was expressed at low levels in PC-3 cells and was also suggested to be AR-regulated in prostate cancer cells.[424] Next, we investigated the expression of p21 mRNA in PC-3 cells. In cells infected with AdE1A12S alone, no effects on cell cycle regulators were detected by immunoblotting analysis. It was previously reported that both E1A13S and E1A12S (to a lesser degree) could induce cell cycle progression, and inhibit p21 expression by direct binding.[425] In contrast, mitoxantrone alone induced the expression of p21 mRNA through a p53-independent pathway in PC-3 cells ($p53^{-/-}$, $AR^{-/-}$). Surprisingly, the combination of mitoxantrone and AdE1A1102 or AdE1A12S further increased p21 mRNA levels in PC-3 cells. Although p21 mRNA levels do not necessarily translate into protein expression, it is plausible that G2/M arrest might be induced through a p53-independent pathway in PC-3 cells in which p21 may contribute even if only as a minor player.[426,427] Furthermore, the upregulation of p21 mRNA by the AdE1A12S mutants has also been reported recently in A549 cancer cells, although these cells express wild type p53.[428] It has also been demonstrated that p21 is p53-dependent and that activation of AR can promote this activation, an observation that was

previously reported for LNCaP cells ($p53^{+}AR^{+}$).[424] However, whether the induction of p21 by AdE1A1102 and AdE1A12S in combination with mitoxantrone contributes to cell sensitization remain unclear; therefore, further investigations will be necessary to conclusively interpret our observations in PC-3 cells.

In contrast, 22Rv1 cells infected with the AdE1A12S mutants showed increased expression of cyclin A and B, and similar increases were observed in response to AdGFP infection. The apparent non-specific virus-induced effects on cyclin expression suggest that E1A-independent viral mechanisms may also regulate cell cycle progression in 22Rv1 cells. However, in 22Rv1 cells treated with mitoxantrone the expression of cyclin A and B was decreased, which is in contrast to the effects observed in PC-3 cells. Moreover, cyclin D did not change in response to any of the non-replicating viral mutants or to mitoxantrone in either PC-3 or 22Rv1 cells. Cyclin E was induced by viral infection similar to both cyclins A and B. In 22Rv1 cells, the upregulation of cyclins A, B and E suggests a drive for cell cycle progression; nonetheless, the combination with mitoxantrone subsequently induced the downregulation of these proteins, an indication of cell cycle arrest possibly in a p53- and p21-dependent manner. It has been established that mitoxantrone can activate p53 in turn contributing to both cyclin A and B degradation which is facilitated by the upregulation of p21. The p21-dependent degradation of cyclin B is essential for G2/M arrest in response to DNA-damaging agents including mitoxantrone, which causes double strand breaks.[392] Despite an increase in the levels of p21 mRNA in PC-3 cells, the corresponding p21 protein expression could not be detected in these cells, possibly because of the absence of p53 as a main regulator of p21. In a p53-independent context E2F1 can regulate p21 at a transcriptional level stimulating the p21-promoter, however, in the presence of p53 it has been reported that p21 expression is strongly enhanced by a combined interaction of p53 with E2F1.[429,430] Therefore, in 22Rv1 cells the presence of p53 is likely to strongly contribute to the stimulation of p21 to regulate the increase in the G2/M cell population.[386,426,431,432] These data are complemented by the activation of p53 (data not shown) by mitoxantrone, although, phospho-p53 was also induced by AdE1A1102 and was not reflected in increased expression of p21. Nevertheless, the contribution of active phospho-p53 to G2/M arrest in 22Rv1 cells is evident. In summary, the responses to

the DNA-damaging drug mitoxantrone suggest that the regulation of the G2/M regulatory cyclins is dependent on the genetic background of the cells.

Another factor that could favour a DNA-damage response induced by mitoxantrone in 22Rv1 cells is the increased expression of topoisomerase II (data not shown), which is consistent with previously published data showing that E1A induces an increase in topoisomerase-II mRNA expression and protein synthesis.[131,433] This upregulation seems to increase the sensitivity of the cells to cytotoxic drugs targeting topoisomerase II.[433] The exact mechanism by which E1A up-regulates topoisomerase II is mainly unknown but it would be expected that E1A interacts with the transcription machinery to enhance topoisomerase levels and facilitate cellular protein synthesis and S-phase entry, to ultimately enable viral replication. However, the downregulation of topoisomerase II with mitoxantrone is consistent with previous reports showing that mitoxantrone inhibits topoisomerase II by inducing DNA-strand breaks and targets the enzyme for degradation.[67]

A G2/M arrest or delay of tumour cells frequently causes apoptotic cell death and the caspase effectors caspase-3 and caspase-7 may be activated. We have shown in 22Rv1 cells that the AdE1A12S-mutants induced sensitization of PCa cells in combination with mitoxantrone was reduced by a pan-caspase inhibitor.[95] Therefore, to verify the activity of caspase-3 and caspase-7 (data not shown) key effector caspases, we assessed the expression of caspase-3 and 7 in response to the combined treatments in PC-3 cells. However, I was unable to detect activation and expression of caspase 3 and 7, and could therefore not show the activity of caspases as part of the apoptotic response, however, cells treated with staurosporin induced the activation of caspase 3 while caspase 7 was not detected.

In order to determine if the differences in the sensitization to chemotherapeutic drugs and cell cycle progression in the PC-3 and 22Rv1 cells were due to sensitivity to infection alone, we attempted to use matched ovarian cancer cell lines; sensitive (Skov3) and less sensitive (Skov3ip1) to viral infection.[371-373] Previous reports demonstrated that Skov3 cells were more sensitive to viral infection than Skov3ip1.[372] However, in my dose-response infectivity assays I found that Skov3ip1 were less sensitive than Skov3. Nevertheless, cytotoxicity was not significantly

different between the two cell lines and was in stark contrast to previously published data.[371] It is possible that the similar responsiveness to virus and combination treatments was due to the absence in both Skov3 and Skov3ip cells of common cell death regulatory mechanisms such as p53 (not expressed in both cell lines) although, this does not explain the contradiction with the published data. While further testing of these cell lines using STR-profiling demonstrated that both cell lines were indeed Skov3, there was no marker for the reported sensitive versus insensitive cell line. In our study the regulatory mechanisms in these cells might be essential in the induction of sensitization to the combination of the drug and the viruses. Thus, we concluded that Skov3ip1 and Skov3 cells could not be used as a tool to investigate differences in chemosensitization in different cell lines (PC-3 and 22Rv1). The aim was to elucidate whether these differences were due to sensitivity to infection and/or additional mechanisms, and consequently other matched cell lines would be required but were not available at the time.

We previously demonstrated that the interactions of AdE1A12S with both mitoxantrone and docetaxel synergistically enhanced cell killing in PCa cells.[95] In order to determine the synergistic interactions in which E1A-deletion mutants (AdE1A-replicating and non-replicating) could best sensitize cells and enhance cell killing in combination with mitoxantrone, I set up synergy assays to determine combination indexes (CI). The results from the studies showed strong synergism between mitoxantrone in combination with AdE1A12S, AdE1A1102 and *dl*1102, but not with mutants with the E1A p300-binding region deleted in PC-3 cells. In 22Rv1 cells the combination of *dl*1102 with mitoxantrone showed the strongest synergy. The sensitization and synergy studies suggested that *dl*1102 was a strong candidate for consideration when improving current vectors, being the most potent and having the strongest synergistic effects in combination with drugs in both cell lines. These findings are in agreement with previous results where the *dl*1102 virus induced more sensitization in cells in response to chemotherapeutic drugs than other viral mutants.[95] These and previous results, contributed to our conclusion that the E1A-p300 binding region (amino acids Δ26-35) was essential for the sensitization of prostate cancer cells to mitoxantrone but not the E1A-p400 binding region (Δ48-60).

However, there is controversy in the literature about the role in drug-sensitization for the p300 and p400 binding sites on E1A.[76,96,100] Both regions have been reported to be responsible for sensitizing cancer cells to cytotoxic agents dependent on cell line. Our data strongly support the E1A-p300 binding region as essential for the sensitization of prostate cancer cells in combination with the currently used clinical cytotoxic drugs for prostate cancer patients; mitoxantrone and docetaxel. However, the mechanisms behind the synergistic interactions remain unclear and further studies will be designed to address these observations in future projects.

In order to generate more selective and potent oncolytic viruses, it was important to determine the selectivity of replication and the potency of the E1A deleted mutants in normal cells. To investigate the safety in normal cells, NHBE and PrEC cells where used to determine replication and virus-mediated sensitivity to chemotherapeutic drugs. The results showed that the replicating AdE1A oncolytic mutants *dl*1102 and *dl*1104 replicated to a significantly lesser degree than Ad5wt in NHBE cells while the mutants replicated as potently as wild type virus in prostate cancer cells. Importantly, the mutants did not sensitize normal cells (NHBE and PrEC cells) to mitoxantrone as previously observed for tumour-selective viruses in combination with other cytotoxic drugs.[131] In contrast, Ad5wt caused more than additive cell death in combination with mitoxantrone in both NHBE and PrEC cell. As previously shown the replication-selective oncolytic AdΔΔ did not enhance cell killing in combination with mitoxantrone in the normal cells.[118] The results demonstrated that *dl*1102, *dl*1104 and AdΔΔ had low cytotoxicity to normal cells. The *dl*1102 were as potent, safe and efficient as AdΔΔ in the PCa cells, in contrast, the *dl*1104 was less effective.

Furthermore, using an *in vivo* murine model with PC-3 xenografts (athymic mice), *dl*1102 in combination with docetaxel was significantly more potent than a similar combination with *dl*1104; prolonged time to tumour progression and reduced tumour growth were significantly higher when *dl*1102 was combined with docetaxel than with either agent alone. In addition, cell death might be induced through apoptosis, as previously shown for AdE1A1102 but remain to be determined in additional studies.

Our results show evidence of apoptotic cell death however, it is not completely clear which mechanisms are interacting and are being regulated to increase the apoptotic death in response to the combination treatments. Therefore, the identification of the mechanisms involved in the E1A-induced sensitization of prostate cancer cells to chemotherapeutic drugs remain elusive.[95] Among the main problems that are hindering the identification of virus-induced sensitization of PCa cells to chemotherapeutic drugs triggering cell death mechanisms are the binding of a plethora of cellular factors to overlapping binding regions within the E1A-protein with the majority having redundant functions.[83,84] Most of these factors are involved in regulation of cell death/survival and cell cycle pathways. Furthermore, to elucidate the mechanisms and pathways involved in synergistic cell killing, an extensive in depth study in each cell line would be required. Therefore, we employed a miRNA array screening that would enable us to identify a broader network of possible mechanisms involved in the sensitization of the PCa cells. We focused on the miRNA analysis in PC-3 cells because of the insensitivity of these cells to each single agents and the significantly synergistic enhancement of cell killing when virus and drug were combined. We postulated that the expression of miRNAs may be affected either by chemotherapeutic drugs and/or expression of E1A12S and that the combination-treated cells would induce a different pattern of miRNA expression.

Interestingly, most of the miRNAs that were upregulated in response to combination of AdE1A12S and mitoxantrone have been reported as downregulated in PCa, (including the miRNAs, hsa-let-7a/b/c/d/e/f/g, hsa-miR-125a-5p, hsa-miR-125b, hsa-miR-128, hsa-miR-15b, hsa-miR-16, hsa-miR-23a, hsa-miR-23b and hsa-miR-27a).[374,389-398] These miRNAs have been established as tumour suppressors contributing to apoptosis by increasing or inhibiting the expression of their respective target genes such as p53, caspase-3 and Bcl-2, or regulating the autophagy pathway through the PI3K/AKT/mTOR pathway.[192,195-199] In contrast, most of the miRNAs that were downregulated in our study were oncomiRs including hsa-miR-93/106b/25, hsa-miR-17-18a, -19a/b, -20a, and miR-92a. Thus, when tumour suppressor miRNAs are upregulated cell death is promoted and inversely, downregulation of oncomiRs also promotes cell death and inhibition of proliferation.[203,228,374,389-398] Some miRNAs were reported to be part of the same

clusters and to be jointly regulated, either by the same promoter and/or the same transcription factors.[231,235-239,388-390] Specific miRNA clusters have been implicated in both tumour suppression and tumour progression. In our study we identified the following miRNA clusters and families; the let-7 family including hsa-let-7d, hsa-let-7e, hsa-let-7f and hsa-let-7g; the hsa-miR-23 cluster including hsa-miR-23, -10, -24, -26, -27 and -30; the cluster 17-92 encoding hsa-miR-17-18a, -19a/b, -20a, and miR-92a; and hsa-miR-183-96-182 cluster including hsa-miR-15/16, hsa-miR-221/222, hsa-miR-93/106b/25, hsa-miR-let-7c/125b-1/99a and hsa-miR-100/7a/125b-2. In summary, the miRNA analysis predicted a role for regulatory factors implicated in cell death and survival pathways, such as autophagy and apoptosis signalling that were further investigated.

4.2 The role of Autophagy in the synergistic cell killing

In addition to the miRNA analysis, previous works in our team (Adam V, unpublished data and Thesis[434]) have shown that both mitoxantrone and docetaxel increased the expression levels of LC3B-II, an indicator of autophagy activation. It was also shown that the replication–selective AdΔΔ mutant could prevent these drug-induced increases in LC3B-II/I ratios.

Several miRNAs have been associated with functions in autophagy flux, and have important roles in autophagy regulation.[352,353,355] The relevant miRNAs related to autophagy that we identified in our screen were the clusters hsa-miR-17-92, hsa-miR-93/106b/25, hsa-miR-183-96-182 and hsa-miR-21 considered as oncomiRs and hsa-miR-128 as a tumour suppressor (Tables 20 and 22).

The oncogenic clusters hsa-miR-17, -20, -93, -106, hsa-miR-21 and hsa-miR-183 were demonstrated to negatively regulate autophagy flux by targeting p62/SQSTM1.[352,353,355] In addition, the hsa-miR-106a targets ULK1 and LC3B.[314,315,317] The hsa-miR-17-92 and Akt forms a positive-feedback loop and hsa-miR-21 were shown to inhibit PTEN enabling the activation of mTOR and consequently blocking autophagy.[390,410] Moreover, Akt has been described as a putative target for hsa-miR-183.[353,355,435,436] In our study, the clusters were induced by AdE1A12S-infection and

were supressed by treatment with mitoxantrone. The combination of AdE1A12S with mitoxantrone resulted in inhibition of these miRNA clusters. We hypothesised that though these changes in miRNA levels AdE1A12S might inhibit autophagy flux while mitoxantrone would induce both autophagy initiation and completion as previously reported for this drug in selected cell lines.[437] To verify our findings and investigate the overall effects on autophagy when virus and mitoxantrone were combined, we determine the levels of expression of the autophagy markers LC3B-II and p62/SQSTM1 in PC-3 and 22Rv1 cells.

In PC3 cells after 24h of treatment, increasing concentrations of mitoxantrone induced autophagy flux determined as increased LC3B-II/LC3B-I ratios and reduced levels of p62/SQSTM1 indicating that autophagosomes accumulated followed by p62/SQSTM1 degradation. In contrast, infection with AdE1A12S maintained basal levels of LC3B-II, although AdE1A12S also seemed to contribute to the degradation of p62/SQSTM1. These data suggest that AdE1A12S might prevent drug-induced autophagy flux. The blockage of autophagy by the AdE1A12S seemed to be overcome by increasing concentrations of the drug.

In PC3 cells the treatment with mitoxantrone for 48h induced higher levels of autophagy-flux than at 24h, observed as increased in LC3B-II/I ratios in a dose-dependent manner indicating accumulation of autophagosomes, in a dose-dependent manner and reduced levels of p62/SQSTM1. In contrast, the AdE1A12S virus impaired autophagy flux seen as decreased LC3B-II/I ratio and increased levels of p62/SQSTM1. However, the combinations of mitoxantrone and AdE1A12S, despite the increased ratio of LC3B-II/I, also induced the accumulation of p62/SQSTM1 suggesting that the virus impaired mitoxantrone-induced autophagy flux and that mitoxantrone was unable to overcome the viral inhibition of autophagy flux. When PC-3 cells were infected with Ad$\Delta\Delta$ for 48h there were no changes in LC3B-II/I ratios. Moreover, Ad$\Delta\Delta$ in combination with mitoxantrone decreased the drug-induced increases in LC3B-II/I ratios. In addition, Ad$\Delta\Delta$ increased the expression of p62/SQSTM1 and in combination with mitoxantrone the virus prevented the mitoxantrone-dependent decreases in p62/SQSTM1, although only at certain doses. Ad5wt reduced the LC3B-II to LC3B-I ratios, in a dose-dependent manner and increased the levels of p62/SQSTM1. In summary, mitoxantrone appeared to induce

complete autophagy flux, while AdE1A12S, AdΔΔ and Ad5wt potently inhibited the flux but only at certain doses in combination with mitoxantrone in PC-3 cells. The effects were more noticeable after 48h of treatment although, a trend was already observed after 24h. The replicative properties of Ad5wt and AdΔΔ might also have influenced the degree of autophagy activity by generating high cellular levels of virus through amplification resulting in more acute induction of cell death. The inhibition of autophagy by Ad5wt and AdΔΔ could serve as a mechanism used to block virus elimination, and allow completion of viral virus entry and replication in infected cells.[438] However, it has also been reported that adenovirus (wild type and a ΔCR2-deleted mutant) can induce autophagy and promote viral replication and oncolysis in glioma and lung cancer cell lines.[344,347] In another reports, the same viruses were demonstrated to promote cell survival in both glioma and ovarian cancer cell lines.[345,349] Moreover, previous reports have shown that autophagy-induction blocks virus infection and replication in sympathetic neurons and mouse embryonic fibroblasts.[438] In contrast, influenza-A virus and human immunodeficiency virus-1 HIV-1 (HSV-1) inhibit autophagy by blocking Beclin-1 or autophagosome formation in U937 and $CD4^+$ T-cells respectively.[439,440] Our results clearly demonstrate that the virus and E1A12S prevent or attenuated complete autophagic flux in PCa cells. The AdE1A12S might inhibit autophagy to promote only cell proliferation; since, the lack of a trans-activating domain does not allow the virus to replicate. Furthermore, the inhibition of autophagy and promotion of cell proliferative pathways might enable viral replication of Ad5wt and the oncolytic AdΔΔ, although only at certain doses of mitoxantrone. The differences between pro- or anti-autophagy responses in different models might indicate that the outcome is virus and cell type dependent.

Our preliminary results were in agreement with our findings from the miRNA analysis, indicating that in PC-3 cells the treatment with mitoxantrone downregulated the oncomiRs and autophagy inhibitors hsa-miR-17-92, hsa-miR-93/106b/25, hsa-miR-183-96-182 and hsa-miR-21. Thus, mitoxantrone promoted the induction of autophagy flux. In contrast, AdE1A12S induced upregulation of these miRNAs and likely impaired autophagy initiation and/or flux.

In 22Rv1 cells, mitoxantrone induced the accumulation of LC3-II only at high cytotoxic concentrations after 48h, accompanied by decreased p62/SQSTM1 levels. Thus, only the highest concentrations of mitoxantrone (still below the EC_{30} values), might induce autophagy in these cells in contrast to findings in PC-3 cells where even low doses of drug induced autophagy. When infected with AdE1A12S a slight dose-dependent decrease in LC3B-II/I ratios and also in the p62/SQSTM1 levels suggest that autophagy activity was likely prevented with no autophagosome formation. It is possible that the decreases in p62/SQSTM1 levels were caused by potent apoptosis-induction in these cells in response to AdE1A12S-expression. Previous reports demonstrated that p62/SQSTM1 is also degraded by caspases and non-autophagy ubiquitination events targeting p62/SQSTM1 to the proteasome.[320] The combination of AdE1A12S with mitoxantrone resulted in attenuation of mitoxantrone-induced autophagy at certain combination-ratios. However, the attenuation was less potent than in PC-3 cells and will require further investigations to generate conclusive data. Infection of 22Rv1 cells with the replicating AdΔΔ resulted in strong depletion of p62/SQSTM1 and decreases in LC3B-II/I ratios. Thus, both viruses seemed to induce a stronger response than mitoxantrone potently preventing autophagy. A possible mechanism for the viral attenuation of autophagy is the strong activation of Akt both in response to the viruses alone and in combination, which would result in activation of mTOR and inhibition of autophagy.

Again, results from these preliminary protein expression studies appeared to be in agreement with our findings from the miRNA analysis, indicating that in PC-3 cells the treatment with mitoxantrone downregulated the oncomiRs and autophagy inhibitors hsa-miR-17-92, hsa-miR-93/106b/25, hsa-miR-183-96-182 and hsa-miR-21 resulting in increased autophagy flux. In contrast, AdE1A12S induced upregulation of these miRNAs. Moreover, the combination of all viruses with mitoxantrone decreased the drug-induced autophagy flux although, at increasing concentrations of mitoxantrone the drug-induced effects dominated. It is likely that viral replication in cells infected with Ad5wt or AdΔΔ could mask the effects on autophagy once the viral amplification reached a certain level, rather causing cell lysis and death than inhibition of autophagy survival mechanisms. Despite the differences in gene expression and viral replication, both AdE1A12S and AdΔΔ had similar effects in

combination with mitoxantrone, suggesting that E1A might play an important role in these mechanisms. Another miRNA that was identified to target the autophagy and the apoptotic pathways is the tumour suppressor hsa-miR-128; when overexpressed it inhibits PCa cell invasion.[400] In addition, the overexpression of hsa-miR-128 was shown to inhibit p-Akt leading to activation and increase in the acetylated and normal forms of FOXO3a enabling the transcription of target genes that contribute to the induction of apoptosis.[441] The hsa-miR-128 was shown to induce apoptosis through both p53-dependent and -independent pathways by direct regulation of p53 upregulated modulator of apoptosis (PUMA).[441] Furthermore, the activation of FOXO3a promotes apoptosis by inhibiting the oncomir hsa-miR-21 that abrogates FasL translation.[407] In our study, hsa-miR-128 and hsa-miR-21 were up- and downregulated respectively in response to the combination treatments, suggesting that this regulatory pathway might contribute to cell killing. Therefore, the targets for hsa-miR-128 seemed to be relevant for analysis. We first analysed the expression of p-Akt in PC-3 cells treated for 24h with mitoxantrone; a dose-dependent decrease in p-Akt was observed. Infection with AdE1A12S inhibited p-Akt at low concentrations, and at higher concentrations basal levels of p-Akt were retained or increased. In contrast, the combination of AdE1A12S with mitoxantrone strongly increased p-Akt. These results suggest that AdE1A12S blocks the mitoxantrone-mediated inhibition of p-Akt and promotes p-Akt activation. In spite of mitoxantrone-mediated attenuation of p-Akt when administered alone, in combination with AdE1A12S, mitoxantrone seemed to potentiate the activation of p-Akt. At 48h p-Akt was still inhibited by mitoxantrone although to a lesser degree than after 24h, indicating that mitoxantrone-mediated inhibition might be strongest early after treatment and subsequently decline. The infection with AdE1A12S for 48h greatly increased the levels of p-Akt, suggesting that virus-induced p-Akt might be triggered at early stages and increase over time. The combination of AdE1A12S and mitoxantrone increased the levels of p-Akt at low concentrations of mitoxantrone however, the effect was not dose-dependent and at higher concentrations of mitoxantrone the activation was less obvious. These results, suggest that the potency of AdE1A12S to increase the levels of p-Akt decrease over time, being abrogated over time but only at high concentrations of mitoxantrone. The infection with Ad$\Delta\Delta$ also

induced a dose-dependent increase in p-Akt levels. Moreover, similarly to AdE1A12S, AdΔΔ in combination with low doses of mitoxantrone increased the levels of p-Akt, and with increasing doses of mitoxantrone the AdΔΔ-dependent increases of p-Akt were impaired.

In 22Rv1 cells no basal levels of p-Akt were detected and the treatment with mitoxantrone did not cause any detectable change. However, infection with AdE1A12S induced a strong dose-dependent increase in p-Akt. In addition, the combination of AdE1A12S with mitoxantrone increased the levels of p-Akt at all combinations compared to untreated control. Moreover, virus-induced increases in p-Akt were potentiated in combination with mitoxantrone, as observed in PC-3 cells at 24h. However, in PC-3 cells at 48h only AdE1A12S in combination with low doses of mitoxantrone increased the levels of p-Akt, whereas in 22Rv1 the levels of p-Akt were increased with all combination ratios. These results suggest that in both PC-3 and 22Rv1 cells mitoxantrone does not cause phosphorylation of Akt at ser-473 although the drug might cause deregulation of other factors enabling AdE1A12S to potently induce p-Akt. Furthermore, infection with AdΔΔ also increased p-Akt levels, although, AdΔΔ was not as potent as AdE1A12S. The combination of AdΔΔ with mitoxantrone strongly enhanced p-Akt at all combinations compared to the virus alone, indicating that, despite that mitoxantrone did not induce p-Akt the drug could potentiate AdΔΔ-dependent increases in p-Akt. Thus, the increased hsa-miR-128 expression and the downregulation of p-Akt seemed to correlate when cells were treated with mitoxantrone. Taken together, Akt is a known negative regulator of autophagy by inducing the activation of mTOR. Therefore, the induction of p-Akt would result in the inhibition of autophagy.[265,301] Moreover, previous reports have shown that adenovirus induce the Akt/mTOR pathway in glioma cells.[349] In agreement with the literature, we demonstrated that all tested adenoviruses (AdE1A12S, AdΔΔ) induced p-Akt. As expected the induction of p-Akt with all viruses alone and in combination (except at high drug doses) correlates with the inhibition of autophagy flux markers. However, despite that Botta and colleagues[349] showed that adenovirus can induce Akt/mTOR-pathway in agreement with our results, they also reported the induction of autophagy in glioma cell lines. These contrasting results

might be due to the genetical background of the cell lines. Nonetheless, other reports showed that adenovirus-5 vectors (with E1 and E3 regions deleted) promotes cell survival mechanisms by activating the PI3K/Akt/mTOR signalling pathway and that re-stimulation of this pathway may have saturating effects, sensitizing HT-29 cells colon carcinoma cells to TNF.[442] It was suggested that virus-induced cell survival mechanism might be counterproductive undermining the cells capacity to overcome the cytotoxic stimulus.[442] In our study, similar results in PCa cells with the combinations at low doses of mitoxantrone make plausible that this mechanism might also contribute to increased cell killing. However, the oncolytic adenovirus used in our study strongly induced cell killing and might be unable to saturate the mechanism before inducing cell death. Nevertheless, this mechanism might be a relevant alternative to be explored under our chemosensitizing conditions.

Furthermore, p-Akt induces FOXO3a phosphorylation blocking its activation and translocation to the nucleus. In contrast, hsa-miR-128 inhibits p-Akt-dependent phosphorylation of FOXO3a and inhibits the deacetylase sirtuin-1 (SIRT-1), promotes FOXO3a acetylation and enables FOXO3a to translocate to the nucleus.[441] Therefore, if the regulatory mechanism driven by hsa-miR-128 correlates with mitoxantrone-dependent attenuation (or no effects) of p-Akt this could lead to the induction of acetylated FOXO3a and increase total levels of FOXO3a leading to increased apoptosis.[441] In melanoma, the transcription factor FOXO3 inhibits cell migration by downregulating hsa-miR-182, in contrast FOXO3 is impaired when the hsa-miR-182 is overexpressed.[408] Additionally, the levels of FOXO3a and hsa-miR-182 are inversely correlated, in our results hsa-miR-182 was inhibited by the combination, thus inhibition of hsa-miR-182 might favoured FOXO3a expression. Another highly expressed miRNA in cancer progression is the hsa-miR-21; its overexpression has been shown to induce cell proliferation in response to androgen-stimulus in PCa. In contrast, the inhibition of hsa-miR-21 facilitates the induction of apoptosis triggered by FOXO3a by repressing hsa-miR-21.[406,407] Therefore, we assessed the expression of FOXO3a, and found that AdE1A12S induced p-Akt 24h after infection as expected,[441] whilst FOXO3a was downregulated by the virus (Fig. 55A). However, the downregulation of p-Akt in response to mitoxantrone did not cause the expected increase in total FOXO3a and in contrast showed a trend towards decreasing levels of

FOXO3a. The combination of virus and mitoxantrone did not cause detectable changes in the expression of FOXO3a. It is known that the inhibition of FOXO3a by p-Akt promotes the translocation of FOXO3a to the cytoplasm where it accumulates and is retained by the protein 14.3.3 through direct binding.[443] To determine the involvement of 14.3.3 in response to the treatments we assessed the levels of expression of 14.3.3. We observed that at the 24h and 48h time-points the virus increased the levels of 14.3.3 while mitoxantrone decreased the levels both alone an in combination with virus (Fig. 55-56). Although, further verification is necessary, the increased expression of 14.3.3 induced by the virus could be due to the accumulation of FOXO3a in response to Akt phosphorylation. However, it is known that 14.3.3 is a carrier protein that translocates phosphorylated proteins from the nucleus to the cytoplasm, the exact function in regard to virus and mitoxantrone treatments in our study remain unclear. After 48h of treatment FOXO3a expression was not affected by mitoxantrone. Surprisingly, at high viral doses the levels of FOXO3a were elevated (Fig. 56). The combination of mitoxantrone with AdE1A12S did not affect the expression of FOXO3a at any combination. These preliminary results suggest that FOXO3a at this time point might not be essential in the mechanism of cell death induced by the combination treatments or that FOXO3a or its role might not be an important factor under these conditions, although more conclusive experiments are required. However, these mechanisms (FOXO3a, 14.3.3 and p-Akt) regulated through hsa-miR-128 might contribute to autophagy and apoptosis; it remains unclear and would require more experiments to validate the involvement of hsa-miR-128.

4.3 Autophagy-apoptosis cross-talk

Numerous reports have demonstrated the presence of complex cellular networks that support cross-talk between autophagy and apoptosis.[265,298,444] Our previous findings indicate that the mechanisms of cell death in response to the combination treatments strongly promoted apoptosis. However, the results were not conclusive and as demonstrated in this thesis autophagy also was found to play a role in the cell death/survival mechanisms. As a result of the combination treatments, we observed

that many upregulated miRNAs coincidentally are reported to be tumour-suppressors and important regulators of the apoptotic pathways. In contrast most downregulated miRNAs are considered as oncomiRs. The cluster miR-106b-25 has been shown to be oncogenic in prostate cancer.[445] The hsa-miR-106b-25 cluster promotes cell proliferation and tumour progression by targeting and inhibiting PTEN, E2F1 and p21/WAF1.[212,226,404,446,447] It was reported in PCa cells, overexpression of hsa-miR-106b induced radiation-therapy resistance, promoting cell-cycle progression and cell proliferation.[445] The hsa-miR-106b-25 cluster inhibits Bim and E2F1-induced apoptosis.[445] Moreover, overexpression of the hsa-miR-106b-25 and hsa-miR-17-92 clusters have been shown to regulate TGFβ signalling by preventing cell cycle arrest and apoptosis in gastrointestinal cells.[405] Another example is the amplification of the hsa-miR-17 cluster that is associated with malignant lymphomas.[288] The hsa-miR-17-92 cluster can also inhibit apoptosis via the inhibition of PTEN through the hsa-miR-19 component, inducing tumour progression.[410]

Overexpression of hsa-miR-1246 a target of the p53 family (H1299 cells), was shown to induce apoptosis by targeting and downregulating DYRK1A (Down-syndrome marker) in U2OS cells.[374] The overexpression of hsa-miR-23b has been shown to target Src kinase and Akt, decreasing tumour growth in nude mice.[393] In an orthotopic xenograft murine model of hepatocellular carcinoma the inhibition of hsa-miR-191 reduced tumour size while *in vitro* cell proliferation was inhibited and apoptosis was induced.[409] Overexpression of the hsa-miR-23a/27a/24-2 cluster has been shown to trigger endoplasmic reticulum stress (ER stress) inducing apoptosis in HEK293T cells.[389] Moreover, cell proliferation induced by Myc is regulated through the repression of hsa-miR-23a and hsa- miR-23b.[401] In contrast, in renal cancer the reduction of hsa-miR-23b was associated with increased expression of PTEN, although a reduction of PI3K and total Akt was also observed.[399] In A549 cells, downregulation of hsa-miR-24 has been shown to inhibit cell growth.[288] The hsa-miR-221/222 have been demonstrated to target and inhibit the tumour suppressor p27, inducing cell proliferation in PC-3 cells, while knock-down of hsa-miR-221/222 increased clonogenicity.[291] In addition, overexpression of hsa-miR-221/222 and the downregulation of hsa-miR-23b/27b are considered as markers for a poor prognosis in metastatic castrate-resistant PCa.[384]

Members of the let-7 family are known to cause tumour suppression, their downregulation or deletion has been associated with breast, lung, ovarian and prostate cancer.[222,396] The downregulation of let-7 promotes cell proliferation and increased clonogenicity contributing to tumour progression, and let-7 has been shown to be downregulated by Myc.[448] In contrast, overexpression of let-7 induces cell cycle arrest at the G1/S-phase by inhibition of E2F2, CCND2, and Enhancer of Zeste homolog 2 (EZH2). Additionally, the let-7 family was reported to induce tumour suppression by inhibiting cell proliferation in PCa models both *in vivo and in vitro.*[395,449] Let-7 is known to target Myc, E2F2, CCND2 and Lin-28, and the downregulation of let-7 results in tumour progression while overexpression correlates with the downregulation of Myc, E2F2, CCND2 and Lin-28 resulting in tumour suppression of PCa. In our study, all the let-7 family members were upregulated (except let-7i), in response to the combination treatments, which would indicate that Myc, E2F2, CCND2 and Lin-28 are be important regulatory factors that play a role in the synergistically enhanced cell killing in response to the combination treatments. Further investigations to determine changes in the expression levels of these factors would be an interesting aspect of the project to pursue in future work.

Additionally, it is important to point out that hsa-let-7c is part of the hsa-miR-99a/let7c/125b cluster, which has been shown to regulate AR expression through the inhibition of Myc.[34] However, hsa-miR-99a was not verified as differentially regulated in our second study. The hsa-miR-99a/let7c/125b cluster has also been shown to be downregulated in the presence of androgens. In contrast, in the absence of androgens and AR-activation the cluster is induced resulting in decreased cell proliferation.[450,451] The hsa-miR-125b has been shown to target and down-regulate Mcl-1, Bcl-w and interleukin (IL)-6R reducing the mitochondrial membrane potential and inducing pro-caspase-3 cleavage, resulting in apoptosis, mainly by the inhibiting of members of the Bcl-2 family.[391] In PCa cells (PC-3) it was shown that hsa-miR-125b contributes to tumour progression by downregulating $p14^{ARF}$ and inducing cell proliferation.[452] However, changes in expression levels of the entire cluster in response to cytotoxic agents were not explored in the same study. In our study hsa-miR-125b was upregulated in response to the combination treatment in addition to let-7c and let-7a. Thus, the contribution of hsa-miR-125b and let-7c might be a

consequence of the entire cluster rather than the sole expression of one miRNA. Nonetheless, the expression of one miRNA could also be determinant for the expression of the cluster. In summary, in our study the Let-7 family and the hsa-miR-99a/let7c/125b cluster might contribute to cell killing although mainly in response to mitoxantrone rather than AdE1A12S.

The hsa-miR-15/16 cluster, which is frequently downregulated in PCa,[225] is a tumour suppressor cluster that contributes to apoptosis by targeting and downregulating Bcl-2, CCND1 and WNT3A in PCa thereby inhibiting cell survival and proliferation. Interestingly, Myc induces the downregulation of this cluster.[397,453,454] In our study, we found that Bcl-2 levels were slightly increased in PC-3 cells infected with AdE1A12S for 24h and this increase was enhanced in combination with mitoxantrone. In contrast after 48h the levels of Bcl-2 were decreased by the combination. Our results suggest that the upregulation of the let-7 family contributes to the induction of the hsa-miR-15/16 cluster through inhibition of Myc. The increase in hsa-miR-15a/16 followed by the decrease in the levels of Bcl-2 might be further regulated by mitoxantrone-induced DNA-damage response that targets E2F1, which is also a direct regulator of hsa-miR-15a/16. Taken together, this indicates that in the absence of viral replication the response might be strongly regulated by mitoxantrone.[455,456] In PC-3 cells infected with AdΔΔ and Ad5wt, the combination treatments caused increased levels of Bcl-2, which was strongest with AdΔΔ. The increased expression of Bcl-2 might be because viral replication could potentially induce an anti-apoptotic response in the cells, at least at earlier time-points (<48h). However, in 22Rv1 cells the combinations of mitoxantrone with either AdE1A12S or AdΔΔ caused a decrease in of Bcl-2 levels, indicating that the genetic background of the cell is also important. Moreover, previous reports have shown that the phosphorylation of Bcl-2 at ser-70 is necessary for full anti-apoptotic activity and that it requires multi-phosphorylation for the induction of autophagy, resulting in the release of Beclin-1 and thus inducing autophagy.[457,458] However, PC-3 (24h) and 22Rv1 (48h) cells infected with AdE1A12S did not show expression of phospho-Bcl-2 (not shown), indicating no activation of the anti-apopototic response at any conditions, although more experiments are needed to conclusively elucidate these preliminary results.

In addition, hsa-miR-107 is part of a group of miRNAs located next to the hsa-miR-15/16 gene cluster and was reported to be upregulated by p53 inhibiting HIF-1 in colon cancer cells, although, these findings have not been validated in PCa.[225,459] The hsa-miR-107 also has high homology with hsa-miR-103 with differences only in one nucleotide.[402] The expression of hsa-miR-103 has been reported as deregulated in PCa,[385] however, in response to the combination treatments the expression remained downregulated. The contribution of both hsa-miR-107 and hsa-miR-103 to cell killing in this study, remain unclear and will require more studies to determine their role in response to the combination treatments.

Nonetheless mitoxantrone is known to induce DNA double strand breaks that could trigger the DNA damage response, induce apoptosis and G2/M arrest. To explore whether DNA-damage was part of the mechanism and if mitoxantrone in combination with the virus increased this damage, we assessed the expression of p-H2AX as a marker for DNA-damage repair response in PC-3 cells.[460] While the infection with AdE1A12S did not activate p-H2AX under our conditions (24h), p-H2AX was induced by mitoxantrone (Fig. 55). Remarkably, the combination of mitoxantrone with AdE1A12S did not affect the activation of p-H2AX and maintained the mitoxantrone-dependent induction of p-H2AX demonstrating activation of the DNA-damage response. The induction of apoptosis by the DNA-damage response is mostly dependent on activation of p53 however induction of cell death in response to DNA-damage can also be caused by p73, a member of the p53-family.[461,462] PC-3 cells are $p53^{-/-}$ and consequently it was important to determine if p73 was involved in the apoptotic response to the combination treatments. Preliminary results in PC-3 cells infected with AdE1A12S indicate that p73 expression was downregulated compared to basal levels (Fig. 56). Moreover, the combination of mitoxantrone with AdE1A12S seemed to decrease p73 levels (Fig. 56). Unfortunately, it was not possible to determine the exact role of mitoxantrone in the expression of p73 due to contradictory results, but it was clear that the virus reduced the levels of p73. Therefore, more conclusive results are needed to determine the role of p73 in response to the treatment combinations.

Additionally, we identified hsa-miR-361-5p, hsa-miR-423-5p, hsa-miR-1826 and hsa-miR-107 as upregulated in response to the combination treatments in our study.

These miRNAs are deregulated in different types of cancer, although none of them has been reported and validated in PCa. Similarly, there is limited information available in the literature regarding hsa-miR-1268 and hsa-miR-1275 and their role(s) is currently incompletely understood. It would therefore be important to determine their function in PCa since like other tumour suppressor miRNAs they were upregulated by the combination treatments. Importantly this work is to my knowledge the first to report on the involvement of these miRNAs in PCa. However, more studies are necessary to validate these initial data and to explore the functional implications.

Taken together, my work presented in this thesis is to the best of my knowledge the first analysis in prostate cancer cells, which demonstrates that binding of AdE1A12S to p300 is essential for the sensitisation of prostate cancer cells to mitoxantrone and docetaxel. Our preliminary results indicate miRNA-driven regulation of cellular pathways in response to the combination of AdE1A12S and mitoxantrone. Furthermore, despite viral induction of cell survival mechanisms, the viruses might also contribute to cell killing complementing mitoxantrone-induced cell death (DNA-damage response-dependent cell death), and favouring enhanced tumour-suppressing signals where the inhibition of autophagy might play a complementing role. Further studies should be aimed at investigating in depth the specific interplay of these mechanisms to develop a better understanding of adenovirus-dependent enhancement of mitoxantrone-mediated apoptotic cell killing and identification of novel therapeutic targets or therapies.

4.4 Summary of this thesis:

- We demonstrate that the E1A-p300 binding region is essential for the synergistic sensitisation to cell killing in combination with the chemotherapeutics mitoxantrone and docetaxel in prostate cancer cell lines.
- We show that the oncolytic mutants *dl*1102 and *dl*1104 potently contribute to prostate cancer cell killing both *in vitro* and *in vivo*.

- The oncolytic mutants *dl*1102 and *dl*1104 are replication-selective with minimal toxicity in two normal cell types.
- Our results indicate that the combination of AdE1A12S and mitoxantrone regulates the expression of miRNAs by downregulating oncoMIRs and upregulating tumour suppressor miRNAs in PCa cells, ultimately affecting the regulation of several key pathways including apoptosis, cell proliferation and autophagy.
- We show that the let-7 family, the hsa-miR-23 cluster (hsa-miR-23, -10, -24, -26, -27 and -30), the 17-92 cluster (hsa-miR-17-18a, -19a/b, -20a, and miR-92a) and the hsa-miR-183-96-182 cluster (hsa-miR-15/16, hsa-miR-221/222, hsa-miR-93/106b/25, hsa-miR-let-7c/125b-1/99a and hsa-miR-100/7a/125b-2) are potentially involved in the miRNA-driven regulation of cell pathways (apoptosis, cell proliferation and autophagy) in response to the combination treatments.
- Our data demonstrate that the changes in expression levels of selected miRNA-targets correlate with the changes in miRNA expression levels.
- We show that while mitoxantrone induces autophagy flux, the viral mutants AdE1A12S, Ad$\Delta\Delta$ and Ad5wt inhibit the autophagy flux both alone and in combination with mitoxantrone in PC-3 and 22Rv1 cells.
- All three viruses AdE1A12S, Ad$\Delta\Delta$ and Ad5wt induce increased expression of p-Akt promoting cell proliferation, while mitoxantrone inhibits this activity in PC-3 and 22Rv1 cells.
- The observed changes in expression of Bcl-2 levels are likely dependent on the replicative properties and promotion of S-phase in response to the viruses

5. Future directions

To further delineate the cellular mechanisms that are activated in response to the viruses and mitoxantrone both alone and in combination including apoptosis and autophagy that appear to be regulated by changes in miRNA processing, it will be important to determine how inhibition or activation of specific miRNAs occurs. For example, are there changes in activity of miRNAs-transcription factors or processing enzymes?.[463,464] The miRNA-regulated pathways that were repressed or activated in our study in response to the different stimuli have been reported to be tightly regulated by transcription factors and miRNAs in a feed-forward loop interaction.[465] Of the miRNAs analysed in this study the majority were regulated by the transcription factors Myc and E2F1.[463,466,467] Both Myc and E2F1 are key regulators of cell death and survival pathways in the absence of p53, and mutually regulated; both Myc and E2F1 can trigger cell survival or apoptosis depending on the stimulus (Fig. 50). Moreover, Myc is the main regulator of oncomiRs while E2F1 mostly regulates tumour suppressor miRNAs.[468-471] E2F1 is a key factor in the DNA-damage response pathway promoting apoptosis and DNA-damage induced autophagy. The DNA-damage response is mediated by ATM/ATR, inducing down-stream activation of E2F1 (Fig. 50).[472-476] Moreover, it has been reported that E2F1 induces cell death in a p53-independent pathway in PCa cells (Fig. 50).[477] Furthermore, E1A and specifically E1A12S have been reported to contribute to the activation and p300-mediated stabilization of E2F1 (Fig. 50).[83,422]

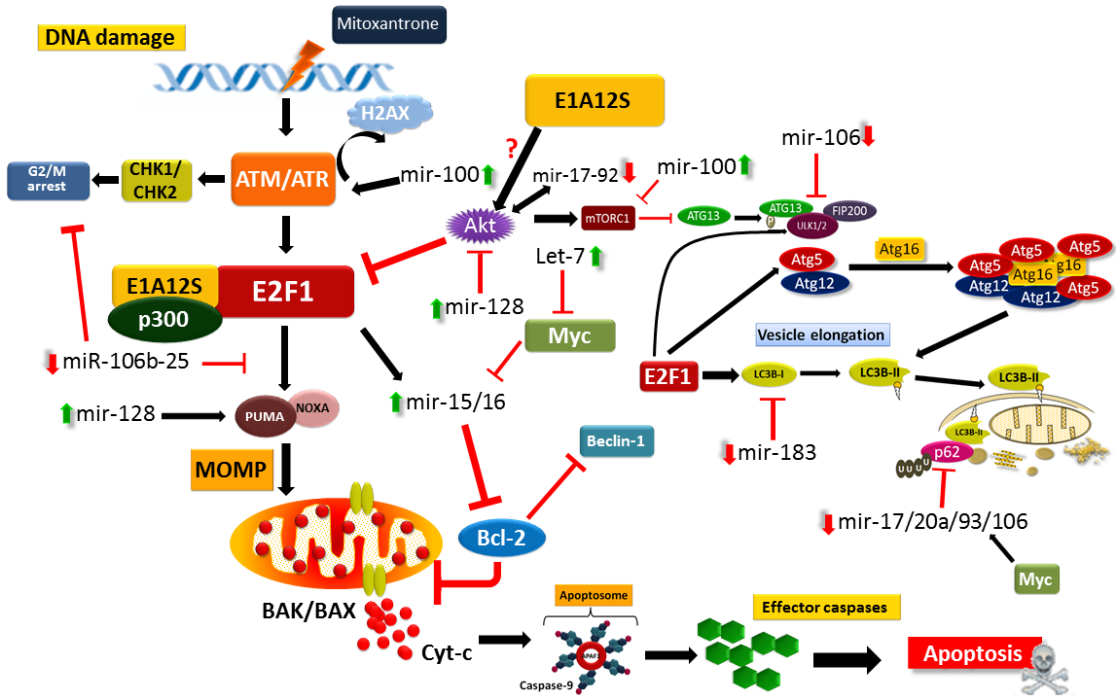

Figure 50. Potential cell death mechanisms involved in the synergistically increased cell killing in response to the combination treatments. The combination of mitoxantrone and AdE1A12S induces the activation of tumour suppressor miRNAs and the downregulation of oncomiRs. Despite mitoxantrone-induced cell death being partly opposed by AdE1A12S, there is an additional pro-apoptotic stimulus driven by E1A12S that contributes to tilting the balance towards enhanced cell killing, in which both apoptosis and autophagy are intimately linked. Based on the results in this thesis and previously published reports [83,203,228,288,353,355,390,395-398,400,410,422,427,436,441,448,450,451,453,455,460,463-467,469-471,473-476,478,479].

Taken together, these reports in addition to our previous results and the findings presented in this thesis suggest that E1A-dependent stabilization of E2F1 is a key factor in the E1A mediated sensitization of prostate cancer cells to the mitoxantrone-induced DNA-damage response. Thus, it is important to determine the involvement of the miRNA-transcription factors E2F1 and Myc in the regulation of autophagy and DNA-damage induced apoptosis and autophagy in response to the combination treatments and also to validate the involvement of the identified miRNAs within these cross-talk pathways. Therefore, to address these issues our future plans are:

- To assess the response of both E2F1 and Myc under chemosensitizing conditions. The expression of E2F1 will be verified in PC-3 cells infected with AdE1A12S, treated with mitoxantrone and both agents in combination by immunoblotting.
- To test the expression of both E2F1 and Myc with the potent viruses AdΔΔ and *dl*1102 to verify the regulation of E2F1 and Myc in response to these

viruses and to validate if AdE1A12S could be the sole core of the mechanism and if this could be extrapolated to the replicating viruses.

- To determine the role of E2F1 and Myc in 22Rv1 cells and test if the inhibition of p53 in 22Rv1 cells changes the regulation of E2F1 to determine if the modulation of these transcription factors is a p53-dependent and/or -independent response.
- To verify the involvement of E2F1 in response to the combination treatments, which will further be used to confirm the regulation of downstream signalling of the DNA-damage response pathway. Specifically the BH3-family members BIM, PUMA and NOXA which are known to be pro-apoptotic targets of E2F1, will be explored for involvement in the response to the combination treatments under chemosensitizing conditions by downregulating each factor by siRNA targeting.[480]

Our results suggest the downregulation of autophagy in response to the combination treatments however, the role and contribution of autophagy to cell death in response to the combination treatments remain unsolved. Therefore, verification of the role of autophagy in cell death will be necessary. Thus, it will be interesting to dissect the autophagy flux in response to the combination treatments in more detail.

- To dissect dynamic autophagy-flux the use of known autophagy inhibitors would add more variables to our current model, while the use of siRNAs to down-regulate key markers of autophagy might be a better solution, by targeting of Beclin-1, Atg-7 and LC3B and measuring the sensitisation of cells in response to the combination treatments. The downregulation of Beclin-1, Atg-7 and LC3B will give us a better understanding if the autophagy flux is contributing to the enhanced cell killing in response to the combination treatments or if it is a side effect. Moreover, the silencing of Beclin-1, Atg-7 and LC3B will enable us to determine if dynamic autophagy flux is essential for this response and how this can be optimized.

In addition, the protein DRAM is known to be a link between apoptosis and autophagy.[265,298,475,481] Therefore, we will need:

- To determine the role of DRAM in response to the treatments, and to determine if the downregulation of DRAM (siRNA) affects the sensitisation of prostate cancer cells induced by the combinations.

Furthermore, we will verify the role of the tumour-suppressor miRNAs and oncomiRs identified in this study to determine their role in the chemosensitization of PCa cells and their regulatory mechanisms. These studies will enable us to validate our findings and to verify the role of miRNAs in response to the combination treatments.

- To overexpress with miRNA mimics of the tumour-suppressor miRNAs including hsa-miR-125/99/let-7, hsa-miR-15/16, 128 and 100 and inhibition of oncomiRs (e.g. hsa-miR-17-92 and hsa-miR-106/93/25) in untreated cells and overexpression of oncomiRs under chemosensitizing conditions. These studies will enable us to verify their role in the regulation of their apoptotic and autophagy targets.

6. Appendix.

6.1 AdE1A mutants characterization

To determine that the viral mutants were functional and expressed appropriate gene-products, E1A protein expression was determined in the replicating and non-replicating *dl*1102 and AdE1A1102, and *dl*1104 and AdE1A1104 viruses by immunoblotting.

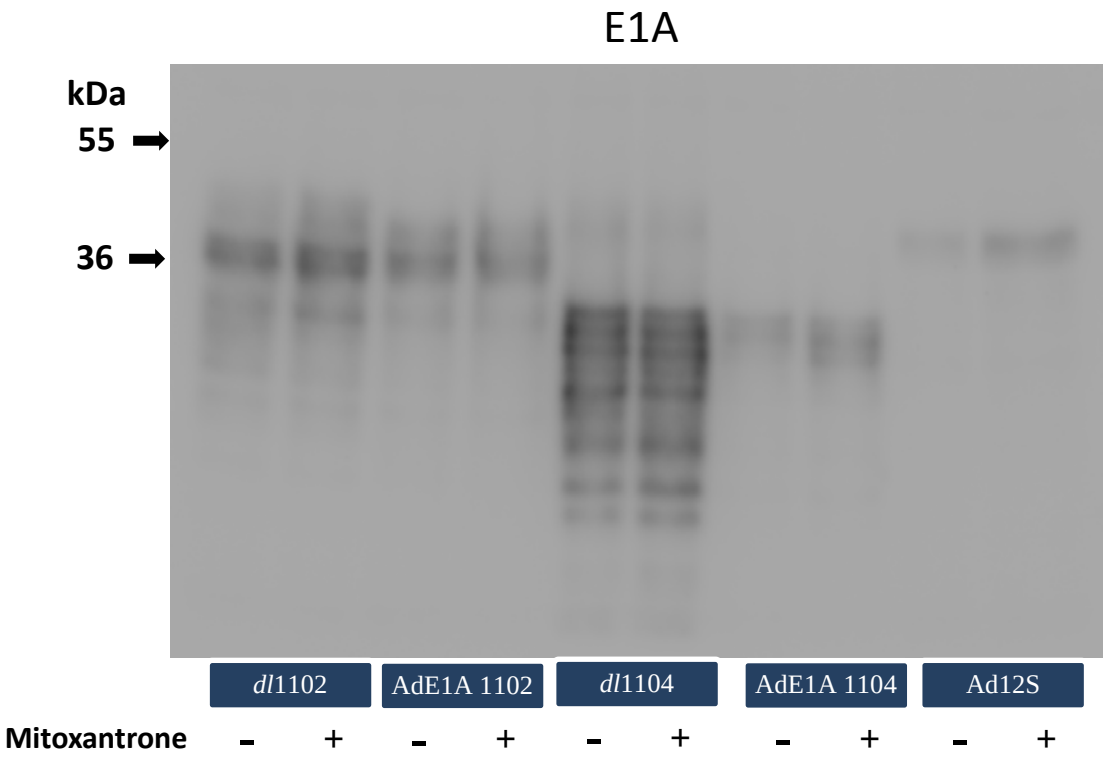

Figure 51. Comparative expression of E1A of replicating and non-replicating AdE1A12S mutants in PC-3 cells. The differential expression of E1A of each viral mutant due to the different deletions is evident in the pattern of expression. Each lane was loaded with 20μg of protein from cells untreated or infected at 100ppc with all viruses alone or in combination with 50nM mitoxantrone Immunoblot representative of three experiments.

The deletions included in each virus are shown in Fig. 19, with AdE1A12S, *dl*1102 and AdE1A1102 being slightly larger than those of *dl*1104 and AdE1A1104. All mutants except *dl*1104 and AdE1A1104 showed the same size and similar expression pattern with several proteins expressed from ~35-45 KDa (Fig.51). However as previously reported [375] *dl*1104 and AdE1A1104 lacked the higher molecular weight proteins

since they do not express exon 1 of the E1A gene. The addition of mitoxantrone did not affect E1A expression.

Replicating *dl*1102, *dl*1104 (Fig. 52, A and B) and non-replicating (Fig. 52, C and D) viruses were characterized using the primer sets described in Table 4, to determine that correct deletions were present and that the viral genome was intact and corresponded to that of Ad5wt after amplification in the producer cell line HEK293.

A) *dl*1102

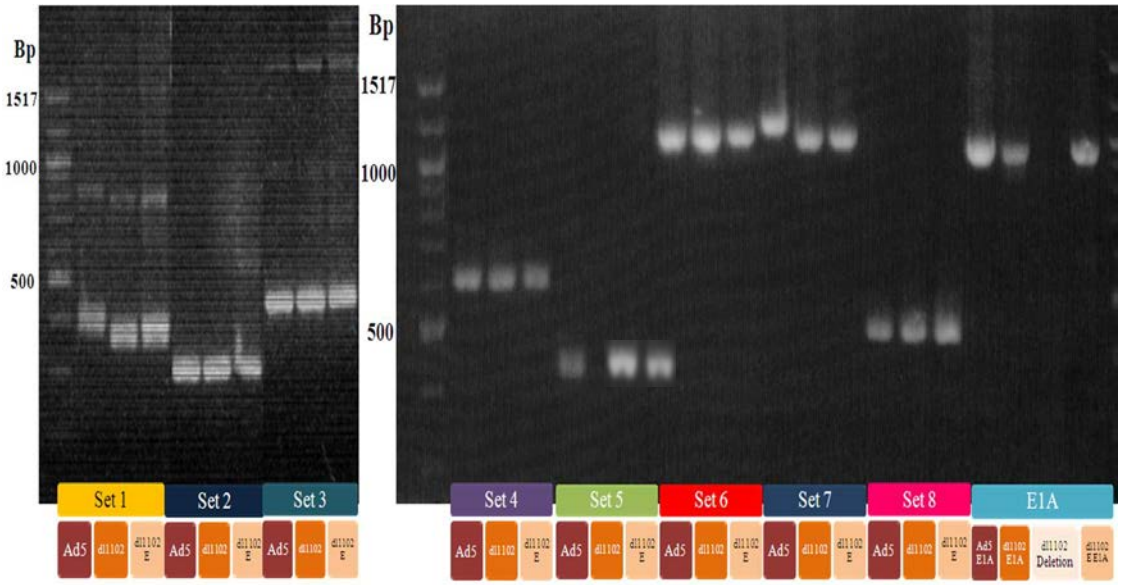

B) *dl*1104

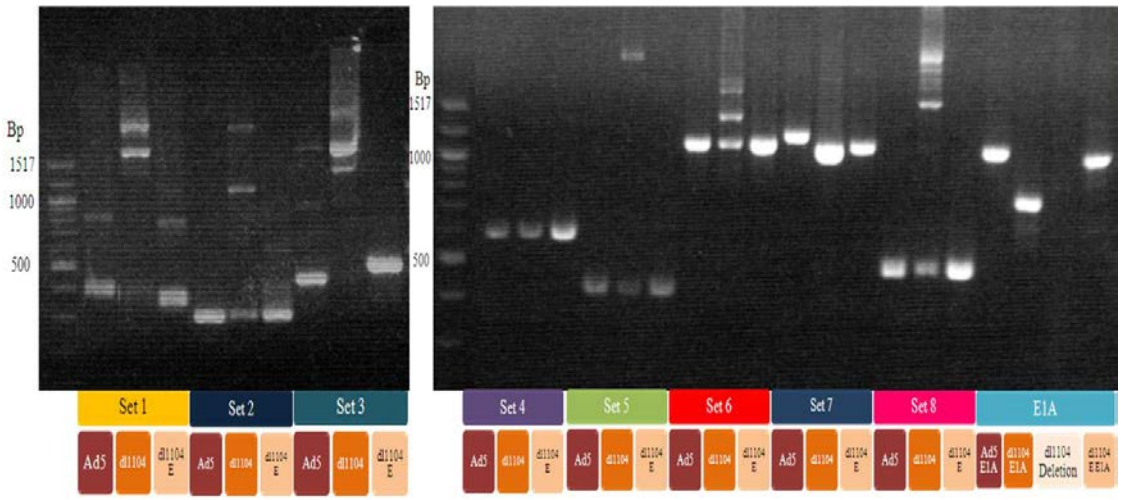

C) AdE1A 1102

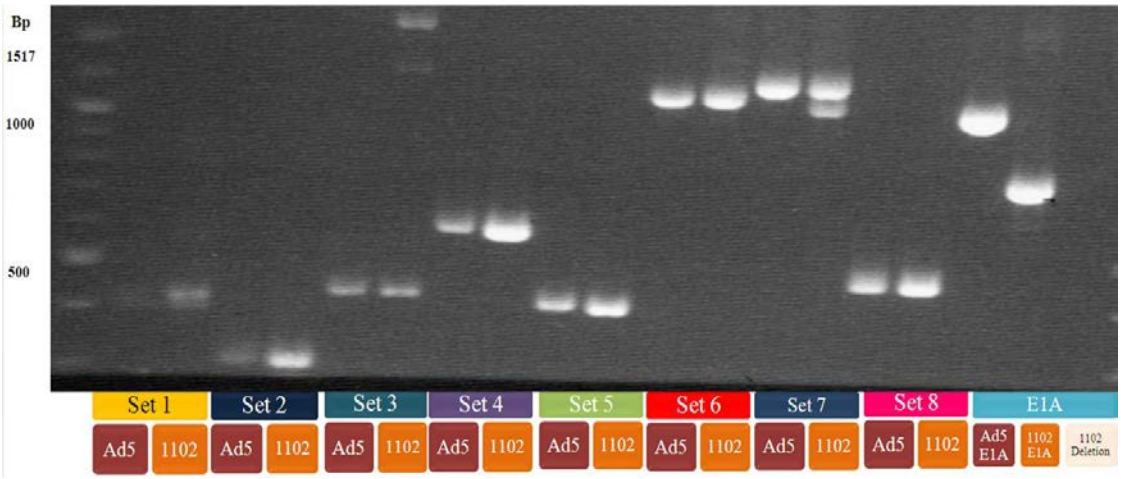

D) AdE1A 1104

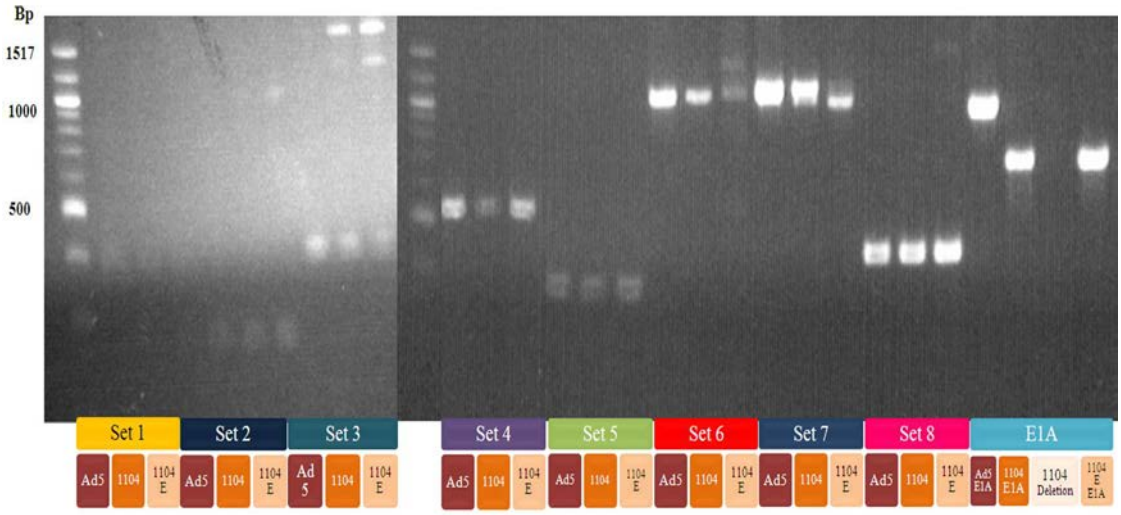

Figure 52. Characterization of viral replicating and non-replicating AdE1A12S mutants used in this project. Viral DNA was extracted to determine the gene size pattern for each set of primers (Table 4). DNA of Ad5wt and mutant viruses previously characterized were extracted and used as reference. Deletion indicates that primers were used for the specific region of the deletion, and as expected no DNA was amplified. The shifts in the bands compared to the Ad5wt virus were caused by the deletions within the genes in each mutant. Other mutants including *dl*922-947, *dl*1520, AdE1A1108, AdΔΔ and AdGFP were produced in the course of other projects by team-members and already characterised aliquots were used in this thesis.

As shown in figure 16 the different mutants (Replicating *dl*1102, *dl*1104 (A and B) and non-replicating (C and D) viruses showed different patterns compared to the corresponding regions in Ad5wt.

6.2 Dose-responses to viral mutants and mitoxantrone in PCa cells tp determine EC_{50} values and relative sensitivity using the MTS- viability assay.

Due to differences in virus and drug batches compared to earlier analysis[362] we conducted a broad screen of virus and drug dose-responses by cell viability assays (Fig 53).

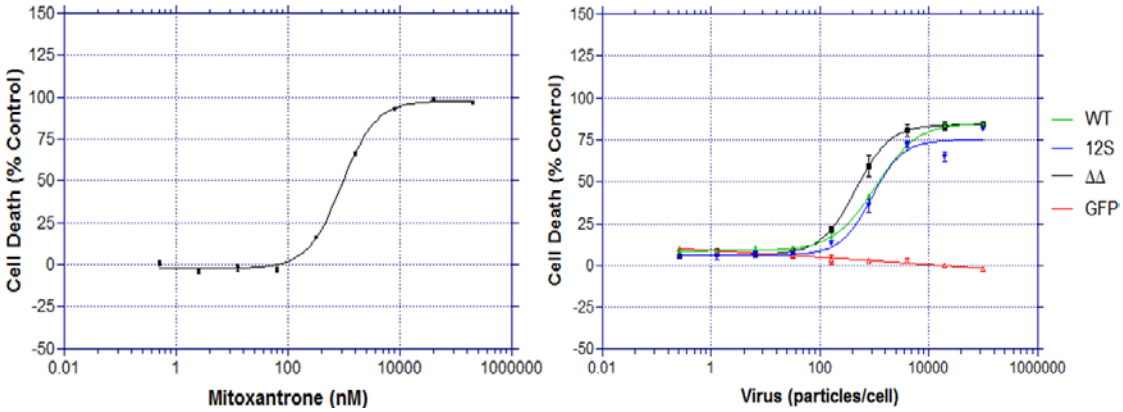

Figure 53. Representative illustration of dose-response assays for Ad5wt, AdE1A12S, AdΔΔ, AdGFP and mitoxantrone in PC-3 cells. The graphics indicate the percentages of cell death *vs* mitoxantrone concentrations (nM) or viral particle per cell (ppc). Data are representative of >5 experiments in triplicates.

Dose-response assays were performed to determine viral and drug concentrations that killed less than 20% of cells in order to investigate key regulatory factors in response to mitoxantrone, viruses and the combinations under synergistic conditions using fixed doses. These dose-response viability assays were routinely performed throughout the thesis work to adjust the doses when necessary for the mechanistic studies.

6.3 The combination of mitoxantrone and AdE1A12S at doses selected in the immunoblot assays enhances cell death.

Previous results showed that the non-replicating AdE1A12S mutants (AdE1A12S, AdE1A1102 and AdE1A1108) increased the percentages of mitochondrial membrane depolarisation membrane as an indication of cell death by apoptosis.[95] The combination of the viruses and mitoxantrone increased cell killing up to 30% after 96h compared to drug alone.[95] In contrast, the AdE1A1104 mutant was unable to

further increase the mitoxantrone-induced apoptosis and had similar effects as the control AdGFP.[95]

A)

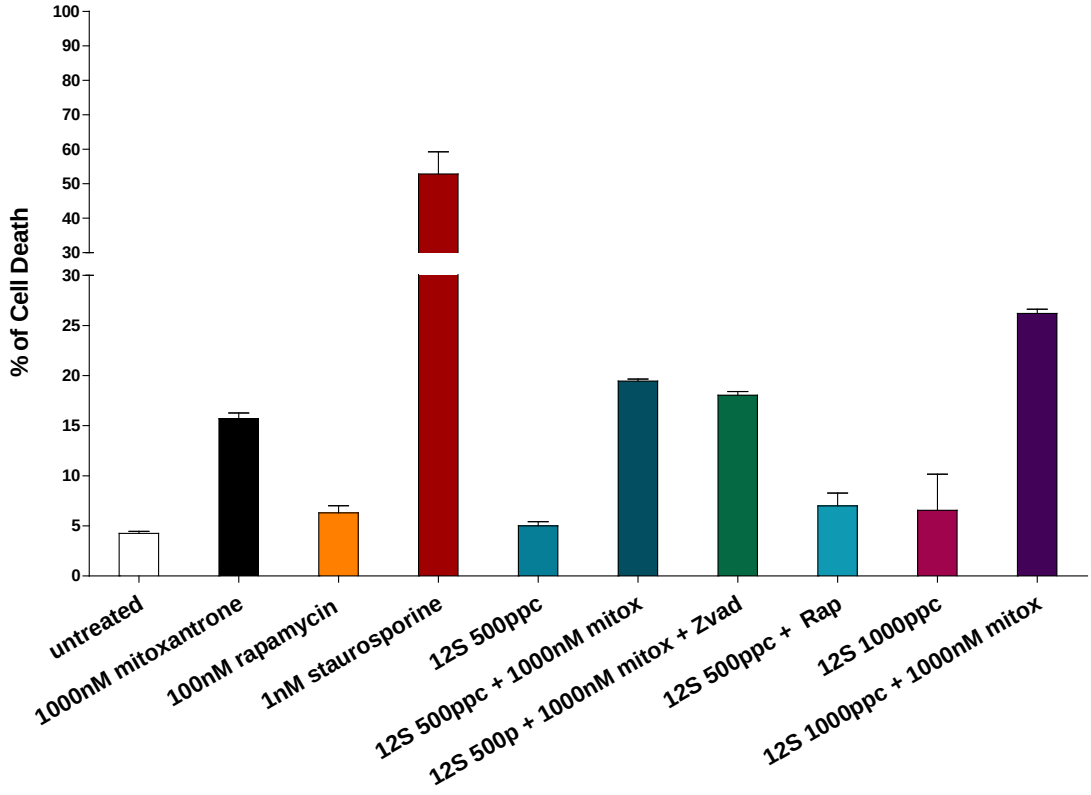

B)

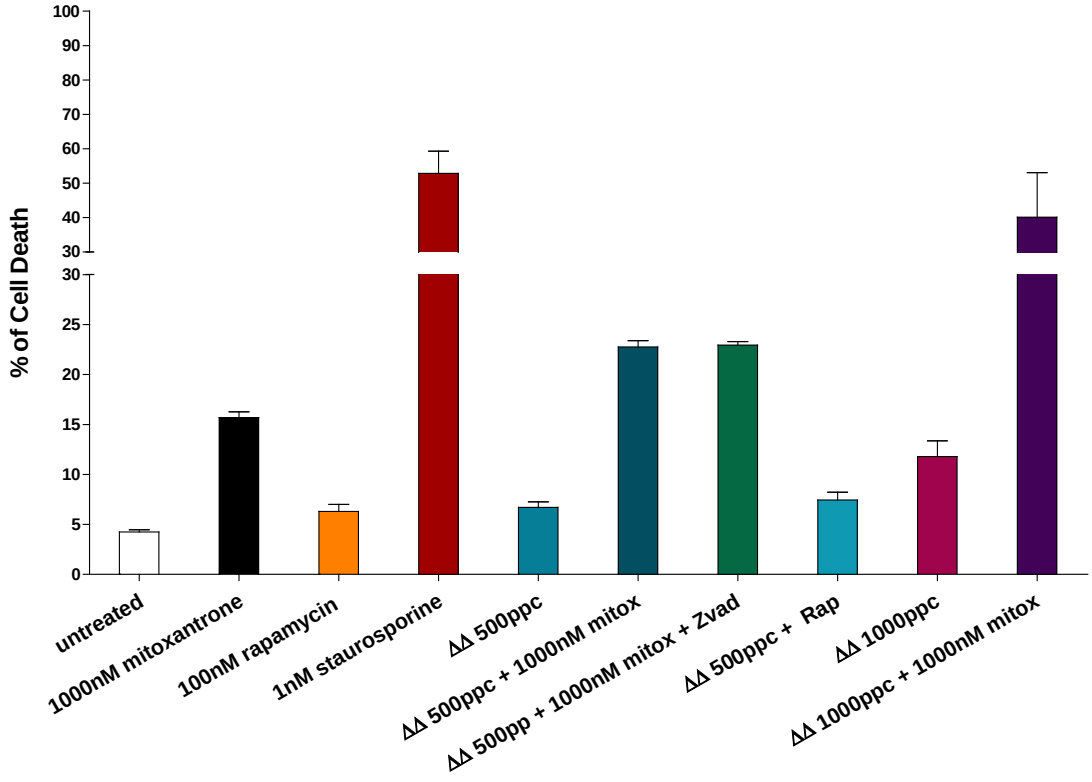

C)

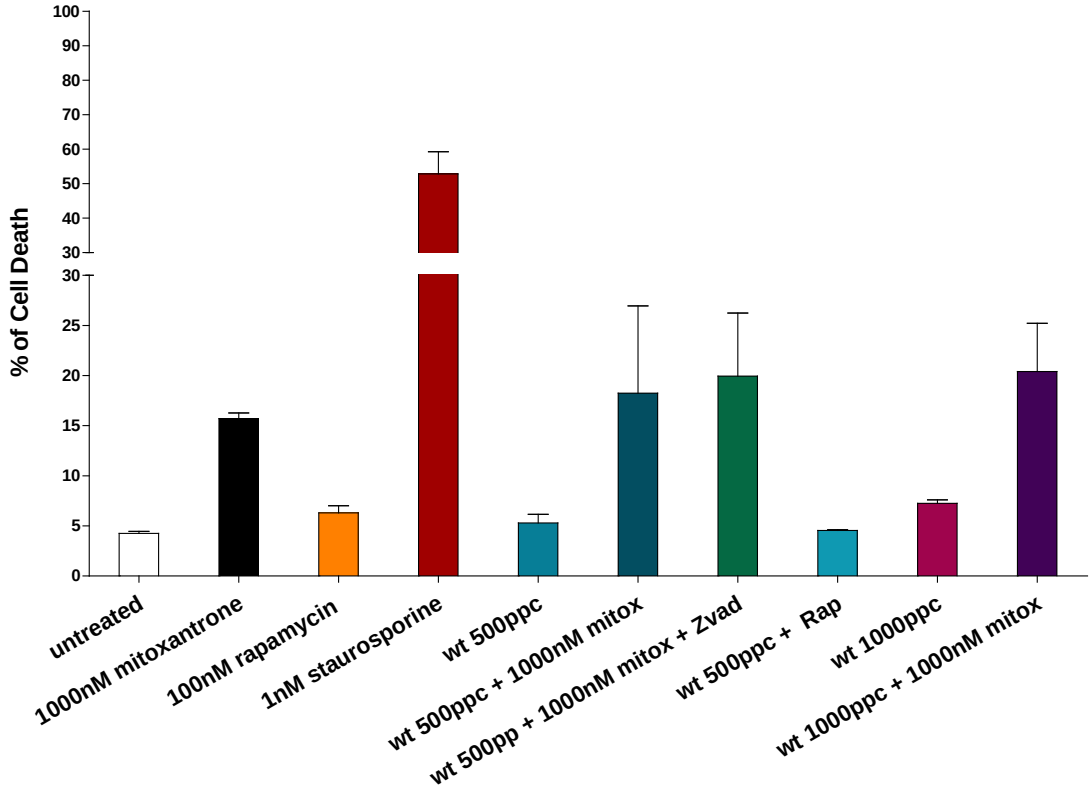

Figure 54. Induction of cell death by the non-replicating AdE1A12S mutant. PC-3 cells were analysed by tetramethylrhodamine uptake (TMRE assay) to measure the mitochondrial membrane potential depolarization and cell death in response to the combination treatments at selected doses. PC-3 cells were treated for 96h with 1000nM mitoxantrone alone or in combination, and infected with: **A)**the non-replicating AdE1A12S mutant at 500ppc and 1000ppc, **B)**AdΔΔ at 500ppc and 1000ppc and **C)**Ad5wt at 500ppc and 1000ppc. PC-3 cells were treated with rapamycin at 100nM, staurosporine at 1nM and zVAD-fmk at 25µM as controls. The percentage of cell death was determined by measuring TMRE and DAPI uptake. Preliminary data, one experiment by duplicate.

My preliminary results testing some of the doses used in the immunoblot screenage, showed that in PC-3 cells at 96h post-treatments, the non-replicating AdE1A12S virus at 500ppc and 1000ppc in combination with mitoxantrone at 1000nM increased the percentages of cells with mitochondrial-depolarised membrane, compared to mitoxantrone alone and showed to be as potent as the wild type virus (Fig. 54A and 54C). However, this increase in cell death was slightly reduced by a pan-caspase inhibitor (Fig. 54A). Moreover, the combination with the replicating oncolytic virus AdΔΔ strongly enhanced cell death with both 500ppc and 1000ppc doses, the combination of mitoxantrone with 1000ppc showed percentage of cell death above 30% similarly to cells treated with staurosporine (Fig. 54B). Interestingly, treatment

with the caspase inhibitor did not seem to reduce cell death (Fig. 54B). Cells infected with Ad5wt showed increased cell death in combination compared to mitoxantrone alone (Fig. 54C), however, both viral doses (500ppc and 1000ppc) induced similar percentages of cell death (Fig. 54C). Furthermore, the percentages of cell death induced by Ad5wt were similar to those showed by the non-replicating AdE1A12S but were less than with the replicating AdΔΔ (Fig. 54A-C). Thus, the differences in cell death were caused by the treatments in combination and not as the result of viral replication. Nonetheless, these results are preliminary and more experiments are needed, although, the results verified that the combination of mitoxantrone and the viruses at these doses sensitize cells and potentiate cell killing.

6.4 Mitoxantrone in combination with the AdE1A12S virus triggers a DNA-damage response but fails to activate the FOXO3a-mediated regulatory mechanism.

In our miRNA study we observed that a recurrent target of deregulated miRNAs was the transcription factor FOXO3a. FOXO3a is a key regulator of the p-53-independent-DNA-damage response which is negatively regulated by p-Akt.[441] In addition, in PCa FOXO3a has been shown to induce apoptosis.[406,407] Therefore, we assessed the expression of FOXO3a at 24h and 48h in PC-3 cells. The expression of FOXO3a at 24h after infection with AdE1A12S showed a trend towards decreased levels (Fig. 55A). The possible decreases in FOXO3a is in agreement with the findings that AdE1A12S induced phospho-Akt (Section 3.5.3) which in turn may inhibit FOXO3a as previously reported.[441] Treatment with mitoxantrone did not significantly affect FOXO3a levels. I previously observed (Section 3.5.3) that mitoxantrone decreased phospho-Akt activation however, this was apparently not reflected in increased levels of FOXO3a (Fig. 55A). The combination of both agents maintained FOXO3a at basal levels except at high concentrations of mitoxantrone where the levels of FOXO3a with 1000nM were slightly increased and decreased with 2000nM, these results did not correlate with expected decreases in p-Akt levels at this time point. FOXO3a might not be an important factor under these conditions, although additional studies will be required to verify these preliminary findings.

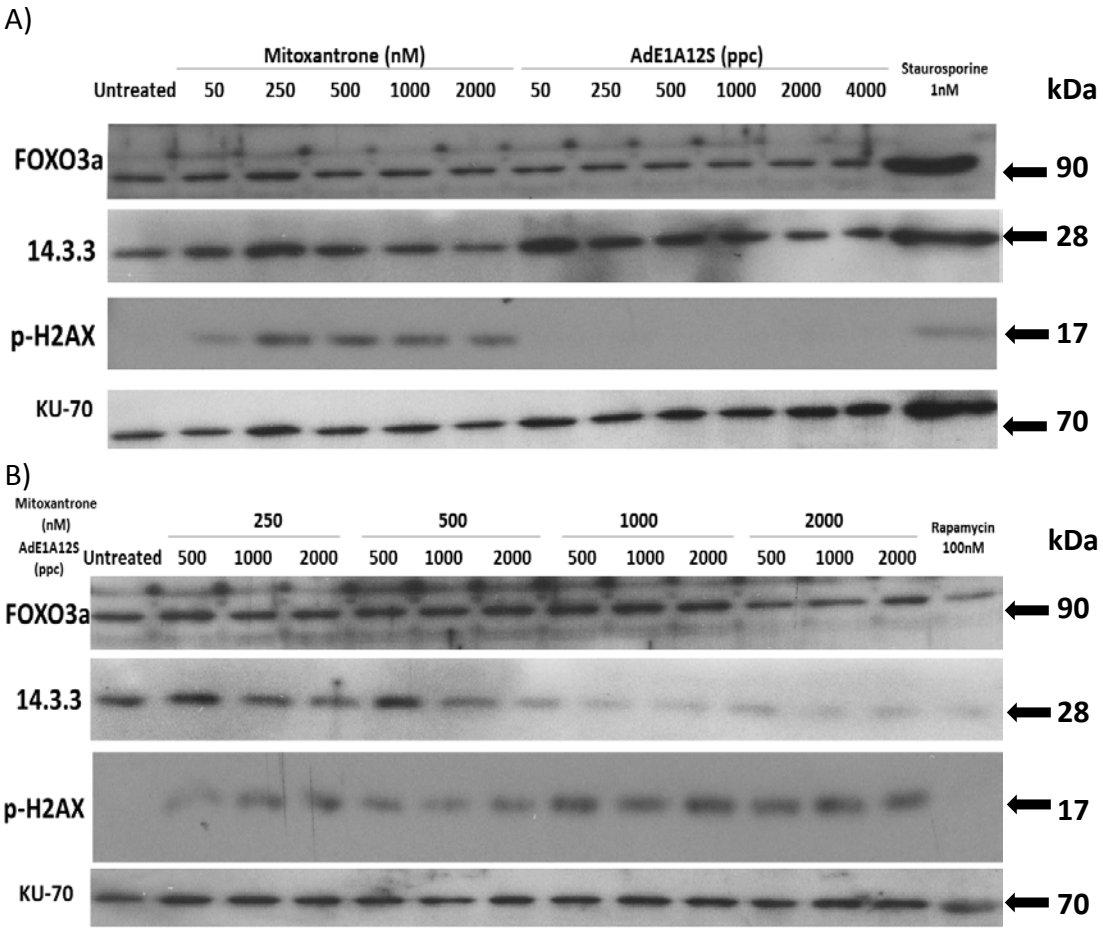

Figure 55. Changes in expression of 14.3.3, FOXO3a and phospho-H2AX in PC-3 cells at 24h post-treatment with mitoxantrone and/or infection with the AdE1A12S virus. **A)** PC-3 cells treated with mitoxantrone at increasing concentrations, 50nM - 2000nM or infected with AdE1A12S,at 50ppc - 4000ppc. Cells were also treated with staurosporine at 1nM and rapamycin 100nM as indicators of apoptotic and autophagic activity. **B)** PC-3 cells treated with mitoxantrone for 24h at 250nM, 500nM, 1000nM and 2000nM in combination with the AdE1A12S virus at 500ppc, 1000ppc and 2000ppc and rapamycin 100nM, loading control KU-70. A-B) Preliminary data, one experiment.

It is known that the inhibition of FOXO3a by Akt promotes the translocation of FOXO3a to the cytoplasm, where it accumulates and is bound and retained by the protein 14.3.3.[443] To determine the involvement of 14.3.3 in response to the treatment we assessed the levels of expression of 14.3.3, we observed that 14.3.3 was strongly induced by the virus and to a lesser extent by mitoxantrone (Fig. 55). These results suggest an accumulation of 14.3.3. In contrast, the combination of AdE1A12S with mitoxantrone reduced the levels of 14.3.3 at increasing concentrations of virus (1000ppc and 2000ppc with 250nM and 500nM mitoxantrone) and was greatly reduced with all combinations at the higher doses

(1000nM and 2000nM) of mitoxantrone. In conclusion, these results are insufficient to elucidate the roles of p-Akt, FOXO3a or 14.3.3, in response to AdE1A12S, mitoxantrone or the combinations. These findings open an interesting area of investigation to identify novel cellular interactions by either E1A or DNA-damaging drugs. It is known that mitoxantrone induces a DNA-damage response which leads to apoptosis. Therefore, we assessed the activation of p-H2AX, a DNA-damage repair marker at 24h in PC-3 cells.[460] As could be expected p-H2AX was activated by mitoxantrone even at low doses (50nM; Fig. 55A). In contrast, infection with AdE1A12S did not activate p-H2AX at any concentration. Interestingly, when mitoxantrone was combined with AdE1A12S the activity of p-H2AX at lower drug doses (250nM and 500nM) was similar to that of drug alone however, at the higher drug doses (1000nM and 2000nM) the expression of E1A12S in combination with mitoxantrone appeared to further activate p-H2AX (Fig. 55B). In conclusion, activation of the DNA-damage repair response is clearly involved in the synergistically enhanced apoptosis in response to the combinations.

A)

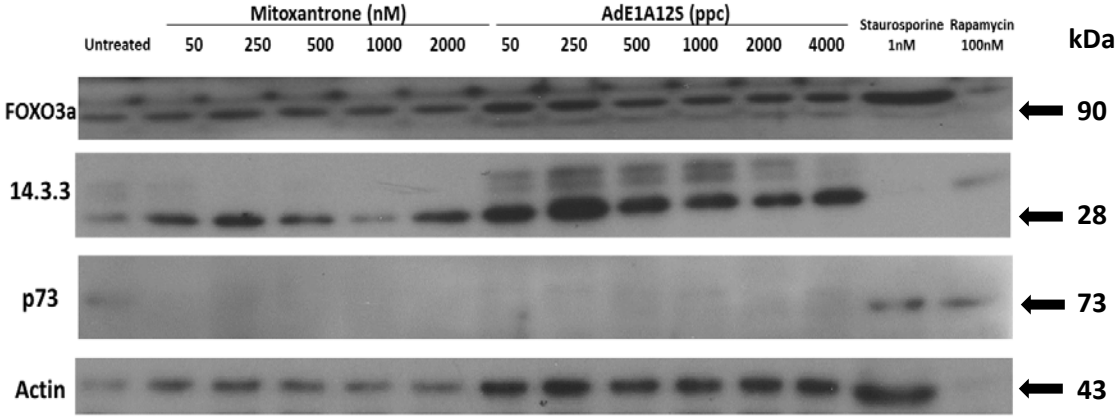

B)

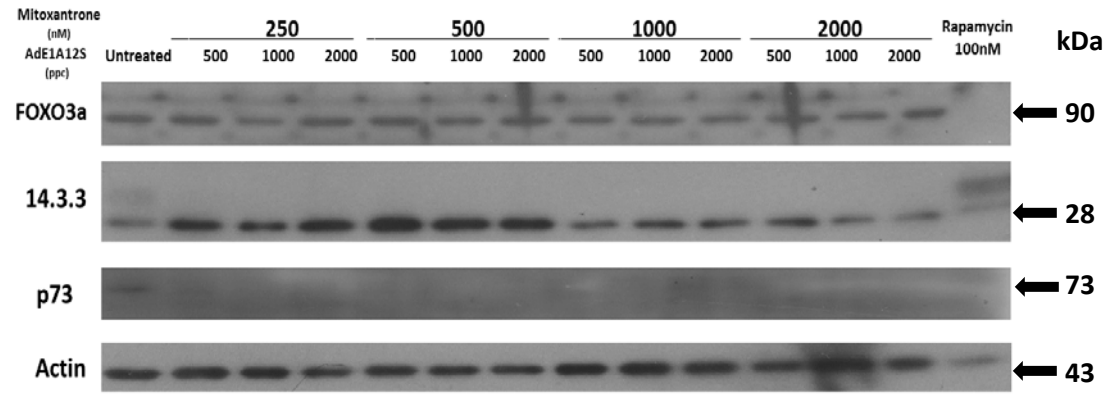

Figure 56. Expression of 14.3.3, FOXO3a and p73 in PC-3 cells at 48h post-treatment with mitoxantrone and/or infection with the AdE1A12S virus. **A)** PC-3 cells treated with mitoxantrone at increasing concentrations, 50nM - 2000nM or infected with AdE1A12S at 50ppc - 4000ppc. Cells were also treated with staurosporine at 1nM as indicators of apoptotic and autophagic activity. **B)** PC-3 cells treated with mitoxantrone for 48h at 250nM, 500nM, 1000nM and 2000nM in combination with the AdE1A12S virus at 500ppc, 1000ppc and 2000ppc and rapamycin 100nM. Loading control Actin. Preliminary data, one experiment.

We also assessed the expression of FOXO3a at 48h. FOXO3a expression-levels were not affected by mitoxantrone at any concentration while AdE1A12S increased the expression at all doses (Fig. 56A). However, when combined, no significant changes in FOXO3a levels were observed compared to basal (Fig. 56B) The levels of 14.3.3 increased similarly at 48h as at the 24h time point in response to both AdE1A12S and mitoxantrone when administered alone (Fig. 55A-56A). In combination, the trend was similar to the 24h findings although the expression levels were more potently increased at all combinations.

In addition, the lack of p53 in PC-3 cells made it interesting to determine the levels of other members of the p53-family that could be regulating the apoptotic pathway in response to the combination treatments. The induction of cell death in response to DNA-damage can also be induced by the p53-family member p73.[461,462] Therefore, we investigated if p73 was involved in the apoptotic cell killing in response to the combination treatments. However, p73 levels were not detectable in PC3 cells after treatment with AdE1A12S, mitoxantrone or the combinations (Fig. 56). Only a faint signal was detectable in untreated and uninfected cells while rapamycin and staurosporine potently induced p73. These studies need further repetitions including loading with more protein lysates (~40μg/lane) and inclusion of loading controls such as β-actin or β-tubulin.

7. References

1 **Jemal, A., Bray, F., Center, M. M., Ferlay, J., Ward, E. & Forman, D.** Global cancer statistics. *CA Cancer J Clin* 61, 69-90 (**2011**).

2 **Attar, R. M., Takimoto, C. H. & Gottardis, M. M.** Castration-resistant prostate cancer: locking up the molecular escape routes. *Clin Cancer Res* 15, 3251-3255 (**2009**).

3 **Hussain, A. & Dawson, N.** Management of advanced/metastatic prostate cancer: 2000 update. *Oncology (Williston Park)* 14, 1677-1688; discussion 1688, 1691-1674 (**2000**).

4 **Altieri, D. C., Languino, L. R., Lian, J. B., Stein, J. L., Leav, I., van Wijnen, A. J., Jiang, Z. & Stein, G. S.** Prostate cancer regulatory networks. *J Cell Biochem* 107, 845-852 (**2009**).

5 **Berthold, D. R., Pond, G. R., de Wit, R., Eisenberger, M. & Tannock, I. F.** Survival and PSA response of patients in the TAX 327 study who crossed over to receive docetaxel after mitoxantrone or vice versa. *Ann Oncol* 19, 1749-1753 (**2008**).

6 **You, Z., Dong, Y., Kong, X., Beckett, L. A., Gandour-Edwards, R. & Melamed, J.** Midkine is a NF-kappaB-inducible gene that supports prostate cancer cell survival. *BMC Med Genomics* 1, 6 (**2008**).

7 **Fusi, A., Procopio, G., Della Torre, S., Ricotta, R., Bianchini, G., Salvioni, R., Ferrari, L., Martinetti, A., Savelli, G., Villa, S. & Bajetta, E.** Treatment options in hormone-refractory metastatic prostate carcinoma. *Tumori* 90, 535-546 (**2004**).

8 **Sciarra, A. & Salciccia, S.** New treatment strategies in the management of hormone refractory prostate cancer (HRPC): only chemotherapy? *Eur Urol* 52, 945-947 (**2007**).

9 **Sawyers, C.** Targeted cancer therapy. *Nature* 432, 294-297 (**2004**).

10 **Strausberg, R. L., Simpson, A. J., Old, L. J. & Riggins, G. J.** Oncogenomics and the development of new cancer therapies. *Nature* 429, 469-474 (**2004**).

11 **Chabner, B. A. & Roberts, T. G., Jr.** Timeline: Chemotherapy and the war on cancer. *Nat Rev Cancer* 5, 65-72 (**2005**).

12 **Bernier, J., Hall, E. J. & Giaccia, A.** Radiation oncology: a century of achievements. *Nat Rev Cancer* 4, 737-747 (**2004**).

13 **Stein, W. D., Bates, S. E. & Fojo, T.** Intractable cancers: the many faces of multidrug resistance and the many targets it presents for therapeutic attack. *Curr Drug Targets* 5, 333-346 (**2004**).

14 **Moul, J. W.** The evolving definition of advanced prostate cancer. *Reviews in urology* 6 Suppl 8, S10-17 (**2004**).

15 **UK, C. R.** *Prostate cancer*, (**2013**).

16 **Kufe, D. W., Frei, E. & Holland, J. F.** ***Cancer medicine 7***. 7th edn, (Elsevier, **2006**).

17 **Schroder, F. H.** Prostate cancer around the world. An overview. *Urol Oncol* 28, 663-667 (**2010**).

18 **De Marzo, A. M., Platz, E. A., Sutcliffe, S., Xu, J., Gronberg, H., Drake, C. G., Nakai, Y., Isaacs, W. B. & Nelson, W. G.** Inflammation in prostate carcinogenesis. *Nat Rev Cancer* 7, 256-269 (**2007**).

19 **Nakai, Y. & Nonomura, N.** Inflammation and prostate carcinogenesis. *International journal of urology : official journal of the Japanese Urological Association* 20, 150-160 (**2013**).

20 **Cohen, R., Shannon, B., McNeal, J., Shannon, T. & Garrett, K.** Propionibacterium acnes associated with inflammation in radical prostatectomy specimens: a possible link to cancer evolution? *The Journal of urology* 173, 1969-1974 (**2005**).

21 **Shinohara, D., Vaghasia, A., Yu, S.-H., Mak, T., Brüggemann, H., Nelson, W., De Marzo, A., Yegnasubramanian, S. & Sfanos, K.** A mouse model of chronic prostatic inflammation using a human prostate cancer-derived isolate of Propionibacterium acnes. *The Prostate* (**2013**).

22 **Urisman, A., Molinaro, R., Fischer, N., Plummer, S., Casey, G., Klein, E., Malathi, K., Magi-Galluzzi, C., Tubbs, R., Ganem, D., Silverman, R. & DeRisi, J.** Identification of a novel Gammaretrovirus in prostate tumors of patients homozygous for R462Q RNASEL variant. *PLoS pathogens* 2 (**2006**).

23 **Whitaker, N., Glenn, W., Sahrudin, A., Orde, M., Delprado, W. & Lawson, J.** Human papillomavirus and Epstein Barr virus in prostate cancer: Koilocytes indicate potential oncogenic influences of human papillomavirus in prostate cancer. *The Prostate* 73, 236-241 (**2013**).

24 **Cunha, G. R., Ricke, W., Thomson, A., Marker, P. C., Risbridger, G., Hayward, S. W., Wang, Y. Z., Donjacour, A. A. & Kurita, T.** Hormonal, cellular, and molecular regulation of normal and neoplastic prostatic development. *J Steroid Biochem Mol Biol* 92, 221-236 (**2004**).

25 **McNeal, J. E.** Normal histology of the prostate. *Am J Surg Pathol* 12, 619-633 (**1988**).

26 **Timms, B. G.** Prostate development: a historical perspective. *Differentiation* 76, 565-577 (**2008**).

27 **Mimeault, M. & Batra, S. K.** Recent advances on multiple tumorigenic cascades involved in prostatic cancer progression and targeting therapies. *Carcinogenesis* 27, 1-22 (**2006**).

28 **Shen, M. M. & Abate-Shen, C.** Molecular genetics of prostate cancer: new prospects for old challenges. *Genes Dev* 24, pp. 1967-2000 (**2010**).

29 **Feldman, B. J. & Feldman, D.** The development of androgen-independent prostate cancer. *Nat Rev Cancer* 1, 34-45 (**2001**).

30 **Clark, J., Attard, G., Jhavar, S., Flohr, P., Reid, A., De-Bono, J., Eeles, R., Scardino, P., Cuzick, J., Fisher, G., Parker, M. D., Foster, C. S., Berney, D., Kovacs, G. & Cooper, C. S.** Complex patterns of ETS gene alteration arise during cancer development in the human prostate. *Oncogene* 27, 1993-2003 (**2008**).

31 **van Leenders, G. J. & Schalken, J. A.** Epithelial cell differentiation in the human prostate epithelium: implications for the pathogenesis and therapy of prostate cancer. *Crit Rev Oncol Hematol* 46 Suppl, S3-10 (**2003**).

32 **Kim, Y. & Nirenberg, M.** Drosophila NK-homeobox genes. *Proceedings of the National Academy of Sciences of the United States of America* 86, 7716-7720 (**1989**).

33 **Bostwick, D. G. & Cheng, L.** Precursors of prostate cancer. *Histopathology* 60, 4-27 (**2012**).

34 **Aschelter, A. M., Giacinti, S., Caporello, P. & Marchetti, P.** Genomic and epigenomic alterations in prostate cancer. *Frontiers in endocrinology* 3, 128 (**2012**).

35 **Holcomb, I. N., Young, J. M., Coleman, I. M., Salari, K., Grove, D. I., Hsu, L., True, L. D., Roudier, M. P., Morrissey, C. M., Higano, C. S., Nelson, P. S., Vessella, R. L. & Trask, B. J.** Comparative analyses of chromosome alterations in soft-tissue metastases within and across patients with castration-resistant prostate cancer. *Cancer Res* 69, 7793-7802 (**2009**).

36 **Bastus, N. C., Boyd, L. K., Mao, X., Stankiewicz, E., Kudahetti, S. C., Oliver, R. T., Berney, D. M. & Lu, Y. J.** Androgen-induced TMPRSS2:ERG fusion in nonmalignant prostate epithelial cells. *Cancer Res* 70, 9544-9548 (**2010**).

37 **McCall, P., Witton, C. J., Grimsley, S., Nielsen, K. V. & Edwards, J.** Is PTEN loss associated with clinical outcome measures in human prostate cancer? *Br J Cancer* 99, 1296-1301 (**2008**).

38 **Barbieri, C. E., Baca, S. C., Lawrence, M. S., Demichelis, F., Blattner, M., Theurillat, J. P., White, T. A., Stojanov, P., Van Allen, E., Stransky, N., Nickerson, E., Chae, S. S., Boysen, G., Auclair, D., Onofrio, R. C., Park, K., Kitabayashi, N., MacDonald, T. Y., Sheikh, K., Vuong, T., Guiducci, C., Cibulskis, K., Sivachenko, A., Carter, S. L., Saksena, G., Voet, D., Hussain, W. M., Ramos, A. H., Winckler, W., Redman, M. C., Ardlie, K., Tewari, A. K., Mosquera, J. M., Rupp, N., Wild, P. J., Moch, H., Morrissey, C., Nelson, P. S., Kantoff, P. W., Gabriel, S. B., Golub, T. R., Meyerson, M., Lander, E. S., Getz, G., Rubin, M. A. & Garraway, L. A.** Exome sequencing identifies recurrent SPOP, FOXA1 and MED12 mutations in prostate cancer. *Nat Genet* 44, 685-689 (**2012**).

39 **Shiota, M., Yokomizo, A. & Naito, S.** Increased androgen receptor transcription: a cause of castration-resistant prostate cancer and a possible therapeutic target. *Journal of molecular endocrinology* 47, R25-41 (**2011**).

40 **Chatterjee, B.** The role of the androgen receptor in the development of prostatic hyperplasia and prostate cancer. *Mol Cell Biochem* 253, 89-101 (**2003**).

41 **Friedlander, T. W. & Ryan, C. J.** Targeting the androgen receptor. *The Urologic clinics of North America* 39, 453-464 (**2012**).

42 **Chen, Y., Sawyers, C. L. & Scher, H. I.** Targeting the androgen receptor pathway in prostate cancer. *Curr Opin Pharmacol* 8, 440-448 (**2008**).

43 **Gottlieb, B., Beitel, L. K., Nadarajah, A., Paliouras, M. & Trifiro, M.** The androgen receptor gene mutations database: 2012 update. *Human mutation* 33, 887-894 (**2012**).

44 **Culig, Z. & Bartsch, G.** Androgen axis in prostate cancer. *J Cell Biochem* 99, 373-381 (**2006**).

45 **Maitland, N. J. & Collins, A. T.** Inflammation as the primary aetiological agent of human prostate cancer: a stem cell connection? *J Cell Biochem* 105, 931-939 (**2008**).

46 **Ilic, D., Neuberger, M. M., Djulbegovic, M. & Dahm, P.** Screening for prostate cancer. *Cochrane Database Syst Rev* 1, CD004720 (**2013**).

47 **Borley, N. & Feneley, M. R.** Prostate cancer: diagnosis and staging. *Asian J Androl* 11, 74-80 (**2009**).

48 **Freedland, S. J.** Screening, risk assessment, and the approach to therapy in patients with prostate cancer. *Cancer* 117, 1123-1135 (**2011**).

49 **Polascik, T. J., Oesterling, J. E. & Partin, A. W.** Prostate specific antigen: a decade of discovery--what we have learned and where we are going. *J Urol* 162, 293-306 (**1999**).

50 **Teeter, A. E., Presti, J. C., Jr., Aronson, W. J., Terris, M. K., Kane, C. J., Amling, C. L. & Freedland, S. J.** Does PSADT after radical prostatectomy correlate with overall survival?--a report from the SEARCH database group. *Urology* 77, 149-153 (**2011**).

51 **Smeenge, M., Barentsz, J., Cosgrove, D., de la Rosette, J., de Reijke, T., Eggener, S., Frauscher, F., Kovacs, G., Matin, S. F., Mischi, M., Pinto, P., Rastinehad, A., Rouviere, O., Salomon, G., Polascik, T., Walz, J., Wijkstra, H. & Marberger, M.** Role of transrectal ultrasonography (TRUS) in focal therapy of prostate cancer: report from a Consensus Panel. *BJU international* 110, 942-948 (**2012**).

52 **Aboumarzouk, O. M., Ogston, S., Huang, Z., Evans, A., Melzer, A., Stolzenberg, J. U. & Nabi, G.** Diagnostic accuracy of transrectal elastosonography (TRES) imaging for the diagnosis of prostate cancer: a systematic review and meta-analysis. *BJU international* 110, 1414-1423; discussion 1423 (**2012**).

53 **Gleason, D. F.** Classification of prostatic carcinomas. *Cancer Chemother Rep* 50, 125-128 (**1966**).

54 **Kollermann, J. & Sauter, G.** [Trends in prostate biopsy interpretation]. *Urologe A* 48, 305-312; quiz 313-304 (**2009**).

55 **Ammon, J., Karstens, J. H. & Rathert, P.** [TNM-system orientated radiological therapy in prostatic carcinoma (author's transl)]. *Urologe A* 16, 73-82 (**1977**).

56 **Cheng, L., Montironi, R., Bostwick, D. G., Lopez-Beltran, A. & Berney, D. M.** Staging of prostate cancer. *Histopathology* 60, 87-117 (**2012**).

57 **Ismail, M., Ferroni, M. & Gomella, L. G.** Androgen suppression strategies for prostate cancer: is there an ideal approach? *Curr Urol Rep* 12, 188-196 (**2011**).

58 **Bill-Axelson, A., Holmberg, L., Ruutu, M., Garmo, H., Stark, J. R., Busch, C., Nordling, S., Haggman, M., Andersson, S. O., Bratell, S., Spangberg, A., Palmgren, J., Steineck, G., Adami, H. O. & Johansson, J. E.** Radical prostatectomy versus watchful waiting in early prostate cancer. *N Engl J Med* 364, 1708-1717 (**2011**).

59 **(U.S.), N. C. I.** Radiation Therapy for Cancer. (**2011**).

60 **Board of Faculty of Clinical Oncology, R. C. o. R.** Radiotherapy Dose-Fractionation. 84 (**2006**).

61 **Ganswindt, U., Stenzl, A., Bamberg, M. & Belka, C.** Adjuvant radiotherapy for patients with locally advanced prostate cancer--a new standard? *Eur Urol* 54, 528-542 (**2008**).

62 **Hammerer, P. & Madersbacher, S.** Landmarks in hormonal therapy for prostate cancer. *BJU international* 110 Suppl 1, 23-29 (**2012**).

63 **Scher, H. I. & Sawyers, C. L.** Biology of progressive, castration-resistant prostate cancer: directed therapies targeting the androgen-receptor signaling axis. *J Clin Oncol* 23, 8253-8261 (**2005**).

64 **de Bono, J. S., Logothetis, C. J., Molina, A., Fizazi, K., North, S., Chu, L., Chi, K. N., Jones, R. J., Goodman, O. B., Jr., Saad, F., Staffurth, J. N., Mainwaring, P., Harland, S., Flaig, T. W., Hutson, T. E., Cheng, T., Patterson, H., Hainsworth, J. D., Ryan, C. J., Sternberg, C. N., Ellard, S. L., Flechon, A., Saleh, M., Scholz, M., Efstathiou, E., Zivi, A., Bianchini, D., Loriot, Y., Chieffo, N., Kheoh, T., Haqq, C. M. & Scher, H. I.** Abiraterone and increased survival in metastatic prostate cancer. *N Engl J Med* 364, 1995-2005 (**2011**).

65 **FDA, U. S. F. a. D. A.** FDA approves Zytiga for late-stage prostate cancer. (**2011**).

66 **Oh, W. K., Logue, J. & Dana-Farber Cancer Institute.** ***Prostate cancer***. (Mosby Elsevier, **2007**).

67 **Mike, S., Harrison, C., Coles, B., Staffurth, J., Wilt, T. J. & Mason, M. D.** Chemotherapy for hormone-refractory prostate cancer. *Cochrane Database Syst Rev*, CD005247 (**2006**).

68 **Ryan, C. W., Stadler, W. M. & Vogelzang, N. J.** Docetaxel and exisulind in hormone-refractory prostate cancer. *Semin Oncol* 28, 56-61 (**2001**).

69 **Knipe, D. M., Howley, P. M. & Griffin, D. E.** ***Fundamental virology***. 4th edn, (Lippincott Williams & Wilkins, **2001**).

70 **Robinson, C. M., Singh, G., Henquell, C., Walsh, M. P., Peigue-Lafeuille, H., Seto, D., Jones, M. S., Dyer, D. W. & Chodosh, J.** Computational analysis and identification of an emergent human adenovirus pathogen implicated in a respiratory fatality. *Virology* 409, 141-147 (**2011**).

71 **Jones, M. S., 2nd, Harrach, B., Ganac, R. D., Gozum, M. M., Dela Cruz, W. P., Riedel, B., Pan, C., Delwart, E. L. & Schnurr, D. P.** New adenovirus species found in a patient presenting with gastroenteritis. *J Virol* 81, 5978-5984 (**2007**).

72 **Sharma, A., Li, X., Bangari, D. S. & Mittal, S. K.** Adenovirus receptors and their implications in gene delivery. *Virus Res* 143, 184-194 (**2009**).

73 **Campos, S. K. & Barry, M. A.** Current advances and future challenges in Adenoviral vector biology and targeting. *Curr Gene Ther* 7, 189-204 (**2007**).

74 **Russell, W. C.** Adenoviruses: update on structure and function. *J Gen Virol* 90, 1-20 (**2009**).

75 **Braithwaite, A. W. & Russell, I. A.** Induction of cell death by adenoviruses. *Apoptosis* 6, 359-370 (**2001**).

76 **Berk, A. J.** Recent lessons in gene expression, cell cycle control, and cell biology from adenovirus. *Oncogene* 24, 7673-7685 (**2005**).

77 **Lauer, K. P., Llorente, I., Blair, E., Seto, J., Krasnov, V., Purkayastha, A., Ditty, S. E., Hadfield, T. L., Buck, C., Tibbetts, C. & Seto, D.** Natural variation among human adenoviruses: genome sequence and annotation of human adenovirus serotype 1. *J Gen Virol* 85, 2615-2625 (**2004**).

78 **Hawkins, L. K. & Hermiston, T.** Gene delivery from the E3 region of replicating human adenovirus: evaluation of the E3B region. *Gene Ther* 8, 1142-1148 (**2001**).

79 **Wang, Y., Hallden, G., Hill, R., Anand, A., Liu, T. C., Francis, J., Brooks, G., Lemoine, N. & Kirn, D.** E3 gene manipulations affect oncolytic adenovirus activity in immunocompetent tumor models. *Nat Biotechnol* 21, 1328-1335 (**2003**).

80 **Gamrot, E.** *The International imMunoGeneTics information system*, <http://www.imgt.org> (**2009**).
81 **Knipe, D., Howley, P., Griffin, D., Lamb, R., Martin, M., Roizman, B. & Straus, S.** Fields Virology, Vols 1 and 2. *Lippincott Willimas & Wilkins, Philadelphia* (**2001**).
82 **Douglas, J. T.** Adenoviral vectors for gene therapy. *Mol Biotechnol* 36, 71-80 (**2007**).
83 **Frisch, S. M. & Mymryk, J. S.** Adenovirus-5 E1A: paradox and paradigm. *Nat Rev Mol Cell Biol* 3, 441-452 (**2002**).
84 **Chakraborty, A. A. & Tansey, W. P.** Adenoviral E1A function through Myc. *Cancer Res* 69, 6-9 (**2009**).
85 **Miller, M. S., Pelka, P., Fonseca, G. J., Cohen, M. J., Kelly, J. N., Barr, S. D., Grand, R. J., Turnell, A. S., Whyte, P. & Mymryk, J. S.** Characterization of the 55-residue protein encoded by the 9S E1A mRNA of species C adenovirus. *J Virol* 86, 4222-4233 (**2012**).
86 **Fueyo, J., Gomez-Manzano, C., Alemany, R., Lee, P. S., McDonnell, T. J., Mitlianga, P., Shi, Y. X., Levin, V. A., Yung, W. K. & Kyritsis, A. P.** A mutant oncolytic adenovirus targeting the Rb pathway produces anti-glioma effect in vivo. *Oncogene* 19, 2-12 (**2000**).
87 **Howe, J. A., Demers, G. W., Johnson, D. E., Neugebauer, S. E., Perry, S. T., Vaillancourt, M. T. & Faha, B.** Evaluation of E1-mutant adenoviruses as conditionally replicating agents for cancer therapy. *Mol Ther* 2, 485-495 (**2000**).
88 **Sauthoff, H., Pipiya, T., Heitner, S., Chen, S., Bleck, B., Reibman, J., Chang, W., Norman, R. G., Rom, W. N. & Hay, J. G.** Impact of E1a modifications on tumor-selective adenoviral replication and toxicity. *Mol Ther* 10, 749-757 (**2004**).
89 **Iyer, N. G., Ozdag, H. & Caldas, C.** p300/CBP and cancer. *Oncogene* 23, 4225-4231 (**2004**).
90 **Goodman, R. H. & Smolik, S.** CBP/p300 in cell growth, transformation, and development. *Genes Dev* 14, 1553-1577 (**2000**).
91 **Chan, H. M. & La Thangue, N. B.** p300/CBP proteins: HATs for transcriptional bridges and scaffolds. *J Cell Sci* 114, 2363-2373 (**2001**).
92 **Chinnadurai, G.** Opposing oncogenic activities of small DNA tumor virus transforming proteins. *Trends in microbiology* 19, 174-183 (**2011**).
93 **Ianculescu, I., Wu, D. Y., Siegmund, K. D. & Stallcup, M. R.** Selective roles for cAMP response element-binding protein binding protein and p300 protein as coregulators for androgen-regulated gene expression in advanced prostate cancer cells. *The Journal of biological chemistry* 287, 4000-4013 (**2012**).
94 **Mymryk, J., Shire, K. & Bayley, S.** Induction of apoptosis by adenovirus type 5 E1A in rat cells requires a proliferation block. *Oncogene* 9, 1187-1193 (**1994**).
95 **Miranda, E., Maya Pineda, H., Öberg, D., Cherubini, G., Garate, Z., Lemoine, N. R. & Halldén, G.** Adenovirus-Mediated Sensitization to the Cytotoxic Drugs Docetaxel and Mitoxantrone Is Dependent on Regulatory Domains in the E1ACR1 Gene-Region. *PloS one* 7, e46617 (**2012**).
96 **Samuelson, A. V., Narita, M., Chan, H. M., Jin, J., de Stanchina, E., McCurrach, M. E., Narita, M., Fuchs, M., Livingston, D. M. & Lowe, S. W.**

p400 is required for E1A to promote apoptosis. *The Journal of biological chemistry* 280, 21915-21923 (**2005**).

97 **Kim, J., Kim, J. H., Choi, K. J., Kim, P. H. & Yun, C. O.** E1A- and E1B-Double mutant replicating adenovirus elicits enhanced oncolytic and antitumor effects. *Hum Gene Ther* 18, 773-786 (**2007**).

98 **Tsantoulis, P. K. & Gorgoulis, V. G.** Involvement of E2F transcription factor family in cancer. *Eur J Cancer* 41, 2403-2414 (**2005**).

99 **Ablack, J. N., Pelka, P., Yousef, A. F., Turnell, A. S., Grand, R. J. & Mymryk, J. S.** Comparison of E1A CR3-dependent transcriptional activation across six different human adenovirus subgroups. *J Virol* 84, 12771-12781 (**2010**).

100 **Pelka, P., Ablack, J. N., Torchia, J., Turnell, A. S., Grand, R. J. & Mymryk, J. S.** Transcriptional control by adenovirus E1A conserved region 3 via p300/CBP. *Nucleic Acids Res* 37, 1095-1106 (**2009**).

101 **Di, L. J., Byun, J. S., Wong, M. M., Wakano, C., Taylor, T., Bilke, S., Baek, S., Hunter, K., Yang, H., Lee, M., Zvosec, C., Khramtsova, G., Cheng, F., Perou, C. M., Miller, C. R., Raab, R., Olopade, O. I. & Gardner, K.** Genome-wide profiles of CtBP link metabolism with genome stability and epithelial reprogramming in breast cancer. *Nature communications* 4, 1449 (**2013**).

102 **Parato, K. A., Senger, D., Forsyth, P. A. & Bell, J. C.** Recent progress in the battle between oncolytic viruses and tumours. *Nat Rev Cancer* 5, 965-976 (**2005**).

103 **Waehler, R., Russell, S. J. & Curiel, D. T.** Engineering targeted viral vectors for gene therapy. *Nat Rev Genet* 8, 573-587 (**2007**).

104 **Young, L. S., Searle, P. F., Onion, D. & Mautner, V.** Viral gene therapy strategies: from basic science to clinical application. *J Pathol* 208, 299-318 (**2006**).

105 **Nemunaitis, J., Cunningham, C., Tong, A. W., Post, L., Netto, G., Paulson, A. S., Rich, D., Blackburn, A., Sands, B., Gibson, B., Randlev, B. & Freeman, S.** Pilot trial of intravenous infusion of a replication-selective adenovirus (ONYX-015) in combination with chemotherapy or IL-2 treatment in refractory cancer patients. *Cancer Gene Ther* 10, 341-352 (**2003**).

106 **Davis, J. J. & Fang, B.** Oncolytic virotherapy for cancer treatment: challenges and solutions. *J Gene Med* 7, 1380-1389 (**2005**).

107 **McCormick, F.** Cancer-specific viruses and the development of ONYX-015. *Cancer Biol Ther* 2, S157-160 (**2003**).

108 **Liu, T. C., Galanis, E. & Kirn, D.** Clinical trial results with oncolytic virotherapy: a century of promise, a decade of progress. *Nat Clin Pract Oncol* 4, 101-117 (**2007**).

109 **Garber, K.** China approves world's first oncolytic virus therapy for cancer treatment. *J Natl Cancer Inst* 98, 298-300 (**2006**).

110 **O'Shea, C. C., Johnson, L., Bagus, B., Choi, S., Nicholas, C., Shen, A., Boyle, L., Pandey, K., Soria, C., Kunich, J., Shen, Y., Habets, G., Ginzinger, D. & McCormick, F.** Late viral RNA export, rather than p53 inactivation, determines ONYX-015 tumor selectivity. *Cancer Cell* 6, 611-623 (**2004**).

111 **Hann, B. & Balmain, A.** Replication of an E1B 55-kilodalton protein-deficient adenovirus (ONYX-015) is restored by gain-of-function rather than loss-of-function p53 mutants. *J Virol* 77, 11588-11595 (**2003**).

112 **Aghi, M. & Martuza, R. L.** Oncolytic viral therapies - the clinical experience. *Oncogene* 24, 7802-7816 (**2005**).

113 **Hecht, J. R., Bedford, R., Abbruzzese, J. L., Lahoti, S., Reid, T. R., Soetikno, R. M., Kirn, D. H. & Freeman, S. M.** A phase I/II trial of intratumoral endoscopic ultrasound injection of ONYX-015 with intravenous gemcitabine in unresectable pancreatic carcinoma. *Clin Cancer Res* 9, 555-561 (**2003**).

114 **Bhattacharyya, M., Francis, J., Eddouadi, A., Lemoine, N. R. & Hallden, G.** An oncolytic adenovirus defective in pRb-binding (dl922-947) can efficiently eliminate pancreatic cancer cells and tumors in vivo in combination with 5-FU or gemcitabine. *Cancer Gene Ther* 18, 734-743 (**2011**).

115 **Cherubini, G., Kallin, C., Mozetic, A., Hammaren-Busch, K., Müller, H., Lemoine, N. & Halldén, G.** The oncolytic adenovirus AdΔΔ enhances selective cancer cell killing in combination with DNA-damaging drugs in pancreatic cancer models. *Gene therapy* 18, 1157-1165 (**2011**).

116 **Raki, M., Kanerva, A., Ristimaki, A., Desmond, R. A., Chen, D. T., Ranki, T., Sarkioja, M., Kangasniemi, L. & Hemminki, A.** Combination of gemcitabine and Ad5/3-Delta24, a tropism modified conditionally replicating adenovirus, for the treatment of ovarian cancer. *Gene Ther* 12, 1198-1205 (**2005**).

117 **Stolarek, R., Gomez-Manzano, C., Jiang, H., Suttle, G., Lemoine, M. G. & Fueyo, J.** Robust infectivity and replication of Delta-24 adenovirus induce cell death in human medulloblastoma. *Cancer Gene Ther* 11, 713-720 (**2004**).

118 **Oberg, D., Yanover, E., Adam, V., Sweeney, K., Costas, C., Lemoine, N. R. & Hallden, G.** Improved potency and selectivity of an oncolytic E1ACR2 and E1B19K deleted adenoviral mutant in prostate and pancreatic cancers. *Clin Cancer Res* 16, 541-553 (**2010**).

119 **Small, E. J., Carducci, M. A., Burke, J. M., Rodriguez, R., Fong, L., van Ummersen, L., Yu, D. C., Aimi, J., Ando, D., Working, P., Kirn, D. & Wilding, G.** A phase I trial of intravenous CG7870, a replication-selective, prostate-specific antigen-targeted oncolytic adenovirus, for the treatment of hormone-refractory, metastatic prostate cancer. *Mol Ther* 14, 107-117 (**2006**).

120 **DeWeese, T. L., van der Poel, H., Li, S., Mikhak, B., Drew, R., Goemann, M., Hamper, U., DeJong, R., Detorie, N., Rodriguez, R., Haulk, T., DeMarzo, A. M., Piantadosi, S., Yu, D. C., Chen, Y., Henderson, D. R., Carducci, M. A., Nelson, W. G. & Simons, J. W.** A phase I trial of CV706, a replication-competent, PSA selective oncolytic adenovirus, for the treatment of locally recurrent prostate cancer following radiation therapy. *Cancer Res* 61, 7464-7472 (**2001**).

121 **Freytag, S. O., Stricker, H., Peabody, J., Pegg, J., Paielli, D., Movsas, B., Barton, K. N., Brown, S. L., Lu, M. & Kim, J. H.** Five-year follow-up of trial of replication-competent adenovirus-mediated suicide gene therapy for treatment of prostate cancer. *Mol Ther* 15, 636-642 (**2007**).

122 **Schepelmann, S., Hallenbeck, P., Ogilvie, L. M., Hedley, D., Friedlos, F., Martin, J., Scanlon, I., Hay, C., Hawkins, L. K., Marais, R. & Springer, C. J.** Systemic gene-directed enzyme prodrug therapy of hepatocellular carcinoma using a targeted adenovirus armed with carboxypeptidase G2. *Cancer Res* 65, 5003-5008 (**2005**).

123 **Johnson, L., Shen, A., Boyle, L., Kunich, J., Pandey, K., Lemmon, M., Hermiston, T., Giedlin, M., McCormick, F. & Fattaey, A.** Selectively replicating adenoviruses targeting deregulated E2F activity are potent, systemic antitumor agents. *Cancer Cell* 1, 325-337 (**2002**).

124 **Lei, N., Shen, F. B., Chang, J. H., Wang, L., Li, H., Yang, C., Li, J. & Yu, D. C.** An oncolytic adenovirus expressing granulocyte macrophage colony-stimulating factor shows improved specificity and efficacy for treating human solid tumors. *Cancer Gene Ther* 16, 33-43 (**2009**).

125 **Schmitz, M., Graf, C., Gut, T., Sirena, D., Peter, I., Dummer, R., Greber, U. F. & Hemmi, S.** Melanoma cultures show different susceptibility towards E1A-, E1B-19 kDa- and fiber-modified replication-competent adenoviruses. *Gene Ther* 13, 893-905 (**2006**).

126 **Ekblad, M. & Halldén, G.** Adenovirus-based therapy for prostate cancer. *Current opinion in molecular therapeutics* 12, 421-431 (**2010**).

127 **Burke, J. M., Lamm, D. L., Meng, M. V., Nemunaitis, J. J., Stephenson, J. J., Arseneau, J. C., Aimi, J., Lerner, S., Yeung, A. W., Kazarian, T., Maslyar, D. J. & McKiernan, J. M.** A first in human phase 1 study of CG0070, a GM-CSF expressing oncolytic adenovirus, for the treatment of nonmuscle invasive bladder cancer. *J Urol* 188, 2391-2397 (**2012**).

128 **Kimball, K. J., Preuss, M. A., Barnes, M. N., Wang, M., Siegal, G. P., Wan, W., Kuo, H., Saddekni, S., Stockard, C. R., Grizzle, W. E., Harris, R. D., Aurigemma, R., Curiel, D. T. & Alvarez, R. D.** A phase I study of a tropism-modified conditionally replicative adenovirus for recurrent malignant gynecologic diseases. *Clin Cancer Res* 16, 5277-5287 (**2010**).

129 **Ueno, N., Bartholomeusz, C., Herrmann, J., Estrov, Z., Shao, R., Andreeff, M., Price, J., Paul, R., Anklesaria, P., Yu, D. & Hung, M.** E1A-mediated paclitaxel sensitization in HER-2/neu-overexpressing ovarian cancer SKOV3.ip1 through apoptosis involving the caspase-3 pathway. *Clinical cancer research : an official journal of the American Association for Cancer Research* 6, 250-259 (**2000**).

130 **Lowe, S., Ruley, H., Jacks, T. & Housman, D.** p53-dependent apoptosis modulates the cytotoxicity of anticancer agents. *Cell* 74, 957-967 (**1993**).

131 **Radhakrishnan, S., Miranda, E., Ekblad, M., Holford, A., Pizarro, M. T., Lemoine, N. R. & Hallden, G.** Efficacy of oncolytic mutants targeting pRb and p53 pathways is synergistically enhanced when combined with cytotoxic drugs in prostate cancer cells and tumour xenografts. *Hum Gene Ther* (**2010**).

132 **Debbas, M. & White, E.** Wild-type p53 mediates apoptosis by E1A, which is inhibited by E1B. *Genes & development* 7, 546-554 (**1993**).

133 **Sharma, A., Tandon, M., Bangari, D. & Mittal, S.** Adenoviral vector-based strategies for cancer therapy. *Current drug therapy* (**2009**).

134 **Cook, J., Miura, T., Iklé, D., Lewis, A. & Routes, J.** E1A oncogene-induced sensitization of human tumor cells to innate immune defenses and chemotherapy-induced apoptosis in vitro and in vivo. *Cancer research* (**2003**).

135 **Liao, Y., Yu, D. & Hung, M.** Novel approaches for chemosensitization of breast cancer cells: the E1A story. *Breast Cancer Chemosensitivity* (**2007**).

136 **Leitner, S., Sweeney, K., Oberg, D., Davies, D., Miranda, E., Lemoine, N. R. & Hallden, G.** Oncolytic adenoviral mutants with E1B19K gene deletions

enhance gemcitabine-induced apoptosis in pancreatic carcinoma cells and anti-tumor efficacy in vivo. *Clin Cancer Res* 15, 1730-1740 (**2009**).

137 **Adam, V., Ekblad, M., Sweeney, K., Müller, H., Busch, K., Johnsen, C., Kang, N., Lemoine, N. & Halldén, G.** Synergistic and Selective Cancer Cell Killing Mediated by the Oncolytic Adenoviral Mutant AdΔΔ and Dietary Phytochemicals in Prostate Cancer Models. *Human gene therapy* 23, 1003-1015 (**2012**).

138 **Gomez-Manzano, C., Alonso, M., Yung, W., McCormick, F., Curiel, D., Lang, F., Jiang, H., Bekele, B., Zhou, X., Alemany, R. & Fueyo, J.** Delta-24 increases the expression and activity of topoisomerase I and enhances the antiglioma effect of irinotecan. *Clinical cancer research : an official journal of the American Association for Cancer Research* 12, 556-562 (**2006**).

139 **Patel, M. R. & Kratzke, R. A.** Oncolytic virus therapy for cancer: the first wave of translational clinical trials. *Translational research : the journal of laboratory and clinical medicine* 161, 355-364 (**2013**).

140 **Liu, T. C. & Kirn, D.** Gene therapy progress and prospects cancer: oncolytic viruses. *Gene Ther* 15, 877-884 (**2008**).

141 **Markert, J. M., Medlock, M. D., Rabkin, S. D., Gillespie, G. Y., Todo, T., Hunter, W. D., Palmer, C. A., Feigenbaum, F., Tornatore, C., Tufaro, F. & Martuza, R. L.** Conditionally replicating herpes simplex virus mutant, G207 for the treatment of malignant glioma: results of a phase I trial. *Gene Ther* 7, 867-874 (**2000**).

142 **Kelly, K. J., Wong, J. & Fong, Y.** Herpes simplex virus NV1020 as a novel and promising therapy for hepatic malignancy. *Expert opinion on investigational drugs* 17, 1105-1113 (**2008**).

143 **Kemeny, N., Brown, K., Covey, A., Kim, T., Bhargava, A., Brody, L., Guilfoyle, B., Haag, N. P., Karrasch, M., Glasschroeder, B., Knoll, A., Getrajdman, G., Kowal, K. J., Jarnagin, W. R. & Fong, Y.** Phase I, open-label, dose-escalating study of a genetically engineered herpes simplex virus, NV1020, in subjects with metastatic colorectal carcinoma to the liver. *Hum Gene Ther* 17, 1214-1224 (**2006**).

144 **Geevarghese, S. K., Geller, D. A., de Haan, H. A., Horer, M., Knoll, A. E., Mescheder, A., Nemunaitis, J., Reid, T. R., Sze, D. Y., Tanabe, K. K. & Tawfik, H.** Phase I/II study of oncolytic herpes simplex virus NV1020 in patients with extensively pretreated refractory colorectal cancer metastatic to the liver. *Hum Gene Ther* 21, 1119-1128 (**2010**).

145 **Hu, J. C., Coffin, R. S., Davis, C. J., Graham, N. J., Groves, N., Guest, P. J., Harrington, K. J., James, N. D., Love, C. A., McNeish, I., Medley, L. C., Michael, A., Nutting, C. M., Pandha, H. S., Shorrock, C. A., Simpson, J., Steiner, J., Steven, N. M., Wright, D. & Coombes, R. C.** A phase I study of OncoVEXGM-CSF, a second-generation oncolytic herpes simplex virus expressing granulocyte macrophage colony-stimulating factor. *Clin Cancer Res* 12, 6737-6747 (**2006**).

146 **Liu, T. C., Zhang, T., Fukuhara, H., Kuroda, T., Todo, T., Canron, X., Bikfalvi, A., Martuza, R. L., Kurtz, A. & Rabkin, S. D.** Dominant-negative fibroblast growth factor receptor expression enhances antitumoral potency of oncolytic herpes simplex virus in neural tumors. *Clin Cancer Res* 12, 6791-6799 (**2006**).

147 **Liu, T. C., Zhang, T., Fukuhara, H., Kuroda, T., Todo, T., Martuza, R. L., Rabkin, S. D. & Kurtz, A.** Oncolytic HSV armed with platelet factor 4, an antiangiogenic agent, shows enhanced efficacy. *Mol Ther* 14, 789-797 (**2006**).

148 **Liu, T. C., Castelo-Branco, P., Rabkin, S. D. & Martuza, R. L.** Trichostatin A and oncolytic HSV combination therapy shows enhanced antitumoral and antiangiogenic effects. *Mol Ther* 16, 1041-1047 (**2008**).

149 **Cozzi, P. J., Burke, P. B., Bhargav, A., Heston, W. D., Huryk, B., Scardino, P. T. & Fong, Y.** Oncolytic viral gene therapy for prostate cancer using two attenuated, replication-competent, genetically engineered herpes simplex viruses. *Prostate* 53, 95-100 (**2002**).

150 **Amgen.** (**2013**).

151 **Lun, X. Q., Jang, J. H., Tang, N., Deng, H., Head, R., Bell, J. C., Stojdl, D. F., Nutt, C. L., Senger, D. L., Forsyth, P. A. & McCart, J. A.** Efficacy of systemically administered oncolytic vaccinia virotherapy for malignant gliomas is enhanced by combination therapy with rapamycin or cyclophosphamide. *Clin Cancer Res* 15, 2777-2788 (**2009**).

152 **Naik, A. M., Chalikonda, S., McCart, J. A., Xu, H., Guo, Z. S., Langham, G., Gardner, D., Mocellin, S., Lokshin, A. E., Moss, B., Alexander, H. R. & Bartlett, D. L.** Intravenous and isolated limb perfusion delivery of wild type and a tumor-selective replicating mutant vaccinia virus in nonhuman primates. *Hum Gene Ther* 17, 31-45 (**2006**).

153 **Hwang, T. H., Moon, A., Burke, J., Ribas, A., Stephenson, J., Breitbach, C. J., Daneshmand, M., De Silva, N., Parato, K., Diallo, J. S., Lee, Y. S., Liu, T. C., Bell, J. C. & Kirn, D. H.** A mechanistic proof-of-concept clinical trial with JX-594, a targeted multi-mechanistic oncolytic poxvirus, in patients with metastatic melanoma. *Mol Ther* 19, 1913-1922 (**2011**).

154 **Park, B. H., Hwang, T., Liu, T. C., Sze, D. Y., Kim, J. S., Kwon, H. C., Oh, S. Y., Han, S. Y., Yoon, J. H., Hong, S. H., Moon, A., Speth, K., Park, C., Ahn, Y. J., Daneshmand, M., Rhee, B. G., Pinedo, H. M., Bell, J. C. & Kirn, D. H.** Use of a targeted oncolytic poxvirus, JX-594, in patients with refractory primary or metastatic liver cancer: a phase I trial. *The lancet oncology* 9, 533-542 (**2008**).

155 **Fukuhara, H., Homma, Y. & Todo, T.** Oncolytic virus therapy for prostate cancer. *International journal of urology : official journal of the Japanese Urological Association* 17, 20-30 (**2010**).

156 **Thorne, S. H., Liang, W., Sampath, P., Schmidt, T., Sikorski, R., Beilhack, A. & Contag, C. H.** Targeting localized immune suppression within the tumor through repeat cycles of immune cell-oncolytic virus combination therapy. *Mol Ther* 18, 1698-1705 (**2010**).

157 **Lun, X., Ruan, Y., Jayanthan, A., Liu, D. J., Singh, A., Trippett, T., Bell, J., Forsyth, P., Johnston, R. N. & Narendran, A.** Double-deleted vaccinia virus in virotherapy for refractory and metastatic pediatric solid tumors. *Molecular oncology* (**2013**).

158 **Kirn, D., Wang, Y., Le Boeuf, F., Bell, J. & Thorne, S.** Targeting of interferon-beta to produce a specific, multi-mechanistic oncolytic vaccinia virus. *PLoS medicine* 4 (**2007**).

159 **Vidal, L., Pandha, H. S., Yap, T. A., White, C. L., Twigger, K., Vile, R. G., Melcher, A., Coffey, M., Harrington, K. J. & DeBono, J. S.** A phase I study of

intravenous oncolytic reovirus type 3 Dearing in patients with advanced cancer. *Clin Cancer Res* 14, 7127-7137 (**2008**).

160 **Russell, S. J., Peng, K. W. & Bell, J. C.** Oncolytic virotherapy. *Nat Biotechnol* 30, 658-670 (**2012**).

161 ***U.S. National Institutes of Health***. *Database of Clinical Trials*, <**www.clinicaltrials.gov** > (**2013**).

162 **Hasegawa, K., Nakamura, T., Harvey, M., Ikeda, Y., Oberg, A., Figini, M., Canevari, S., Hartmann, L. C. & Peng, K. W.** The use of a tropism-modified measles virus in folate receptor-targeted virotherapy of ovarian cancer. *Clin Cancer Res* 12, 6170-6178 (**2006**).

163 **Noyce, R. S. & Richardson, C. D.** Nectin 4 is the epithelial cell receptor for measles virus. *Trends in microbiology* 20, 429-439 (**2012**).

164 **Fabre-Lafay, S., Monville, F., Garrido-Urbani, S., Berruyer-Pouyet, C., Ginestier, C., Reymond, N., Finetti, P., Sauvan, R., Adelaide, J., Geneix, J., Lecocq, E., Popovici, C., Dubreuil, P., Viens, P., Goncalves, A., Charafe-Jauffret, E., Jacquemier, J., Birnbaum, D. & Lopez, M.** Nectin-4 is a new histological and serological tumor associated marker for breast cancer. *BMC cancer* 7, 73 (**2007**).

165 **Takano, A., Ishikawa, N., Nishino, R., Masuda, K., Yasui, W., Inai, K., Nishimura, H., Ito, H., Nakayama, H., Miyagi, Y., Tsuchiya, E., Kohno, N., Nakamura, Y. & Daigo, Y.** Identification of nectin-4 oncoprotein as a diagnostic and therapeutic target for lung cancer. *Cancer Res* 69, 6694-6703 (**2009**).

166 **Derycke, M. S., Pambuccian, S. E., Gilks, C. B., Kalloger, S. E., Ghidouche, A., Lopez, M., Bliss, R. L., Geller, M. A., Argenta, P. A., Harrington, K. M. & Skubitz, A. P.** Nectin 4 overexpression in ovarian cancer tissues and serum: potential role as a serum biomarker. *American journal of clinical pathology* 134, 835-845 (**2010**).

167 **Galanis, E., Hartmann, L. C., Cliby, W. A., Long, H. J., Peethambaram, P. P., Barrette, B. A., Kaur, J. S., Haluska, P. J., Jr., Aderca, I., Zollman, P. J., Sloan, J. A., Keeney, G., Atherton, P. J., Podratz, K. C., Dowdy, S. C., Stanhope, C. R., Wilson, T. O., Federspiel, M. J., Peng, K. W. & Russell, S. J.** Phase I trial of intraperitoneal administration of an oncolytic measles virus strain engineered to express carcinoembryonic antigen for recurrent ovarian cancer. *Cancer Res* 70, 875-882 (**2010**).

168 **Gauvrit, A., Brandler, S., Sapede-Peroz, C., Boisgerault, N., Tangy, F. & Gregoire, M.** Measles virus induces oncolysis of mesothelioma cells and allows dendritic cells to cross-prime tumor-specific CD8 response. *Cancer Res* 68, 4882-4892 (**2008**).

169 **Ong, H. T., Hasegawa, K., Dietz, A. B., Russell, S. J. & Peng, K. W.** Evaluation of T cells as carriers for systemic measles virotherapy in the presence of antiviral antibodies. *Gene Ther* 14, 324-333 (**2007**).

170 **Power, A., Wang, J., Falls, T., Paterson, J., Parato, K., Lichty, B., Stojdl, D., Forsyth, P., Atkins, H. & Bell, J.** Carrier cell-based delivery of an oncolytic virus circumvents antiviral immunity. *Molecular therapy : the journal of the American Society of Gene Therapy* 15, 123-130 (**2007**).

171 **Noser, J., Mael, A., Sakuma, R., Ohmine, S., Marcato, P., Lee, P. & Ikeda, Y.** The RAS/Raf1/MEK/ERK signaling pathway facilitates VSV-mediated oncolysis: implication for the defective interferon response in cancer cells. *Molecular therapy : the journal of the American Society of Gene Therapy* 15, 1531-1536 (**2007**).

172 **Carey, B., Ahmed, M., Puckett, S. & Lyles, D.** Early steps of the virus replication cycle are inhibited in prostate cancer cells resistant to oncolytic vesicular stomatitis virus. *Journal of virology* 82, 12104-12115 (**2008**).

173 **Stanford, M., Barrett, J., Nazarian, S., Werden, S. & McFadden, G.** Oncolytic virotherapy synergism with signaling inhibitors: Rapamycin increases myxoma virus tropism for human tumor cells. *Journal of virology* 81, 1251-1260 (**2007**).

174 **Berry, L., Au, G., Barry, R. & Shafren, D.** Potent oncolytic activity of human enteroviruses against human prostate cancer. *The Prostate* 68, 577-587 (**2008**).

175 **Wheelock, E. & Dingle, J.** OBSERVATIONS ON THE REPEATED ADMINISTRATION OF VIRUSES TO A PATIENT WITH ACUTE LEUKEMIA. A PRELIMINARY REPORT. *The New England journal of medicine* 271, 645-651 (**1964**).

176 **Pecora, A. L., Rizvi, N., Cohen, G. I., Meropol, N. J., Sterman, D., Marshall, J. L., Goldberg, S., Gross, P., O'Neil, J. D., Groene, W. S., Roberts, M. S., Rabin, H., Bamat, M. K. & Lorence, R. M.** Phase I trial of intravenous administration of PV701, an oncolytic virus, in patients with advanced solid cancers. *J Clin Oncol* 20, 2251-2266 (**2002**).

177 **Cassel, W. A. & Garrett, R. E.** Newcastle disease virus as an antineoplastic agent. *Cancer* 18, 863-868 (**1965**).

178 **Phuangsab, A., Lorence, R., Reichard, K., Peeples, M. & Walter, R.** Newcastle disease virus therapy of human tumor xenografts: antitumor effects of local or systemic administration. *Cancer letters* 172, 27-36 (**2001**).

179 **Lorence, R. M., Roberts, M. S., O'Neil, J. D., Groene, W. S., Miller, J. A., Mueller, S. N. & Bamat, M. K.** Phase 1 clinical experience using intravenous administration of PV701, an oncolytic Newcastle disease virus. *Current cancer drug targets* 7, 157-167 (**2007**).

180 **Bartel, D.** MicroRNAs: target recognition and regulatory functions. *Cell* 136, 215-233 (**2009**).

181 **Du, T. & Zamore, P. D.** microPrimer: the biogenesis and function of microRNA. *Development* 132, 4645-4652 (**2005**).

182 **Zhang, B., Pan, X., Cobb, G. P. & Anderson, T. A.** microRNAs as oncogenes and tumor suppressors. *Developmental biology* 302, 1-12 (**2007**).

183 **Waldman, S. A. & Terzic, A.** Applications of microRNA in cancer: Exploring the advantages of miRNA. *Clinical and translational science* 2, 248-249 (**2009**).

184 **Cheng, A., Byrom, M., Shelton, J. & Ford, L.** Antisense inhibition of human miRNAs and indications for an involvement of miRNA in cell growth and apoptosis. *Nucleic acids research* 33, 1290-1297 (**2005**).

185 **Lee, R. C., Feinbaum, R. L. & Ambros, V.** The C. elegans heterochronic gene lin-4 encodes small RNAs with antisense complementarity to lin-14. *Cell* 75, 843-854 (**1993**).

186 **Reinhart, B. J., Slack, F. J., Basson, M., Pasquinelli, A. E., Bettinger, J. C., Rougvie, A. E., Horvitz, H. R. & Ruvkun, G.** The 21-nucleotide let-7 RNA regulates developmental timing in Caenorhabditis elegans. *Nature* 403, 901-906 (**2000**).

187 **Lim, L. P., Glasner, M. E., Yekta, S., Burge, C. B. & Bartel, D. P.** Vertebrate microRNA genes. *Science* 299, 1540 (**2003**).

188 **Lewis, B. P., Burge, C. B. & Bartel, D. P.** Conserved seed pairing, often flanked by adenosines, indicates that thousands of human genes are microRNA targets. *Cell* 120, 15-20 (**2005**).

189 **Rodriguez, A., Griffiths-Jones, S., Ashurst, J. L. & Bradley, A.** Identification of mammalian microRNA host genes and transcription units. *Genome research* 14, 1902-1910 (**2004**).

190 **Baskerville, S. & Bartel, D. P.** Microarray profiling of microRNAs reveals frequent coexpression with neighboring miRNAs and host genes. *Rna* 11, 241-247 (**2005**).

191 **Lu, J., Getz, G., Miska, E. A., Alvarez-Saavedra, E., Lamb, J., Peck, D., Sweet-Cordero, A., Ebert, B. L., Mak, R. H., Ferrando, A. A., Downing, J. R., Jacks, T., Horvitz, H. R. & Golub, T. R.** MicroRNA expression profiles classify human cancers. *Nature* 435, 834-838 (**2005**).

192 **Krol, J., Loedige, I. & Filipowicz, W.** The widespread regulation of microRNA biogenesis, function and decay. *Nature reviews. Genetics* 11, 597-610 (**2010**).

193 **Lee, Y., Kim, M., Han, J., Yeom, K. H., Lee, S., Baek, S. H. & Kim, V. N.** MicroRNA genes are transcribed by RNA polymerase II. *The EMBO journal* 23, 4051-4060 (**2004**).

194 **Cai, X., Hagedorn, C. H. & Cullen, B. R.** Human microRNAs are processed from capped, polyadenylated transcripts that can also function as mRNAs. *Rna* 10, 1957-1966 (**2004**).

195 **Lee, Y., Jeon, K., Lee, J.-T., Kim, S. & Kim, V.** MicroRNA maturation: stepwise processing and subcellular localization. *The EMBO journal* 21, 4663-4670 (**2002**).

196 **Bartel, D. P.** MicroRNAs: genomics, biogenesis, mechanism, and function. *Cell* 116, 281-297 (**2004**).

197 **Denli, A., Tops, B., Plasterk, R., Ketting, R. & Hannon, G.** Processing of primary microRNAs by the Microprocessor complex. *Nature* 432, 231-235 (**2004**).

198 **Gregory, R. I., Yan, K. P., Amuthan, G., Chendrimada, T., Doratotaj, B., Cooch, N. & Shiekhattar, R.** The Microprocessor complex mediates the genesis of microRNAs. *Nature* 432, 235-240 (**2004**).

199 **Han, J., Lee, Y., Yeom, K. H., Kim, Y. K., Jin, H. & Kim, V. N.** The Drosha-DGCR8 complex in primary microRNA processing. *Genes Dev* 18, 3016-3027 (**2004**).

200 **Landthaler, M., Yalcin, A. & Tuschl, T.** The human DiGeorge syndrome critical region gene 8 and Its D. melanogaster homolog are required for miRNA biogenesis. *Current biology : CB* 14, 2162-2167 (**2004**).

201 **Yi, R., Qin, Y., Macara, I. G. & Cullen, B. R.** Exportin-5 mediates the nuclear export of pre-microRNAs and short hairpin RNAs. *Genes Dev* 17, 3011-3016 (**2003**).

202 **Okamura, K., Hagen, J. W., Duan, H., Tyler, D. M. & Lai, E. C.** The mirtron pathway generates microRNA-class regulatory RNAs in Drosophila. *Cell* 130, 89-100 (**2007**).
203 **Esquela-Kerscher, A. & Slack, F. J.** Oncomirs - microRNAs with a role in cancer. *Nat Rev Cancer* 6, 259-269 (**2006**).
204 **Tomari, Y. & Zamore, P. D.** MicroRNA biogenesis: drosha can't cut it without a partner. *Current biology : CB* 15, R61-64 (**2005**).
205 **Zhang, H., Kolb, F. A., Jaskiewicz, L., Westhof, E. & Filipowicz, W.** Single processing center models for human Dicer and bacterial RNase III. *Cell* 118, 57-68 (**2004**).
206 **Ketting, R. F., Fischer, S. E., Bernstein, E., Sijen, T., Hannon, G. J. & Plasterk, R. H.** Dicer functions in RNA interference and in synthesis of small RNA involved in developmental timing in C. elegans. *Genes Dev* 15, 2654-2659 (**2001**).
207 **Chendrimada, T. P., Gregory, R. I., Kumaraswamy, E., Norman, J., Cooch, N., Nishikura, K. & Shiekhattar, R.** TRBP recruits the Dicer complex to Ago2 for microRNA processing and gene silencing. *Nature* 436, 740-744 (**2005**).
208 **Gregory, R. I., Chendrimada, T. P., Cooch, N. & Shiekhattar, R.** Human RISC couples microRNA biogenesis and posttranscriptional gene silencing. *Cell* 123, 631-640 (**2005**).
209 **Hafner, M., Ascano, M., Jr. & Tuschl, T.** New insights in the mechanism of microRNA-mediated target repression. *Nature structural & molecular biology* 18, 1181-1182 (**2011**).
210 **Olena, A. F. & Patton, J. G.** Genomic organization of microRNAs. *Journal of cellular physiology* 222, 540-545 (**2010**).
211 **Lim, L. P., Lau, N. C., Garrett-Engele, P., Grimson, A., Schelter, J. M., Castle, J., Bartel, D. P., Linsley, P. S. & Johnson, J. M.** Microarray analysis shows that some microRNAs downregulate large numbers of target mRNAs. *Nature* 433, 769-773 (**2005**).
212 **Carthew, R. & Sontheimer, E.** Origins and Mechanisms of miRNAs and siRNAs. *Cell* 136, 642-655 (**2009**).
213 **Chekulaeva, M. & Filipowicz, W.** Mechanisms of miRNA-mediated post-transcriptional regulation in animal cells. *Current opinion in cell biology* 21, 452-460 (**2009**).
214 **Ricci, E., Limousin, T., Soto-Rifo, R., Rubilar, P., Decimo, D. & Ohlmann, T.** miRNA repression of translation in vitro takes place during 43S ribosomal scanning. *Nucleic acids research* 41, 586-598 (**2013**).
215 **Cifuentes, D., Xue, H., Taylor, D. W., Patnode, H., Mishima, Y., Cheloufi, S., Ma, E., Mane, S., Hannon, G. J., Lawson, N. D., Wolfe, S. A. & Giraldez, A. J.** A novel miRNA processing pathway independent of Dicer requires Argonaute2 catalytic activity. *Science* 328, 1694-1698 (**2010**).
216 **Fabian, M. R. & Sonenberg, N.** The mechanics of miRNA-mediated gene silencing: a look under the hood of miRISC. *Nature structural & molecular biology* 19, 586-593 (**2012**).
217 **Kolupaeva, V. G., Unbehaun, A., Lomakin, I. B., Hellen, C. U. & Pestova, T. V.** Binding of eukaryotic initiation factor 3 to ribosomal 40S subunits and its role in ribosomal dissociation and anti-association. *Rna* 11, 470-486 (**2005**).

218 **Le, H., Browning, K. S. & Gallie, D. R.** The phosphorylation state of poly(A)-binding protein specifies its binding to poly(A) RNA and its interaction with eukaryotic initiation factor (eIF) 4F, eIFiso4F, and eIF4B. *The Journal of biological chemistry* 275, 17452-17462 (**2000**).

219 **Filipowicz, W., Bhattacharyya, S. N. & Sonenberg, N.** Mechanisms of post-transcriptional regulation by microRNAs: are the answers in sight? *Nat Rev Genet* 9, 102-114 (**2008**).

220 **Liu, J., Rivas, F. V., Wohlschlegel, J., Yates, J. R., 3rd, Parker, R. & Hannon, G. J.** A role for the P-body component GW182 in microRNA function. *Nature cell biology* 7, 1261-1266 (**2005**).

221 **Hutvagner, G. & Zamore, P. D.** RNAi: nature abhors a double-strand. *Current opinion in genetics & development* 12, 225-232 (**2002**).

222 **Calin, G. A., Sevignani, C., Dumitru, C. D., Hyslop, T., Noch, E., Yendamuri, S., Shimizu, M., Rattan, S., Bullrich, F., Negrini, M. & Croce, C. M.** Human microRNA genes are frequently located at fragile sites and genomic regions involved in cancers. *Proceedings of the National Academy of Sciences of the United States of America* 101, 2999-3004 (**2004**).

223 **Huse, J., Brennan, C., Hambardzumyan, D., Wee, B., Pena, J., Rouhanifard, S., Sohn-Lee, C., le Sage, C., Agami, R., Tuschl, T. & Holland, E.** The PTEN-regulating microRNA miR-26a is amplified in high-grade glioma and facilitates gliomagenesis in vivo. *Genes & development* 23, 1327-1337 (**2009**).

224 **Garofalo, M. & Croce, C.** microRNAs: Master regulators as potential therapeutics in cancer. *Annual review of pharmacology and toxicology* 51, 25-43 (**2011**).

225 **Finnerty, J., Wang, W.-X., Hébert, S., Wilfred, B., Mao, G. & Nelson, P.** The miR-15/107 group of microRNA genes: evolutionary biology, cellular functions, and roles in human diseases. *Journal of molecular biology* 402, 491-509 (**2010**).

226 **Poliseno, L., Salmena, L., Riccardi, L., Fornari, A., Song, M., Hobbs, R., Sportoletti, P., Varmeh, S., Egia, A., Fedele, G., Rameh, L., Loda, M. & Pandolfi, P.** Identification of the miR-106b~25 microRNA cluster as a proto-oncogenic PTEN-targeting intron that cooperates with its host gene MCM7 in transformation. *Science signaling* 3 (**2010**).

227 **Jazbutyte, V. & Thum, T.** MicroRNA-21: from cancer to cardiovascular disease. *Current drug targets* 11, 926-935 (**2010**).

228 **Farazi, T., Spitzer, J., Morozov, P. & Tuschl, T.** miRNAs in human cancer. *The Journal of pathology* 223, 102-115 (**2011**).

229 **Zhang, L., Huang, J., Yang, N., Greshock, J., Megraw, M., Giannakakis, A., Liang, S., Naylor, T., Barchetti, A., Ward, M., Yao, G., Medina, A., O'Brien-Jenkins, A., Katsaros, D., Hatzigeorgiou, A., Gimotty, P., Weber, B. & Coukos, G.** microRNAs exhibit high frequency genomic alterations in human cancer. *Proceedings of the National Academy of Sciences of the United States of America* 103, 9136-9141 (**2006**).

230 **Lynam-Lennon, N., Maher, S. & Reynolds, J.** The roles of microRNA in cancer and apoptosis. *Biological reviews of the Cambridge Philosophical Society* 84, 55-71 (**2009**).

231 **Porkka, K. P., Pfeiffer, M. J., Waltering, K. K., Vessella, R. L., Tammela, T. L. & Visakorpi, T.** MicroRNA expression profiling in prostate cancer. *Cancer Res* 67, 6130-6135 (**2007**).

232 **Barbarotto, E., Schmittgen, T. D. & Calin, G. A.** MicroRNAs and cancer: profile, profile, profile. *International journal of cancer. Journal international du cancer* 122, 969-977 (**2008**).

233 **Heneghan, H., Miller, N. & Kerin, M.** MiRNAs as biomarkers and therapeutic targets in cancer. *Current opinion in pharmacology* 10, 543-550 (**2010**).

234 **Jiang, Q., Wang, Y., Hao, Y., Juan, L., Teng, M., Zhang, X., Li, M., Wang, G. & Liu, Y.** miR2Disease: a manually curated database for microRNA deregulation in human disease. *Nucleic Acids Res* 37, D98-104 (**2009**).

235 **Volinia, S., Calin, G. A., Liu, C. G., Ambs, S., Cimmino, A., Petrocca, F., Visone, R., Iorio, M., Roldo, C., Ferracin, M., Prueitt, R. L., Yanaihara, N., Lanza, G., Scarpa, A., Vecchione, A., Negrini, M., Harris, C. C. & Croce, C. M.** A microRNA expression signature of human solid tumors defines cancer gene targets. *Proceedings of the National Academy of Sciences of the United States of America* 103, 2257-2261 (**2006**).

236 **Ambs, S., Prueitt, R. L., Yi, M., Hudson, R. S., Howe, T. M., Petrocca, F., Wallace, T. A., Liu, C. G., Volinia, S., Calin, G. A., Yfantis, H. G., Stephens, R. M. & Croce, C. M.** Genomic profiling of microRNA and messenger RNA reveals deregulated microRNA expression in prostate cancer. *Cancer Res* 68, 6162-6170 (**2008**).

237 **Ozen, M., Creighton, C. J., Ozdemir, M. & Ittmann, M.** Widespread deregulation of microRNA expression in human prostate cancer. *Oncogene* 27, 1788-1793 (**2008**).

238 **Tong, A. W., Fulgham, P., Jay, C., Chen, P., Khalil, I., Liu, S., Senzer, N., Eklund, A. C., Han, J. & Nemunaitis, J.** MicroRNA profile analysis of human prostate cancers. *Cancer Gene Ther* 16, 206-216 (**2009**).

239 **Coppola, V., De Maria, R. & Bonci, D.** MicroRNAs and prostate cancer. *Endocrine-related cancer* 17, F1-17 (**2010**).

240 **Chiosea, S., Jelezcova, E., Chandran, U., Acquafondata, M., McHale, T., Sobol, R. & Dhir, R.** Up-regulation of dicer, a component of the MicroRNA machinery, in prostate adenocarcinoma. *The American journal of pathology* 169, 1812-1820 (**2006**).

241 **Pang, Y., Young, C. Y. F. & Yuan, H.** MicroRNAs and prostate cancer. *Acta Biochimica et Biophysica Sinica* 42 (**2010**).

242 **Vrba, L., Jensen, T., Garbe, J., Heimark, R., Cress, A., Dickinson, S., Stampfer, M. & Futscher, B.** Role for DNA methylation in the regulation of miR-200c and miR-141 expression in normal and cancer cells. *PloS one* 5 (**2010**).

243 **Papagiannakopoulos, T., Shapiro, A. & Kosik, K. S.** MicroRNA-21 targets a network of key tumor-suppressive pathways in glioblastoma cells. *Cancer Res* 68, 8164-8172 (**2008**).

244 **Ribas, J. & Lupold, S. E.** The transcriptional regulation of miR-21, its multiple transcripts, and their implication in prostate cancer. *Cell cycle* 9, 923-929 (**2010**).

245 **DeVere White, R., Vinall, R., Tepper, C. & Shi, X.-B.** MicroRNAs and their potential for translation in prostate cancer. *Urologic oncology* 27, 307-311 (**2009**).
246 **Dhar, S., Hicks, C. & Levenson, A.** Resveratrol and prostate cancer: promising role for microRNAs. *Molecular nutrition & food research* 55, 1219-1229 (**2011**).
247 **Chang, T.-C., Yu, D., Lee, Y.-S., Wentzel, E., Arking, D., West, K., Dang, C., Thomas-Tikhonenko, A. & Mendell, J.** Widespread microRNA repression by Myc contributes to tumorigenesis. *Nature genetics* 40, 43-50 (**2008**).
248 **O'Donnell, K., Wentzel, E., Zeller, K., Dang, C. & Mendell, J.** c-Myc-regulated microRNAs modulate E2F1 expression. *Nature* 435, 839-843 (**2005**).
249 **Kerr, J., Wyllie, A. & Currie, A.** Apoptosis: a basic biological phenomenon with wide-ranging implications in tissue kinetics. *British journal of cancer* 26, 239-257 (**1972**).
250 **Zeiss, C.** The apoptosis-necrosis continuum: insights from genetically altered mice. *Veterinary Pathology Online* (**2003**).
251 **Elmore, S.** Apoptosis: a review of programmed cell death. *Toxicologic pathology* 35, 495-516 (**2007**).
252 **Fadok, V., Bratton, D., Frasch, S., Warner, M. & Henson, P.** The role of phosphatidylserine in recognition of apoptotic cells by phagocytes. *Cell death and differentiation* 5, 551-562 (**1998**).
253 **Häcker, G.** The morphology of apoptosis. *Cell and tissue research* 301, 5-17 (**2000**).
254 **Horvitz, H.** Genetic control of programmed cell death in the nematode Caenorhabditis elegans. *Cancer research* 59 (**1999**).
255 **Norbury, C. & Hickson, I.** Cellular responses to DNA damage. *Annual review of pharmacology and toxicology* 41, 367-401 (**2001**).
256 **Long, J. & Ryan, K.** New frontiers in promoting tumour cell death: targeting apoptosis, necroptosis and autophagy. *Oncogene* (**2012**).
257 **Walczak, H. & Krammer, P.** The CD95 (APO-1/Fas) and the TRAIL (APO-2L) apoptosis systems. *Experimental cell research* 256, 58-66 (**2000**).
258 **Fulda, S. & Debatin, K. M.** Extrinsic versus intrinsic apoptosis pathways in anticancer chemotherapy. *Oncogene* 25, 4798-4811 (**2006**).
259 **Ashkenazi, A. & Dixit, V. M.** Death receptors: signaling and modulation. *Science* 281, 1305-1308 (**1998**).
260 **Martin, D., Siegel, R., Zheng, L. & Lenardo, M.** Membrane oligomerization and cleavage activates the caspase-8 (FLICE/MACHalpha1) death signal. *The Journal of biological chemistry* 273, 4345-4349 (**1998**).
261 **Schug, Z., Gonzalvez, F., Houtkooper, R., Vaz, F. & Gottlieb, E.** BID is cleaved by caspase-8 within a native complex on the mitochondrial membrane. *Cell death and differentiation* 18, 538-548 (**2011**).
262 **Lavrik, I., Golks, A. & Krammer, P.** Death receptor signaling. *Journal of cell science* 118, 265-267 (**2005**).
263 **Scaffidi, C., Fulda, S., Srinivasan, A., Friesen, C., Li, F., Tomaselli, K., Debatin, K., Krammer, P. & Peter, M.** Two CD95 (APO-1/Fas) signaling pathways. *The EMBO journal* 17, 1675-1687 (**1998**).

264 **Krammer, P.** CD95's deadly mission in the immune system. *Nature* 407, 789-795 (**2000**).
265 **Maiuri, M. C., Zalckvar, E., Kimchi, A. & Kroemer, G.** Self-eating and self-killing: crosstalk between autophagy and apoptosis. *Nat Rev Mol Cell Biol* 8, 741-752 (**2007**).
266 **Mayer, B. & Oberbauer, R.** Mitochondrial regulation of apoptosis. *News in physiological sciences : an international journal of physiology produced jointly by the International Union of Physiological Sciences and the American Physiological Society* 18, 89-94 (**2003**).
267 **Tait, S. & Green, D.** Mitochondria and cell death: outer membrane permeabilization and beyond. *Nature reviews. Molecular cell biology* 11, 621-632 (**2010**).
268 **Cain, K., Bratton, S., Langlais, C., Walker, G., Brown, D., Sun, X. & Cohen, G.** Apaf-1 oligomerizes into biologically active approximately 700-kDa and inactive approximately 1.4-MDa apoptosome complexes. *The Journal of biological chemistry* 275, 6067-6070 (**2000**).
269 **Sakahira, H., Enari, M. & Nagata, S.** Cleavage of CAD inhibitor in CAD activation and DNA degradation during apoptosis. *Nature* 391, 96-99 (**1998**).
270 **Degterev, A., Boyce, M. & Yuan, J.** A decade of caspases. *Oncogene* 22, 8543-8567 (**2003**).
271 **Yang, Q.-H., Church-Hajduk, R., Ren, J., Newton, M. & Du, C.** Omi/HtrA2 catalytic cleavage of inhibitor of apoptosis (IAP) irreversibly inactivates IAPs and facilitates caspase activity in apoptosis. *Genes & development* 17, 1487-1496 (**2003**).
272 **Verhagen, A., Ekert, P., Pakusch, M., Silke, J., Connolly, L., Reid, G., Moritz, R., Simpson, R. & Vaux, D.** Identification of DIABLO, a mammalian protein that promotes apoptosis by binding to and antagonizing IAP proteins. *Cell* 102, 43-53 (**2000**).
273 **Deveraux, Q., Takahashi, R., Salvesen, G. & Reed, J.** X-linked IAP is a direct inhibitor of cell-death proteases. *Nature* 388, 300-304 (**1997**).
274 **Youle, R. & Strasser, A.** The BCL-2 protein family: opposing activities that mediate cell death. *Nature reviews. Molecular cell biology* 9, 47-59 (**2008**).
275 **Kroemer, G., Galluzzi, L. & Brenner, C.** Mitochondrial membrane permeabilization in cell death. *Physiological reviews* 87, 99-163 (**2007**).
276 **Vousden, K. & Lane, D.** p53 in health and disease. *Nature reviews. Molecular cell biology* 8, 275-283 (**2007**).
277 **Tinel, A., Janssens, S., Lippens, S., Cuenin, S., Logette, E., Jaccard, B., Quadroni, M. & Tschopp, J.** Autoproteolysis of PIDD marks the bifurcation between pro-death caspase-2 and pro-survival NF-kappaB pathway. *The EMBO journal* 26, 197-208 (**2007**).
278 **Igney, F. & Krammer, P.** Death and anti-death: tumour resistance to apoptosis. *Nature reviews. Cancer* 2, 277-288 (**2002**).
279 **Tsujimoto, Y., Finger, L., Yunis, J., Nowell, P. & Croce, C.** Cloning of the chromosome breakpoint of neoplastic B cells with the t(14;18) chromosome translocation. *Science (New York, N.Y.)* 226, 1097-1099 (**1984**).

280 **Vaux, D., Cory, S. & Adams, J.** Bcl-2 gene promotes haemopoietic cell survival and cooperates with c-myc to immortalize pre-B cells. *Nature* 335, 440-442 (**1988**).

281 **Hockenbery, D., Nuñez, G., Milliman, C., Schreiber, R. & Korsmeyer, S.** Bcl-2 is an inner mitochondrial membrane protein that blocks programmed cell death. *Nature* 348, 334-336 (**1990**).

282 **Fecker, L., Geilen, C., Tchernev, G., Trefzer, U., Assaf, C., Kurbanov, B., Schwarz, C., Daniel, P. & Eberle, J.** Loss of proapoptotic Bcl-2-related multidomain proteins in primary melanomas is associated with poor prognosis. *The Journal of investigative dermatology* 126, 1366-1371 (**2006**).

283 **Olopade, O., Adeyanju, M., Safa, A., Hagos, F., Mick, R., Thompson, C. & Recant, W.** Overexpression of BCL-x protein in primary breast cancer is associated with high tumor grade and nodal metastases. *The cancer journal from Scientific American* 3, 230-237 (**1997**).

284 **Cheung, W., Kim, J., Linden, M., Peng, L., Van Ness, B., Polakiewicz, R. & Janz, S.** Novel targeted deregulation of c-Myc cooperates with Bcl-X(L) to cause plasma cell neoplasms in mice. *The Journal of clinical investigation* 113, 1763-1773 (**2004**).

285 **McDonnell, T. & Korsmeyer, S.** Progression from lymphoid hyperplasia to high-grade malignant lymphoma in mice transgenic for the t(14; 18). *Nature* 349, 254-256 (**1991**).

286 **Vousden, K. & Lu, X.** Live or let die: the cell's response to p53. *Nature reviews. Cancer* 2, 594-604 (**2002**).

287 **Wu, Y., Mehew, J., Heckman, C., Arcinas, M. & Boxer, L.** Negative regulation of bcl-2 expression by p53 in hematopoietic cells. *Oncogene* 20, 240-251 (**2001**).

288 **Jovanovic, M. & Hengartner, M.** miRNAs and apoptosis: RNAs to die for. *Oncogene* 25, 6176-6187 (**2006**).

289 **Garofalo, M., Quintavalle, C., Di Leva, G., Zanca, C., Romano, G., Taccioli, C., Liu, C., Croce, C. & Condorelli, G.** MicroRNA signatures of TRAIL resistance in human non-small cell lung cancer. *Oncogene* 27, 3845-3855 (**2008**).

290 **Felli, N., Fontana, L., Pelosi, E., Botta, R., Bonci, D., Facchiano, F., Liuzzi, F., Lulli, V., Morsilli, O., Santoro, S., Valtieri, M., Calin, G., Liu, C.-G., Sorrentino, A., Croce, C. & Peschle, C.** MicroRNAs 221 and 222 inhibit normal erythropoiesis and erythroleukemic cell growth via kit receptor down-modulation. *Proceedings of the National Academy of Sciences of the United States of America* 102, 18081-18086 (**2005**).

291 **Galardi, S., Mercatelli, N., Giorda, E., Massalini, S., Frajese, G., Ciafrè, S. & Farace, M.** miR-221 and miR-222 expression affects the proliferation potential of human prostate carcinoma cell lines by targeting p27Kip1. *The Journal of biological chemistry* 282, 23716-23724 (**2007**).

292 **Lankat-Buttgereit, B. & Göke, R.** Programmed cell death protein 4 (pdcd4): a novel target for antineoplastic therapy? *Biology of the cell / under the auspices of the European Cell Biology Organization* 95, 515-519 (**2003**).

293 **de Reuck AVS, C. M.** *Ciba Foundation Symposium on Lysosomes.*, London: J.A. Churchill Ltd,, (**1963**).

294 **Yang, Z. J., Chee, C. E., Huang, S. & Sinicrope, F. A.** The role of autophagy in cancer: therapeutic implications. *Molecular cancer therapeutics* 10, 1533-1541 (**2011**).
295 **Klionsky, D.** The molecular machinery of autophagy: unanswered questions. *Journal of cell science* 118, 7-18 (**2005**).
296 **Hansen, T. & Johansen, T.** Following autophagy step by step. *BMC biology* 9, 39 (**2011**).
297 **Eskelinen, E.-L.** Maturation of autophagic vacuoles in Mammalian cells. *Autophagy* 1, 1-10 (**2005**).
298 **Rosenfeldt, M. & Ryan, K.** The role of autophagy in tumour development and cancer therapy. *Expert reviews in molecular medicine* 11 (**2009**).
299 **Simonsen, A. & Tooze, S.** Coordination of membrane events during autophagy by multiple class III PI3-kinase complexes. *The Journal of cell biology* 186, 773-782 (**2009**).
300 **Jung, C., Jun, C., Ro, S.-H., Kim, Y.-M., Otto, N., Cao, J., Kundu, M. & Kim, D.-H.** ULK-Atg13-FIP200 complexes mediate mTOR signaling to the autophagy machinery. *Molecular biology of the cell* 20, 1992-2003 (**2009**).
301 **Jung, C., Ro, S.-H., Cao, J., Otto, N. & Kim, D.-H.** mTOR regulation of autophagy. *FEBS letters* 584, 1287-1295 (**2010**).
302 **Heitman, J., Movva, N. & Hall, M.** Targets for cell cycle arrest by the immunosuppressant rapamycin in yeast. *Science (New York, N.Y.)* 253, 905-909 (**1991**).
303 **Sarbassov, D., Ali, S., Kim, D.-H., Guertin, D., Latek, R., Erdjument-Bromage, H., Tempst, P. & Sabatini, D.** Rictor, a novel binding partner of mTOR, defines a rapamycin-insensitive and raptor-independent pathway that regulates the cytoskeleton. *Current biology : CB* 14, 1296-1302 (**2004**).
304 **Ganley, I., Lam, D. H., Wang, J., Ding, X., Chen, S. & Jiang, X.** ULK1.ATG13.FIP200 complex mediates mTOR signaling and is essential for autophagy. *The Journal of biological chemistry* 284, 12297-12305 (**2009**).
305 **Yang, Z. & Klionsky, D. J.** Mammalian autophagy: core molecular machinery and signaling regulation. *Current opinion in cell biology* 22, 124-131 (**2010**).
306 **Cebollero, E., van der Vaart, A. & Reggiori, F.** Understanding phosphatidylinositol-3-phosphate dynamics during autophagosome biogenesis. *Autophagy* 8, 1868-1870 (**2012**).
307 **Tooze, S., Jefferies, H., Kalie, E., Longatti, A., McAlpine, F., McKnight, N., Orsi, A., Polson, H., Razi, M., Robinson, D. & Webber, J.** Trafficking and signaling in mammalian autophagy. *IUBMB life* 62, 503-508 (**2010**).
308 **Rubinsztein, D., Codogno, P. & Levine, B.** Autophagy modulation as a potential therapeutic target for diverse diseases. *Nature reviews. Drug discovery* 11, 709-730 (**2012**).
309 **Wirawan, E., Lippens, S., Vanden Berghe, T., Romagnoli, A., Fimia, G., Piacentini, M. & Vandenabeele, P.** Beclin1: a role in membrane dynamics and beyond. *Autophagy* 8, 6-17 (**2012**).
310 **Molejon, M. I., Ropolo, A., Re, A. L., Boggio, V. & Vaccaro, M. I.** The VMP1-Beclin 1 interaction regulates autophagy induction. *Scientific reports* 3, 1055 (**2013**).

311 **Walczak, M. & Martens, S.** Dissecting the role of the Atg12-Atg5-Atg16 complex during autophagosome formation. *Autophagy* 9 (**2013**).
312 **Ohsumi, Y. & Mizushima, N.** Two ubiquitin-like conjugation systems essential for autophagy. *Seminars in cell & developmental biology* 15, 231-236 (**2004**).
313 **Mizushima, N. & Yoshimori, T.** How to interpret LC3 immunoblotting. *Autophagy* 3, 542-545 (**2007**).
314 **Kabeya, Y., Kamada, Y., Baba, M., Takikawa, H., Sasaki, M. & Ohsumi, Y.** Atg17 functions in cooperation with Atg1 and Atg13 in yeast autophagy. *Molecular biology of the cell* 16, 2544-2553 (**2005**).
315 **Kabeya, Y., Mizushima, N., Ueno, T., Yamamoto, A., Kirisako, T., Noda, T., Kominami, E., Ohsumi, Y. & Yoshimori, T.** LC3, a mammalian homologue of yeast Apg8p, is localized in autophagosome membranes after processing. *The EMBO journal* 19, 5720-5728 (**2000**).
316 **Hamasaki, M., Furuta, N., Matsuda, A., Nezu, A., Yamamoto, A., Fujita, N., Oomori, H., Noda, T., Haraguchi, T., Hiraoka, Y., Amano, A. & Yoshimori, T.** Autophagosomes form at ER-mitochondria contact sites. *Nature* (**2013**).
317 **Rowland, A. & Voeltz, G.** Endoplasmic reticulum-mitochondria contacts: function of the junction. *Nature reviews. Molecular cell biology* 13, 607-625 (**2012**).
318 **Liang, C., Lee, J.-s., Inn, K.-s., Gack, M., Li, Q., Roberts, E., Vergne, I., Deretic, V., Feng, P., Akazawa, C. & Jung, J.** Beclin1-binding UVRAG targets the class C Vps complex to coordinate autophagosome maturation and endocytic trafficking. *Nature cell biology* 10, 776-787 (**2008**).
319 **Mizushima, N., Ohsumi, Y. & Yoshimori, T.** Autophagosome formation in mammalian cells. *Cell structure and function* 27, 421-429 (**2002**).
320 **Moscat, J. & Diaz-Meco, M.** p62 at the crossroads of autophagy, apoptosis, and cancer. *Cell* 137, 1001-1004 (**2009**).
321 **Tanida, I.** Autophagosome formation and molecular mechanism of autophagy. *Antioxidants & redox signaling* 14, 2201-2214 (**2011**).
322 **Yang, Z., Huang, J., Geng, J., Nair, U. & Klionsky, D.** Atg22 recycles amino acids to link the degradative and recycling functions of autophagy. *Molecular biology of the cell* 17, 5094-5104 (**2006**).
323 **Yang, Z. & Klionsky, D.** Permeases recycle amino acids resulting from autophagy. *Autophagy* 3, 149-150 (**2007**).
324 **Levine, B. & Klionsky, D.** Development by self-digestion: molecular mechanisms and biological functions of autophagy. *Developmental cell* 6, 463-477 (**2004**).
325 **Zhang, H., Bosch-Marce, M., Shimoda, L., Tan, Y., Baek, J., Wesley, J., Gonzalez, F. & Semenza, G.** Mitochondrial autophagy is an HIF-1-dependent adaptive metabolic response to hypoxia. *The Journal of biological chemistry* 283, 10892-10903 (**2008**).
326 **Ravikumar, B., Berger, Z., Vacher, C., O'Kane, C. & Rubinsztein, D.** Rapamycin pre-treatment protects against apoptosis. *Human molecular genetics* 15, 1209-1216 (**2006**).
327 **Vazquez-Martin, A., Oliveras-Ferraros, C. & Menendez, J.** Autophagy facilitates the development of breast cancer resistance to the anti-HER2 monoclonal antibody trastuzumab. *PloS one* 4 (**2009**).

328 **Bray, K., Mathew, R., Lau, A., Kamphorst, J., Fan, J., Chen, J., Chen, H.-Y., Ghavami, A., Stein, M., DiPaola, R., Zhang, D., Rabinowitz, J. & White, E.** Autophagy suppresses RIP kinase-dependent necrosis enabling survival to mTOR inhibition. *PloS one* 7 (**2012**).

329 **Yang, S., Wang, X., Contino, G., Liesa, M., Sahin, E., Ying, H., Bause, A., Li, Y., Stommel, J., Dell'antonio, G., Mautner, J., Tonon, G., Haigis, M., Shirihai, O., Doglioni, C., Bardeesy, N. & Kimmelman, A.** Pancreatic cancers require autophagy for tumor growth. *Genes & development* 25, 717-729 (**2011**).

330 **Guo, J., Chen, H.-Y., Mathew, R., Fan, J., Strohecker, A., Karsli-Uzunbas, G., Kamphorst, J., Chen, G., Lemons, J., Karantza, V., Coller, H., Dipaola, R., Gelinas, C., Rabinowitz, J. & White, E.** Activated Ras requires autophagy to maintain oxidative metabolism and tumorigenesis. *Genes & development* 25, 460-470 (**2011**).

331 **Gong, C., Bauvy, C., Tonelli, G., Yue, W., Deloménie, C., Nicolas, V., Zhu, Y., Domergue, V., Marin-Esteban, V., Tharinger, H., Delbos, L., Gary-Gouy, H., Morel, A. P., Ghavami, S., Song, E., Codogno, P. & Mehrpour, M.** Beclin 1 and autophagy are required for the tumorigenicity of breast cancer stem-like/progenitor cells. *Oncogene* (**2012**).

332 **Carew, J., Kelly, K. & Nawrocki, S.** Autophagy as a target for cancer therapy: new developments. *Cancer management and research* 4, 357-365 (**2012**).

333 **Kimmelman, A.** The dynamic nature of autophagy in cancer. *Genes & development* 25, 1999-2010 (**2011**).

334 **Takamura, A., Komatsu, M., Hara, T., Sakamoto, A., Kishi, C., Waguri, S., Eishi, Y., Hino, O., Tanaka, K. & Mizushima, N.** Autophagy-deficient mice develop multiple liver tumors. *Genes & development* 25, 795-800 (**2011**).

335 **Inami, Y., Waguri, S., Sakamoto, A., Kouno, T., Nakada, K., Hino, O., Watanabe, S., Ando, J., Iwadate, M., Yamamoto, M., Lee, M.-S., Tanaka, K. & Komatsu, M.** Persistent activation of Nrf2 through p62 in hepatocellular carcinoma cells. *The Journal of cell biology* 193, 275-284 (**2011**).

336 **Mathew, R., Karp, C., Beaudoin, B., Vuong, N., Chen, G., Chen, H.-Y., Bray, K., Reddy, A., Bhanot, G., Gelinas, C., Dipaola, R., Karantza-Wadsworth, V. & White, E.** Autophagy suppresses tumorigenesis through elimination of p62. *Cell* 137, 1062-1075 (**2009**).

337 **Degenhardt, K., Mathew, R., Beaudoin, B., Bray, K., Anderson, D., Chen, G., Mukherjee, C., Shi, Y., Gélinas, C., Fan, Y., Nelson, D., Jin, S. & White, E.** Autophagy promotes tumor cell survival and restricts necrosis, inflammation, and tumorigenesis. *Cancer cell* 10, 51-64 (**2006**).

338 **Shimizu, S., Kanaseki, T., Mizushima, N., Mizuta, T., Arakawa-Kobayashi, S., Thompson, C. & Tsujimoto, Y.** Role of Bcl-2 family proteins in a non-apoptotic programmed cell death dependent on autophagy genes. *Nature cell biology* 6, 1221-1228 (**2004**).

339 **Scherz-Shouval, R., Shvets, E., Fass, E., Shorer, H., Gil, L. & Elazar, Z.** Reactive oxygen species are essential for autophagy and specifically regulate the activity of Atg4. *The EMBO journal* 26, 1749-1760 (**2007**).

340 **Espert, L., Denizot, M., Grimaldi, M., Robert-Hebmann, V., Gay, B., Varbanov, M., Codogno, P. & Biard-Piechaczyk, M.** Autophagy is involved in

T cell death after binding of HIV-1 envelope proteins to CXCR4. *The Journal of clinical investigation* 116, 2161-2172 (**2006**).

341 **Pattingre, S., Tassa, A., Qu, X., Garuti, R., Liang, X., Mizushima, N., Packer, M., Schneider, M. & Levine, B.** Bcl-2 antiapoptotic proteins inhibit Beclin 1-dependent autophagy. *Cell* 122, 927-939 (**2005**).

342 **Zhang, H., Kong, X., Kang, J., Su, J., Li, Y., Zhong, J. & Sun, L.** Oxidative stress induces parallel autophagy and mitochondria dysfunction in human glioma U251 cells. *Toxicological sciences : an official journal of the Society of Toxicology* 110, 376-388 (**2009**).

343 **Yousefi, S., Perozzo, R., Schmid, I., Ziemiecki, A., Schaffner, T., Scapozza, L., Brunner, T. & Simon, H.-U.** Calpain-mediated cleavage of Atg5 switches autophagy to apoptosis. *Nature cell biology* 8, 1124-1132 (**2006**).

344 **Rodriguez-Rocha, H., Gomez-Gutierrez, J., Garcia-Garcia, A., Rao, X.-M., Chen, L., McMasters, K. & Zhou, H.** Adenoviruses induce autophagy to promote virus replication and oncolysis. *Virology* 416, 9-15 (**2011**).

345 **Baird, S., Aerts, J., Eddaoudi, A., Lockley, M., Lemoine, N. & McNeish, I.** Oncolytic adenoviral mutants induce a novel mode of programmed cell death in ovarian cancer. *Oncogene* 27, 3081-3090 (**2008**).

346 **Ito, H., Aoki, H., Kühnel, F., Kondo, Y., Kubicka, S., Wirth, T., Iwado, E., Iwamaru, A., Fujiwara, K., Hess, K., Lang, F., Sawaya, R. & Kondo, S.** Autophagic cell death of malignant glioma cells induced by a conditionally replicating adenovirus. *Journal of the National Cancer Institute* 98, 625-636 (**2006**).

347 **Jiang, H., White, E., Ríos-Vicil, C., Xu, J., Gomez-Manzano, C. & Fueyo, J.** Human adenovirus type 5 induces cell lysis through autophagy and autophagy-triggered caspase activity. *Journal of virology* 85, 4720-4729 (**2011**).

348 **Piya, S., White, E., Klein, S., Jiang, H., McDonnell, T., Gomez-Manzano, C. & Fueyo, J.** The E1B19K oncoprotein complexes with Beclin 1 to regulate autophagy in adenovirus-infected cells. *PloS one* 6 (**2011**).

349 **Botta, G., Passaro, C., Libertini, S., Abagnale, A., Barbato, S., Maione, A., Hallden, G., Beguinot, F., Formisano, P. & Portella, G.** Inhibition of autophagy enhances the effects of E1A-defective oncolytic adenovirus dl922-947 against glioma cells in vitro and in vivo. *Human gene therapy* 23, 623-634 (**2012**).

350 **Hasei, J., Sasaki, T., Tazawa, H., Osaki, S., Yamakawa, Y., Kunisada, T., Yoshida, A., Hashimoto, Y., Onishi, T., Uno, F., Kagawa, S., Urata, Y., Ozaki, T. & Fujiwara, T.** Dual programmed cell death pathways induced by p53 transactivation overcome resistance to oncolytic adenovirus in human osteosarcoma cells. *Molecular cancer therapeutics* (**2013**).

351 **Zhu, H., Wu, H., Liu, X., Li, B., Chen, Y., Ren, X., Liu, C.-G. & Yang, J.-M.** Regulation of autophagy by a beclin 1-targeted microRNA, miR-30a, in cancer cells. *Autophagy* 5, 816-823 (**2009**).

352 **Xu, J., Wang, Y., Tan, X. & Jing, H.** MicroRNAs in autophagy and their emerging roles in crosstalk with apoptosis. *Autophagy* 8, 873-882 (**2012**).

353 **Fu, L.-l., Wen, X., Bao, J.-k. & Liu, B.** MicroRNA-modulated autophagic signaling networks in cancer. *The international journal of biochemistry & cell biology* 44, 733-736 (**2012**).

354 **Huang, Y., Chuang, A. & Ratovitski, E.** Phospho-ΔNp63α/miR-885-3p axis in tumor cell life and cell death upon cisplatin exposure. *Cell cycle (Georgetown, Tex.)* 10, 3938-3947 (**2011**).
355 **Frankel, L. & Lund, A.** MicroRNA regulation of autophagy. *Carcinogenesis* 33, 2018-2025 (**2012**).
356 **Tekirdag, K., Korkmaz, G., Ozturk, D., Agami, R. & Gozuacik, D.** MIR181A regulates starvation- and rapamycin-induced autophagy through targeting of ATG5. *Autophagy* 9, 374-385 (**2013**).
357 **Zou, Z., Wu, L., Ding, H., Wang, Y., Zhang, Y., Chen, X., Chen, X., Zhang, C.-Y., Zhang, Q. & Zen, K.** MicroRNA-30a sensitizes tumor cells to cis-platinum via suppressing beclin 1-mediated autophagy. *The Journal of biological chemistry* 287, 4148-4156 (**2012**).
358 **Yu, Y., Cao, L., Yang, L., Kang, R., Lotze, M. & Tang, D.** microRNA 30A promotes autophagy in response to cancer therapy. *Autophagy* 8, 853-855 (**2012**).
359 **Yu, Y., Yang, L., Zhao, M., Zhu, S., Kang, R., Vernon, P., Tang, D. & Cao, L.** Targeting microRNA-30a-mediated autophagy enhances imatinib activity against human chronic myeloid leukemia cells. *Leukemia* 26, 1752-1760 (**2012**).
360 **Halldén, G. & Portella, G.** Oncolytic virotherapy with modified adenoviruses and novel therapeutic targets. *Expert opinion on therapeutic targets* 16, 945-958 (**2012**).
361 **Cheong, S. C., Wang, Y., Meng, J. H., Hill, R., Sweeney, K., Kirn, D., Lemoine, N. R. & Hallden, G.** E1A-expressing adenoviral E3B mutants act synergistically with chemotherapeutics in immunocompetent tumor models. *Cancer Gene Ther* 15, 40-50 (**2008**).
362 **Miranda Rota, E. & Barts & the London Queen Mary's School of Medicine and Dentistry. Institute of Cancer.** *Identification of adenovirus E1A gene regions involved in chemosensitisation of prostate cancer cells. Thesis (PhD).* Queen Mary, University of London, 2009., (**2009**).
363 **Kaighn, M. E., Narayan, K. S., Ohnuki, Y., Lechner, J. F. & Jones, L. W.** Establishment and characterization of a human prostatic carcinoma cell line (PC-3). *Investigative urology* 17, 16-23 (**1979**).
364 (**2013**).
365 **Sramkoski, R. M., Pretlow, T. G., 2nd, Giaconia, J. M., Pretlow, T. P., Schwartz, S., Sy, M. S., Marengo, S. R., Rhim, J. S., Zhang, D. & Jacobberger, J. W.** A new human prostate carcinoma cell line, 22Rv1. *In vitro cellular & developmental biology. Animal* 35, 403-409 (**1999**).
366 **Stone, K. R., Mickey, D. D., Wunderli, H., Mickey, G. H. & Paulson, D. F.** Isolation of a human prostate carcinoma cell line (DU 145). *International journal of cancer. Journal international du cancer* 21, 274-281 (**1978**).
367 **Horoszewicz, J. S., Leong, S. S., Kawinski, E., Karr, J. P., Rosenthal, H., Chu, T. M., Mirand, E. A. & Murphy, G. P.** LNCaP model of human prostatic carcinoma. *Cancer Res* 43, 1809-1818 (**1983**).
368 **Heemers, H. V., Sebo, T. J., Debes, J. D., Regan, K. M., Raclaw, K. A., Murphy, L. M., Hobisch, A., Culig, Z. & Tindall, D. J.** Androgen deprivation increases p300 expression in prostate cancer cells. *Cancer Res* 67, 3422-3430 (**2007**).

369 **Skjoth, I. H. & Issinger, O. G.** Profiling of signaling molecules in four different human prostate carcinoma cell lines before and after induction of apoptosis. *International journal of oncology* 28, 217-229 (**2006**).
370 **Buick, R. N., Pullano, R. & Trent, J. M.** Comparative properties of five human ovarian adenocarcinoma cell lines. *Cancer Res* 45, 3668-3676 (**1985**).
371 **Flak, M. B., Connell, C. M., Chelala, C., Archibald, K., Salako, M. A., Pirlo, K. J., Lockley, M., Wheatley, S. P., Balkwill, F. R. & McNeish, I. A.** p21 Promotes oncolytic adenoviral activity in ovarian cancer and is a potential biomarker. *Mol Cancer* 9, 175 (**2010**).
372 **Leath, C. A., 3rd, Kataram, M., Bhagavatula, P., Gopalkrishnan, R. V., Dent, P., Fisher, P. B., Pereboev, A., Carey, D., Lebedeva, I. V., Haisma, H. J., Alvarez, R. D., Curiel, D. T. & Mahasreshti, P. J.** Infectivity enhanced adenoviral-mediated mda-7/IL-24 gene therapy for ovarian carcinoma. *Gynecol Oncol* 94, 352-362 (**2004**).
373 **Bai, F., Feng, J., Cheng, Y., Shi, J., Yang, R. & Cui, H.** Analysis of gene expression patterns of ovarian cancer cell lines with different metastatic potentials. *Int J Gynecol Cancer* 16, 202-209 (**2006**).
374 **Zhang, Y., Liao, J.-M., Zeng, S. & Lu, H.** p53 downregulates Down syndrome-associated DYRK1A through miR-1246. *EMBO reports* 12, 811-817 (**2011**).
375 **Mymryk, J. S., Lee, R. W. & Bayley, S. T.** Ability of adenovirus 5 E1A proteins to suppress differentiation of BC3H1 myoblasts correlates with their binding to a 300 kDa cellular protein. *Mol Biol Cell* 3, 1107-1115 (**1992**).
376 **Cook, J. L., Krantz, C. K. & Routes, B. A.** Role of p300-family proteins in E1A oncogene induction of cytolytic susceptibility and tumor cell rejection. *Proceedings of the National Academy of Sciences of the United States of America* 93, 13985-13990 (**1996**).
377 **Tony, N. J., John, A. H., Carole, M. E., Nina, F. C., Mario, H. S., Michael, R. F., Judy, E. D. & Stanley, T. B.** Use of deletion and point mutants spanning the coding region of the adenovirus 5 E1A gene to define a domain that is essential for transcriptional activation. *Virology* 163 (**1988**).
378 **O'Reilly, D. M. & VA, L.** 132-134 (**1994**).
379 **Chou, T. C.** Drug combination studies and their synergy quantification using the Chou-Talalay method. *Cancer Res* 70, 440-446 (**2010**).
380 **Halldén, G., Thorne, S., Yang, J. & Kirn, D.** Replication-selective oncolytic adenoviruses. *Methods in molecular medicine* 90, 71-90 (**2004**).
381 **Chou, T. C.** Theoretical basis, experimental design, and computerized simulation of synergism and antagonism in drug combination studies. *Pharmacol Rev* 58, 621-681 (**2006**).
382 **Griffiths-Jones, S., Saini, H., van Dongen, S. & Enright, A.** miRBase: tools for microRNA genomics. *Nucleic acids research* 36, 8 (**2008**).
383 **Sharov, V., Kwong, K., Frank, B. & Chen…, E.** The limits of log-ratios. *BMC …* (**2004**).
384 **Sun, T., Yang, M., Chen, S., Balk, S., Pomerantz, M., Hsieh, C.-L., Brown, M., Lee, G.-S. M. & Kantoff, P.** The altered expression of MiR-221/-222 and MiR-23b/-27b is associated with the development of human castration resistant prostate cancer. *The Prostate* 72, 1093-1103 (**2012**).

385 **Hessvik, N., Phuyal, S., Brech, A., Sandvig, K. & Llorente, A.** Profiling of microRNAs in exosomes released from PC-3 prostate cancer cells. *Biochimica et biophysica acta* 1819, 1154-1163 (**2012**).

386 **Venkatakrishnan, C. D., Dunsmore, K., Wong, H., Roy, S., Sen, C. K., Wani, A., Zweier, J. L. & Ilangovan, G.** HSP27 regulates p53 transcriptional activity in doxorubicin-treated fibroblasts and cardiac H9c2 cells: p21 upregulation and G2/M phase cell cycle arrest. *American journal of physiology. Heart and circulatory physiology* 294, H1736-1744 (**2008**).

387 **Mirbase**. <**www.mirbase.org**> (

388 **Rogler, C. E., Levoci, L., Ader, T., Massimi, A., Tchaikovskaya, T., Norel, R. & Rogler, L. E.** MicroRNA-23b cluster microRNAs regulate transforming growth factor-beta/bone morphogenetic protein signaling and liver stem cell differentiation by targeting Smads. *Hepatology* 50, 575-584 (**2009**).

389 **Chhabra, R., Adlakha, Y., Hariharan, M., Scaria, V. & Saini, N.** Upregulation of miR-23a-27a-24-2 cluster induces caspase-dependent and -independent apoptosis in human embryonic kidney cells. *PloS one* 4 (**2009**).

390 **Catto, J., Alcaraz, A., Bjartell, A., De Vere White, R., Evans, C., Fussel, S., Hamdy, F., Kallioniemi, O., Mengual, L., Schlomm, T. & Visakorpi, T.** MicroRNA in prostate, bladder, and kidney cancer: a systematic review. *European urology* 59, 671-681 (**2011**).

391 **Gong, J., Zhang, J. P., Li, B., Zeng, C., You, K., Chen, M. X., Yuan, Y. & Zhuang, S. M.** MicroRNA-125b promotes apoptosis by regulating the expression of Mcl-1, Bcl-w and IL-6R. *Oncogene* (**2012**).

392 **Cui, F., Li, X., Zhu, X., Huang, L., Huang, Y., Mao, C., Yan, Q., Zhu, J., Zhao, W. & Shi, H.** MiR-125b Inhibits Tumor Growth and Promotes Apoptosis of Cervical Cancer Cells by Targeting Phosphoinositide 3-Kinase Catalytic Subunit Delta. *Cellular physiology and biochemistry : international journal of experimental cellular physiology, biochemistry, and pharmacology* 30, 1310-1318 (**2012**).

393 **Majid, S., Dar, A., Saini, S., Arora, S., Shahryari, V., Zaman, M., Chang, I., Yamamura, S., Tanaka, Y., Deng, G. & Dahiya, R.** miR-23b represses proto-oncogene Src kinase and functions as methylation-silenced tumor suppressor with diagnostic and prognostic significance in prostate cancer. *Cancer research* 72, 6435-6446 (**2012**).

394 **Adlakha, Y. & Saini, N.** MicroRNA-128 downregulates Bax and induces apoptosis in human embryonic kidney cells. *Cellular and molecular life sciences : CMLS* 68, 1415-1428 (**2011**).

395 **Dong, Q., Meng, P., Wang, T., Qin, W., Qin, W., Wang, F., Yuan, J., Chen, Z., Yang, A. & Wang, H.** MicroRNA let-7a inhibits proliferation of human prostate cancer cells in vitro and in vivo by targeting E2F2 and CCND2. *PloS one* 5 (**2010**).

396 **Nadiminty, N., Tummala, R., Lou, W., Zhu, Y., Shi, X.-B., Zou, J., Chen, H., Zhang, J., Chen, X., Luo, J., deVere White, R., Kung, H.-J., Evans, C. & Gao, A.** MicroRNA let-7c is downregulated in prostate cancer and suppresses prostate cancer growth. *PloS one* 7 (**2012**).

397 **Bonci, D., Coppola, V., Musumeci, M., Addario, A., Giuffrida, R., Memeo, L., D'Urso, L., Pagliuca, A., Biffoni, M., Labbaye, C., Bartucci, M., Muto, G.,**

Peschle, C. & De Maria, R. The miR-15a-miR-16-1 cluster controls prostate cancer by targeting multiple oncogenic activities. *Nature medicine* 14, 1271-1277 (**2008**).

398 **Fendler, A., Stephan, C., Yousef, G. & Jung, K.** MicroRNAs as regulators of signal transduction in urological tumors. *Clinical chemistry* 57, 954-968 (**2011**).

399 **Zaman, M., Thamminana, S., Shahryari, V., Chiyomaru, T., Deng, G., Saini, S., Majid, S., Fukuhara, S., Chang, I., Arora, S., Hirata, H., Ueno, K., Singh, K., Tanaka, Y. & Dahiya, R.** Inhibition of PTEN gene expression by oncogenic miR-23b-3p in renal cancer. *PloS one* 7 (**2012**).

400 **Khan, A., Poisson, L., Bhat, V., Fermin, D., Zhao, R., Kalyana-Sundaram, S., Michailidis, G., Nesvizhskii, A., Omenn, G., Chinnaiyan, A. & Sreekumar, A.** Quantitative proteomic profiling of prostate cancer reveals a role for miR-128 in prostate cancer. *Molecular & cellular proteomics : MCP* 9, 298-312 (**2010**).

401 **Gao, P., Tchernyshyov, I., Chang, T.-C., Lee, Y.-S., Kita, K., Ochi, T., Zeller, K., De Marzo, A., Van Eyk, J., Mendell, J. & Dang, C.** c-Myc suppression of miR-23a/b enhances mitochondrial glutaminase expression and glutamine metabolism. *Nature* 458, 762-765 (**2009**).

402 **Moncini, S., Salvi, A., Zuccotti, P., Viero, G., Quattrone, A., Barlati, S., De Petro, G., Venturin, M. & Riva, P.** The role of miR-103 and miR-107 in regulation of CDK5R1 expression and in cellular migration. *PloS one* 6, e20038 (**2011**).

403 **Hirata, H., Hinoda, Y., Ueno, K., Nakajima, K., Ishii, N. & Dahiya, R.** MicroRNA-1826 directly targets beta-catenin (CTNNB1) and MEK1 (MAP2K1) in VHL-inactivated renal cancer. *Carcinogenesis* 33, 501-508 (**2012**).

404 **Ivanovska, I., Ball, A., Diaz, R., Magnus, J., Kibukawa, M., Schelter, J., Kobayashi, S., Lim, L., Burchard, J., Jackson, A., Linsley, P. & Cleary, M.** MicroRNAs in the miR-106b family regulate p21/CDKN1A and promote cell cycle progression. *Molecular and cellular biology* 28, 2167-2174 (**2008**).

405 **Petrocca, F., Vecchione, A. & Croce, C.** Emerging role of miR-106b-25/miR-17-92 clusters in the control of transforming growth factor beta signaling. *Cancer research* 68, 8191-8194 (**2008**).

406 **Ribas, J., Ni, X., Haffner, M., Wentzel, E., Salmasi, A., Chowdhury, W., Kudrolli, T., Yegnasubramanian, S., Luo, J., Rodriguez, R., Mendell, J. & Lupold, S.** miR-21: an androgen receptor-regulated microRNA that promotes hormone-dependent and hormone-independent prostate cancer growth. *Cancer research* 69, 7165-7169 (**2009**).

407 **Wang, K. & Li, P.-F.** Foxo3a regulates apoptosis by negatively targeting miR-21. *The Journal of biological chemistry* 285, 16958-16966 (**2010**).

408 **Segura, M., Hanniford, D., Menendez, S., Reavie, L., Zou, X., Alvarez-Diaz, S., Zakrzewski, J., Blochin, E., Rose, A., Bogunovic, D., Polsky, D., Wei, J., Lee, P., Belitskaya-Levy, I., Bhardwaj, N., Osman, I. & Hernando, E.** Aberrant miR-182 expression promotes melanoma metastasis by repressing FOXO3 and microphthalmia-associated transcription factor. *Proceedings of the National Academy of Sciences of the United States of America* 106, 1814-1819 (**2009**).

409 **Elyakim, E., Sitbon, E., Faerman, A., Tabak, S., Montia, E., Belanis, L., Dov, A., Marcusson, E., Bennett, C., Chajut, A., Cohen, D. & Yerushalmi, N.** hsa-miR-

191 is a candidate oncogene target for hepatocellular carcinoma therapy. *Cancer research* 70, 8077-8087 (**2010**).

410 **Hong, L., Lai, M., Chen, M., Xie, C., Liao, R., Kang, Y., Xiao, C., Hu, W.-Y., Han, J. & Sun, P.** The miR-17-92 cluster of microRNAs confers tumorigenicity by inhibiting oncogene-induced senescence. *Cancer research* 70, 8547-8557 (**2010**).

411 **Tanida, I., Ueno, T. & Kominami, E.** in *Autophagosome and Phagosome* Vol. 445 *Methods in Molecular Biology™* (ed Vojo Deretic) 77-88 (Humana Press, **2008**).

412 **Bjorkoy, G., Lamark, T., Brech, A., Outzen, H., Perander, M., Overvatn, A., Stenmark, H. & Johansen, T.** p62/SQSTM1 forms protein aggregates degraded by autophagy and has a protective effect on huntingtin-induced cell death. *The Journal of cell biology* 171, 603-614 (**2005**).

413 **Kuusisto, E., Suuronen, T. & Salminen, A.** Ubiquitin-binding protein p62 expression is induced during apoptosis and proteasomal inhibition in neuronal cells. *Biochemical and biophysical research communications* 280, 223-228 (**2001**).

414 **Sarker, D., Reid, A., Yap, T. & de Bono, J.** Targeting the PI3K/AKT pathway for the treatment of prostate cancer. *Clinical cancer research : an official journal of the American Association for Cancer Research* 15, 4799-4805 (**2009**).

415 **Zhang, X., Tang, N., Hadden, T. & Rishi, A.** Akt, FoxO and regulation of apoptosis. *Biochimica et biophysica acta* 1813, 1978-1986 (**2011**).

416 **Floc'h, N., Kinkade, C., Kobayashi, T., Aytes, A., Lefebvre, C., Mitrofanova, A., Cardiff, R., Califano, A., Shen, M. & Abate-Shen, C.** Dual targeting of the Akt/mTOR signaling pathway inhibits castration-resistant prostate cancer in a genetically engineered mouse model. *Cancer research* 72, 4483-4493 (**2012**).

417 **Yap, T., Garrett, M., Walton, M., Raynaud, F., de Bono, J. & Workman, P.** Targeting the PI3K-AKT-mTOR pathway: progress, pitfalls, and promises. *Current opinion in pharmacology* 8, 393-412 (**2008**).

418 **Zhou, F., Yang, Y. & Xing, D.** Bcl-2 and Bcl-xL play important roles in the crosstalk between autophagy and apoptosis. *The FEBS journal* 278, 403-413 (**2011**).

419 **Massague, J.** G1 cell-cycle control and cancer. *Nature* 432, 298-306 (**2004**).

420 **Vermeulen, K., Van Bockstaele, D. R. & Berneman, Z. N.** The cell cycle: a review of regulation, deregulation and therapeutic targets in cancer. *Cell Prolif* 36, 131-149 (**2003**).

421 **Potter, A. J. & Rabinovitch, P. S.** The cell cycle phases of DNA damage and repair initiated by topoisomerase II-targeting chemotherapeutic drugs. *Mutat Res* 572, 27-44 (**2005**).

422 **Trouche, D. & Kouzarides, T.** E2F1 and E1A(12S) have a homologous activation domain regulated by RB and CBP. *Proceedings of the National Academy of Sciences of the United States of America* 93, 1439-1442 (**1996**).

423 **Satyanarayana, A. & Kaldis, P.** Mammalian cell-cycle regulation: several Cdks, numerous cyclins and diverse compensatory mechanisms. *Oncogene* 28, 2925-2939 (**2009**).

424 **Kadowaki, Y., Chari, N. S., Teo, A. E., Hashi, A., Spurgers, K. B. & McDonnell, T. J.** PI3 Kinase inhibition on TRAIL-induced apoptosis correlates with

androgen-sensitivity and p21 expression in prostate cancer cells. *Apoptosis* 16, 627-635 (**2011**).

425 **Chattopadhyay, D., Ghosh, M. K., Mal, A. & Harter, M. L.** Inactivation of p21 by E1A leads to the induction of apoptosis in DNA-damaged cells. *J Virol* 75, 9844-9856 (**2001**).

426 **Koniaras, K., Cuddihy, A. R., Christopoulos, H., Hogg, A. & O'Connell, M. J.** Inhibition of Chk1-dependent G2 DNA damage checkpoint radiosensitizes p53 mutant human cells. *Oncogene* 20, 7453-7463 (**2001**).

427 **Chung, J. H. & Bunz, F.** Cdk2 is required for p53-independent G2/M checkpoint control. *PLoS Genet* 6, e1000863 (**2010**).

428 **Savelyeva, I. & Dobbelstein, M.** Infection with E1B-mutant adenovirus stabilizes p53 but blocks p53 acetylation and activity through E1A. *Oncogene* 30, 865-875 (**2011**).

429 **Fogal, V., Hsieh, J. K., Royer, C., Zhong, S. & Lu, X.** Cell cycle-dependent nuclear retention of p53 by E2F1 requires phosphorylation of p53 at Ser315. *The EMBO journal* 24, 2768-2782 (**2005**).

430 **Hiyama, H., Iavarone, A., LaBaer, J. & Reeves, S. A.** Regulated ectopic expression of cyclin D1 induces transcriptional activation of the cdk inhibitor p21 gene without altering cell cycle progression. *Oncogene* 14, 2533-2542 (**1997**).

431 **Gillis, L. D., Leidal, A. M., Hill, R. & Lee, P. W.** p21Cip1/WAF1 mediates cyclin B1 degradation in response to DNA damage. *Cell cycle* 8, 253-256 (**2009**).

432 **Furuta, T., Hayward, R. L., Meng, L. H., Takemura, H., Aune, G. J., Bonner, W. M., Aladjem, M. I., Kohn, K. W. & Pommier, Y.** p21CDKN1A allows the repair of replication-mediated DNA double-strand breaks induced by topoisomerase I and is inactivated by the checkpoint kinase inhibitor 7-hydroxystaurosporine. *Oncogene* 25, 2839-2849 (**2006**).

433 **Zhou, Z., Guan, H. & Kleinerman, E. S.** E1A specifically enhances sensitivity to topoisomerase IIalpha targeting anticancer drug by up-regulating the promoter activity. *Mol Cancer Res* 3, 271-275 (**2005**).

434 **Adam, V. S.** *Prostate cancer targeting using replication-selective adenoviruses in combination with phytochemicals. Thesis (PhD)*, Queen Mary, University of London, 2009., (**2009**).

435 **Gundara, J. S., Robinson, B. G. & Sidhu, S. B.** Evolution of the "autophagamiR". *Autophagy* 7, 1553-1554 (**2011**).

436 **Meenhuis, A., van Veelen, P., de Looper, H., van Boxtel, N., van den Berge, I., Sun, S., Taskesen, E., Stern, P., de Ru, A., van Adrichem, A., Demmers, J., Jongen-Lavrencic, M., Löwenberg, B., Touw, I., Sharp, P. & Erkeland, S.** MiR-17/20/93/106 promote hematopoietic cell expansion by targeting sequestosome 1-regulated pathways in mice. *Blood* 118, 916-925 (**2011**).

437 **Michaud, M., Martins, I., Sukkurwala, A., Adjemian, S., Ma, Y., Pellegatti, P., Shen, S., Kepp, O., Scoazec, M., Mignot, G., Rello-Varona, S., Tailler, M., Menger, L., Vacchelli, E., Galluzzi, L., Ghiringhelli, F., di Virgilio, F., Zitvogel, L. & Kroemer, G.** Autophagy-dependent anticancer immune responses induced by chemotherapeutic agents in mice. *Science (New York, N.Y.)* 334, 1573-1577 (**2011**).

438 **Dreux, M. & Chisari, F. V.** Viruses and the autophagy machinery. *Cell cycle* 9, 1295-1307 (**2010**).
439 **Zhou, D. & Spector, S. A.** Human immunodeficiency virus type-1 infection inhibits autophagy. *Aids* 22, 695-699 (**2008**).
440 **Gannage, M., Dormann, D., Albrecht, R., Dengjel, J., Torossi, T., Ramer, P. C., Lee, M., Strowig, T., Arrey, F., Conenello, G., Pypaert, M., Andersen, J., Garcia-Sastre, A. & Munz, C.** Matrix protein 2 of influenza A virus blocks autophagosome fusion with lysosomes. *Cell host & microbe* 6, 367-380 (**2009**).
441 **Adlakha, Y. K. & Saini, N.** miR-128 exerts pro-apoptotic effect in a p53 transcription-dependent and -independent manner via PUMA-Bak axis. *Cell death & disease* 4, e542 (**2013**).
442 **Miller-Jensen, K., Janes, K. A., Wong, Y. L., Griffith, L. G. & Lauffenburger, D. A.** Adenoviral vector saturates Akt pro-survival signaling and blocks insulin-mediated rescue of tumor necrosis-factor-induced apoptosis. *J Cell Sci* 119, 3788-3798 (**2006**).
443 **Littlewood, T. & Bennett, M.** Foxing smooth muscle cells: FOXO3a-CYR61 connection. *Circulation research* 100, 302-304 (**2007**).
444 **Baehrecke, E.** Autophagy: dual roles in life and death? *Nature reviews. Molecular cell biology* 6, 505-510 (**2005**).
445 **Hudson, R. S., Yi, M., Esposito, D., Glynn, S. A., Starks, A. M., Yang, Y., Schetter, A. J., Watkins, S. K., Hurwitz, A. A., Dorsey, T. H., Stephens, R. M., Croce, C. M. & Ambs, S.** MicroRNA-106b-25 cluster expression is associated with early disease recurrence and targets caspase-7 and focal adhesion in human prostate cancer. *Oncogene* (**2012**).
446 **Trompeter, H.-I., Abbad, H., Iwaniuk, K., Hafner, M., Renwick, N., Tuschl, T., Schira, J., Müller, H. & Wernet, P.** MicroRNAs MiR-17, MiR-20a, and MiR-106b act in concert to modulate E2F activity on cell cycle arrest during neuronal lineage differentiation of USSC. *PloS one* 6 (**2011**).
447 **Petrocca, F., Visone, R., Onelli, M., Shah, M., Nicoloso, M., de Martino, I., Iliopoulos, D., Pilozzi, E., Liu, C.-G., Negrini, M., Cavazzini, L., Volinia, S., Alder, H., Ruco, L., Baldassarre, G., Croce, C. & Vecchione, A.** E2F1-regulated microRNAs impair TGFbeta-dependent cell-cycle arrest and apoptosis in gastric cancer. *Cancer cell* 13, 272-286 (**2008**).
448 **Roush, S. & Slack, F.** The let-7 family of microRNAs. *Trends in cell biology* 18, 505-516 (**2008**).
449 **Kong, D., Heath, E., Chen, W., Cher, M. L., Powell, I., Heilbrun, L., Li, Y., Ali, S., Sethi, S., Hassan, O., Hwang, C., Gupta, N., Chitale, D., Sakr, W. A., Menon, M. & Sarkar, F. H.** Loss of let-7 up-regulates EZH2 in prostate cancer consistent with the acquisition of cancer stem cell signatures that are attenuated by BR-DIM. *PloS one* 7, e33729 (**2012**).
450 **Sun, D., Layer, R., Mueller, A. C., Cichewicz, M. A., Negishi, M., Paschal, B. M. & Dutta, A.** Regulation of several androgen-induced genes through the repression of the miR-99a/let-7c/miR-125b-2 miRNA cluster in prostate cancer cells. *Oncogene* (**2013**).
451 **Nadiminty, N., Tummala, R., Lou, W., Zhu, Y., Zhang, J., Chen, X., eVere White, R. W., Kung, H. J., Evans, C. P. & Gao, A. C.** MicroRNA let-7c

suppresses androgen receptor expression and activity via regulation of Myc expression in prostate cancer cells. *The Journal of biological chemistry* 287, 1527-1537 (**2012**).

452 **Amir, S., Ma, A. H., Shi, X. B., Xue, L., Kung, H. J. & Devere White, R. W.** Oncomir miR-125b Suppresses p14(ARF) to Modulate p53-Dependent and p53-Independent Apoptosis in Prostate Cancer. *PloS one* 8, e61064 (**2013**).

453 **Cimmino, A., Calin, G., Fabbri, M., Iorio, M., Ferracin, M., Shimizu, M., Wojcik, S., Aqeilan, R., Zupo, S., Dono, M., Rassenti, L., Alder, H., Volinia, S., Liu, C.-G., Kipps, T., Negrini, M. & Croce, C.** miR-15 and miR-16 induce apoptosis by targeting BCL2. *Proceedings of the National Academy of Sciences of the United States of America* 102, 13944-13949 (**2005**).

454 **Zhang, X., Chen, X., Lin, J., Lwin, T., Wright, G., Moscinski, L. C., Dalton, W. S., Seto, E., Wright, K., Sotomayor, E. & Tao, J.** Myc represses miR-15a/miR-16-1 expression through recruitment of HDAC3 in mantle cell and other non-Hodgkin B-cell lymphomas. *Oncogene* 31, 3002-3008 (**2012**).

455 **Ofir, M., Hacohen, D. & Ginsberg, D.** MiR-15 and miR-16 are direct transcriptional targets of E2F1 that limit E2F-induced proliferation by targeting cyclin E. *Mol Cancer Res* 9, 440-447 (**2011**).

456 **Engelmann, D. & Putzer, B. M.** The dark side of E2F1: in transit beyond apoptosis. *Cancer Res* 72, 571-575 (**2012**).

457 **Ruvolo, P. P., Deng, X. & May, W. S.** Phosphorylation of Bcl2 and regulation of apoptosis. *Leukemia* 15, 515-522 (**2001**).

458 **Wei, Y., Pattingre, S., Sinha, S., Bassik, M. & Levine, B.** JNK1-mediated phosphorylation of Bcl-2 regulates starvation-induced autophagy. *Molecular cell* 30, 678-688 (**2008**).

459 **Yamakuchi, M., Lotterman, C., Bao, C., Hruban, R., Karim, B., Mendell, J., Huso, D. & Lowenstein, C.** P53-induced microRNA-107 inhibits HIF-1 and tumor angiogenesis. *Proceedings of the National Academy of Sciences of the United States of America* 107, 6334-6339 (**2010**).

460 **Podhorecka, M., Skladanowski, A. & Bozko, P.** H2AX Phosphorylation: Its Role in DNA Damage Response and Cancer Therapy. *Journal of nucleic acids* 2010 (**2010**).

461 **Allocati, N., Di Ilio, C. & De Laurenzi, V.** p63/p73 in the control of cell cycle and cell death. *Exp Cell Res* 318, 1285-1290 (**2012**).

462 **Bitomsky, N. & Hofmann, T. G.** Apoptosis and autophagy: Regulation of apoptosis by DNA damage signalling - roles of p53, p73 and HIPK2. *FEBS J* 276, 6074-6083 (**2009**).

463 **Yan, Z., Shah, P., Amin, S., Samur, M., Huang, N., Wang, X., Misra, V., Ji, H., Gabuzda, D. & Li, C.** Integrative analysis of gene and miRNA expression profiles with transcription factor-miRNA feed-forward loops identifies regulators in human cancers. *Nucleic acids research* 40 (**2012**).

464 **Lin, C.-C., Chen, Y.-J., Chen, C.-Y., Oyang, Y.-J., Juan, H.-F. & Huang, H.-C.** Crosstalk between transcription factors and microRNAs in human protein interaction network. *BMC systems biology* 6, 18 (**2012**).

465 **Arora, S., Rana, R., Chhabra, A., Jaiswal, A. & Rani, V.** miRNA-transcription factor interactions: a combinatorial regulation of gene expression. *Molecular genetics and genomics : MGG* 288, 77-87 (**2013**).

466 **Wang, J., Lu, M., Qiu, C. & Cui, Q.** TransmiR: a transcription factor-microRNA regulation database. *Nucleic Acids Res* 38, D119-122 (**2010**).
467 **El Baroudi, M., Corà, D., Bosia, C., Osella, M. & Caselle, M.** A curated database of miRNA mediated feed-forward loops involving MYC as master regulator. *PloS one* 6 (**2011**).
468 **Wong, J. V., Yao, G., Nevins, J. R. & You, L.** Viral-mediated noisy gene expression reveals biphasic E2f1 response to MYC. *Molecular cell* 41, 275-285 (**2011**).
469 **Hallstrom, T. C., Mori, S. & Nevins, J. R.** An E2F1-dependent gene expression program that determines the balance between proliferation and cell death. *Cancer Cell* 13, 11-22 (**2008**).
470 **Ginsberg, D.** E2F1 pathways to apoptosis. *FEBS Lett* 529, 122-125 (**2002**).
471 **Croce, C. M.** Causes and consequences of microRNA dysregulation in cancer. *Nat Rev Genet* 10, 704-714 (**2009**).
472 **Saha, A., Lu, J., Morizur, L., Upadhyay, S. K., Aj, M. P. & Robertson, E. S.** E2F1 mediated apoptosis induced by the DNA damage response is blocked by EBV nuclear antigen 3C in lymphoblastoid cells. *PLoS Pathog* 8, e1002573 (**2012**).
473 **Lin, W. C., Lin, F. T. & Nevins, J. R.** Selective induction of E2F1 in response to DNA damage, mediated by ATM-dependent phosphorylation. *Genes Dev* 15, 1833-1844 (**2001**).
474 **Polager, S., Ofir, M. & Ginsberg, D.** E2F1 regulates autophagy and the transcription of autophagy genes. *Oncogene* 27, 4860-4864 (**2008**).
475 **Rodriguez-Rocha, H., Garcia-Garcia, A., Panayiotidis, M. I. & Franco, R.** DNA damage and autophagy. *Mutat Res* 711, 158-166 (**2011**).
476 **Garcia-Garcia, A., Rodriguez-Rocha, H., Tseng, M. T., Montes de Oca-Luna, R., Zhou, H. S., McMasters, K. M. & Gomez-Gutierrez, J. G.** E2F-1 lacking the transcriptional activity domain induces autophagy. *Cancer Biol Ther* 13, 1091-1101 (**2012**).
477 **Udayakumar, T. S., Stoyanova, R., Hachem, P., Ahmed, M. M. & Pollack, A.** Adenovirus E2F1 overexpression sensitizes LNCaP and PC3 prostate tumor cells to radiation in vivo. *International journal of radiation oncology, biology, physics* 79, 549-558 (**2011**).
478 **Xu, C., Zeng, Q., Xu, W., Jiao, L., Chen, Y., Zhang, Z., Wu, C., Jin, T., Pan, A., Wei, R., Yang, B. & Sun, Y.** miRNA-100 inhibits human bladder urothelial carcinogenesis by directly targeting mTOR. *Molecular cancer therapeutics* 12, 207-219 (**2013**).
479 **Sun, D., Lee, Y., Malhotra, A., Kim, H., Matecic, M., Evans, C., Jensen, R., Moskaluk, C. & Dutta, A.** miR-99 family of MicroRNAs suppresses the expression of prostate-specific antigen and prostate cancer cell proliferation. *Cancer research* 71, 1313-1324 (**2011**).
480 **Hershko, T. & Ginsberg, D.** Up-regulation of Bcl-2 homology 3 (BH3)-only proteins by E2F1 mediates apoptosis. *The Journal of biological chemistry* 279, 8627-8634 (**2004**).
481 **Crighton, D., Wilkinson, S., O'Prey, J., Syed, N., Smith, P., Harrison, P., Gasco, M., Garrone, O., Crook, T. & Ryan, K.** DRAM, a p53-induced modulator of autophagy, is critical for apoptosis. *Cell* 126, 121-134 (**2006**).